Kinetic and Product Studies of the Hydroxyl Radical Initiated Oxidation of Dimethyl Sulfide in the Temperature Range 250 - 300 K

Thesis submitted to the Faculty of Mathematics and Natural Sciences

Bergische Universität Wuppertal

for the Degree of Doctor of Natural Sciences

(Dr. rer. nat.)

by

Mihaela Albu

born in Iasi, Romania

February, 2008

The work described in this thesis was carried out in the Department of Physical Chemistry, Bergische Universität Wuppertal, under the supervision of Prof. Dr. Karl Heinz Becker.

Referee: Prof. Dr. Karl Heinz Becker
Co-referee: Prof. Dr. Thorsten Benter

Acknowledgements

I would like to express my sincere thanks to Prof. Dr. Karl Heinz Becker for the opportunity of doing this Ph.D. in his research group and for the supervision of this work. Thanks also for his support and encouragement.

I am very grateful to Prof. Dr. Thorsten Benter for agreeing to co-referee the thesis and his many useful comments. Very special thanks for his support and encouragement and also for the fruitful discussions and his appreciation of my work during the “Wednesday” seminars.

I would like to express my appreciation to Prof. Dr. Siegmar Gäb and Prof. Dr. Joachim M. Marzinkowski for their kindness to be co-examiners.

My sincere and distinguished thanks are also due to Dr. Ian Barnes who not only helped me to understand at least a part of the vast and fascinating domain of the atmospheric chemistry but also followed with his special care my scientific work. His guidance, sugestions, support and encouragement have been of immense help to me during the whole course of my work.

I would like to express my sincere gratitude to Prof. Dr. Raluca Delia Mocanu for trusting me and for giving me the chance to open a window to atmospheric chemistry. Distinguished thanks for her parental attitude and warm encouragements when times were hard.

I wish to thank all my former and current colleagues from the Department of Physical Chemistry, Bergische Universität Wuppertal, for the pleasant working atmosphere, for helpful discussions and for the experience they shared with me. Special thanks are due to Dr. Klaus Brockmann for his help, support, encouragement and constant friendliness. Thanks are due to Dr. Cecilia Arsene for her help given at the beginning of my work on atmospheric chemistry and to Dr. Romeo Olariu for his unconditional help. Distinguished thanks are also due to Dr. Iulia Patroesu-Klotz and Dr. Markus Spitler. Special thanks to my office colleagues, Ana Lydia Mangas Suárez, Anne Heinrich, Hendrik Kersten and Matthias Lorenz, together with them, I was feeling like in a family.

Thanks are also due to the technical and secretarial staff of this group; my special thanks to Ronald Giese for his excellent technical support in the experimental part of this work and to Wilhelm Nelsen for his always-kindly help in solving technical problems.

My special thanks to all my former colleagues from the Department of Analytical Chemistry, Faculty of Chemistry, “Al. I. Cuza” University of Iasi, which have a special place in my heart.

And last but certainly not the least, my most sincere and deepest thanks are to my family, particularly my parents, my twin brother and my sister-in-law for their great love, care, support, and encouragement from the distance, all the time being spiritually near by me.

Familiei mele

Abstract

This work presents investigations on the gas-phase chemistry of dimethyl sulfide (DMS: CH_3-S-CH_3) with hydroxyl (OH) radicals performed in a 336 l quartz glass reactor in the laboratory of the Department of Physical Chemistry of the University of Wuppertal, Germany. In this work kinetic, product and mechanistic data for the reaction of OH radicals with DMS were obtained. The investigations were aimed at achieving a better understanding of the oxidation mechanism for DMS as a function of temperature. Such an insight will help to provide a basis for understanding the atmospheric processes that link DMS photooxidation to particle formation and climate change.

Relative rate coefficients were measured for the first time for the gas-phase reactions of hydroxyl radicals with dimethyl sulfide for a wide range of temperature (250 - 299 K) and different partial pressures of oxygen (~0, 205 and 500 mbar) at 1000 mbar total pressure. Using *in situ* Fourier transform infrared (FTIR) spectroscopy for the analyses the following averaged values of the rate coefficients for the reaction of OH radicals with DMS were obtained:

Temperature (K)	$k_{DMS} \times 10^{11}$ (cm^3 $molecule^{-1}$ s^{-1})		
	~0 mbar O_2	205 mbar O_2	500 mbar O_2
299	0.50 ± 0.10	0.78 ± 0.18	0.95 ± 0.19
290	0.57 ± 0.11	0.98 ± 0.23	1.34 ± 0.27
280	0.62 ± 0.13	1.20 ± 0.26	1.54 ± 0.31
270	0.63 ± 0.14	1.51 ± 0.34	1.85 ± 0.37
260	0.64 ± 0.13	1.99 ± 0.47	2.38 ± 0.47
250	0.66 ± 0.14	2.82 ± 0.77	2.83 ± 0.62

From the kinetic data the following Arrhenius expressions for the reaction of OH radicals with DMS, valid in the temperature range 250 to 299 K, have been obtained:

O_2 partial pressure (mbar)	k_{DMS} (cm^3 $molecule^{-1}$ s^{-1})
~ 0	$(1.56 \pm 0.20) \times 10^{-12} \exp[(369 \pm 27) / T]$
205	$(1.31 \pm 0.08) \times 10^{-14} \exp[(1910 \pm 69) / T]$
500	$(5.18 \pm 0.71) \times 10^{-14} \exp[(1587 \pm 24) / T]$

Detailed product studies were performed on the OH radical initiated oxidation of dimethyl sulfide for different conditions of temperature (260, 270, 280, 290 and 298 K), oxygen partial pressure (~0, 250 and 500 mbar) and initial NO_x concentrations ($NO + NO_2$: 0 - 3215 ppbv + 0 - 106 ppbv). The present work represents the first product study at low temperatures (260 - 280 K).

The major sulfur-containing products identified in the OH radical initiated oxidation of DMS using *in situ* FTIR spectroscopy were: dimethyl sulfoxide (DMSO: $CH_3S(O)CH_3$) and sulfur dioxide (SO_2), in the absence of NO_x, and dimethyl sulfoxide, dimethyl sulfone ($DMSO_2$: $CH_3S(O)_2CH_3$) and sulfur dioxide, in the presence of NO_x. Formation of dimethyl sulfone, methyl thiol formate (MTF: CH_3SCHO) and carbonyl sulfide (OCS), in the absence of NO_x, and of methyl sulfonyl peroxynitrate

(MSPN: $CH_3S(O)_2OONO_2$) and methane sulfonic acid (MSA: $CH_3S(O)_2OH$), in the presence of NO_x, has also been observed. Using Ion Chromatography (IC) evidence has been found for the formation of methane sulfinic acid (MSIA: $CH_3S(O)OH$) and methane sulfonic acid, both in the absence and presence of NO_x.

The variation of the product yields with temperature, NO_x concentration and partial pressure of oxygen is consistent with the occurrence of both addition and abstraction channels in the OH radical initiated oxidation of DMS. At all temperatures and reaction conditions studied, in the presence of oxygen, the combined yields of dimethyl sulfoxide and dimethyl sulfone are roughly equal to the fraction of the reaction proceeding *via* the addition channel.

The DMSO/$DMSO_2$ yield ratio observed in the reaction system was sensitive to the initial NO concentration. Increasing NO caused a decrease in the DMSO concentration with an approximately equivalent increase in the $DMSO_2$ concentration. A reaction sequence involving a DMS-OH adduct and O_2 has been proposed to explain the observation. The observations, however, support that this sequence will be unimportant under most atmospheric conditions and that reaction of the DMS-OH adduct with molecular oxygen will mainly produce DMSO. Based on the work it is suggested that in the OH radical initiated photooxidation of DMS in the remote marine atmosphere, where NO levels are extremely low, the major product of the O_2-dependent pathway will be DMSO with a branching ratio of $\geq$0.95 and $DMSO_2$, if formed at all, with a ratio of $\leq$0.05.

The work has confirmed that the reaction of CH_3S radicals with O_2 to produce CH_2S and its further oxidation is the most probable pathway for the production of carbonyl sulfide (OCS) under NO_x-free experimental systems. At around room temperature the measured yield is similar to that reported in other studies; the present study, however, indicates that the process forming OCS may not be efficient at temperatures below 290 K.

In all of the experimental systems the yield of SO_2 was always lower than the fraction of the reaction proceeding *via* the O_2-independent pathway. In the NO_x-free systems this has been attributed to the formation of products such as CH_3SCHO (methyl thiol formate), CH_3SCH_2OH (methyl thiomethanol) and possibly CH_3SCH_2OOH. Of these products only CH_3SCHO has been positively identified. The results support that in the remote marine atmosphere the yield of this compound in the oxidation of DMS will not be more than a few percent even at low temperatures. In the presence of high levels of NO_x the low SO_2 yields can be explained by the formation of sulfur reservoir species such as $CH_3S(O)_2OONO_2$, $CH_3S(O)OONO_2$, $CH_3S(O)ONO_2$, $CH_3S(O)NO_2$ and $CH_3S(O)NO$. The low levels of SO_2 observed also support that the further oxidation of DMSO formed in the O_2-dependent pathway is not leading to formation of high yields of SO_2 under the conditions of the experiments.

The results from the kinetic and product studies have been used to propose a reaction mechanism for the reaction of OH radicals with DMS which can be implemented over the temperature range 260 - 306 K.

Contents

Chapter 1:

Introduction 1

1.1 Importance of sulfur chemistry in the atmosphere 1

1.2 Sulfur compounds in the atmosphere 2

1.3 Atmospheric sulfur cycle 3

1.4 Dimethyl sulfide in the atmosphere 5

Chapter 2:

Gas-phase chemistry of dimethyl sulfide (DMS) with hydroxyl (OH) radicals: state of knowledge 11

2.1 Kinetics of the reaction of OH radicals with DMS 11

2.2 Product and mechanistic studies of the reaction of OH radicals with DMS 14

2.2.1 O_2-dependent channel 15

2.2.2 O_2-independent channel 18

2.3 Aim of the work 30

Chapter 3:

Experimental section 31

3.1 Experimental set-up 31

3.1.1 Description of the reaction chamber 31

3.1.2 Description of the sampling system for ion chromatography analysis 33

3.2 Typical experimental procedure 34

3.2.1 Kinetic experiments on the system DMS + OH radicals 35

3.2.2 Product study experiments on the system DMS + OH radicals 35

3.3 Generation of OH radicals 36

3.4 Data analysis 37

3.4.1 Relative rate method 37

3.4.2 Product analysis 39

Chapter 4:

Kinetic study of the OH radical initiated oxidation of dimethyl sulfide 43

4.1 Results 44

4.2 Discussion 48

4.2.1 Possible source of errors in the system 48

4.2.2 Comparison with previous work 49

4.3 Summary of the kinetic results 56

Chapter 5:

Product study of the OH radical initiated oxidation of dimethyl sulfide 59

5.1 Experimental results 59

5.1.1 Dimethyl sulfoxide (DMSO) 67

5.1.2 Dimethyl sulfone ($DMSO_2$) 75

5.1.3 Sulfur dioxide (SO_2) 82

5.1.4 Methyl sulfonyl peroxynitrate (MSPN) 88

5.1.5 Methyl thiol formate (MTF) 91

5.1.6 Carbonyl sulfide (OCS) 94

5.1.7. Methane sulfonic acid (MSA) and methane sulfinic acid (MSIA) 96

5.2 Discussion of the results and comparison with literature data 100

5.2.1 Dimethyl sulfoxide (DMSO) and dimethyl sulfone ($DMSO_2$) formation 102

5.2.2 Sulfur dioxide (SO_2), methyl thiol formate (MTF), methane sulfonic acid (MSA), and methyl sulfonyl peroxynitrate (MSPN) formation 110

5.2.3 Carbonyl sulfide (OCS) formation 116

5.2.4 Methane sulfonic acid (MSA) and methane sulfinic acid (MSIA) formation ... 118

5.3 Summary of the product results 120

Chapter 6:

Atmospheric implications 127

Summary 131

Appendix I:

Synthesis of methyl nitrite (CH_3ONO) 135

Appendix II:

Gas-phase infrared absorption cross sections 137

Appendix III:

Literature product yields in the reaction of dimethyl sulfide with OH radicals 141

Appendix IV:

Gases and chemicals 147

Appendix V:

Abbreviations 149

References 151

Chapter 1

Introduction

The atmosphere forms mainly a gaseous envelope that surrounds the earth. It is composed primarily of nitrogen, oxygen and several noble gases; the concentrations of which have remained remarkably constant over time. Also present are so-called trace gases that occur in relatively small (in the ppmv* range and below) and sometimes highly variable amounts. The atmosphere contains a myriad of trace species with levels as low as 1 pptv* which comprise less than 1% of the atmosphere. The trace gas abundances have changed rapidly and remarkably over the last two centuries. The role of trace species is disproportionate to their atmospheric abundance. In the earth's radiative balance and in the chemical properties of the atmosphere they play a crucial role.

1.1 Importance of sulfur chemistry in the atmosphere

Even though gas-phase sulfur compounds represent only a small fraction of the earth's atmospheric composition, comprising less than 1 ppmv (Tyndall and Ravishankara, 1991; Seinfeld and Pandis, 1998), these minor constituents have a significant impact on the atmosphere, hydrosphere and biosphere. The gas- and liquid-phase oxidation of sulfur dioxide (SO_2) to sulfuric acid (H_2SO_4) is the predominant source of acidic precipitation (Wayne, 2000). The gas-phase oxidation of reduced sulfur to sulfuric acid can promote the formation of aerosol which reduces visibility and may pose a risk to human health (Dockery *et al.*, 1993; Finlayson-Pitts and Pitts, 2000). These aerosols have a direct impact on the earth-atmosphere radiation budget by reflecting surface bound solar radiation (Jonas *et al.*, 1995). Additionally, atmospheric aerosols may participate in cloud formation processes by serving as cloud condensation nuclei; in this role, aerosols generated by gas phase sulfuric acid possess the potential to have an impact on the earth's radiation budget by influencing the radiative properties of clouds and the cloud aerial distribution (Jonas *et al.*, 1995).

**1 ppmv = 1 part in 10^6 parts of air by volume*
1 pptv = 1 part in 10^{12} parts of air by volume

The potential of a given sulfur compound to make an impact on the environment is dependent on a variety of factors that include distribution of the emission source, photochemistry, physical processes (i.e. susceptibility to removal *via* wet and dry deposition) and local environment (e.g. humidity and temperature, meteorology, concentration and properties of pre-existing particulates, mixing ratios of oxidants and other reactive trace species). Upon careful consideration of these factors, it becomes apparent that in addition to being major sources of atmospheric acidity in remote regions (i.e. non-continental), organosulfur compounds may constitute an important component in the earth's climate system by making an impact on the earth-atmosphere radiation budget (Shaw, 1983; Charlson *et al.*, 1987). A thorough understanding of the atmospheric oxidation of organosulfur compounds is necessary to evaluate accurately the importance of their role in the earth-atmosphere radiation budget and how this role changes with the fluxes of these gases into the atmosphere.

1.2 Sulfur compounds in the atmosphere

Sulfur in the atmosphere originates either from natural processes or anthropogenic activity. Numerous gas-phase sulfur compounds have been observed in the atmosphere; the most important ones are listed in Table 1.1.

Table 1.1: Atmospheric sulfur compounds.

Name of compound	Symbol	Chemical structure	Oxidation state
Hydrogen sulfide	H_2S	H-S-H	−2
Dimethyl sulfide	DMS	CH_3-S-CH_3	−2
Carbon disulfide	CS_2	S=C=S	−2
Carbonyl sulfide	OCS	O=C=S	−2
Methyl mercaptan	MeSH	CH_3-S-H	−2
Dimethyl disulfide	DMDS	CH_3-S-S-CH_3	−1
Dimethyl sulfoxide	DMSO	CH_3-S(O)-CH_3	0
Dimethyl sulfone	$DMSO_2$	CH_3-$S(O)_2$-CH_3	2
Methane sulfonic acid	MSA	CH_3-$S(O)_2$-OH	4
Sulfur dioxide	SO_2	O=S=O	4
Sulfuric acid	H_2SO_4	OH-$S(O)_2$-OH	6

Sulfur occurs in the atmosphere in various oxidation states (Andreae, 1990). The chemical reactivity of atmospheric sulfur compounds is inversely related to their sulfur oxidation state. The water solubility of sulfur species increases with their oxidation state.

Reduced sulfur species occur preferentially in the gas phase, whereas the S(+6) compounds often tend to be found in particles or droplets. Six of the compounds listed in the above table (H_2S, DMS, CS_2, OCS, MeSH and DMDS) are reduced sulfur compounds which are emitted directly into the atmosphere from various sources. Carbonyl sulfide (OCS) is also produced in the atmosphere by the oxidation of CS_2, making it the only atmospheric reduced sulfur compound with both primary and secondary sources of significance. The other five compounds (SO_2, DMSO, H_2SO_4, MSA and $DMSO_2$) listed in Table 1.1 are oxysulfur compounds, among which only SO_2 has significant primary sources. The remaining oxysulfur compounds are products resulting from the oxidation of SO_2 and reduced sulfur species.

1.3 Atmospheric sulfur cycle

Approximately 110 Tg sulfur per year are emitted into the atmosphere (Berresheim *et al.*, 1995). Anthropogenic emissions account for ca. 70% of sulfur emissions and are overwhelmingly in the form of SO_2, with the vast majority of these emissions occurring in the Northern Hemisphere. In the Southern Hemisphere organosulfur compounds from natural sources constitute ca. 70% of total sulfur emissions. Due to the skewed emissions of SO_2, natural organosulfur compounds, mainly dimethyl sulfide, are the most important reactive sulfur gases in the Southern Hemisphere and in the Northern Hemisphere marine atmosphere, excluding regions associated with coastal waters and areas of the open ocean where air masses of continental origin predominate.

The major processes involved in the atmospheric sulfur cycle are depicted in Figure 1.1. The atmospheric sulfur cycle begins with the introduction of a sulfur compound into the atmosphere. The sulfur compound is subjected to physical transport and may endure chemical and/or physical transformations prior to being removed from the atmosphere *via* wet or dry deposition.

For sulfur compounds of atmospheric interest, photolysis by actinic radiation is not an important process. With the exception of OCS, the dominant fate of reduced sulfur compounds in the troposphere is chemical transformation. The primary oxidants responsible for the initiation of atmospheric oxidation are the hydroxyl (OH) radical in the daytime and the nitrate (NO_3) radical at night. Because OCS is very unreactive, it is the only sulfur compound that diffuses into the stratosphere (excluding the injection of sulfur compounds into the stratosphere by volcanoes).

Of the oxysulfur compounds, SO_2 and DMSO are the species for which gas-phase oxidation is an important process. However, removal by physical processes (uptake by aerosol and cloud droplets in particular) followed by heterogeneous chemical reaction is a

viable process for both species. On a global scale, up to ca. 90% of SO_2 is removed from the atmosphere by heterogeneous processes (Jonas *et al.*, 1995). Wet and dry deposition account for just over half of SO_2 heterogeneous removal and the remainder is removed *via* in-cloud aqueous phase oxidation to sulfate (Jonas *et al.*, 1995). The balance of atmospheric SO_2, less than 10% of total emissions (primary and secondary), is thought to be converted to H_2SO_4 by gas-phase oxidation (Jonas *et al.*, 1995). The remainder of the oxysulfur compounds shown in Table 1.1 are hexavalent and thus highly unreactive in the gas phase over the range of tropospheric conditions. Wet and dry depositions are the dominant removal processes for these species.

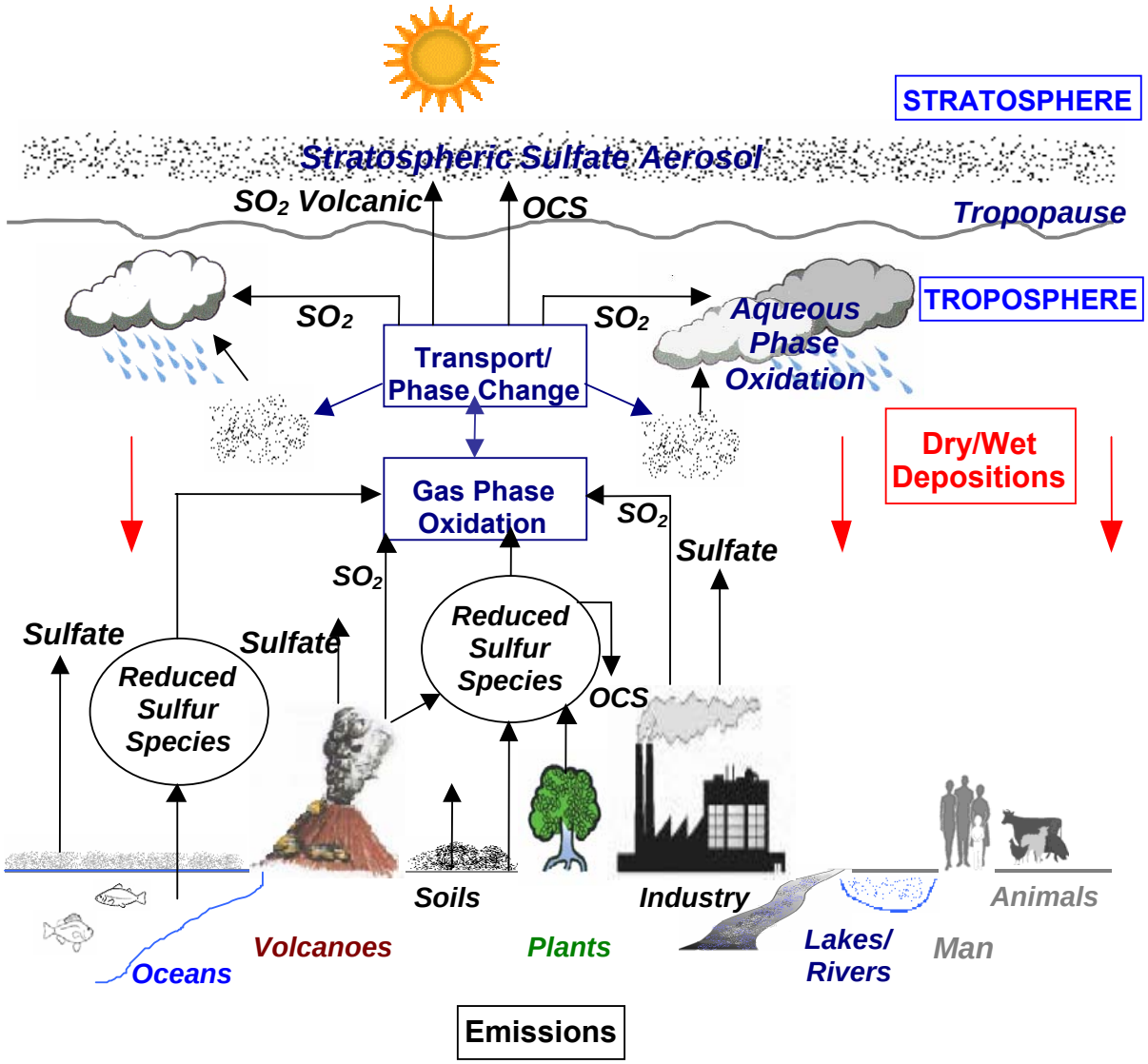

Figure 1.1: Major processes involved in the atmospheric sulfur cycle.

1.4 Dimethyl sulfide in the atmosphere

The main questions in atmospheric chemistry that need answering in order to asses the role of dimethyl sulfide (DMS) are as follows: (i) how is DMS emitted to the atmosphere? (ii) how much DMS is released into the atmosphere? (iii) how rapidly is DMS oxidized in the atmosphere and by what chemical agent? (iv) what are the end products of its oxidation and what stable intermediates are produced? (v) how does the presence of DMS and its chemical transformation affect the composition of the atmosphere? To answer these questions, a combination of field measurements, laboratory studies and numerical modelling studies have been carried out by numerous research groups.

Dimethyl sulfide is the dominant natural sulfur compound emitted from the oceans to the atmosphere (Bates *et al.*, 1992; Spiro *et al.*, 1992; Beresheim *et al.*, 1995; Urbanski and Wine, 1999a), accounting for about one quarter of global sulfur emissions in the gaseous phase. DMS was discovered in the surface ocean by Lovelock *et al.* (1972), who suggested that DMS may be the biogenic sulfur species that was needed at the time to balance the global sulfur budget. Since its discovery, DMS has been the subject of continuously increasing interest by the scientific community. DMS was immediately recognized as an important component of the biogeochemical sulfur cycle, and is now indicated as the second most important source of sulfur in the atmosphere, after anthropogenic SO_2 emission from fossil fuel combustion and industry.

The predominant oceanic source of DMS is dimethyl sulfonium propionate (DMSP), a compatible solute synthesized by phytoplankton for osmoregulation (Vairavamurthy *et al.*, 1985) and/or cryoprotection (Kirst *et al.*, 1991). The emission of dimethyl sulfide by macro algae was discovered by Haas (1935). Challenger and Simpson (1948) showed that dimethyl sulfonium propionate was its precursor. The enzymatic cleavage of DMSP produces DMS along with acrylic acid:

$(CH_3)_2S^+CH_2CH_2COO^-$	$\rightarrow$	CH_3SCH_3	+	CH_2=CHCOOH
Dimethyl sulfonium propionate		Dimethyl sulfide		Acrylic acid

Laboratory (Keller, 1989) and field (Malin *et al.*, 1993; Liss *et al.*, 1994) studies have shown that both DMSP production and DMS release is species specific (for example, diatoms generally produce little DMSP, whereas prymnesiophytes and dinoflagellates make significantly larger amounts). The biological processes involved in the DMS production from phytoplanktonic DMSP are metabolic excretion (Vairavamurthy *et al.*, 1985), grazing (Dacey and Wakeham, 1986; Leck *et al.*, 1990) and senescence (Nguyen *et al.*, 1988; Leck *et al.*,

1990), the two last processes being probably the major DMS sources. Concentrations of both DMS and DMSP typically show a maximum a few meters below the ocean surface and a sharp decline at about 100 m depths where the light intensity is reduced to 1% (Georgii and Warnek, 1999).

The removal pathways of DMS in seawater are emission to the atmosphere, bacterial consumption/transformation, photochemical oxidation and downward mixing, with a total turnover time of one to a few days (Kieber *et al.*, 1996; Ledyard and Dacey, 1996). The rates of the first three dominant sinks are highly variable as a function of time, place and meteorological conditions, but are of comparable overall importance for the removal of dissolved DMS. Atmospheric ventilation might predominate removal of DMS in the upper meter of the water column. Because of its high concentration in seawater relative to that in air and its insolubility in water, DMS is transferred across the water-air interface and enters the atmosphere. The first detection of DMS in marine air was reported by Maroulis and Bandy (1977). The flux of DMS from the seawater into the atmosphere is primarily controlled by the wind speed, the water concentration of DMS and the sea surface temperature. There have been numerous estimates of the sea-air flux of DMS, by extrapolating the measurement results to the global scale or by atmospheric models (e.g. Nguyen *et al.*, 1978; Barnard *et al.*, 1982; Andreae and Raemdonck, 1983; Cline and Bates, 1983; Andreae *et al.*, 1985; Bates *et al.*, 1987; Andreae, 1990; Aneja, 1990; Erickson III *et al.*, 1990; Langner and Rodhe, 1991; Andreae and Jaeschke, 1992; Bates *et al.*, 1992; Spiro *et al.*, 1992; Staubes and Georgii, 1993; Pham *et al.*, 1995; Chin *et al.*, 1996; Feichter *et al.*, 1996; Restad *et al.*, 1998). The recent estimates of the ocean to air flux of DMS are: 20.7 $\pm$ 5.2 Tg S year^{-1} (Watts, 2000), 13 to 37 Tg S year^{-1} (Kettle and Andreae, 2000), 17 to 26.7 Tg S year^{-1} (Aumont *et al.*, 2002), 15.4 to 26 Tg S year^{-1} (Bopp *et al.*, 2003) and 28 Tg S year^{-1} (Kloster *et al.*, 2006), i.e. enough to make a significant contribution to the global atmospheric sulfur burden (Gondwe *et al.*, 2003).

Oceanic DMS concentrations have changed over geological time scales and continue to vary both regionally and seasonally. Ice core measurements of the atmospheric DMS oxidation product, methane sulfonate, suggest that DMS emissions (and presumably oceanic DMS concentrations) may have changed by a factor of 6 between glacial and interglacial times (Legrand *et al.*, 1991). The spatial and temporal variation of sea surface concentration of DMS is summarized in Kettle *et al.* (1999). The DMS distribution in highly productive oceanic regions is characterized by pronounced patchiness on a relatively small scale (100 m, Andreae and Raemdonck, 1983). On an annual basis, large scale variations are less pronounced, but seem to follow a general trend towards higher DMS concentrations and sea-

to-air fluxes with increasing primary production (Andreae and Barnard, 1984). Seasonal studies have revealed strong annual variations in some mid to high latitude regions, in particular in coastal and shelf seas (Bates *et al.*, 1987; Leck *et al.*, 1990; Turner *et al.*, 1996; Dacey *et al.*, 1998; Preunkert *et al.*, 2007).

The other sources of DMS (especially terrestrial): tropical forests, vegetation (maize, wheat, lichens), soils, freshwater wetlands, salt-marshes and estuaries, and anthropogenic sources are minor compared to oceanic sources and were estimated to be 1.60 $\pm$ 0.50, 1.58 $\pm$ 0.86, 0.29 $\pm$ 0.17, 0.12 $\pm$ 0.07, 0.07 $\pm$ 0.06, and 0.13 $\pm$ 0.04 Tg S $year^{-1}$, respectively (Watts, 2000).

In the atmosphere, DMS reacts predominantly with the hydroxyl (OH) radical and also with the nitrate (NO_3) radical (Tyndall and Ravishankara, 1991; Berresheim *et al.*, 1995; Wilson and Hirst, 1996; Stark *et al.*, 2007). Because the OH radical has a photochemical source, DMS is removed more effectively during daylight hours rather than at night when the NO_3 radical reaction could be important. As a result marine boundary layer DMS concentrations exhibit a diurnal cycle, with a night-time maximum and daytime minimum. However, the relative importance of these two pathways is most likely a strong function of latitude, altitude and season of the year.

It has been speculated that halogen atoms (X atoms) and halogen oxides (XO radicals) might also play a role in the chemistry of the marine boundary layer and consequently in the chemistry of DMS oxidation (Andreae and Crutzen, 1997; Platt and Honninger, 2003); many experimental studies (Barnes *et al.*, 1987a; Martin *et al.*, 1987; Daykin and Wine, 1990; Nielsen *et al.*, 1990; Barnes *et al.*, 1991; Maguin *et al.*, 1991; Stickel *et al.*, 1992; Barnes, 1993; Wine *et al.*, 1993; Jefferson *et al.*, 1994; Butkovskaya *et al.*, 1995; Bedjanian *et al.*, 1996; Kinnison *et al.*, 1996; Zhao *et al.*, 1996; Ingham *et al.*, 1999; Maurer *et al.*, 1999; Urbanski and Wine, 1999b; Knight and Crowley, 2001; Nakano *et al.*, 2001; Arsene *et al.*, 2002a, b; Ballesteros *et al.*, 2002; Diaz-de-Mera *et al.*, 2002; Nakano *et al.*, 2003; Enami *et al.*, 2004; Ghosh *et al.*, 2004; Arsene *et al.*, 2005, Dyke *et al.*, 2005) and theoretical studies (McKee, 1993a; Resende and De Almeida, 1997; Wilson and Hirst, 1997; Thompson *et al.*, 2002; Enami *et al.*, 2004; Sayin and McKee, 2004; Gravestock *et al.*, 2005; Zhang *et al.*, 2007) have been carried out on this subject.

The rate coefficients for the initiation reactions of DMS with the OH radicals are reasonably well established and are presented in detail in Chapter 2, Paragraph 2.1.

The reaction between DMS and NO_3 radicals (kinetics, products and mechanism) has also been studied (Atkinson *et al.*, 1984; MacLeod *et al.*, 1986; Tyndall *et al.*, 1986;

Wallington *et al.*, 1986a, b; Dlugokencky and Howard, 1988; Daykin and Wine, 1990; Jensen *et al.*, 1991, 1992; Butkovskaya and Le Bras, 1994; Arsene *et al.*, 2003).

Based on the current values for the initiation reactions and the concentration of the oxidants in the atmosphere, the atmospheric lifetime of DMS is believed to be a few days, with the majority of the oxidation being initiated by OH radicals in warm sunny regions, and by NO_3 radicals in colder, darker regions. In the remote marine boundary layer, the reaction of DMS with NO_3 radicals will be of little significance, due to the predicted low ambient NO_3 radical concentrations in these regions.

The oxidation mechanism of DMS with OH radicals is very complex and still not well defined (Yin *et al.*, 1990a; Barone *et al.*, 1995; Barnes *et al.*, 2006). This complexity has to be understood to assess the role of DMS in the atmosphere. The oxidation steps involve many species, competing reactions and multiple branch points, which are discussed in detail in Chapter 2, Paragraph 2.2. The end products from the atmospheric oxidation of DMS have been deduced from laboratory investigations, field observations and modelling studies.

The oxidation mechanism of DMS with OH radicals under NO_x-free or NO_x-containing conditions and the relative yields of the products SO_2, DMSO, $DMSO_2$, MSA, MSIA (methane sulfinic acid), MSPN (methyl sulfonyl peroxynitrate), OCS and MTF (methyl thiol formate) have been extensively studied in laboratory experiments (Grosjean and Lewis, 1982; Hatakeyama *et al.*, 1982; Hatakeyama and Akimoto, 1983; Niki *et al.*, 1983a, b; Atkinson *et al.*, 1984; Grosjean, 1984; Hatakeyama *et al.*, 1985; Hynes *et al.*, 1986; Barnes *et al.*, 1988; Hynes *et al.*, 1993; Barnes *et al.*, 1994a, b, 1996; Patroescu, 1996; Sørensen *et al.*, 1996; Turnipseed *et al.*, 1996; Arsene *et al.*, 1999; Patroescu *et al.*, 1999; Arsene *et al.*, 2001; Albu *et al.*, 2002; Arsene, 2002; Albu *et al.*, 2003, 2004a; Arsene *et al.*, 2004; Librando *et al.*, 2004; Albu *et al.*, 2007, 2008). In most cases large volume photoreactors were employed for the investigations. Laboratory reaction chamber studies provide information about product yields for various reactions and conditions. Drawbacks to these chamber studies include a general disagreement between different groups because of differing chamber environments, problems in applying the results to the real atmosphere because of the pseudo atmospheric chamber conditions and difficulties in defining mechanisms at the elementary reaction level. Despite these drawbacks laboratory-based investigations of DMS oxidation using chemical kinetic and reaction chamber techniques have provided many mechanistic details.

To complement laboratory investigations, field observations of DMS and its oxidation products can be used to deduce mechanistic information. Field studies on DMS oxidation have provided evidence for SO_2, H_2SO_4, DMSO, $DMSO_2$, nss-SO_4^{2-} (non-sea-salt sulfate) in the aerosol phase and MSA, also largely present in the aerosol phase (Berresheim, 1987; Bandy *et al.*, 1992; Mihalopoulos *et al.*, 1992a; Nguyen *et al.*, 1992; Putaud *et al.*, 1992;

Berresheim *et al.*, 1993a, b, c; Davison and Hewitt, 1994; Bandy *et al.*, 1996; Davison *et al.*, 1996; Hewitt and Davison, 1997; Berresheim and Eisele, 1998; Berresheim *et al.*, 1998; Davis *et al.*, 1998; Jefferson *et al.*, 1998a, b; Legrand and Pasteur, 1998; Minikin *et al.*, 1998; Davis *et al.*, 1999; Mauldin III *et al.*, 1999; Putaud *et al.*, 1999; Chen *et al.*, 2000; Kim *et al.*, 2000; Sciare *et al.*, 2001; Shon *et al.*, 2001; De Bruyn *et al.*, 2002; Bardouki *et al.*, 2003). MSA and nss-SO_4^{2-} ions have also been measured in ice cores (Legrand *et al.*, 1991; Legrand *et al.*, 1997).

The direct interpretation of field data is, however, often difficult because photochemical changes have to be separated from the transport tendencies, aerosol-cloud interactions and other physical processes that are occurring simultaneously. Modelling approaches overcome this difficulty by incorporating these additional processes into a model containing a DMS oxidation mechanism. The resulting model simulations can then be compared with the field observations and used to assess the mechanism. There have been many recent modelling studies using both comprehensive (Koga and Tanaka, 1993; Hertel *et al.*, 1994; Saltelli and Hjorth, 1995; Campologno *et al.*, 1999; Lucas and Prinn, 2002, 2005; Karl *et al.*, 2007) and parameterized (Chin *et al.*, 1996; Davis *et al.*, 1999; Mari *et al.*, 1999; Chen *et al.*, 2000) versions of DMS mechanisms. The comprehensive mechanisms are modified or reduced forms from the work of Yin *et al.* (1990a). Detailed reviews of comprehensive DMS oxidation mechanisms are given by Yin *et al.* (1990a), Turnipseed and Ravishankara (1993), Urbanski and Wine (1999a) and Barnes *et al.* (2006).

The ocean covers approximately two-thirds of the earth's surface, and this relatively dark water surface could absorb over 90% of the incident solar radiation (Pandis *et al.*, 1994). About 50% of the ocean is covered by stratus clouds (Katoshevski *et al.*, 1999), which decreases the amount of energy reaching the sea-surface. Through reflection of incoming solar radiation back to space this type of cloud exerts a profound influence in governing the planetary albedo and can influence the earth's climate. Aerosols present in the marine boundary layer, MBL, serve as cloud condensation nuclei (CCN) and are actively involved in regulation of the formation of marine stratus clouds. There are three main sources of aerosol in the remote marine boundary layer: sea-salt, non-sea-salt (nss) sources and entrainment of free tropospheric aerosol. The principal component of nss-aerosol is sulfate originating from the oxidation of gaseous dimethyl sulfide produced by phytoplankton in surface water (Charlson *et al.*, 1987; Andreae *et al.*, 1994; Cainey *et al.*, 1996). The relative contributions of the three marine aerosol sources are dependent upon many factors such as wind speed, frequency of occurrence of clouds and precipitation, sea-surface DMS emission rates, oxidation mechanism of DMS to SO_2 and MSA, rate of entrainment of free trophospheric aerosol etc.

It has been postulated that emission of DMS from the oceans may have a significant influence on the earth's radiation budget and possibly in climate regulation (CLAW hypothesis, Charlson *et al.*, 1987). Substantial amounts of DMS may also reach the upper trophosphere (even lower stratosphere) over convective regions. Thus, DMS may also influence sulfate aerosol formation in the upper troposphere and lower stratosphere.

The Intergovernmental Panel on Climate Change (Denman *et al.*, 1995) has classified the coupling between DMS and aerosols as an important component of the planetary climate system which needs to be understood in detail. The major question concerning DMS in the marine atmosphere is the extent it plays in controlling the levels of aerosol in the MBL. Any effect that DMS will have on the climate is critically dependent on the production of gas-phase sulfuric acid (H_2SO_4) and new particles. Despite intensive efforts determination of the quantitative contribution of DMS-derived non-sea-salt sulfate to CCN in the marine boundary layer has remained elusive and model studies of global SO_2 indicate that there may be as yet unaccounted for oxidants involved in the DMS oxidation (Chin *et al.*, 1998). Further progress in the elucidation of the DMS oxidation mechanism requires further advances in field studies as well as detailed kinetic/product studies combined with modelling of the field data.

Chapter 2

Gas-phase chemistry of dimethyl sulfide (DMS) with hydroxyl (OH) radicals: state of knowledge

The reactions of DMS with OH radicals have been studied extensively using experimental and theoretical methods. There have been many studies aimed at understanding the kinetics and mechanism of the oxidation of DMS by OH radicals, and identification of the products and their yields. However, some aspects are not yet fully understood, and a number of reaction steps of atmospheric importance involving this species still need to be better described. Detailed information about the gas-phase oxidation of atmospheric sulfur compounds, and in particular DMS, can be found in Plane (1989), Tyndall and Ravishankara (1991), Barone et *al.* (1995), Berresheim *et al.* (1995), Wilson and Hirst (1996), Ravishankara *et al.* (1997), Urbanski and Wine (1999a), Barnes *et al.* (2006).

2.1 Kinetics of the reaction of OH radicals with DMS

The kinetics of the reaction of OH radicals with DMS have been studied by a variety of techniques. The three early studies, two flash photolysis/resonance fluorescence studies (in Ar/SF_6 buffer gases) by Atkinson *et al.* (1978) and Kurylo (1978) and a competitive rate study (in 760 Torr of air) by Cox and Sheppard (1980), agreed that the rate coefficient is approximately 9×10^{-12} cm^3 $molecule^{-1}$ s^{-1} at ambient temperature. Atkinson *et al.* (1978) and Kurylo (1978) reported a small *negative* activation energy for the reaction. In addition, Atkinson *et al.* (1978) suggested that the mechanism of the reaction was a hydrogen abstraction. These three studies seemed to indicate that the rate coefficient was well defined and unaffected by the presence of O_2. However, a later flash-photolysis/resonance fluorescence study by Wine *et al*. (1981) yielded a rate coefficient of 4.3×10^{-12} cm^3 $molecule^{-1}$ s^{-1} and a small *positive* activation energy. The authors suggested that in the previous studies, impurities in the DMS samples used may have affected the results. Also the results of Cox and Sheppard (1980) could have been affected by secondary reactions leading to the loss of DMS. MacLeod *et al.* (1984) measured the rate coefficient at 373 and

573 K (no air present) and a value of 10.4×10^{-12} cm^3 molecule^{-1} s^{-1} at room temperature was obtained from their data. They also reported a small *positive* activation energy. Atkinson *et al.* (1984) reinvestigated the reaction using a relative rate technique and reported a rate coefficient of 10.3×10^{-12} cm^3 molecule^{-1} s^{-1} at room temperature in the presence of 760 Torr of air. This was in reasonable agreement with Cox and Sheppard's value in air and the first two studies in the absence of air, but is not in agreement with the value of Wine *et al*. (1981). At this time, the situation was confused. But numerous later studies (Martin *et al.*, 1985; Wallington *et al.*, 1986c; Hynes *et al.*, 1986; Hsu *et al.*, 1987; Barnes *et al.*, 1988; Nielsen *et al.*, 1989; Abbatt *et al.*, 1992; Barone *et al.*, 1996) were carried out. The value of the activation energy was not satisfactorily resolved by these studies. Martin *et al.* (1985) and Wallington *et al.* (1986c) reported small *negative* values for activation energy, whereas Hynes *et al*. (1986) and Hsu *et al.* (1987) reported small *positive* values. Several authors have shown that rate coefficient was affected by the presence of O_2 (Wallington *et al.*, 1986c; Hynes *et al.*, 1986; Barnes *et al.*, 1988). In their comprehensive work, Hynes *et al.* (1986) found that the effective rate coefficient for the reaction of OH radicals with DMS and its deuterated analogue (DMS-d_6) was dependent on oxygen concentration, increasing as the partial pressure of oxygen was increased. The "oxygen enhancement" was the same for both DMS and its deuterated analogue, showing no kinetic isotope but a significant *negative* temperature dependence.

The experimental kinetic observations for the reaction of OH radicals with DMS and DMS-d_6 are consistent with a two-channel reaction mechanism involving both hydrogen abstraction (O_2-independent channel) and reversible adduct formation in competition with adduct reaction with O_2 (O_2-dependent channel):

$$OH + CH_3SCH_3 \rightarrow CH_3SCH_2 + H_2O \quad (2.1a)$$

$$OH + CH_3SCH_3 + M \leftrightarrow CH_3S(OH)CH_3 + M \quad (2.1b, -b)$$

$$CH_3S(OH)CH_3 + O_2 \rightarrow \text{products} \quad (2.1c)$$

$$OH + CD_3SCD_3 \rightarrow CD_3SCD_2 + HDO \quad (2.2a)$$

$$OH + CD_3SCD_3 + M \leftrightarrow CD_3S(OH)CD_3 + M \quad (2.2b, -b)$$

$$CD_3S(OH)CD_3 + O_2 \rightarrow \text{products} \quad (2.2c)$$

In the work of Hynes *et al.* (1986) the temperature dependence of the rate coefficient for the reaction of DMS with OH radicals in 760 Torr air together with temperature

dependence of the branching ratio were determined. The authors obtained the following expression for k_{obs} for one atmosphere of air:

$$k_{obs} = \{T \exp(-234/T) + 8.46 \times 10^{-10} \exp(7230/T) + 2.68 \times 10^{-10} \exp(7810/T)\}/ \{1.04 \times 10^{11} T + 88.1 \exp(7460/T)\}.$$

The branching ratio for abstraction was given by:

$$k_{2.1a}/k_{obs} = 9.6 \times 10^{-12} \exp(-234/T)/k_{obs}.$$

For many years, the two-channel mechanism has been widely accepted as the operative mechanism for the OH radical initiated oxidation of DMS and expressions for the rate coefficient and inferred branching ratio have been recommended as the best currently available for mechanistic interpretation and atmospheric modelling purposes.

A recent re-evaluation of the rate coefficient and the branching ratio has been made by Williams *et al.* (2001) using the pulsed laser photolysis/pulsed laser induced fluorescence (PLP-PLIF) technique. The effective rate coefficient for the reaction of OH radicals with DMS and DMS-d_6 was determined as a function of O_2 partial pressure at 600 Torr total pressure in N_2/O_2 mixtures; the temperature was 240 K for DMS and 240, 261 and 298 K for DMS-d_6. This new work shows that at low temperatures the currently recommended expression underestimates both the effective rate coefficient for the reaction and also the branching ratio between addition and abstraction. For example, at 261 K a branching ratio of 3.6 was obtained as opposed to the value of 2.8 based on the work of Hynes *et al.* (1986) and at 240 K the discrepancy increases between a measured value of 7.8 and a value of 3.9 using the extrapolated values from the 1986 work (the branching ratio is defined here as $(k_{obs}-k_{2.1a})/k_{2.1a}$); at 240 K the expression for k_{obs} in 1 atm of air based on the work of Hynes *et al.* (1986) predicts a value which is a factor of 2 lower then the value observed at 600 Torr. Because of the discrepancies at low temperatures, further kinetic studies are necessary to confirm the results of Williams *et al.* (2001).

The preferred value for the rate coefficient for reaction (2.1a) from the review of Atkinson *et al.* (2004) is:

$$k_{2.1a} = 1.13 \times 10^{-11} \exp(-253/T) \text{ cm}^3 \text{ molecule}^{-1} \text{ s}^{-1}$$

over the temperature range 240 - 400 K ($k_{2.1a}$ = 4.8 × 10^{-12} cm^3 $molecule^{-1}$ s^{-1} at 298 K). This value is based on the studies of Wine *et al*. (1981), Hynes *et al.* (1986), Hsu *et al.* (1987), Abbatt *et al.* (1992) and Barone *et al.* (1996). Sekušak *et al.* (2000), El-Nahas *et al.* (2005) and González-Garcia *et al.* (2007) calculated theoretically the gas-phase rate coefficient for the abstraction of hydrogen by the hydroxyl radical from dimethyl sulfide. Sekušak *et al.* (2000) found that the computed thermal rate coefficient is in good agreement with that determined experimentally within a factor of 2; the calculations of El-Nahas *et al.* (2005) gave a rate coefficient which is a factor of 4 lower than the experimentally determined values; the value of González-Garcia *et al.* (2007) at 298 K is 1.8 times slower than the recommended experimental value.

The preferred value for the rate coefficient for reaction (2.1b) from the review of Atkinson *et al.* (2004) is:

$$k_{2.1b} = 1.0 \times 10^{-39} [O_2] \exp(5820/T)/\{1 + 5.0 \times 10^{-30} [O_2] \exp(6280/T)\}$$

over the temperature range 240 - 360 K ($k_{2.1b}$= 1.7 × 10^{-12} cm^3 $molecule^{-1}$ s^{-1} at 298 K, 1 bar air). This value is based on the studies of Hynes *et al.* (1986) and Williams *et al.* (2001).

2.2 Product and mechanistic studies of the reaction of OH radicals with DMS

The reaction of OH radicals with DMS ($OH + CH_3SCH_3 \rightarrow$ Products (2.1)) can proceed *via* several possible channels:

$OH + CH_3SCH_3 \rightarrow CH_3SCH_2 + H_2O$	$\Delta H^0 = -25.5$ kcal mol^{-1}	(2.1a)
$OH + CH_3SCH_3 + M \leftrightarrow CH_3S(OH)CH_3 + M$	$\Delta H^0 = -10.7$ kcal mol^{-1}	(2.1b, -b)
$OH + CH_3SCH_3 \rightarrow CH_3 + CH_3SOH$	$\Delta H^0 = 0 \pm 3$ kcal mol^{-1}	(2.1d)
$OH + CH_3SCH_3 \rightarrow CH_3S + CH_3OH$	$\Delta H^0 = -18.8$ kcal mol^{-1}	(2.1e)

The values of ΔH^0 for the reactions are taken from the literature (Barone *et al.*, 1996 and references therein).

The reaction of OH radicals with the deuterated analogue of DMS has the same possible product channels, with approximately the same reaction enthalpies.

As outlined in Paragraph 2.1 it is well established that the reaction of OH radicals with DMS proceeds through two channels: H atom abstraction by OH radical from a methyl group and OH radical addition to the S atom (Hynes *et al.*, 1986, 1995; Barone *et al.*, 1996). Attack

of OH radicals at the CH_3 group produces water and the methyl thiomethyl radical (CH_3SCH_2) (Hynes *et al.*, 1986; Stikel *et al.*, 1993; Hynes *et al.*, 1995; Barone *et al.*, 1996; Zhao *et al.*, 1996), while addition to the S atom produces the dimethyl hydroxysulfuranyl radical, $(CH_3)_2S$-OH, an adduct, which can either dissociate back to reactants or react further with O_2 to form products (Hynes *et al.*, 1986, 1995; Barone *et al.*, 1996). The relative importance of the addition versus abstraction channels is temperature dependent (Hynes *et al.*, 1986; Williams *et al.*, 2001; Albu *et al.*, 2004b, 2006a; Williams *et al.*, 2007). In 1 atm of air the channels have approximately equal rates at ~290 K, with the addition channel being favored at lower temperatures.

The reactions discussed above, however, exclude a possible mechanism consisting of an initial addition of OH radical to DMS followed by rearrangement of the DMS-OH adduct to form the "bimolecular" products, $H_2O + CH_3SCH_2$:

$$OH + CH_3SCH_3 + M \leftrightarrow CH_3S(OH)CH_3 + M \qquad \Delta H^0 = -10.7 \text{ kcal mol}^{-1} \quad (2.1b, -b)$$

$$CH_3S(OH)CH_3 + M \rightarrow H_2O + CH_3SCH_2 + M \qquad \Delta H^0 = 0 \pm 3 \text{ kcal mol}^{-1} \quad (2.1f)$$

Such a reaction sequence would make it impossible to decouple the abstraction and addition pathways in the atmosphere. On the basis of a comparison of the measured O_2 behaviour of the rate coefficients for the reaction of OH radicals with DMS and DMS-d_6, Barone *et al.* (1996) and Ravishankara *et al.* (1997) argued that two uncoupled independent reaction channels must exist. The evidence presented by Barone *et al.* (1996) and Ravishankara *et al.* (1997) is convincing and in the following discussion two independent reaction channels, addition and abstraction, are assumed. The very recent work of Williams *et al.* (2007) demonstrates consistency of the two-channel reaction mechanism too.

2.2.1 O_2-dependent channel

The existence of the DMS-OH adduct was a controversial subject. Although kinetic experiments claimed to have "proved" the existence of this species, experimental and computational studies had yet to resolve the issue. While Hynes *et al.* (1986) estimated the S-O bond strength in OH-DMS-d_6 at ca. 13 kcal mol^{-1}, Gu and Tureček (1992) presented experimental and theoretical evidence which led them to conclude that the adduct does not exist at all except as a transition state. Subsequently, McKee (1993a) published results of a theoretical study indicating that the adduct was indeed stable and reported a binding energy of 6 kcal mol^{-1}. McKee (1993a) concluded that the description of the two-centre, three-electron bond (2c-3e), which binds the OH radical to a lone pair on DMS, requires a higher

level of theory for binding, which is why the earlier study failed to find a complex. Tureček (1994) published another theoretical study which again concluded that the adduct is not bound. Two other kinetic studies (Hynes *et al.*, 1995; Barone *et al.*, 1996) confirmed the existence of the OH-DMS-d_6 adduct at low temperature. Hynes *et al.* (1995) reported an adduct bond strength of 13.0 kcal mol^{-1} (second law method) and 10.1 kcal mol^{-1} (third law method), while Barone *et al.* (1996) reported a value of 10.7 kcal mol^{-1}. Recent computational studies: Tureček (2000), Wang and Zhang (2001) and McKee (2003), reported values of 9.6, 7.41 and 8.7 kcal mol^{-1}, respectively, for the S-OH binding enthalpy for DMS. In the work of Tureček (2000), the structure and energetics of the DMS-OH adduct were revisited and were found to be similar to those of the most stable adduct structure (with the 2c-3e bonding) identified in the work of Wang and Zhang (2001). The recent paper on this subject by Uchimaru *et al.* (2005) reports for 298 K a value of 9.0 kcal mol^{-1} for the dissociation enthalpy of the S-O bond in the DMS-OH adduct. In the study of Gross *et al.* (2004) the geometries of the DMS-OH adduct have been investigated. In the very recent work of Williams *et al.* (2007) the structures of the DMS-OH adduct and its deuterated isotopomer have been studied.

In the atmosphere, the DMS-OH adduct has three subsequent reaction pathways: re-dissociation back to DMS + OH, decomposition to $CH_3SOH + CH_3$ and reaction with O_2. The energy barrier of 7.34 kcal mol^{-1} and the endothermicity of the reaction to form $CH_3SOH + CH_3$, however, hinder the dissociation of the OH-DMS complex to $CH_3SOH + CH_3$. Thus, the $CH_3SOH + CH_3$ product channel can be excluded from the reaction mechanism of DMS with OH radicals at room temperature. Nielsen *et al.* (1989) have observed the formation of CH_3 radicals following the reaction of OH radicals with DMS without O_2 and suggested that the formation takes place through reaction 2.1d. However, the formation of sulfenic acid (CH_3SOH) has never been observed in any oxidation study of DMS:

$$OH + CH_3SCH_3 \rightarrow CH_3S(OH)CH_3 \rightarrow CH_3SOH + CH_3 \qquad (2.1d)$$

They also determined a rate coefficient for reaction (2.1d) of $(9.1 \pm 1.0) \times 10^{-14}$ cm^3 $molecule^{-1}$ s^{-1} and concluded that this reaction is an insignificant pathway for the fate of the DMS-OH adduct in the absence of O_2, compared to the H atom abstraction pathway and provided additional support for the conclusion by Hynes *et al.* (1986) that the addition channel is only important in the presence of O_2.

Reaction of DMS-OH adduct with O_2 is proposed to be responsible for the formation of DMSO (dimethyl sulfoxide) and $DMSO_2$ (dimethyl sulfone) in the DMS + OH reaction system in the presence of O_2 (Barnes *et al.*, 1988; Hynes *et al.*, 1993; Barnes *et al.*, 1996;

Barone *et al.*, 1996; Patroescu, 1996; Sørensen *et al.*, 1996; Patroescu *et al.*, 1999; Arsene *et al.*, 1999; Patroescu-Klotz, 1999; Arsene *et al.*, 2001; Arsene, 2002).

Experimental investigations of the reactions $CH_3S(OH)CH_3 + O_2 \rightarrow$ products (2.1c) and $CD_3S(OH)CD_3 + O_2 \rightarrow$ products (2.2c) have been performed. Hynes *et al.* (1986, 1995) have studied the reaction (2.2c). Hynes *et al.* (1986) estimated the rate coefficient to be $(4.2 \pm 2.2) \times 10^{-12}$ cm^3 molecule^{-1} s^{-1} at a pressure of 700 Torr $N_2 + O_2$ and a temperature of 261 K. Hynes *et al.* (1995) estimated the rate coefficient to be $(0.8 \pm 0.3) \times 10^{-12}$ cm^3 molecule^{-1} s^{-1} independent of pressure (100 - 700 Torr of N_2) and temperature (250 - 300 K). Barone *et al.* (1996) studied both (2.1c) and (2.2c) reactions and they estimated the rate coefficient to be $(1.00 \pm 0.33) \times 10^{-12}$ cm^3 molecule^{-1} s^{-1} independent of pressure in the range 30 - 200 Torr of N_2 and temperature in the range of 222 - 258 K, which is in excellent agreement with the value reported by Hynes *et al.* (1995). A theoretical study of the reaction between $CH_3S(OH)CH_3$ and O_2 has been performed (Gross *et al.*, 2004). The very new study of Williams *et al.* (2007) investigated both (2.1c) and (2.2c) reactions; the average value for the rate coefficient of $(0.63 \pm 0.12) \times 10^{-12}$ cm^3 molecule^{-1} s^{-1} determined in this study is independent of pressure (over the range 200 - 600 Torr) and shows no isotopic dependence (in the region of ~ 240 K).

Thermodynamically allowed product channels for the reaction of DMS-OH adduct with O_2 are:

$$CH_3S(OH)CH_3 + O_2 \rightarrow CH_3S(O)CH_3 + HO_2 \quad (2.1c\text{-}1)$$

$$CH_3S(OH)CH_3 + O_2 + M \rightarrow CH_3S(OH)(OO)CH_3 + M \quad (2.1c\text{-}2)$$

$$CH_3S(OH)CH_3 + O_2 \rightarrow CH_3SOH + CH_3O_2 \quad (2.1c\text{-}3)$$

$$CH_3S(OH)CH_3 + O_2 \rightarrow CH_3S(O)_2CH_3 + OH \quad (2.1c\text{-}4)$$

$$CH_3S(OH)CH_3 + O_2 \rightarrow CH_3S(OH)(OO) + CH_3 \quad (2.1c\text{-}5)$$

Hynes *et al.* (1986, 1995) could not observe channel (2.1c-4) since they monitored OH radical loss in a pseudo first-order excess of DMS. However, they specified that if channel (2.1c-4) is occurring to any significant extent, their measured rates would underestimate the effective rate of DMS removal. This could account for the discrepancy between the values of the rate constants obtained from direct and relative kinetic studies for the reaction of OH radicals with DMS.

Gross *et al.* (2004) estimated the rate coefficients at 298 K for reactions (2.1c-1) and (2.1c-2) to be 1.74×10^{-12} cm^3 molecule^{-1} s^{-1} and 8.63×10^{-34} cm^3 molecule^{-1} s^{-1}, respectively.

The studies by Hynes *et al.* (1986), Hynes *et al.* (1995) and Barone *et al.* (1996) did not investigate the branching ratio of reaction (2.1c), however, experimental mechanistic studies (Hynes *et al.*, 1993; Turnipseed *et al.*, 1996; Arsene *et al.*, 1999) have reported estimates for the branching ratios of reaction (2.1c). In the laser flash photolysis/pulsed laser induced fluorescence study of Hynes *et al.* (1993) and in the pulsed laser photolysis/pulsed laser induced fluorescence study of Turnipseed *et al.* (1996) similar branching ratios of ~0.5 (at 267 K and 100 Torr of O_2) and 0.50 $\pm$ 0.15 (at 234 and 258 K and 100 Torr, either N_2 or He), respectively, have been reported for the production of DMSO based on the conversion of the HO_2 produced to OH by reaction with NO. The product study of Arsene *et al.* (1999) supports that the major product channel of reaction (2.1c) under NO_x-free conditions is channel (2.1c-1). The reason for the discrepancy between these studies is not completely clear, but it could be related to the reaction conditions employed, i.e., presence or absence of NO in the reaction system. Gross *et al.* (2004) concluded from their theoretical study of the reaction between $CH_3S(OH)CH_3$ and O_2 that the dominant channel for the reaction is the formation of DMSO + HO_2. The very recent work of Williams *et al.* (2007) indicates that the channel (2.1c-4) is insignificant.

2.2.2 O_2-independent channel

There is considerable evidence for the existence of an H atom abstraction channel in the reaction of OH radicals with DMS. Stickel *et al.* (1993) directly measured the yield of HDO from the reaction of OD radicals with DMS to be $\Phi_{2.1a}$ = 0.84 $\pm$ 0.15 at 298 K. In the study of Turnipseed *et al.* (1996) the yield of channel 2.1a was determined indirectly by converting the methyl thiomethyl radical (MTM: CH_3SCH_2) to CH_3S *via* the addition of high concentrations of O_2 and sufficient NO (see reaction sequence 2.3 - 2.5). This method gave an average value for $\Phi_{2.1a}$ of 0.86 $\pm$ 0.26 in excellent agreement with the results of Stickel *et al.* (1993). End product studies also support that H atom abstraction is a major pathway for reaction (2.1) at atmospheric pressure (Hatakeyama *et al.*, 1982; Grosjean and Lewis, 1982; Niki *et al.*, 1983a, b; Hatakeyama and Akimoto, 1983; Grosjean, 1984; Hatakeyama *et al.*, 1985; Barnes *et al.*, 1988; Yin *et al.*, 1990b; Patroescu, 1996; Sørensen *et al.*, 1996; Patroescu *et al.*, 1999; Patroescu-Klotz, 1999; Arsene *et al.*, 2001; Arsene, 2002; Librando *et al.*, 2004). Theoretical studies have also been performed on the methyl thiomethyl radical (Baker and Dyke, 1993; McKee, 1993a; Kuhns *et al.*, 1994; Tureček, 1994; Mousavipour *et al.*, 2002).

The methyl thiomethyl radical has never been directly observed, which indicates that it may be very reactive. It will react mainly with atmospheric O_2, to produce the methyl thiyl peroxy radical (MTP: CH_3SCH_2OO):

$$CH_3SCH_2 + O_2 + M \rightarrow CH_3SCH_2OO + M \quad (2.3)$$

The reaction has been studied by Wallington *et al.* (1993a) and Butkovskaya and Le Bras (1994). The preferred value of rate coefficient for this reaction is 5.7×10^{-12} cm^3 molecule^{-1} s^{-1} at 298 K and 1 bar (Atkinson *et al.*, 2004). There is also a theoretical study of reaction (2.3) by Resende and De Almeida (1999a), in which they established a bimolecular mechanism and a transition state for the reaction; the calculated *negative* activation energy of – 3.31 kcal mol^{-1}, but the high-spin contamination of the transition state prohibited the calculation of a rate coefficient for the reaction.

The methyl thiyl peroxy radical, CH_3SCH_2OO, will react with trace species in the atmosphere, such as NO, NO_2, HO_2 or other peroxy radicals (RO_2), to give a variety of products.

The following mechanism, proposed by Niki *et al.* (1983a) for the atmospheric oxidation of the methyl thiomethyl radical in the presence of NO (based on an analogy with alkyl radical oxidation chemistry), has been validated by subsequent laboratory investigations (Wallington *et al.*, 1993; Butkovskaya and Le Bras, 1994; Turnipseed *et al.*, 1996; Urbanski *et al.*, 1997):

$$CH_3SCH_2 + O_2 + M \rightarrow CH_3SCH_2OO + M \quad (2.3)$$
$$CH_3SCH_2OO + NO \rightarrow CH_3SCH_2O + NO_2 \quad (2.4)$$
$$CH_3SCH_2O + M \rightarrow CH_3S + CH_2O + M \quad (2.5)$$

Wallington *et al.* (1993) observed the NO_2 production from reaction (2.4) and measured an NO_2 yield of 0.81 ± 0.15 as well as a room temperature rate coefficient of $k_{2.4}$ = (1.9 ± 0.6) × 10^{-11} cm^3 molecule^{-1} s^{-1} in 750 Torr SF_6. Turnipseed *et al.* (1996) have provided evidence that CH_3S is the dominant sulfur-containing product generated by the sequence of reactions (2.3) - (2.5); a CH_3S yield of 0.81 ± 0.15 was estimated along with a room temperature rate coefficient for reaction (2.4) of (8.0 ± 3.1) × 10^{-12} cm^3 molecule^{-1} s^{-1} in 22 Torr of O_2. In the work of Urbanski *et al.* (1997) the rate coefficient for reaction (2.4) was found to decrease slightly with increasing temperature and they reported the Arrhenius expression: $k_{2.4}$ = 4.9 × 10^{-12} exp(263/T) cm^3 molecule^{-1} s^{-1} for the temperature range 261 - 400 K; a yield of 1.04 ± 0.13 was determined for CH_2O, and the lifetime of CH_3SCH_2O was found to be less than 30 µs at 261 K and 10 Torr total pressure. In the study of Turnipseed *et al.* (1996) modelled fits of the results suggested that the lifetime of CH_3SCH_2O is less than 10 µs at 298 K. CH_3SCH_2O has been calculated to be thermally unstable at 298 K (McKee, 1994) and should

dissociate to CH_3S and CH_2O. However, it may be that in the atmosphere reaction of CH_3SCH_2O radicals with O_2 can compete with the thermal decomposition. The likely product of the reaction of CH_3SCH_2O with O_2 is CH_3SCHO (methyl thiol formate, MTF):

$$CH_3SCH_2O + O_2 \rightarrow CH_3SCHO + HO_2 \quad (2.6)$$

This product has been observed in several studies of the photooxidation of DMS under conditions of low NO_x (Barnes *et al.*, 1996; Arsene *et al.*, 1999; Patroescu *et al.*, 1999), but in these studies it is not clear whether the MTF is formed *via* reaction (2.6) or by other routes, i.e. *via* reactions such as $CH_3SCH_2OO + HO_2$, CH_3SCH_2OO or other alkyl peroxy radicals.

No direct study of the $CH_3SCH_2OO + HO_2$ reaction has been performed, but indirect experimental evidence for the occurrence of this reaction has been reported. Butkovskaya and Le Bras (1994) detected CH_3SCH_2OOH *via* mass spectrometry in flow-tube experiments performed on a Cl/Cl_2 + DMS + O_2 system. Recently Butkovskaya and Barnes (2003) reported tentative FTIR detection of CH_3SCH_2OOH in studies on the UV photolysis of bis(methyltio)methane ($CH_3SCH_2SCH_3$) in air in a photoreactor. By analogy with other HO_2 + RO_2 reactions, the resulting product is expected to be a stable hydroperoxide species, CH_3SCH_2OOH (Lightfoot *et al.*, 1992; Wallington *et al.*, 1992):

$$CH_3SCH_2OO + HO_2 \rightarrow CH_3SCH_2OOH + O_2 \quad (2.7)$$

Depending on the efficiency of the CH_3SCH_2OO reaction with HO_2, the CH_3SCH_2OO self- and cross-reaction with other alkyl peroxy radicals (RO_2, represented by CH_3SO_2) could be of significance under some atmospheric conditions. The CH_3SCH_2OO self-reaction is fast, the rate coefficient being approximately 1×10^{-11} cm^3 $molecule^{-1}$ s^{-1} at 298 K (Atkinson *et al.*, 2004 and references therein) and could proceed *via* the following routes:

$$CH_3SCH_2O_2 + CH_3SCH_2O_2 \rightarrow 2CH_3SCH_2O + O_2 \quad (2.8)$$

$$\rightarrow CH_3SCHO + CH_3SCH_2OH + O_2 \quad (2.9)$$

In the self-reaction the CH_3SCH_2OO radical is converted to CH_2O with a yield of 0.97 ± 0.08 at 298 K (Urbanski *et al.*, 1997), indicating that CH_3S is also produced with unit yield. It was concluded that the reaction leads to formation of CH_3SCH_2O radicals *via* pathway (2.8), with the CH_3SCH_2O radical rapidly decomposing to form CH_2O and CH_3S.

By analogy with other alkyl peroxy radicals, NO_2 may be expected to add to CH_3SCH_2OO and establish the equilibrium:

$$CH_3SCH_2OO + NO_2 + M \leftrightarrow CH_3SCH_2OONO_2 + M \qquad (2.10)$$

Rate coefficients of $(9.2 \pm 0.9) \times 10^{-12}$ cm^3 $molecule^{-1}$ s^{-1} and $(7.1 \pm 0.9) \times 10^{-12}$ cm^3 $molecule^{-1}$ s^{-1} at 296 K in 1000 and 300 mbar SF_6 diluent, respectively, have been measured for the reaction of CH_3SCH_2OO with NO_2 (Nielsen *et al.*, 1995). In two product studies of the NO_3 radical initiated oxidation of DMS in air (Jensen *et al.*, 1991, 1992), a species observed in the FTIR spectrum was tentatively identified as $CH_3SCH_2OONO_2$. However, Mayer-Figge (1997) observed similar bands in studies on the photolysis of CH_3SNO in O_2 where this compound cannot be formed, suggesting that the assignment might be in error.

In a theoretical study, Resende and De Almeida (1999b) have examined the thermodynamic properties of nine possible reactions for the atmospheric fate of the CH_3SCH_2OO radical. They found that the reactions of the CH_3SCH_2OO radical with NO, NO_2, HO_2, CH_3S, CH_3SO, CH_3SO_2 and O are all exothermic and have negative reaction Gibbs free energies. For the reaction with NO_2, the equilibrium in the atmosphere will be displaced towards the reactants; the present evidence would suggest that the peroxynitrate is probably not important in the atmosphere. The reaction with CH_3O_2 radical is endothermic by a small quantity and it will be not important in the atmosphere. Reaction with O_2 leading to formation of CH_3SCH_2O and O_3 is thermodynamically unfavourable, having a positive reaction enthalpy; therefore, it will not occur in the atmosphere.

Chemistry of CH_3S and associated CH_3SO_x (x = 1-3) species

While the reactions initiating the atmospheric oxidation of DMS are reasonably well understood, the ultimate fate of the sulfur-containing species produced by these reactions is uncertain. On the basis of the laboratory kinetic and end product analysis studies, it has been postulated that the key intermediates of the H atom abstraction initited oxidation pathway of DMS are CH_3SO_x (x = 0, 1, 2, 3) radicals (Turnipseed and Ravishankara, 1993; Ravishankara *et al.*, 1997).

The methyl thiyl radical (CH_3S) is formed from reactions of CH_3SCH_2 (methyl thiomethyl radical) as disscused above. CH_3S is one of the key intermediates of the OH radical initiated oxidation of DMS (Yin *et al.*, 1990a, b) and is believed to be the principal source of the products SO_2, MSA (methane sulfonic acid) and H_2SO_4. Oxidation of CH_3S radicals under

atmospheric conditions may involve numerous reactions whose relative importance will vary with ambient conditions such as temperature and the concentrations of reactive species. Kinetic information for CH_3S reactions of atmospheric importance are presented in Table 2.1.

Reaction of CH_3S with O_2 is the most significant oxidation pathway for this radical in the atmosphere; kinetic information for the reaction of CH_3S with O_2 can be found in literature (Balla *et al.*, 1986; Black and Jusinski, 1986; Tyndall and Ravishankara, 1989a; Turnipseed *et al.*, 1992, 1993; Atkinson *et al.*, 2004). The reaction of CH_3S with O_2 forms a weakly bound adduct CH_3SOO (methyl thioperoxyl radical) with a bond strength of ~11 kcal mol^{-1} (Turnipseed *et al.*, 1992). The adduct formed has a peroxy-structure, CH_3S-O-O, and not a sulfone-structure, $CH_3(O=)S(=O)$, where both oxygen atoms are bound to the sulfur atom, otherwise it could not rapidly decomposes back to CH_3S and O_2. Even though it is weakly bound, the large abundance of O_2 makes the CH_3SOO adduct a significant atmospheric species. Under atmospheric conditions equilibrium between CH_3S and CH_3SOO is established rapidly and between 20 - 80% of CH_3S is tied up as CH_3SOO. The CH_3S/ CH_3SOO yield ratio is strongly temperature dependent. For example, at 298 K and at sea level, approximately one-third of CH_3S would be present as the CH_3SOO adduct and the equilibration would be established rapidly ($\leq$ 3 μs); at 273 K, about 75% of CH_3S would be in the adduct form. Formation of the CH_3SOO adduct suggests that other weakly bound adducts such as $CH_3SO(OO)$, $CH_3SO_2(OO)$ could exist (Barone *et al.*, 1995). No other reaction channel for $CH_3S + O_2$ than adduct formation has been positively identified. However, Barnes *et al.* (1994b) have observed OCS (carbonyl sulfide) as a minor product of the OH radical initiated oxidation of DMS and have suggested that CH_2S, generated by $CH_3S + O_2 \rightarrow CH_2S + HO_2$, is the likely OCS precursor. The rapid establishment of equilibrium between CH_3S and O_2 has complicated attempts to establish the rate coefficient for other $CH_3S + O_2$ reactions; extrapolation of the equilibrium data to 298 K, leads to an equilibrium-corrected upper limit of 6×10^{-18} cm^3 $molecule^{-1}$ s^{-1} at 298 K on the rate coefficient for the reaction of CH_3S with O_2 leading to products other than CH_3SOO (Turnipseed *et al.*, 1993).

Rate coefficients for the reaction of CH_3S with other trace gas species such as O_3 (Tyndall and Ravishankara, 1989b; Dominé *et al.*, 1992; Turnipseed *et al.*, 1993; Martinez *et al.*, 2000; Atkinson *et al.*, 2004), NO (Balla *et al.*, 1986; Turnipseed *et al.*, 1993; Atkinson *et al.*, 2004) and NO_2 (Balla *et al.*, 1986; Tyndall and Ravishankara, 1989a; Dominé *et al.*, 1990; Turnipseed *et al.*, 1993; Martinez *et al.*, 1999; Chang *et al.*, 2000; Atkinson *et al.*, 2004) are reasonably well established.

Table 2.1: Kinetic information for CH_3S reactions of atmospheric importance.

Reaction	k(298 K) (cm^3 $molecule^{-1}$ s^{-1})	k(T) = A exp(-E/RT)	References and notes
$CH_3S+O_2+M\leftrightarrow$ CH_3SOO+M[a]		1.2×10^{-16} exp(1580/T)[b]	Turnipseed *et al.* (1992)[a] Atkinson *et al.* (2004)[b], 210-250 K
CH_3S+O_2[c]$\rightarrow$ Products	$< 6\times10^{-18}$		Turnipseed *et al.* (1993)[d]
	$< 2.5\times10^{-18}$		Tyndall and Ravishankara (1989a)
	$< 1\times10^{-16}$		Black and Jusinski (1986)
	$\leq 2\times10^{-17}$		Balla *et al.* (1986)
$CH_3S+O_3\rightarrow$ Products	4.9×10^{-12}	1.15×10^{-12} exp(430/T)	Atkinson *et al.* (2004)[e], 250-390 K
	$(4.6\pm0.6)\times10^{-12}$	$(1.02\pm0.30)\times10^{-12}$ exp[(432±77)/T]	Martinez *et al.* (2000)[f]
	$(5.2\pm0.5)\times10^{-12}$	$(1.98\pm0.38)\times10^{-12}$ exp[(290±40)/T]	Turnipseed *et al.* (1993)[g]
	$(5.7\pm1.4)\times10^{-12}$		Dominé *et al.* (1992), 300 K
	$(4.1\pm2.0)\times10^{-12}$		Tyndall and Ravishankara (1989b)[h]
$CH_3S+NO+M\rightarrow$ products		4.0×10^{-11}[e]	Atkinson *et al.* (2004)[e], 290-450 K Turnipseed *et al.* (1993) Balla *et al.* (1986)
$CH_3S+NO_2\rightarrow$ products	6.0×10^{-11}	3×10^{-11} exp(210/T)	Atkinson *et al.* (2004)[e], 240-350 K
	$(10.1\pm1.5)\times10^{-11}$	$(4.3\pm1.3)\times10^{-11}$ exp[(240±100)/T]	Chang *et al.* (2000)[i]
	$(6.6\pm1.0)\times10^{-11}$	$(3.8\pm0.3)\times10^{-11}$ exp[(160±22)/T]	Martinez *et al.* (1999)[j]
	$(6.28\pm0.28)\times10^{-11}$	$(2.06\pm0.44)\times10^{-11}$ exp[(320±40/T)]	Turnipseed *et al.* (1993)[k]
	$(5.1\pm0.9)\times10^{-11}$		Dominé *et al.* (1990)[l], 1 Torr He
	$(6.1\pm0.9)\times10^{-11}$		Tyndall and Ravishankara (1989a)[m]
	$(10.6\pm0.6)\times10^{-11}$	$(8.3\pm1.4)\times10^{-11}$ exp[(160±120)/T]	Balla *et al.* (1986), 295-511 K

[a]Forward and reverse rate constants have been measured over T = 216-258 K and P = 80 Torr He; [b]Preferred values for forward rate constants; [c]Rate constants are for products other than CH_3SOO; [d]Corrected for $CH_3S+O_2\leftrightarrow CH_3SOO$; [e]Preferred values; [f]Study over T = 259-381 K and P = 25-300 Torr He; [g]Study over T = 295-359 K and P = 75-325 Torr He; [h]Study at P = 38-300 Torr N_2 or O_2; [i]Study over T = 222-420 K and P = 55-202 Torr He; [j]Study over T = 263-381 K and P = 30-300 Torr He; [k]Study over T = 242-350 K and P = 25-200 Torr He or N_2; [l]Φ(NO) = 1.07±0.15; [m]Study at P = 40-140 Torr N_2 or O_2, Φ(NO) = 0.8±0.2.

On the basis of the available kinetic data, reaction with O_2 and O_3 will determine the fate of CH_3S in the atmosphere. Although the kinetics of the reaction of CH_3S with O_3 are well established, the mechanism is still very speculative (Barnes *et al.*, 2006 and references therein).

Reaction of the methyl thiyl radical with NO_2 will be of atmospheric importance only under conditions of elevated NO_x concentrations, for example, in coastal areas or in air masses influenced by long range transport from the continents. The rate coefficient for the reaction $CH_3S + NO_2$ is independent of pressure, exhibits a slightly *negative* activation energy and proceeds primarily *via* O atom transfer. While the dominant reaction channel is generation of the methyl sulfinyl radical (CH_3SO) and NO (Tyndall and Ravishankara, 1989a; Dominé *et al.*, 1990):

$$CH_3S + NO_2 \rightarrow CH_3SO + NO \qquad (2.11)$$

another possible product, methyl thionitrate (CH_3SNO_2), has been observed as a minor product in some chamber studies, although the source could not be definitively identified (Barnes *et al.*, 1987b; Jensen *et al.*, 1991).

In the case of $CH_3S + NO$, the product has been identified as methyl thionitrite (CH_3SNO) (Hatakeyama and Akimoto, 1983; Niki *et al.*, 1983b; Balla and Heicklen, 1984; Barnes *et al.*, 1987b):

$$CH_3S + NO + M \rightarrow CH_3SNO + M \qquad (2.12)$$

No direct studies of CH_3S reactions with HO_2 or organic peroxy radicals have been reported. Indirect experimental evidence suggests that the methyl thiyl radical reacts with both HO_2 and CH_3O_2 *via* O atom transfer (Hynes and Wine, 1987; Barnes *et al.*, 1994a).

The methyl sulfinyl radical (CH_3SO)

Studies on the reactions of CH_3SO radicals with O_2 (Tyndall and Ravishankara, 1989a), O_3 (Tyndall and Ravishankara, 1989b; Dominé *et al.*, 1992; Borissenko *et al.*, 2003; Atkinson *et al.*, 2004) and NO_2 (Mellouki *et al.*, 1988; Tyndall and Ravishankara, 1989a; Dominé *et al.*, 1990; Kukui *et al.*, 2000; Borissenko *et al.*, 2003; Atkinson *et al.*, 2004) have been carried out. The kinetic informations on these reactions are listed in Table 2.2.

Table 2.2: Kinetic information for CH_3SO_x (x = 1-3) reactions of atmospheric importance.

Reaction	*k*(298 K) (cm^3 $molecule^{-1}$ s^{-1})	References and notes
$CH_3SO+O_2+M\rightarrow$products	$< 5\times10^{-13}$	Tyndall and Ravishankara (1989a), 300 Torr N_2
$CH_3SO+O_3\rightarrow$products	6×10^{-13}	Atkinson *et al.* (2004)[a]
	$(3.2\pm0.9)\times10^{-13}$	Borissenko *et al.* (2003)[b]
	$(6\pm3)\times10^{-13}$	Dominé *et al.* (1992)[c], 300 K, 1 Torr He
	1×10^{-12}	Tyndall and Ravishankara (1989b)
$CH_3SO+NO_2\rightarrow$products	1.2×10^{-11}	Atkinson *et al.* (2004)[a]
		Borissenko *et al.* (2003)[d]
	$(1.5\pm0.4)\times10^{-11}$	Kukui *et al.* (2000)[e]
	$(1.2\pm0.25)\times10^{-11}$	Dominé *et al.* (1990), 1 Torr He
	$(0.8\pm0.5)\times10^{-11}$	Tyndall and Ravishankara (1989a)
	$(3.0\pm2.0)\times10^{-11}$	Mellouki *et al.* (1988)
$CH_3SOO+O_2\rightarrow$products	$< 6\times10^{-18}$	Turnipseed *et al.* (1993)[f]
	$< 4\times10^{-17}$	Turnipseed *et al.* (1992), 258 K
$CH_3SOO+O_3\rightarrow$products	$< 8\times10^{-13}$	Turnipseed *et al.* (1993), 227 K
$CH_3SOO+NO\rightarrow$products	$(1.1\pm0.4)\times10^{-11}$	Turnipseed *et al.* (1993), 227-255 K
$CH_3SOO+NO_2\rightarrow$products	$(2.2\pm0.6)\times10^{-11}$	Turnipseed *et al.* (1993), 227-246 K
$CH_3SO_2+M\rightarrow CH_3+SO_2$	$1\ s^{-1}$	Borissenko *et al.* (2003)[g]
	$(0.4\pm0.2)\ s^{-1}$	Butkovskaya and Barnes (2001, 2002)[h]
	$< 100\ s^{-1}$	Kukui *et al.* (2000), 300 K, 1-612 Torr He
	$510\pm150\ s^{-1}$	Ray *et al.* (1996), 1 Torr He
	$\leq 10\ s^{-1}$	Mellouki *et al.* (1988)
$CH_3SO_2+O_2+M\rightarrow$products	2.6×10^{-18}	Yin *et al.* (1990a)[i]
$CH_3SO_2+O_3\rightarrow$products	5×10^{-15}	Yin *et al.* (1990a), estimate
$CH_3SO_2+NO_2\rightarrow$products	$\leq 1\times10^{-15}$	Atkinson *et al.* (2004)[a], 300 K
		Kukui *et al.* (2000)
	$(2.2\pm1.1)\times10^{-11}$	Ray *et al.* (1996), 1 Torr He
$CH_3SO_2OO+NO\rightarrow$ $CH_3SO_3+NO_2$	1×10^{-11}	Yin *et al.* (1990a), estimate
$CH_3SO_2OO+NO_2\rightarrow$ $CH_3SO_2OONO_2$	1×10^{-12}	Yin *et al.* (1990a), estimate
$CH_3SO_3+HO_2\rightarrow CH_3SO_3H+O_2$	5×10^{-11}	Yin *et al.* (1990a), estimate

[a]Preferred values; [b]Study at T = 300 K and P = 140-660 Torr N_2, $\Phi(SO_2)$ = 1.0±0.12 at 660 Torr N_2; [c]$\Phi(CH_3)$ = 0.13±0.06; [d]Study at T = 300 K and P = 140-660 Torr N_2, $\Phi(SO_2)$ = 0.40±0.12 at 100 Torr N_2 falling to 0.25±0.05 at 664 Torr N_2; [e]Study at T = 300 K and P = 1-612 Torr He, $\Phi(SO_2)$ = 1 at 1 Torr of He falling to 0.18±0.03 at 612 Torr of He; [f]Study over T = 295-359 K and P = 20-200 Torr, value corrected for $CH_3S+O_2\leftrightarrow CH_3SOO$ equilibrium data (Turnipseed et al., 1992) extrapolated to 298 K; [g]Estimate at T = 300 K from an analysis of a DMDS/NO_2 system, $\Phi(CH_3)$ = 0.13±0.06; [h]Chamber study of the 254 nm photolysis of $CH_3SO_2SCH_3$ with simulation of the products; [i]No measurement, estimate, not corrected for $CH_3SO_2+O_2+M\leftrightarrow CH_3SO_2OO+M$ equilibrium.

CH_3SO may react with O_2 to form an adduct (Barnes *et al.*, 1987b; Jensen *et al.*, 1991, 1992). End product studies of sulfide oxidation have detected a species believed to be methyl sulfinyl peroxynitrate ($CH_3S(O)OONO_2$) (Barnes *et al.*, 1987b; Jensen *et al.*, 1991, 1992). The apparent observation of $CH_3S(O)OONO_2$ implies that O_2 can add to CH_3SO to form $CH_3S(O)OO$. However, Van Dingen *et al.* (1994) suggest that the species tentatively identified as $CH_3S(O)OONO_2$, could also be methyl sulfonyl peroxynitrate ($CH_3S(O)_2OONO_2$). The $CH_3S(O)_2OONO_2$ intermediate proposed by Van Dingen *et al.* (1994) and Sørensen *et al.* (1996) would result from the reactions of CH_3SO_2, not CH_3SO. Mayer-Figge (1997) observed a product in a study of the photolysis of CH_3SNO at low temperature which is assigned to $CH_3S(O)OONO_2$. In a qualitative study on the thermal stability of the species it was found that the thermal decomposition of the species was more than a factor of 3 faster than that of CH_3OONO_2. Thus, if the species observed in the various systems is indeed $CH_3S(O)OONO_2$, the measurements of Mayer-Figge (1997) imply negligible importance for the species under atmospheric conditions.

The reaction of CH_3SO with NO_2 is known to produce NO with a yield of 0.80 ± 0.20 (Tyndall and Ravishankara, 1989a), and studies of the $CH_3S + NO_2$ system suggest that CH_3SO_2 is produced in high yield, $\geq 80\%$ (Mellouki *et al.*, 1988; Ray *et al.*, 1996). In two recent studies (Kukui *et al.*, 2000; Borissenko *et al.*, 2003) the reaction of CH_3SO with NO_2 has been found to form CH_3 and SO_2; the yield of SO_2 was found to be pressure dependent varying from (0.33 ± 0.05) at 13 Torr to (0.18 ± 0.03) at 612 Torr of He (Kukui *et al.*, 2000) and from (0.4 ± 0.12) at 100 Torr to (0.25 ± 0.05) at 664 Torr of N_2 (Borissenko *et al.*, 2003). On the basis of *ab initio* calculations these experimental results have been interpreted as involving the formation of a chemically activated CH_3SO_2* radical, which may undergo either prompt decomposition to CH_3 and SO_2 or collisional stabilization followed by thermal decomposition:

$$CH_3SO + NO_2 \rightarrow CH_3S(O)ONO^* \rightarrow CH_3SO_2^* + NO \quad (2.13)$$

$$CH_3SO_2^* \rightarrow CH_3 + SO_2 \quad (2.14)$$

$$CH_3SO_2^* + M \rightarrow CH_3SO_2 + M \quad (2.15)$$

The methyl thiyl peroxyl radical (CH_3SOO)

As discussed in the section of CH_3S radical, under atmospheric conditions 20 - 80% of CH_3S is partitioned into the CH_3SOO adduct, with the partitioning being a strong function of temperature (Turnipseed *et al.*, 1993). Thus, reactions of the CH_3SOO adduct are important in determining the ultimate fate of CH_3S. Kinetic data of CH_3SOO are presented in Table 2.2.

While CH_3SOO is apparently unreactive towards O_2 and O_3, this species does react with both NO and NO_2.

Similar to other alkyl peroxyl radicals, reaction of CH_3SOO with NO_2 is expected to occur *via* a termolecular combination pathway, to form a thio peroxynitrate:

$$CH_3SOO + NO_2 + M \rightarrow CH_3SOONO_2 + M \qquad (2.16)$$

The $CH_3SOO + NO_2$ rate coefficient was found to be independent of pressure (65 - 360 Torr), suggesting, either that the proposed addition channel to form CH_3SOONO_2 has reached its high pressure limit at 65 Torr or that the reaction proceeds *via* a bimolecular reaction channel, probably producing $CH_3SO + NO_3$ (Turnipseed *et al.*, 1993). In a search for the existence of methyl thiomethyl peroxynitrate (CH_3SOONO_2) and other sulfur peroxynitrates Mayer-Figge (1997) examined the photolysis of CH_3SNO at low temperatures. Using *in situ* FTIR spectroscopy for the analysis of products, the photolysis of CH_3SNO by 258 K in 1013 mbar of O_2 was invstigated in hope that following reactions would initially dominate:

$$CH_3SNO + h\nu \rightarrow CH_3S + NO \qquad (2.17)$$

$$CH_3S + O_2 + M \leftrightarrow CH_3SOO + M \qquad (2.18)$$

$$CH_3SOO + NO_2 + M \leftrightarrow CH_3SOONO_2 + M \qquad (2.16)$$

In the system SO_2 and methyl sulfonyl peroxynitrate ($CH_3S(O)_2OONO_2$) were positively identified and evidence was found for the presence of a further peroxynitrate compound. However, the IR evidence was more in keeping with the formation of methyl sulfinyl peroxynitrate ($CH_3S(O)OONO_2$) rather than CH_3SOONO_2. The conclusion from the study was that either CH_3SOONO_2 is much less thermally stable than, for example, CH_3OONO_2 or the competing reaction of CH_3S with NO_2 was dominantig over $CH_3S + O_2$, despite 1 atm of O_2 in the reaction system.

The rate coefficient for the reaction of CH_3SOO with NO was found to be independent of temperature over the small temperature range 228 - 258 K (Turnipseed *et al.*, 1993). The most likely channel for the reaction is:

$$CH_3SOO + NO \rightarrow CH_3SO + NO_2 \qquad (2.19)$$

Despite the low upper limits placed on the rate coefficient for the reaction of CH_3SOO with O_2, this pathway may be the dominant fate of the CH_3SOO adduct in the atmosphere.

It is also possible that thermal izomerization of CH_3SOO to CH_3SO_2 (where both oxygens are bound to the sulfur atom) could be important, resulting in a net loss of CH_3S. From the data of Tyndall and Ravishankara (1989a) and Turnipseed *et al.* (1993) an upper limit of only 20 - 25 s^{-1} can be placed on this process. To explain their experimental observations Butkovskaya and Barnes (2001), in a model study of the photooxidation of DMDS at a total pressure of 1013 mbar ($N_2 + O_2$) and different partial pressures of oxygen, suggest that the CH_3SOO radical undergoes transformation to $CH_3 + SO_2$ with a first order rate constant of about 8 s^{-1} in synthetic air at room temperature. In view of the existing high equilibrium CH_3SOO/CH_3S ratio the limiting step of this transformation is the thermal isomerization to a CH_3SO_2 ring structure. The barrier to formation of the three-membered SOO-ring structure, the first step of the isomerisation, has been estimated by *ab initio* calculation to be 21.6 kcal mol^{-1} by McKee (1993b). However, this calculation was performed at a low level of theory. For comparison, at this level the CH_3SOO complex is predicted to be unbound by 0.8 kcal mol^{-1}, whereas the experimental equilibrium value is about 11 kcal mol^{-1} below $CH_3S + O_2$. It is quite probable that the barrier for rearrangement to the ring S(O)O structure is less and that it is a thermally effective process at room temperature. In the work of Barnes *et al.* (2006) is presented the energy diagram for the species related to the $CH_3S + O_2$ reaction system. Since the C-S bond energy in CH_3SO_2 radical is evaluated to be less than 20 kcal mol^{-1}, the release of about 90 kcal mol^{-1} energy after forming two S=O bonds will lead to immediate (with respect to the frequency of collisions) decomposition. Taking into account the high equilibrium CH_3SOO/CH_3S ratio in air, the CH_3SOO isomerisation will be a rate-determining step in the conversion of CH_3S to SO_2.

The methyl sulfonyl radical (CH_3SO_2)

The methyl sulfonyl radical may be formed either in the oxidation reactions of the CH_3S and CH_3SO intermediate or *via* isomerisation of the CH_3SOO adduct. The CH_3SO radical is produced in the abstraction route of the OH radical initiated oxidation mechanism of DMS. CH_3SO has also been suggested to be formed in the OH radical addition reaction of DMS, through DMSO in a mechanism involving H atom abstraction from DMSO by OH radical (Sørensen *et al*., 1996). However, it has recently been shown in a more direct study that the OH radical reaction with DMSO produces mainly MSIA (methane sulfinic acid), which may react with OH radical to produce CH_3SO_2 (Urbanski *et al*., 1998). Therefore, the CH_3SO_2 radical can be an intermediate in both the abstraction and addition oxidation routes of DMS.

Both laboratory product studies (Hatakeyama *et al.*, 1982; Hatakeyama and Akimoto, 1983; Hatakeyama *et al.*, 1985; Barnes *et al.*, 1987b, 1988; Yin *et al.*, 1990b; Arsene *et al.*,

1999; Patroescu *et al.*, 1999; Arsene *et al.*, 2001; Librando *et al.*, 2004) and field observations (Bandy *et al.*, 1992, 1996; Huebert *et al.*, 1996; Allen *et al.*, 1997) suggest that SO_2 and MSA (methane sulfonic acid) are the dominant sulfur-containing end products in the atmospheric oxidation of DMS, and the CH_3SO_2 radical has been proposed as a potential major branching point leading to SO_2 and MSA (Yin *et al.*, 1990b). The CH_3SO_2 branching point involves thermal decoposition of CH_3SO_2 to form SO_2 competing with the further oxidation of CH_3SO_2 to form CH_3SO_3 and eventually MSA. The partitioning of sulfur between SO_2 and MSA will be highly dependent on ambient conditions (in particular, temperature and the concentrations of various reactive trace gases).

Kinetic data on reactions of the CH_3SO_2 radical are presented in Table 2.2. Considering the potential importance of the CH_3SO_2 radical the kinetic database for its atmospheric reactions, as listed in Table 2.2, is very sparse. Experimental kinetic information is available only on the thermal decomposition of CH_3SO_2 and its reaction with NO_2.

The value for the thermal decomposition of CH_3SO_2 has oscillated between low values (Mellouki *et al.*, 1988; Butkovskaya and Barnes, 2001, 2002; Borissenko *et al.*, 2003) and high values (Ray *et al.*, 1996; Kukui *et al.*, 2000) with the newest determinations favoring a low value (Butkovskaya and Barnes, 2001, 2002; Borissenko *et al.*, 2003). It would now appear that the high values for the thermal decomposition are in error (Borissenko *et al.*, 2003) and that the value is $< 1\ s^{-1}$ (Butkovskaya and Barnes, 2001, 2002; Borissenko *et al.*, 2003). It is difficult to explain the high yields of MSA observed by Butkovskaya and Barnes (2001, 2002) in their study on UV photolysis of $CH_3SO_2CH_3$ and also other NO_x-free chamber studies without invoking a low value for the thermal decomposition of CH_3SO_2. The use of a lower value for the thermal decomposition of CH_3SO_2 in atmospheric models of DMS chemistry would lead to somewhat higher formation yields of MSA and slightly lower SO_2 yields.

It seems beyond reasonable doubt that the identity of one of the peroxynitrates observed in many chamber studies is methyl sulfonyl peroxynitrate (MSPN: $CH_3S(O)_2OONO_2$). This is evident from the behaviour of IR absorption bands assigned to the compound as monitored in many photoreactor systems using different precursors (Barnes *et al.*, 1996; Patroescu *et al.*, 1999; Arsene *et al.*, 2001; Jensen *et al.*, 1991, 1992; Mayer-Figge, 1997). MSPN will result from reactions of the methyl sufonyl radical (CH_3SO_2):

$$CH_3SO_2 + O_2 + M \leftrightarrow CH_3S(O)_2OO + M \quad (2.20)$$

$$CH_3S(O)_2OO + NO_2 + M \leftrightarrow CH_3S(O)_2OONO_2 + M \quad (2.21)$$

Wang and Zhang (2002a) made calculations on the enthalpies of formation of CH_3SO_xH (x = 1 - 3) and H_2SO_y (y = 2, 3) and they reported values of −134.69, −79,19, −35.17, −126.32 and −69.38 kcal mol^{-1} for $CH_3S(O)_2OH$, $CH_3S(O)OH$, CH_3SOH, H_2SO_3 and HOSOH, respectively. On the basis of the calculated enthalpies of formation the O-H bond dissociation energies (BDE) of MSA, MSIA and CH_3SOH at 298 K are estimated to be 112.68, 81.34 and 71.53 kcal mol^{-1}, respectively. Hydrogen abstraction from H-R species by the CH_3SO_2 radical is energetically possible only from HONO. Hence, it is unlikely that $CH_3S(O)OH$ will be produced from H atom abstraction reactions of CH_3SO_2 radicals. Given the much higher BDE of H-O in MSA compared to MSIA, H atom abstraction reactions appear more likely to be of importance in the case of the CH_3SO_3 radical. The observations of MSA formation in the studies of Butkovskaya and Barnes (2001, 2002) on CH_3SO_2 radical in a laboratory photoreactor are indicative that H atom abstraction reactions by CH_3SO_3 forming MSA were occuring.

2.3 Aim of the work

A detailed understanding of the rates, mechanisms and ultimate products of the atmospheric degradation of DMS by OH radicals is required in order to assess the contribution of DMS to aerosol formation. The important mechanistic question is how the stable products are formed and which factors influence the branching ratio between the different product channels under the different conditions in the atmosphere. Information on intermediates and end products in OH radical initiated oxidation of DMS is mainly available only at room temperature and very little work has been perfomed on their temperature dependence especially at low temperatures. In order to properly represent DMS chemistry in models under all the conditions prevailing in the troposphere, further investigations on the temperature dependence of DMS photooxidation products are needed.

The general objectives of the present work are as follows:

- Determination of rate coefficients for the reaction of DMS with OH radicals as a function of temperature and O_2 partial pressure.
- Determination of the influence of temperature, O_2 partial pressure and NO_x on the relative yields of measurable stable products, especially, sulfur dioxide (SO_2), dimethyl sulfoxide (DMSO) and dimethyl sulfone ($DMSO_2$).
- Identification of possible intermediate products, e.g. methane sulfinic acid (MSIA).

Chapter 3

Experimental section

3.1 Experimental set-up

3.1.1 Description of the reaction chamber

All experiments performed in this work were carried out in a 336 l reaction chamber, a schematic diagram of which is presented in Figure 3.1. A detailed description of the reactor can be found in the literature (Albu *et al.*, 2006b). The reactor is built from 2 borosilicate glass cylinders of length 150 cm and different diameters, which are mounted concentrically one within the other. The inner tube has a diameter of 60 cm. Both ends of the cylinders are closed with stainless steel flanges. Elastic KEL-F-seals (GDF Bauart 314) have been used as the sealing material in the entire reactor. The volume of the reactor after deduction of the volume for various fittings is 336 l. The reactor can be temperature regulated to within ± 1 in the range 230 to 300 K. Isododecane (Maloterm P1), which is used as the coolant, is circulated continuously through the cavity between the two glass cylinders. The isododecane is cooled by three cryostats (HAAKE N3) connected in series. The temperature of the coolant in the cavity is controlled continuously by 8 platinum resistance thermometers. The reactor is isolated by several layers of the elastomeric nitrile rubber material Armaflex and the entire system is encased in a rectangular aluminum housing. The space between the outer housing and the end flanges is flushed with dry air to avoid condensation of water.

Two other quartz glass tubes with diameters of 230 and 244 mm are mounted (concentrically one within the other) and centrally within the inner main reactor cylinder. The smaller of these central tubes contains 12 photolysis lamps. The lamps are of 2 types: 6 Philips TLA 40W ($300 \leq \lambda \leq 450$ nm, λ_{max} = 360 nm) and 6 Philips TUV 40W (main emission at λ_{max} = 254 nm). The area between the glass cylinders can be cooled either by flowing coolant or dry air.

The reactor is equipped with 2 White mirrors systems, one for UV spectroscopy and one for FTIR spectroscopy. The mirror systems are mounted on the end flanges. The in and

out coupling of the probing light is through windows (KCl for the IR and quartz for the UV) mounted on the flange containing the field mirror of the White system. The multi-reflection White mirror system (used for FTIR spectroscopy) is set to a total optical path length of 47.7 m and is coupled to a FTIR spectrometer, Nicolet Magna 550, equipped with a liquid nitrogen cooled mercury-cadmium-tellurium (MCT) detector. The spectrometer is directly controlled using the software OMNIC provided by Nicolet, which runs on a PC where raw data are stored. The adjacent flange has connectors for the pumping system, pressure gauges and gas bottles. In addition an easy to open smaller flange is mounted on the main flange for checking the condition of the reactor interior or placing samples inside the reactor. This small flange also contains a window for visual inspection of samples or chemical gas mixtures during measurements. The spectrometers and the outer reactor housing are connected with one another by a plastic housing through which the analysing light beams pass. The housing is continuously flushed with dry air.

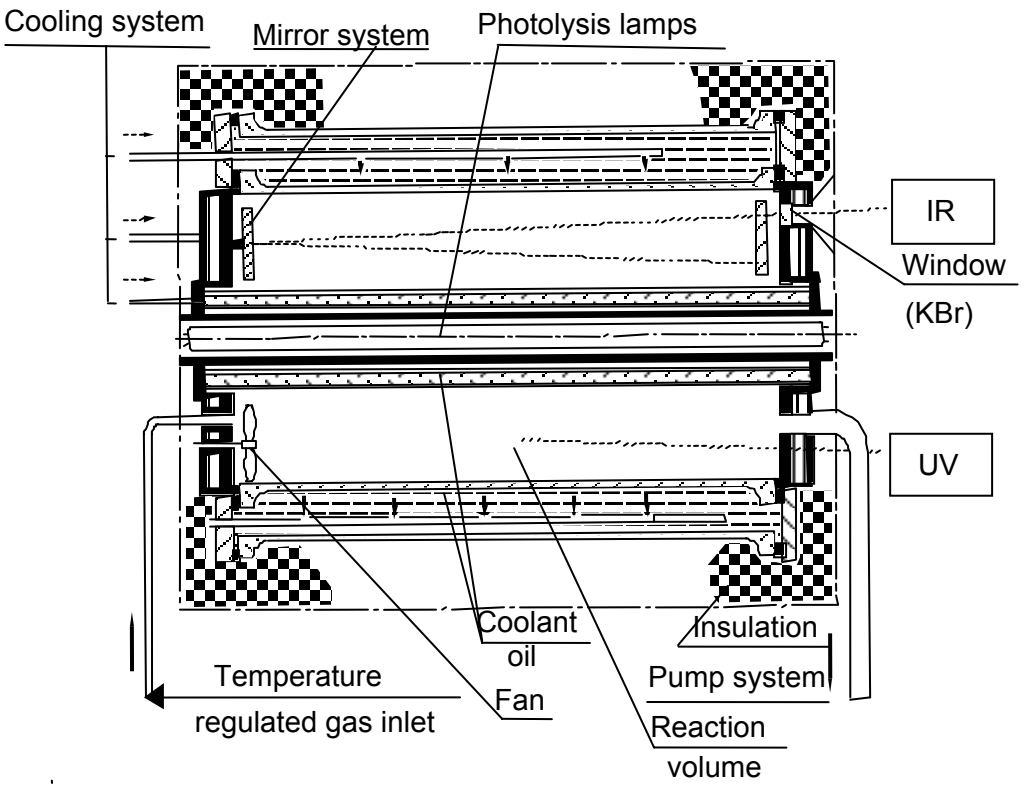

Figure 3.1: Schematic diagram of the 336 l reaction chamber.

3.1.2 Description of the sampling system for ion chromatography analysis

An external system was used for the sampling of methane sulfinic and methane sulfonic acids from the reaction chamber. This system consists of a short Teflon tube attached to two empty glass cryogenic U-tube traps connected in series, a flow controller and a pump, as indicated in Figure 3.2. The glass cryogenic U-tubes were immersed in an ethanol-liquid nitrogen slush bath (-112^{o}C). The pump was adjusted to pass air from the reactor at a rate of 1 l min^{-1} through the cold trap, and 20 l were sampled. To improve the efficiency of trapping, a glass sinter was inserted into the sampling tubes.

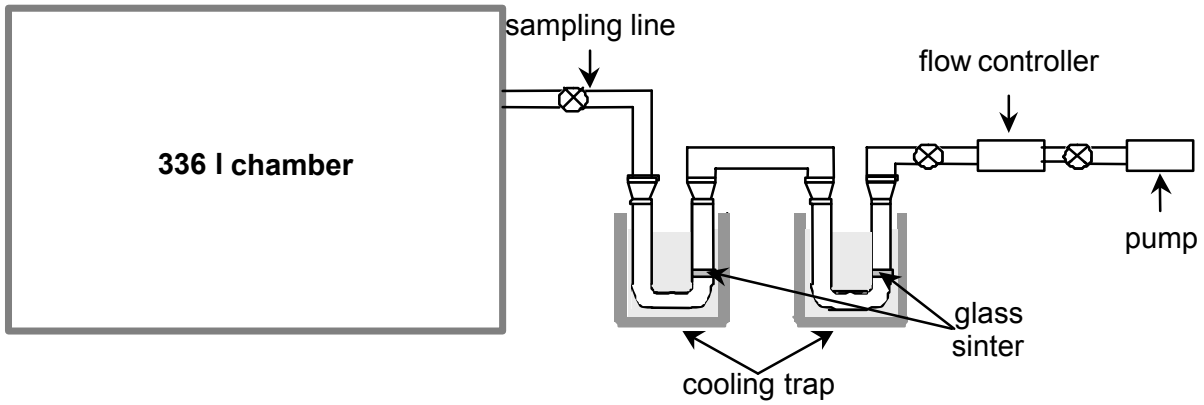

Figure 3.2: The sampling system for ion chromatography analysis.

Methane sulfinic acid (MSIA) along with methane sulfonic acid (MSA) was determined using the Odyssey ion chromatography (IC) system (Figure 3.3). The IC consists of a 526 HPLC pump, an Alltech ERIS 1000 HP autosuppresor, a 550 conductivity detector and a 7725/7725i Rheodyne injection valve. An Allsep hydrophilic anion exchange column filled with methyl acrylate containing quaternary amine functional groups (particle size 7 µm, 100 mm length × 4.6 mm ID) operated at ambient temperature was used for the anion separation. To analyse methane sulfinate and methane sulfonate, a mobile phase consisting of a mixture of bicarbonate (0.24 mM) and carbonate (0.30 mM) sodium salts solutions was chosen as eluent. During the analysis, the flow of the eluent was maintained at a rate of 1.0 ml min^{-1}.

Figure 3.3: Ion chromatography system.

3.2 Typical experimental procedure

The reaction chamber was evacuated by a pump which was able to reduce the pressure inside the chamber below 10^{-3} mbar. The valve to the vacuum pump was then closed and the chamber was filled to a total pressure of 1000 mbar with synthetic air or nitrogen. After approximately 3 min a background spectrum was recorded.

The compounds under investigation were introduced into the evacuated chamber: gas and liquid substances were injected by means of syringes (gas-tight syringes and microliter syringes), either directly into the reactor or in a stream of gas; in the case of substances with high boiling points, the inlet port to the reactor was also heated. Solid compounds were placed in a glass bulb attached to the injection port of the chamber; they were then heated and flushed into the reaction chamber with diluent gas. The reaction chamber was subsequently filled to a total pressure of 1000 mbar with the bath gas. Before commencing a measurement, the reaction mixture was kept in the dark for approximately 5 min to allow thorough mixing of the reactants and thermal equilibrium to be established.

FTIR spectra were recorded regularly over the wavelength range 690 - 4000 cm^{-1} with a resolution of 1 cm^{-1}.

3.2.1 Kinetic experiments on the system DMS + OH radicals

In order to determine the rate coefficients of the DMS with OH radicals a relative rate method (Paragraph 3.4.1) was used. The kinetic experiments were performed at a total pressure of 1000 mbar (N_2, synthetic air or N_2/O_2 mixtures) and different temperatures (ranging from 250 to 299 K). The photolysis of hydrogen peroxide (H_2O_2) was used as the OH radical source. Ethene, propene and 2-methylpropene have been used as the organic reference compounds.

In the following concentrations of the species are expressed as volum mixing ratios and not in absolute concentration units.

The starting concentrations (calculated at the working temperature) of DMS and of the organic reference compounds were typically in the range 1 to 3 ppmv and that of H_2O_2 was approximately 20 ppmv. After introducing the reactants into the chamber, the reaction chamber was pressurized to 1000 mbar with nitrogen, synthetic air or nitrogen/oxygen mixtures.

The concentration-time behaviours of DMS and the reference organic compounds were followed over 40 - 50 min time periods by FTIR spectroscopy. After acquiring 10 - 15 spectra of the mixture in the dark (to control that no dark reaction takes place and to follow possible wall losses), the photooxidation was initiated by switching on the lamps (6 Philips TUV 40W) and then 15 - 20 spectra were recorded. After switching off the lamps, 10 - 15 spectra were recorded in the dark, in order to check that the wall loss was constant over the entire time period of the experiments. Spectra were obtained by co-adding 64 scans which yielded a time resolution of 1 min. The light intensity, measured by the NO_2 photodissociation rate in N_2, was 4.48×10^{-4}, 4.35×10^{-4}, 3.34×10^{-4}, 2.35×10^{-4}, 1.16×10^{-4} and 1.03×10^{-4} s^{-1} at 299, 290, 280, 270, 260 and 250 K, respectively.

3.2.2 Product study experiments on the system DMS + OH radicals

The experiments to determine the gas-phase oxidation products from the OH radical initiated oxidation of DMS were performed at a total pressure of 1000 mbar (N_2, synthetic air or N_2/O_2 mixtures) and different temperatures (ranging from 260 to 298 K). The photolysis of hydrogen peroxide (H_2O_2) and of methyl nitrite (CH_3ONO) were used as OH radicals sources.

The starting concentrations (calculated at the working temperature) of DMS were in the range from 14 to 25 ppmv, H_2O_2 in the range from 25 to 50 ppmv, CH_3ONO in the range from 10 to 15 ppmv and NO_x in the range from 0 to 3315 ppbv. After introducing the reactants into the chamber, the reaction chamber was filled to 1000 mbar with nitrogen, synthetic air or nitrogen/oxygen mixtures. Reactants and products were monitored by FTIR

spectroscopy over a time period of 40 - 50 min. After acquiring 10 - 15 spectra of the mixture in the dark (to control that no dark reaction takes place and to follow possible wall losses), the photooxidation was initiated by switching on the lamps (6 Philips TUV 40W or 6 Philips TLA 40W) and then 15 - 20 spectra were recorded. The lamps were then switched off and 10 - 15 spectra were recorded in the dark in order to follow the stability of the products formed in the reaction. Spectra were obtained by co-adding 64 scans which yielded a time resolution of 1 min.

In order to determine methane sulfinic acid (MSIA) and methane sulfonic acid (MSA), samples were taken continuously from the reactor during the irradiation period of the experiments using the sampling system described in Paragraph 3.1.2. Due to the low temperature, any methane sulfinate or methane sulfonate passing through the trap was condensed on the walls of the tube. After collection, 10 ml of reagent grade water was added to the U-tube to dissolve the sampled material, which was then transferred to a small storage flask. The samples were analysed as soon as posible after collection by ion chromatography.

3.3 Generation of OH radicals

The photolysis of either hydrogen peroxide (H_2O_2) or of methyl nitrite (CH_3ONO) was used to generate OH radicals.

Photolysis of H_2O_2: Hydrogen peroxide provides a clean source of OH radicals, which allows experiments to be performed under NO_x free conditions.

$$H_2O_2 + h\nu\ (\lambda < 370\ nm) \rightarrow 2\ OH \qquad (3.1)$$

In the system hydroperoxy (HO_2) radicals can also be produced by the reaction:

$$H_2O_2 + OH \rightarrow H_2O + HO_2 \qquad (3.2)$$

The rate coefficient for the reaction (3.2) is 1.7×10^{-12} cm^3 $molecule^{-1}$ s^{-1} at 298 K ($2.9 \times 10^{-12} \exp(-160/T)$ in the temperature range 240 - 460 K) (Atkinson *et al.*, 2004).

HO_2 radicals can react with OH radicals:

$$HO_2 + OH \rightarrow H_2O + O_2 \qquad (3.3)$$

However, the rate coefficient for the reaction (3.3) of 1.1×10^{-10} cm^3 $molecule^{-1}$ s^{-1} at 298 K (4.8×10^{-11} exp(250/T) in the temperature range 250 - 400 K) is high enough to suppress the HO_2 radicals produced in the system (Atkinson *et al.*, 2004).

Reaction (3.3) will always provide small quantities of oxygen, leading to the formation of oxygenated compounds even when nitrogen is used as bath gas.

The decomposition of H_2O_2 at the reactor walls will be the major source of O_2 in the nitrogen systems. Small leaks might also introduce some oxygen.

Photolysis of methyl nitrite in the presence of NO: Photolysis of methyl nitrite produces OH radicals in the following sequence of reactions:

$$CH_3ONO + h\nu\ (\lambda_{max} = 360\ nm) \rightarrow CH_3O + NO \quad (3.4)$$

$$CH_3O + O_2 \rightarrow CH_2O + HO_2 \quad (3.5)$$

$$HO_2 + NO \rightarrow OH + NO_2 \quad (3.6)$$

When photolysis of methyl nitrate in synthetic air was used as the hydroxyl radical source NO was added to the reaction mixture to accelerate the convertion of HO_2 to OH (reaction 3.6) and to suppress the formation of ozone and hence of nitrate radicals.

The synthesis of methyl nitrite is described in Appendix I.

3.4 Data analysis

3.4.1 Relative rate method

Rate coefficients for the reaction of DMS with OH radicals were determined using a relative rate method in which the relative disappearance rates of DMS and of a reference compound, whose rate coefficient with OH radicals is known are monitored parallel in the presence of OH radicals:

$$OH + DMS \rightarrow \text{products} \qquad k_{DMS}$$

$$OH + \text{reference} \rightarrow \text{products} \qquad k_{reference}$$

Providing that DMS and the reference compound are removed solely by reaction with the OH radicals, it follows:

$$\ln\left\{\frac{[\mathrm{DMS}]_{t_0}}{[\mathrm{DMS}]_t}\right\} = \frac{k_{\mathrm{DMS}}}{k_{\mathrm{reference}}} \ln\left\{\frac{[\mathrm{reference}]_{t_0}}{[\mathrm{reference}]_t}\right\} \quad \text{(I)}$$

where $[\mathrm{DMS}]_{t_0}$ and $[\mathrm{reference}]_{t_0}$ are the concentrations of DMS and the reference compound, respectively, at time t_0; $[\mathrm{DMS}]_t$ and $[\mathrm{reference}]_t$ are the corresponding concentrations at time t; k_{DMS} and $k_{\mathrm{reference}}$ are the rate coefficients for the reaction with OH radicals of DMS and the reference compound, respectively. Thus, the concentrations of DMS and the reference as a function of reaction time, plotted according to Eqn (I), can be used to derive the rate coefficient ratio $k_{\mathrm{DMS}}/k_{\mathrm{reference}}$. Plots of $\ln\{[\mathrm{DMS}]_{t_0}/[\mathrm{DMS}]_t\}$ versus $\ln\{[\mathrm{reference}]_{t_0}/[\mathrm{reference}]_t\}$ should give straight lines with slopes $k_{\mathrm{DMS}}/k_{\mathrm{reference}}$ and zero intercept. If the value of the rate coefficient of the reference $k_{\mathrm{reference}}$ is known, then k_{DMS} can be obtained. Under the experimental conditions, DMS and the reference compounds may additionally undergo photodissociation and/or be lost to the chamber surface. The photostability of DMS and of each reference compound was established by irradiation of DMS/reference compound/diluent gas mixtures in the absence of OH radical precursors for a time period as long as that employed in the kinetic experiments, after switching on the lamps. The possibility of adsorption of DMS or of the reference compound on the wall of the chamber was tested at the beginning and at the end of every experiment. The reference compounds employed were not photolysed and their wall losses were also very low, often below the detection limit. For DMS, the wall losses accounted for approximately 5% of its measured decay at room temperature and this increased gradually to around 30% at the lowest temperature employed in the experiments:

DMS (+ wall) $\rightarrow$ loss $\qquad k_{\mathrm{DMS}}^{\mathrm{loss}}$

The wall loss of DMS was measured at the beginning of every experiment by recording 10 - 15 spectra prior to irradiation. To check that the wall loss of DMS was constant over the entire time period of the experiments its loss was measured on a regular basis after termination of the irradiation. No significant change in the DMS wall loss rate was ever observed between the pre- and post-irradiation periods.

Incorporation of a first-order loss process for DMS into Eqn (I) leads to:

$$\ln\left\{\frac{[\mathrm{DMS}]_{t_0}}{[\mathrm{DMS}]_t}\right\} - k_{\mathrm{DMS}}^{\mathrm{loss}} \times \mathrm{t} = \frac{k_{\mathrm{DMS}}}{k_{\mathrm{reference}}} \ln\left\{\frac{[\mathrm{reference}]_{t_0}}{[\mathrm{reference}]_t}\right\} \quad \text{(II)}$$

or

$$\ln\left\{\frac{[\mathrm{DMS}]_{t_0}}{[\mathrm{DMS}]_t}\right\} - k_{\mathrm{DMS}}^{\mathrm{loss}} \times \mathrm{t} = k_{\mathrm{DMS}}\left(\ln\left\{\frac{[\mathrm{reference}]_{t_0}}{[\mathrm{reference}]_t}\right\} \Big/ k_{\mathrm{reference}}\right) \qquad \text{(III)}$$

where t is the reaction time and $k_{\mathrm{DMS}}^{\mathrm{loss}}$ is the first-order loss rate of DMS.

According to Eqn (III), a plot of $\ln\{[\mathrm{DMS}]_{t_0}/[\mathrm{DMS}]_t\} - k_{\mathrm{DMS}}^{\mathrm{loss}} \times \mathrm{t}$ as a function of $\ln\{[\mathrm{reference}]_{t_0}/[\mathrm{reference}]_t\}/k_{\mathrm{reference}}$ should give a straight line directly yielding k_{DMS} as the slope. Eqn (II) allows the data for all reference hydrocarbons employed for a set of experimental conditions to be plotted and evaluated simultaneously and gives a direct visual view of the quality of the agreement of the experimental data obtained for the different reference compounds.

3.4.2 Product analysis

Product studies were carried out in the 336 l reactor described in Paragraph 3.1.1, using FTIR spectroscopy and the IC method.

FTIR spectroscopy was used to analyze products like sulfur dioxide (SO_2), dimethyl sulfoxide (DMSO), dimethyl sulfone ($DMSO_2$), methyl sulfonyl peroxynitrate (MSPN), methane sulfonic acid (MSA), carbonyl sulfide (OCS) and methyl thiol formate (MTF). Reactants and products were identified by comparison of the infrared spectra of the reaction mixture with the reference spectra of the pure compounds; the complex spectra were analyzed by successively subtracting the characteristic absorptions of identified compounds using the calibrated spectra. From the calibrated spectra the concentration of the related species could be derived.

The molar formation yield of each product was derived by plotting the amount of the product formed against the amount of the reactant (DMS) consumed. Least-square analysis of the slopes of such plots gives the molar formation yield of the individual product. The indicated error of the product formation yields is twice the standard deviation of the linear regression.

For some of the identified products, plots of their concentration against the amounts of DMS consumed showed curvature, indicating that secondary reactions of these primary products occurred during the time period of the experiments. In order to derive the formation yields of these products, their measured concentrations had to be corrected for further reactions with OH radicals, wall loss and photolysis. Corrections have been performed using

the mathematical procedure described by Tuazon *et al.* (1986), which is based on the reaction sequence:

OH + DMS $\rightarrow$ Y (product)	k_{DMS}
DMS (+ wall) $\rightarrow$ loss	k_{DMS}^{loss}
OH + product $\rightarrow$ secondary products	$k_{product}$
product (+ wall/hν) $\rightarrow$ loss	$k_{product}^{loss}$

In this sequence, Y is the formation yield of the primary product from the oxidation of the dimethyl sulfide and k_{DMS} and $k_{product}$ are the rate coefficients for reaction with OH radicals.

By making the reasonable assumption that the OH radical concentration was essentially constant over the time intervals between the measurement points, then:

$$[DMS]_{t_2} = [DMS]_{t_1} e^{-\left(k_{DMS}[OH]+k_{DMS}^{loss}\right)(t_2-t_1)} \quad \text{(IV)}$$

and

$$[product]_{t_2} = [product]_{t_1} e^{-\left(k_{product}[OH]+k_{product}^{loss}\right)(t_2-t_1)} + \frac{Y_{t_2-t_1}[DMS]_{t_1} k_{DMS}[OH]}{\left(k_{product}-k_{DMS}\right)[OH]+k_{product}^{loss}} \left[e^{-\left(k_{DMS}[OH]+k_{DMS}^{loss}\right)(t_2-t_1)} - e^{-\left(k_{product}[OH]+k_{product}^{loss}\right)(t_2-t_1)}\right] \quad \text{(V)}$$

where $[DMS]_{t_1}$, $[product]_{t_1}$, and $[DMS]_{t_2}$, $[product]_{t_2}$ are the reactant (DMS) and product concentrations measured at times t_1 and t_2, respectively, and $Y_{t_2-t_1}$ is the formation yield of the individual product over the period time t_2 - t_1. The OH radical concentration was calculated from the decay of the DMS using the rate coefficient for the reaction of DMS with OH radicals, according to the following equation:

$$[OH] = \frac{\ln\left([DMS]_{t_2}/[DMS]_{t_1}\right)}{k_{DMS}\times\left(t_2-t_1\right)} \quad \text{(VI)}$$

Rate coefficients k_{DMS} and $k_{product}$ were determined in this study or taken from the literature.

The product concentrations, corrected for reaction with OH radicals, are then given by:

$$[\text{product}]_{t_2}^{\text{corrected}} = [\text{product}]_{t_1}^{\text{corrected}} + Y_{t_2-t_1}\left([\text{DMS}]_{t_1} - [\text{DMS}]_{t_2}\right) \quad \text{(VII)}$$

where $[\text{product}]_{t_1}^{\text{corrected}}$ and $[\text{product}]_{t_2}^{\text{corrected}}$ are the corrected product concentrations at times t_1 and t_2, respectively. The corrected product concentrations were, then, plotted against the consumed amount of the reactant to derive the molar formation yield of the products (this was the case for products like DMSO, $DMSO_2$, MTF and SO_2). In the case of MSPN, OCS and MSA secondary formation or other removal processes occurring in the system rendered the procedure for the correction of the measured concentrations difficult. Therefore, the molar formation yield of the product was derived from the uncorrected concentrations plotted against the consumption of the reactant.

IC was used to determine methane sulfinic acid (MSIA) and methane sulfonic acid (MSA). The samples were analysed by injecting a 200 µl aliquot of the collected sample *via* an injection loop into the IC system. Calibrations of the methane sulfinate ($CH_3S(O)O^-$) and methane sulfonate ($CH_3S(O)_2O^-$) ions were performed using standard solutions of sodium salts of methane sulfinic acid and methane sulfonic acid. It was observed that the heights of the IC peaks corresponding to the $CH_3S(O)O^-$ and $CH_3S(O)_2O^-$ anions were proportional to the concentration of $CH_3S(O)O^-$ and $CH_3S(O)_2O^-$, respectively, and in the range of 0.2 - 12 µg ml^{-1} good correlation coefficients were obtained. Calibrations were performed weekly, and every day a few working standards were injected for comparison. The compounds were identified by comparison of the retention time of the peaks of the unknown samples with the retention times of peaks in the chromatograms of standard solutions.

Chapter 4

Kinetic study of the OH radical initiated oxidation of dimethyl sulfide

The rate coefficients reported in this work, for the reaction of OH radicals with dimethyl sulfide (DMS), were determined using a relative rate method (see Chapter 3, Paragraph 3.4.1.). The kinetic experiments were performed at a total pressure of 1000 mbar diluent gas (N_2, synthetic air or N_2/O_2 mixtures), at three different O_2 partial pressures (~0, 205 and 500 mbar) and six different temperatures (250, 260, 270, 280, 290 and 299 K). The photolysis of hydrogen peroxide (H_2O_2) was used as the OH radical source. Ethene, propene and 2-methylpropene (*iso*-buthene) were used as the reference compounds in the investigations. The rate coefficients for the reactions of these compounds with OH radicals are well established (Atkinson, 1997) and listed in Table 4.1.

Table 4.1: Rate coefficients for reaction of the reference compounds with OH radicals ($k = A\ e^{-Ea/RT}$, T = ~ 250 - 425 K) (Atkinson, 1997).

Reference compound	10^{12} *k* (298 K) (cm^3 $molecule^{-1}$ s^{-1})	10^{12} A (cm^3 $molecule^{-1}$ s^{-1})	$-E_a/R$ (K)
Ethene	8.52	1.96	438
Propene	26.3	4.85	504
2-Methylpropene	51.4	9.47	504

Test experiments were performed both for dimethyl sulfide and the reference compounds to check that unwanted adsorptions on the wall of the reactor, dark reaction and photolysis were not occurring under the experimental conditions employed. For the reference compounds employed in this study, these loss processes were found to be negligible on the time scale of the experiments. For DMS the wall losses accounted for approximately 5% of its measured decay at room temperature and increased gradually to around 30% at the lowest temperature employed in the experiments. These losses were taken into account using Eqn (II) or Eqn (III) to determine the corrected reaction rate coefficients.

For each temperature and pO_2 = ~0 mbar and pO_2 = 500 mbar, one reference compound (ethene) was employed, and for each temperature and pO_2 = 205 mbar, two or three different reference compounds (ethene, propene, *iso*-buthene) were employed. For each set of experimental conditions, at least three experimental runs were performed.

4.1 Results

The kinetic data obtained from the investigations on the reaction of OH radicals with DMS at 6 temperatures for different partial pressures of O_2 are shown plotted according to Eqn (III) in Figure 4.1. Reasonably linear plots were obtained in all cases. Significant scatter in the measurement points was only observed at the lowest temperature investigated, i.e. 250 K.

Table 4.2 Rate coefficient ratios $k_{DMS}/k_{reference}$ and rate coefficients k_{DMS} for the gas-phase reaction of OH radicals with DMS at different temperatures and various O_2 partial pressures.

Temperature (K)	pO_2 (mbar)	reference	$k_{DMS}/k_{reference}$	$k_{DMS}\times10^{11a}$	$k_{DMS\ (average)}\times10^{11a}$	$\tau_{DMS} = 1/k_{DMS}$ [OH] (h)
299	~0	ethene	0.59 ± 0.01	0.50 ± 0.10		
	205	ethene	0.94 ± 0.02	0.80 ± 0.16	0.78 ± 0.18	35.6
		propene	0.28 ± 0.01	0.75 ± 0.15		
	500	ethene	1.13 ± 0.02	0.95 ± 0.19		
290	~0	ethene	0.64 ± 0.02	0.57 ± 0.11		
	205	ethene	1.13 ± 0.02	1.00 ± 0.20	0.98 ± 0.23	28.3
		propene	0.33 ± 0.01	0.93 ± 0.18		
	500	ethene	1.51 ± 0.04	1.34 ± 0.27		
280	~0	ethene	0.67 ± 0.02	0.62 ± 0.13		
	205	ethene	1.27 ± 0.03	1.19 ± 0.24	1.20 ± 0.26	23.1
		propene	0.42 ± 0.01	1.22 ± 0.24		
	500	ethene	1.64 ± 0.03	1.54 ± 0.31		
270	~0	ethene	0.64 ± 0.02	0.63 ± 0.14		
	205	ethene	1.53 ± 0.06	1.52 ± 0.31	1.51 ± 0.34	18.4
		propene	0.47 ± 0.01	1.47 ± 0.30		
	500	ethene	1.87 ± 0.05	1.85 ± 0.37		
260	~0	ethene	0.60 ± 0.03	0.64 ± 0.13		
	205	ethene	1.93 ± 0.04	2.04 ± 0.40	1.99 ± 0.47	13.9
		propene	0.58 ± 0.01	1.97 ± 0.39		
		i-buthene	0.30 ± 0.01	2.00 ± 0.40		
	500	ethene	2.25 ± 0.12	2.38 ± 0.47		
250	~0	ethene	0.58 ± 0.05	0.66 ± 0.14		
	205	ethene	2.37 ± 0.30	2.68 ± 0.63	2.82 ± 0.77	9.85
		propene	0.77 ± 0.04	2.80 ± 0.57		
		i-buthene	0.41 ± 0.02	2.96 ± 0.60		
	500	ethene	2.51 ± 0.23	2.83 ± 0.62		

[a] *units: in cm^3 $molecule^{-1}$ s^{-1}*

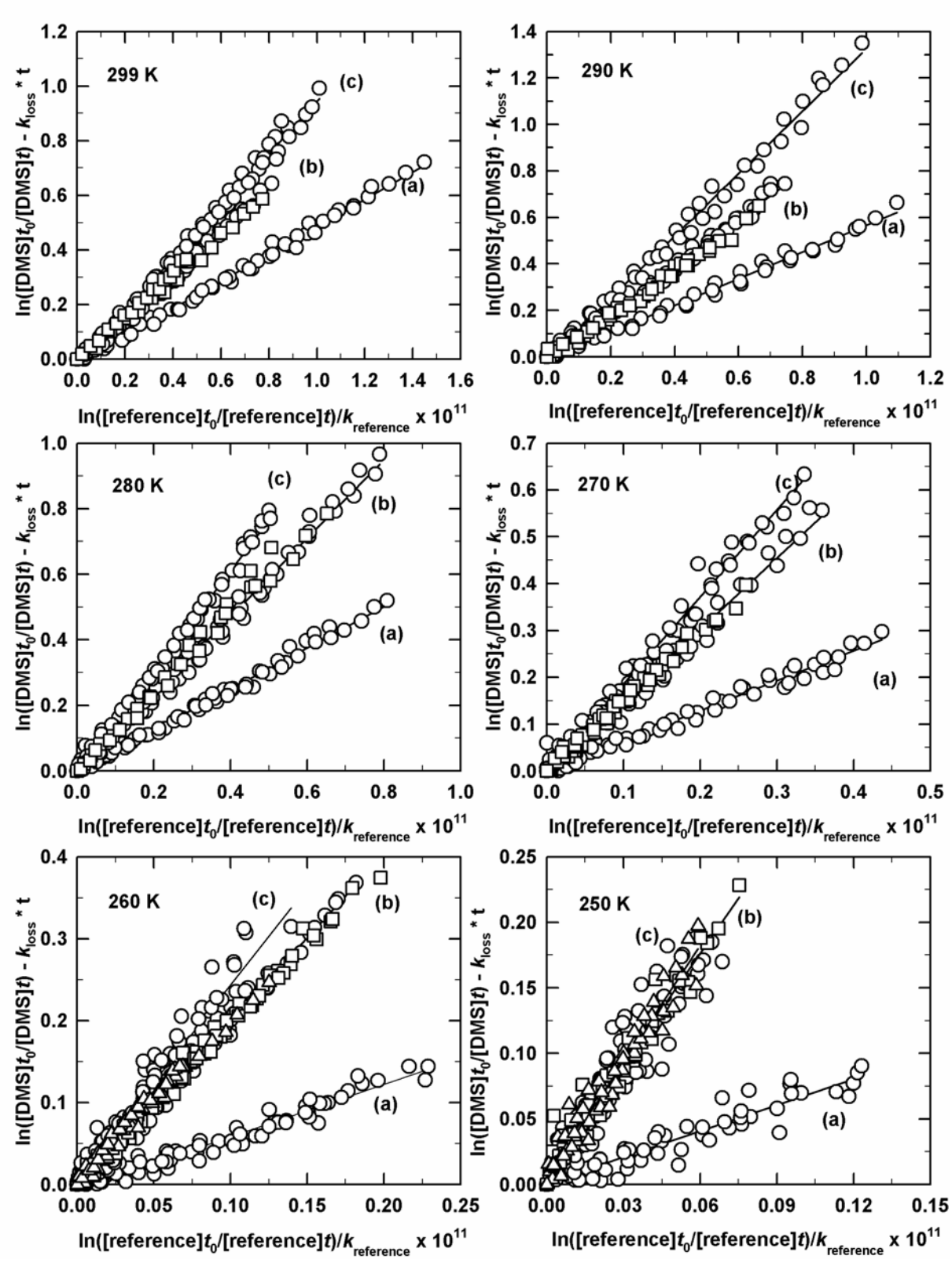

Figure 4.1: Plot of the kinetic data according to Eqn (III) for the reaction of DMS with OH radicals at different temperatures and oxygen partial pressures: (a) = ~0 mbar O_2, (b) = 205 mbar O_2, (c) = 500 mbar O_2; references: ○ - ethene, □ - propene, △ - *iso*-butene.

Table 4.2 lists the reference compounds used for each set of experimental conditions, the rate coefficient ratios obtained from an analysis of the data according to Eqn (II) and the rate coefficients for the reaction of OH radicals with DMS as determined from the data plotted according to Eqn (III). The errors given for the rate coefficient ratios in Table 4.2 are two least-squares standard deviations ($\pm 2\sigma$); the quoted errors for the rate coefficients in Table 4.2 are a combination of the 2σ statistical errors from the linear regression analysis plus an additional 20% to cover uncertainties associated with the values of the reference rate coefficients. For every temperature and pO_2 = 205 mbar, the rate coefficients were measured relative to two or three different references, thus, the final values given in Table 4.2 for these conditions of the rate coefficients ($k_{DMS(average)}$) are averages of those determined using the two or three different reference compounds together with error limits which encompass the extremes of the individual determinations.

Given in Table 4.2 is the tropospheric lifetime of DMS at each temperature, calculated using an annually averaged global tropospheric hydroxyl radical concentration of ~1 $\times$ 10^6 molecule cm^{-3} (24 h average) (Prinn *et al.*, 1995).

For ease of comparison the final averaged values of the rate coefficients for the reaction of DMS with OH radicals determined in this work are summarized in the Table 4.3.

Table 4.3: Summary of rate coefficients for the reaction of DMS with OH radicals determined at different temperatures and O_2 partial pressures.

Temperature (K)	$k_{DMS} \times 10^{11}$ (cm^3 $molecule^{-1}$ s^{-1})		
	~0 mbar O_2	205 mbar O_2	500 mbar O_2
299	0.50 $\pm$ 0.10	0.78 $\pm$ 0.18	0.95 $\pm$ 0.19
290	0.57 $\pm$ 0.11	0.98 $\pm$ 0.23	1.34 $\pm$ 0.27
280	0.62 $\pm$ 0.13	1.20 $\pm$ 0.26	1.54 $\pm$ 0.31
270	0.63 $\pm$ 0.14	1.51 $\pm$ 0.34	1.85 $\pm$ 0.37
260	0.64 $\pm$ 0.13	1.99 $\pm$ 0.47	2.38 $\pm$ 0.47
250	0.66 $\pm$ 0.14	2.82 $\pm$ 0.77	2.83 $\pm$ 0.62

Several trends can be seen in the kinetic data listed in Table 4.3:

- At a fixed temperature the overall rate coefficient for the reaction of DMS with OH radicals increases with increasing partial pressure of oxygen.
- At a constant O_2 partial pressure the rate coefficient is observed to increase quite appreciably with decreasing temperature, i.e. by factors of 3.6 and 3.0 for pO_2 = 205 and 500 mbar between 299 and 250 K, respectively.
- In N_2 with pO_2 = ~0 mbar where the abstraction pathway for the reaction will dominate the rate coefficient for the reaction of DMS with OH radicals is observed to increase

very slightly with decreasing temperature. However, the observed increase does not exceed the combined error limits of the two measurements at the lowest and highest temperatures.

The data listed in Table 4.3 are plotted in Arrhenius form in Figure 4.2 for the three O_2 partial pressures investigated. The solid lines are the least-squares fits of the data. The Arrhenius expressions derived from these fits are given in Table 4.4 for the individual O_2 partial pressures.

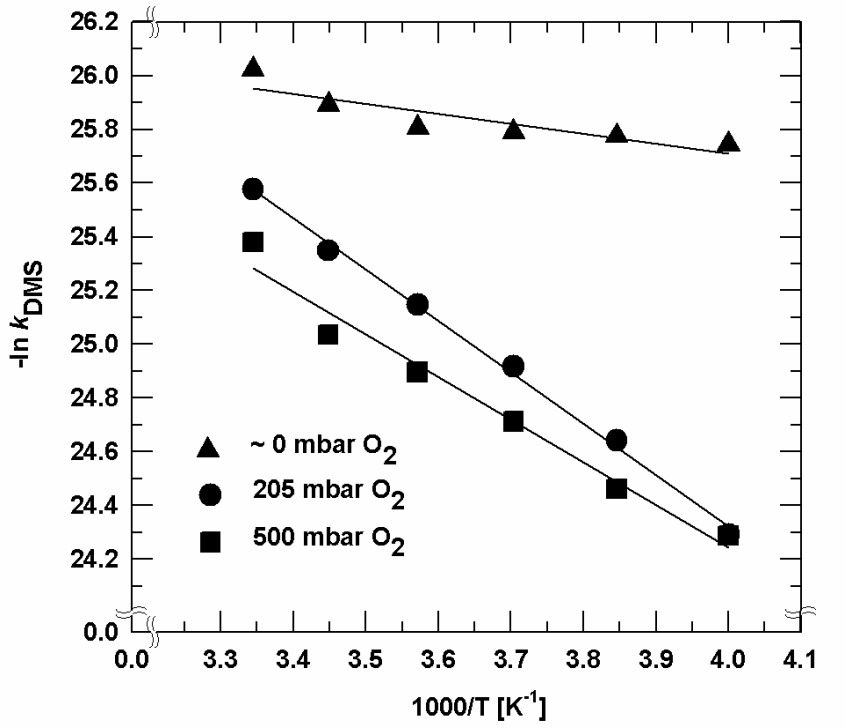

Figure 4.2: Arrhenius plots of the rate coefficients determined for the reaction of DMS with OH radicals in the temperature range 250 to 299 K for various O_2 partial pressures.

Table 4.4: Arrhenius expressions for the reaction of OH radicals with DMS as a function of O_2 partial pressure valid in the temperature range 250 to 299 K.

O_2 partial pressure (mbar)	k_{DMS} (cm^3 $molecule^{-1}$ s^{-1})
~0	$(1.56 \pm 0.20) \times 10^{-12}$ exp[(369 ± 27) / T]
205	$(1.31 \pm 0.08) \times 10^{-14}$ exp[(1910 ± 69) / T]
500	$(5.18 \pm 0.71) \times 10^{-14}$ exp[(1587 ± 24) / T]

4.2 Discussion

4.2.1 Possible source of errors in the system

Although results are reported here for experiments performed in 1000 mbar N_2 with pO_2 = ~0 mbar in reality the system will contain very small concentrations of O_2. Apart from O_2 entering the system through leaks in the apparatus the use of hydrogen peroxide (H_2O_2) as OH radical source can lead to production of O_2 *via* (i) heterogeneous decomposition on the reactor surface (possibly the largest source) and (ii) chemical reactions in the system.

Hydroperoxy (HO_2) radicals are produced in the reaction of OH radicals with DMS and they are produced also by the reaction:

$$H_2O_2 + OH \rightarrow H_2O + HO_2 \qquad (4.1)$$

The self-reaction of HO_2 radical and the reaction with OH radical result in the formation of O_2:

$$HO_2 + HO_2 \rightarrow H_2O_2 + O_2 \qquad (4.2)$$

$$HO_2 + OH \rightarrow H_2O + O_2 \qquad (4.3)$$

The above reactions in combination with heterogeneous decay of H_2O_2 will always provide small quantities of oxygen in the system, leading to the formation of oxygenated compounds even when pure nitrogen is used as the bath gas. Based on the known leak rate of the reactor under vacuum it is estimated that in the nitrogen experiments the concentration of O_2 is probably less than 30 ppmv. From the measured O_2 enhancement on the rate coefficients for the reaction of DMS with OH radicals it is, however, apparent that this low O_2 concentration in the N_2 experiments will make a negligible contribution to the measured rate coefficient.

Another potential source of error is the reaction of HO_2 radicals with DMS:

$$HO_2 + CH_3SCH_3 \rightarrow OH + CH_3S(O)CH_3 \qquad (4.4)$$

An upper limit of the rate coefficient for reaction (4.4) of $< 5 \times 10^{-15}$ cm^3 $molecule^{-1}$ s^{-1} at 298 K has been reported (Atkinson *et al.*, 2004).

However, the good agreement between the rate coefficient for the reaction of OH radicals with DMS determined in N_2 at 299 K in this study with those obtained by other

groups (as discussed later) leads to the conclusion that both reaction (4.4) and the low traces of O_2 have a negligible influence on the measurements.

4.2.2 Comparison with previous work

For ease of comprehension, the rate coefficients determined in the absence of O_2 will be discussed first, followed by a discussion on the determinations performed in the presence of O_2. Earlier determinations, which are now thought to be flawed because of reactive impurities in the DMS samples (Atkinson *et al.*, 1978; Kurylo, 1978) or heterogeneous effects (MacLeod *et al.*, 1984), are not considered in the comparison. Also excluded from the comparison are relative studies where NO was present (Cox and Sheppard, 1980; Atkinson *et al.*, 1984; Wallington *et al.*, 1986c; Nielsen *et al.*, 1989), since these studies are believed to be in error due to secondary reactions in the systems. The exclusions, however, underline the variety of complications which can arise in studies of the kinetics of the DMS with OH radical reaction.

In Table 4.5 a comparison is made of the data obtained in this work at 299 K and 760 Torr N_2 (pO_2 = ~0 mbar) with other room temperature values reported in the literature.

This comparison shows that the value obtained in this study (k_{DMS} = (5.00 ± 1.00) × 10^{-12} cm^3 $molecule^{-1}$ s^{-1}) is in very good agreement with most of the other determinations obtained using absolute (Wine *et al.*, 1981; Hynes *et al.*, 1986; Hsu *et al.*, 1987; Abbat *et al.*, 1992; Barone *et al.*, 1996) and relative (Wallington *et al.*, 1986c; Barnes *et al.*, 1988) methods. There are, however, three absolute studies (Martin *et al.*, 1985; Wallington *et al.*, 1986c; Nielsen *et al.*, 1989) which report room temperature rate coefficient in the absence of O_2 which are substantially lower; potential production of O atoms in these systems which can react with DMS to regenerate OH radicals on the time scale of the experiment and thus lead to a low effective rate constant has been postulated as an explanation for the low values. O atoms can be formed either in high concentrations from microwave discharges (which could affect flow tube experiments) or from high concentrations of OH radicals *via* the reaction OH + OH → H_2O + O. The experiments of Martin *et al.* (1985) and Nielsen *et al.* (1989), for example, used extremely high OH radical concentrations.

The new recommended Arrhenius expression for the reaction: OH + CH_3SCH_3 → CH_3SCH_2 + H_2O of $k_{2.1a}$ = 1.13 × 10^{-11} exp(–253/T) cm^3 $molecule^{-1}$ s^{-1} over the temperature range 240 - 400 K from the review of Atkinson *et al.* (2004) gives $k_{2.1a}$ = 4.8 × 10^{-12} cm^3 $molecule^{-1}$ s^{-1} at 298 K. The value of (5.00 ± 1.00) × 10^{-12} cm^3 $molecule^{-1}$ s^{-1} determined in this study at 299 K is in good agreement with the recommended value.

Table 4.5: Room temperature rate coefficients for the reaction of DMS with OH radicals in the absence of O_2.

$k_{DMS} \times 10^{12a}$	Temperature (K)	Pressure (Torr) / Bath gas	Technique	Reference
4.26 ± 0.56	298	50/Ar	FP-RF[b]	Wine *et al.* (1981)
3.22 ± 1.16	293	0.5/He	DF-EPR[b]	Martin *et al.* (1985)
4.09 ± 1.16	298	40/Ar	FP-RF[b]	Hynes *et al.* (1986)
4.44 ± 0.23	298	30/Ar	FP-RF[b]	Hynes *et al.* (1986)
4.75 ± 0.15	298	500/SF_6	PLP-PLIF[b]	Hynes *et al.* (1986)
4.80 ± 0.11	298	40/N_2	PLP-PLIF[b]	Hynes *et al.* (1986)
3.60 ± 0.20	297	50-400/Ar	FP-RF[b]	Wallington *et al.* (1986c)
5.50 ± 1.00	298	0.8-3/He	DF-RF[b]	Hsu *et al.* (1987)
3.50 ± 0.20	295	760/Ar	PR-KS[b]	Nielsen *et al.* (1989)
4.98 ± 0.46	297	10-100/N_2	HPF-LIF[b]	Abbat *et al.* (1992)
4.95 ± 0.35	298	100/He/N_2/SF_6	PLP-PLIF[b]	Barone *et al.* (1996)
5.30 ± 0.50	296	740/Ar	DS-FTIR[c]	Wallington *et al.* (1986c)
4.40 ± 0.40	298	760/N_2	CP-GC[c]	Barnes *et al.* (1988)
4.80	298	-	review	Atkinson *et al.* (2004)
5.00 ± 1.00	299	760/N_2	CP-FTIR[c]	This work

[a]units: in cm^3 $molecule^{-1}$ s^{-1}; [b]absolute technique: FP = flash photolysis, RF = resonance fluorescence, DF = discharge flow, EPR = electron paramagnetic resonance, PLP = pulsed laser photolysis, PLIF = pulsed laser induced fluorescence, PR = pulse radiolysis, KS = kinetic spectroscopy, HPF = high pressure flow, LIF = laser induced fluorescence; [c]relative technique: DS = dark source of OH (O_3 + N_2H_4), FTIR = Fourier transform infrared spectroscopy, CP = continuous photolysis, GC = gas chromatography.

The Arrhenius expression derived in this work from the measurement in N_2 with pO_2 = ~0 mbar for the reaction of DMS with OH radicals in the temperature range 250 to 299 K is compared with other determinations in the absence of O_2 and also the most recent kinetic review in Table 4.6.

The activation energy of reaction (2.1a) is still not well characterized. The studies of Wine *et al.* (1981), Hynes *et al.* (1986), Hsu *et al.* (1987) and Abbat *et al.* (1992) report a *positive* Arrhenius activation energy, while Wallington *et al.* (1986c) report a *negative* Arrhenius activation energy. The latest IUPAC data evaluation (Atkinson *et al.*, 2004) recommends a *positive* Arrhenius activation energy. The observation of a *positive* activation energy has been taken as indicating the dominance of the hydrogen abstraction reaction (2.1a) in the systems used to study the reaction, while measurement of a *negative* Arrhenius activation energy has been taken as an indication that the association reaction (2.1b) is also probably contributing to the rate coefficient measurement under the conditions employed. In this work a *negative* Arrhenius activation energy has been obtained. Although very low

concentrations of O_2 are always present in the system, even in 1000 mbar N_2, the reasonable agreement with other determinations of the rate coefficient would suggest that the O_2 is not making a large contribution, at least at room temperature. However, with decrease in temperature, the formation of the $(CH_3)_2S$-OH adduct will become more important and it cannot be excluded that the system may be more sensitive to the presence of small quantities of O_2 at lower temperatures. As stated previously, the increase in the rate coefficient of DMS with OH radicals with decreasing temperature in N_2 observed in this study does not exceed the combined error limits of the measurements at the temperature extremes. Similarly, for all of the other investigations the determined activation energy is associated with quite sizeable errors and the observed increase in the rate coefficient does not exceed the combined error limits of the measurements at the temperature extremes. Further measurements with higher precision are required to determine more accurately the Arrhenius parameters for the abstraction channel (2.1a) in the reaction of DMS with OH radicals.

Table 4.6: Arrhenius expressions for the reaction of DMS with OH radicals in the absence of O_2 for different ranges of temperature.

k_{DMS}[a] Arrhenius expression	Temperature range (K)	Pressure (Torr)/ Bath gas	Technique	Reference
$(6.8 \pm 1.1) \times 10^{-12}$ exp[(−138 ± 46)/T]	248 - 363	50-200/Ar	FP-RF[b]	Wine *et al.* (1981)
$(13.6 \pm 4.0) \times 10^{-12}$ exp[(−332 ± 96)/T]	276 - 397	30-40/Ar	FP-RF[b]	Hynes *et al.* (1986)
$(2.5 \pm 0.9) \times 10^{-12}$ exp[(130 ± 102)/T]	297 - 400	50/Ar	FP-RF[b]	Wallington *et al.* (1986c)
$(11.8 \pm 2.2) \times 10^{-12}$ exp[(−236 ± 150)/T]	260 - 393	0.8-3/He	DF-RF[b]	Hsu *et al.* (1987)
$(13.5 \pm 6.2) \times 10^{-12}$ exp[(−285 ± 135)/T]	297 - 368	10-100/N_2	HPF-LIF[b]	Abbat *et al.* (1992)
1.13×10^{-11} exp(−253/T)	240 - 400	-	review	Atkinson *et al.* (2004)
$(1.56 \pm 0.20) \times 10^{-12}$ exp[(369 ± 27)/T]	250 - 299	760/N_2	CP-FTIR[c]	This work

[a]units: in cm^3 $molecule^{-1}$ s^{-1}; [b]absolute technique: FP = flash photolysis, RF = resonance fluorescence, DF = discharge flow, HPF = high pressure flow, LIF = laser induced fluorescence; [c]relative technique: CP = continuous photolysis, FTIR = Fourier transform infrared spectroscopy.

The observed increase in the rate coefficient for the reaction of OH radicals with DMS with increase in the partial pressure of O_2 for each temperature studied is in agreement with

the observations from the studies at room temperature of Wallington *et al.* (1986c), Hynes *et al.* (1986) and Barnes *et al.* (1988) (Figure 4.3) as well as from the studies of Hynes *et al.* (1986) and Williams *et al.* (2001) made at different temperatures (Figure 4.4).

In the work of Wallington *et al.* (1986c), the experiments were carried out at 296 K and 740 Torr total pressure at different O_2 partial pressures between 0 and 740 Torr; the rate coefficient of 5.3×10^{-12} cm^3 $molecule^{-1}$ s^{-1} measured in the absence of O_2 was found to increase by factors of 1.3, 1.6 and ~2.0 in the presence of 50, 160 and 740 Torr O_2, respectively. In the work of Barnes *et al.* (1988) carried out at a total pressure of 760 Torr at 298 K, the rate coefficient was observed to increase from 4.4×10^{-12} cm^3 $molecule^{-1}$ s^{-1} in the absence of O_2 by factors of 1.2, 1.5, 1.8 and 2.6 with 50, 100, 155 and 760 Torr partial pressures of O_2. In this work at 299 K, the rate coefficient increases from 5.0×10^{-12} cm^3 $molecule^{-1}$ s^{-1} with ~0 mbar O_2 by factors of approximately 1.6 and 2.0 with 205 and 500 mbar of O_2.

In the work of Hynes *et al.* (1986) at 298 K the measured rate coefficient was found to increase from 4.8×10^{-12} cm^3 $molecule^{-1}$ s^{-1} in 40 Torr N_2 by a factor of 1.3 on replacing N_2 by 750 Torr air, and at 261 K from 4.29×10^{-12} cm^3 $molecule^{-1}$ s^{-1} in 700 Torr N_2 by a factor of approximately 3.0 when measured in 700 Torr of air.

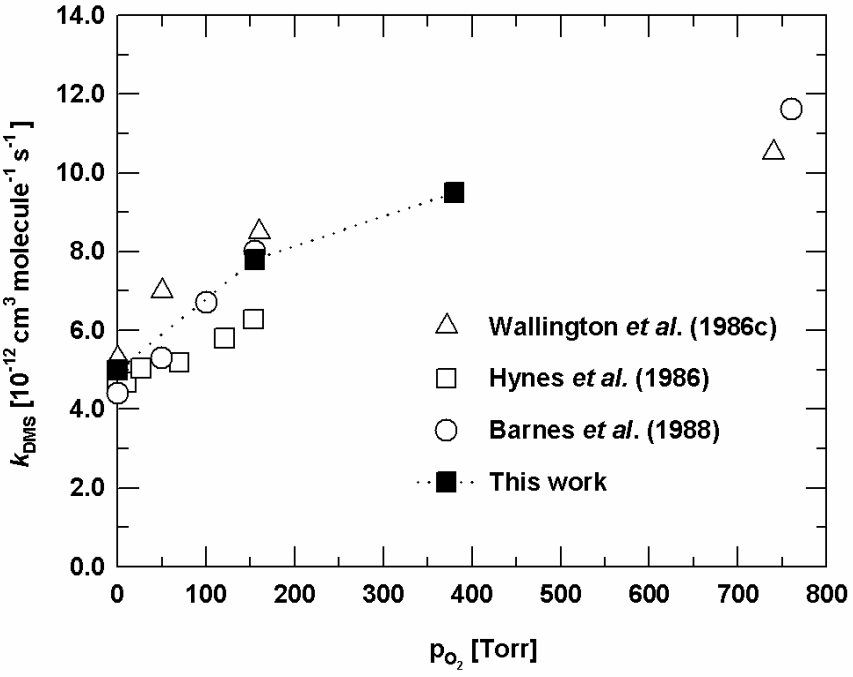

Figure 4.3: Comparison of the literature values with those of the present study for the rate coefficient of DMS with OH radicals as a function of the O_2 partial pressure at room temperature.

In the work of Williams *et al.* (2001) at a temperature of 240 K and a total pressure of 600 Torr, the rate coefficient was found to increase from 5.4 × 10^{-12} cm^3 $molecule^{-1}$ s^{-1} with 5 Torr O_2 by factors of approximately 2.9, 3.9 and 5.2 when using 15, 30 and 120 Torr partial pressures of O_2, respectively. In this work at 260 K, the rate coefficient increases from 6.4 × 10^{-12} cm^3 $molecule^{-1}$ s^{-1} with ~0 mbar O_2 by factors of approximately 3.1 and 3.7 with 205 and 500 mbar of O_2.

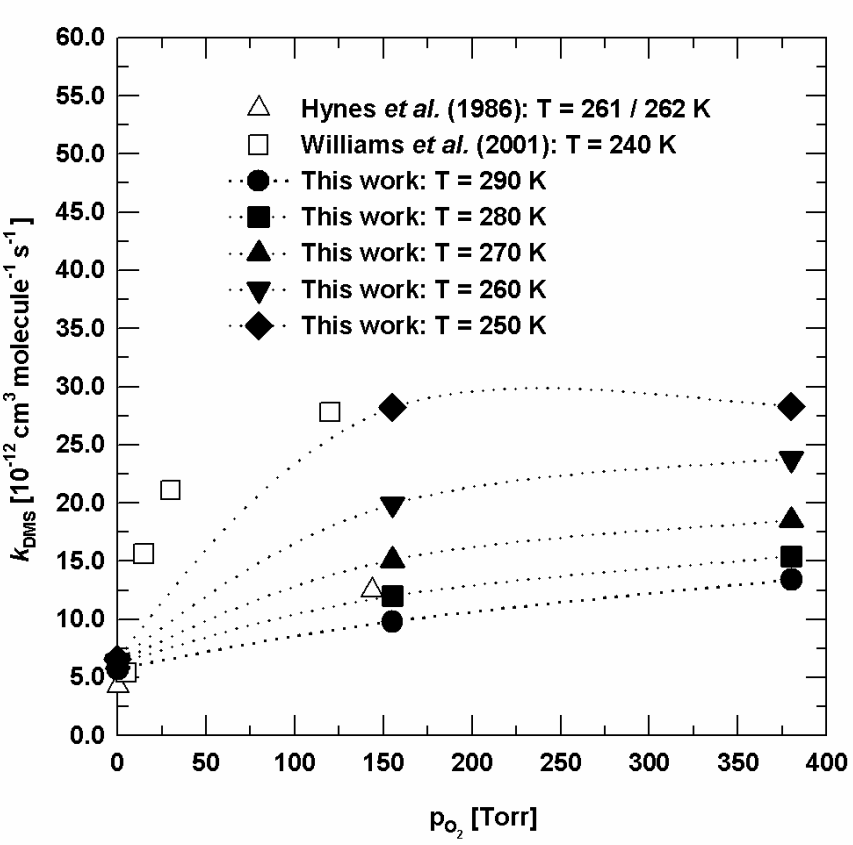

Figure 4.4: Comparison of the literature values with those of the present study for the rate coefficient of DMS with OH radicals as a function of the O_2 partial pressure at temperatures below room temperature.

Table 4.7 shows a comparison between the overall rate coefficient obtained in this work for the reaction of DMS with OH radicals in 1 atm of synthetic air at 299 K and those reported in other studies under similar conditions which are considered free of potential artifacts. The value obtained in this work for atmospheric conditions is in reasonable agreement with the other values determined using relative kinetic techniques (Wallington *et al.*, 1986c; Barnes *et al.*, 1988) but is approximately 20% higher than that determined using an absolute technique (Hynes *et al.*, 1986).

Table 4.7: Rate coefficients for the reaction of DMS with OH radicals at room temperature in air.

$k_{DMS} \times 10^{12a}$	Temperature (K)	Pressure (Torr)	Technique	Authors
6.28 ± 0.10	298	750	PLP-PLIF[b]	Hynes *et al.* (1986)
8.50 ± 0.20	296	740	DS-FTIR[c]	Wallington *et al.* (1986c)
8.00 ± 0.50	298	760	CP-GC[c]	Barnes *et al.* (1988)
7.80 ± 1.80	299	760	CP-FTIR[c]	This work

[a]units: in cm^3 $molecule^{-1}$ s^{-1}; [b]absolute technique: PLP = pulsed laser photolysis, PLIF = pulsed laser induced fluorescence; [c]relative technique: DS = dark source of OH (O_3 + N_2H_4), FTIR = Fourier transform infrared spectroscopy, CP = continuous photolysis, GC = gas chromatography.

Figure 4.5 shows plots of the overall rate coefficients k_{DMS} (abstraction + addition channels) for the reaction of DMS with OH radicals as a function of temperature for:

- Values calculated from the fit expression of Hynes *et al*. (1986) for 1 atm of air.
- Values measured in this work at 1 atm of air (pO_2 = 205 mbar).
- Values calculated from the new recommended fit expression of Atkinson *et al*. (2004) for 1 atm of air (pO_2 = 205 mbar).
- Values measured in this work at 1 atm total pressure and pO_2 = 500 mbar.
- Values calculated from the new recommended fit expression of Atkinson *et al*. (2004) for 1 atm total pressure and pO_2 = 500 mbar.

Unfortunately, the rate coefficient data in the paper of Williams *et al*. (2001) were not given in a tabulated form and thus could not be plotted in Figure 4.5. The data is, however, incorporated into the fit expression given by Atkinson *et al*. (2004) which is plotted in Figure 4.5. An inspection of Figure 4.5 shows that for 1 atmosphere of air and in the temperature range 270 to 299 K, the values determined in this work are somewhat higher but are generally in fair agreement with those calculated from the old fit of Hynes *et al.* (1986) and the new recommended fit given in Atkinson *et al*. (2004) which incorporates the new Williams *et al*. (2001) data. Also shown in Figure 4.5, just for comparison purposes, is a plot of the rate coefficients measured in this study for pO_2 = 500 mbar and the corresponding values calculated with the Atkinson *et al.* (2004) expression. The agreement here is also reasonably good. At temperatures below 270 K our rate coefficient values show a strong increase compared to the values predicted by the empirical fit expression of Hynes *et al*. (1986). The values are, however, in good agreement with the new preferred values calculated from the recommended expression of Atkinson *et al.* (2004) which took into account the data of Williams *et al.* (2001). This work thus confirms the measurements reported by Williams *et al.* (2001).

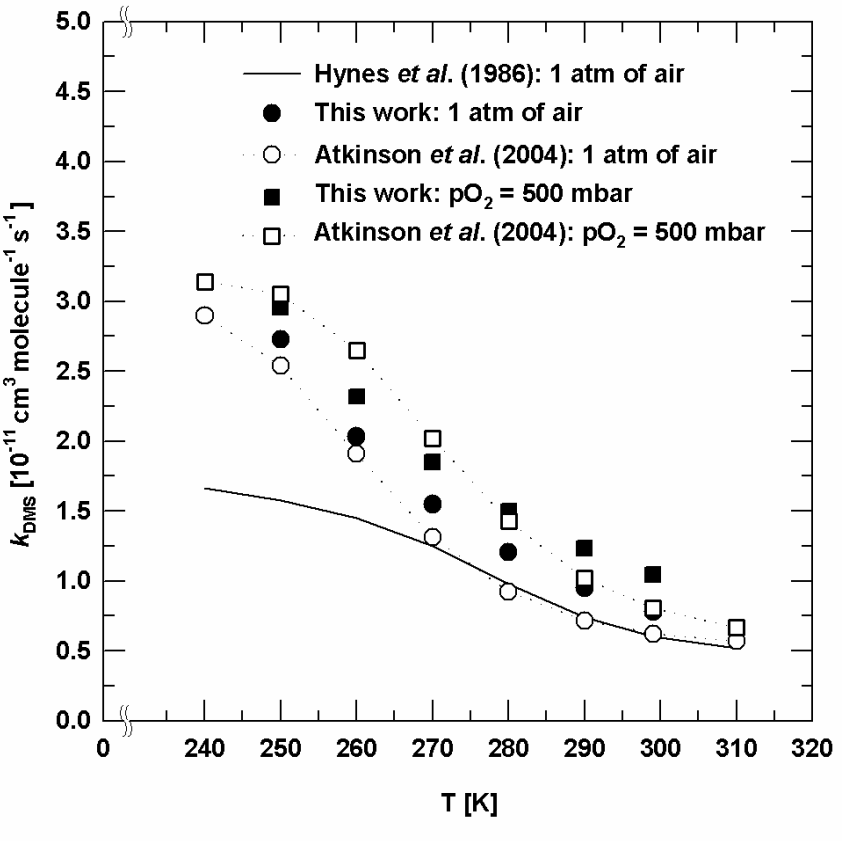

Figure 4.5: Variation in the overall rate coefficient k_{DMS} for the reaction of DMS with OH radicals as a function of temperature as estimated or measured (see text for details).

Figure 4.6 compares the temperature dependence of the branching ratio between the addition and abstraction channel for the reaction of DMS with OH radicals obtained from:

- The empirical expression given in Hynes *et al.* (1986).
- The values given in Williams *et al.* (2001).
- The values measured in this study for the overall reaction at pO_2 = 205 mbar and the value for the abstraction channel taken from Atkinson *et al.* (2004).

The branching ratio is defined as $(k_{obs}-k_{2.1a})/k_{2.1a}$. As is to be expected from the kinetic data, above 270 K there is good agreement between the branching ratios calculated from the different data sets, while below 270 K there is a sharp increase in the branching ratio calculated using the data from this work which matches very well that obtained in the study of Williams *et al*. (2001), but deviates strongly from the values obtained from an extrapolation of the empirical expression of Hynes *et al*. (1986).

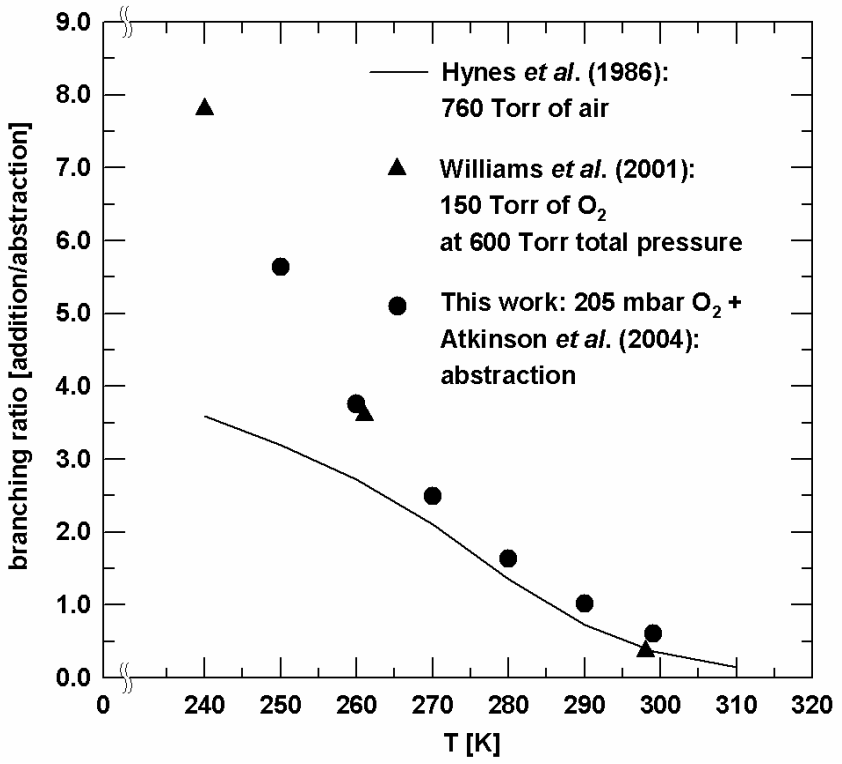

Figure 4.6: Temperature dependence of the branching ratio between the addition and abstraction channel for the reaction of DMS with OH radicals as estimated or measured (see text for details).

At the time of writing, has been published the new work on the kinetics of DMS with OH radicals of Williams *et al*. (2007). They measured the effective rate coefficients as a function of pressure and gas composition at 240 K. In this work they present a predictive expression that gives the effective rate coefficient and branching ratio at low temperature (220 - 260 K) for any atmospheric pressure and oxygen concentration. The expression reproduces the data presented here and published in Albu *et al.* (2006a) at 760 Torr over the range 250 - 270 K.

4.3 Summary of the kinetic results

The kinetics of the OH radical initiated oxidation of DMS in the gas phase were investigated as a function of temperature (250, 260, 270, 280, 290 and 299 K) and O_2 partial pressures (~0, 205 and 500 mbar) at a total pressure of 1000 mbar (O_2 + N_2) using the relative kinetic technique and FTIR spectroscopy for the analysis.

The results obtained in this work using the relative kinetic technique have confirmed the sharp increase in the rate coefficient for the reaction of OH radicals with DMS at temperatures below 270 K observed by Williams *et al*. (2001) using an absolute kinetic

method. The results of this study confirmed the findings of Williams *et al*. (2001) that for 1 atm of air and at temperatures below ~270 K the contribution of the addition pathway is considerably more than was predicted by extrapolation using the previously recommended expression of Hynes *et al*. (1986).

Chapter 5

Product study of the OH radical initiated oxidation of dimethyl sulfide

In this chapter the products observed in the reaction between dimethyl sulfide (DMS) and OH radicals, both in the presence and in the absence of NO_x, will be presented. This study aimed at clarifying the OH radical initiated oxidation mechanism of DMS over an extended temperature range and especially at low temperatures, which has been done for the first time.

Two different series of product experiments were carried out. In the first series of experiments the products of the OH radical initiated oxidation of DMS have been investigated at five different temperatures (260, 270, 280, 290 and 298 K) using the photolysis of methyl nitrite (CH_3ONO) as the OH radical source; the experiments were performed at a total pressure of 1000 mbar synthetic air at different initial NO_x ($NO + NO_2$) concentrations. The initial NO concentration was varied between 0 - 3215 ppbv and that of NO_2 between 0 - 106 ppbv. The results are presented in Paragraph 5.1.1.

In the second series of experiments, the products of the OH radical initiated oxidation of DMS have been investigated at the same five temperatures using the photolysis of hydrogen peroxide (H_2O_2) as the OH radical source, which allows experiments to be performed under NO_x-free conditions. The experiments were performed at a total pressure of 1000 mbar diluent gas ($N_2 + O_2$) at three different O_2 partial pressures (~0, 205 and 500 mbar). The results are also presented in Paragraph 5.1.1.

5.1 Experimental results

In the experiments on the OH radical initiated oxidation of DMS, conducted in the presence of NO_x, the sulfur-containing products identified and quantified by FTIR were dimethyl sulfoxide (DMSO: $CH_3S(O)CH_3$), dimethyl sulfone ($DMSO_2$: $CH_3S(O)_2CH_3$), sulfur dioxide (SO_2) and methyl sulfonyl peroxynitrate (MSPN: $CH_3S(O)_2OONO_2$). The formation of trace amounts of methane sulfonic acid (MSA: $CH_3S(O)_2OH$) was also observed. Non-sulfur-

containing products detected by FTIR included methanol (CH_3OH), formic acid (HCOOH), formaldehyde (HCHO), carbon monoxide (CO), carbon dioxide (CO_2), nitric acid (HNO_3), nitrous acid (HONO), peroxynitric acid (PNA: HO_2NO_2) and methyl nitrate (CH_3ONO_2).

An example of the FTIR spectral data obtained from the evaluation of an experiment on the reaction of OH radicals with DMS in the presence of NO_x is presented in Figure 5.1. Figure 5.1, panel (a) shows the IR spectrum of a DMS (~23.5 ppmv)/CH_3ONO (~15 ppmv)/NO_x (911 ppbv NO + 27 ppbv NO_2) mixture in 1000 mbar synthetic air at 270 K before irradiation. Figure 5.1, panel (b), shows the spectrum obtained after ~12 min irradiation, i.e. ~10% DMS consumption and subtraction of the reactant spectral features. Figure 5.1, panel (c), shows the product spectrum obtained from (b) after subtraction of the spectral features belonging to HCOOH, HCHO, CH_3ONO_2, CH_3OH, HNO_3, PNA, HONO, CO and CO_2. Figure 5.2 shows the concentration-time profiles of DMS and the identified sulfur-containing products for the same experiment.

Examples of the concentration-time profiles of the major sulfur-containing products oberved in the OH radical initiated oxidation of DMS in the presence of NO_x are presented for experiments performed at 260, 270, 280, 290 and 298 K in Figures 5.3 - 5.6.

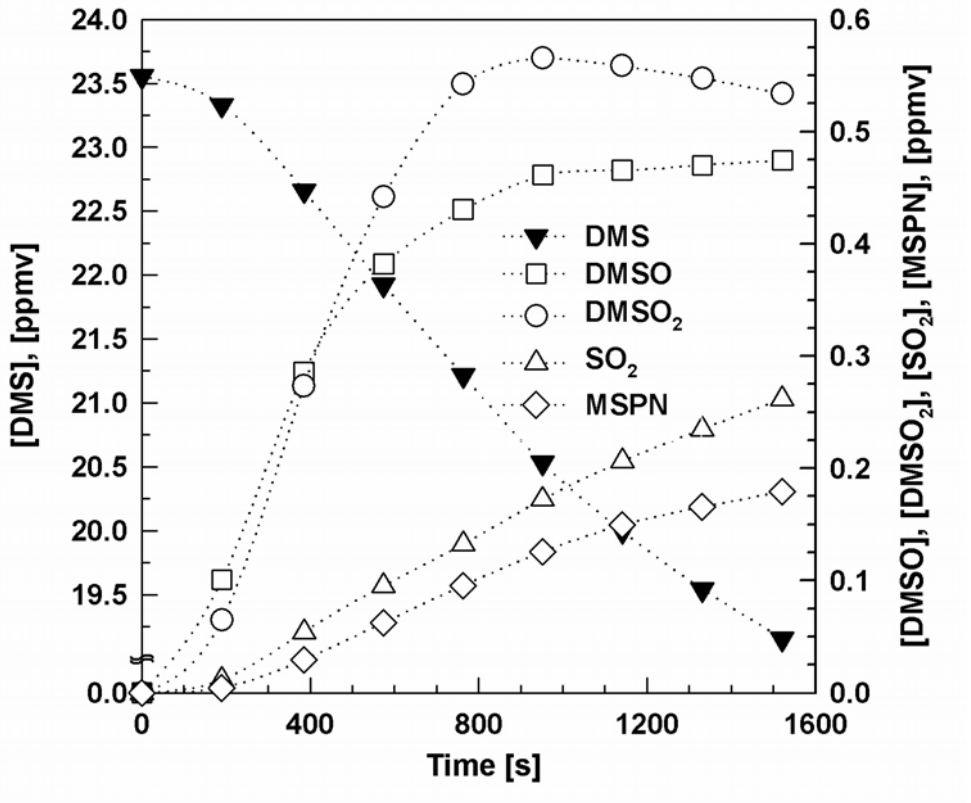

Figure 5.2: Concentration-time profiles of DMS and sulfur-containing oxidation products identified in the reaction of OH radicals with DMS from an experiment performed at 270 K on a DMS (~23.5 ppmv)/CH_3ONO (~15 ppmv)/NO_x (911 ppbv NO + 27 ppbv NO_2) mixture in 1000 mbar total pressure of synthetic air.

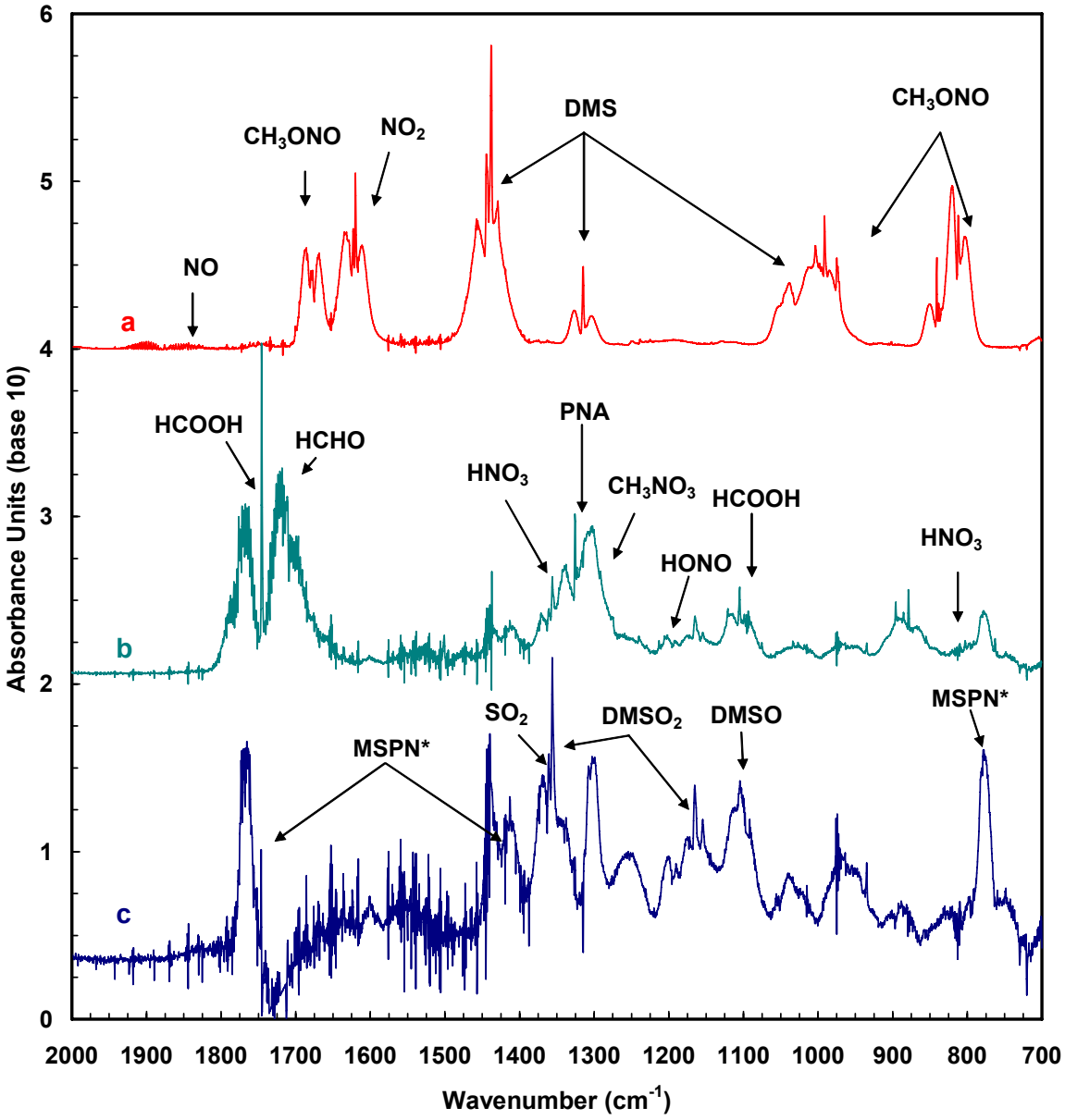

Figure 5.1: IR spectra in the region 2000 - 700 cm^{-1} obtained from the evaluation of a photolysis experiment on a DMS (~23.5 ppmv)/CH_3ONO (~15 ppmv)/NO_x (911 ppbv NO + 27 ppbv NO_2) mixture performed at 270 K in 1000 mbar synthetic air:

a) Spectrum recorded prior to irradiation.

b) Spectrum obtained after ~12 min irradiation (~10% DMS consumed) and subtraction of the reactant spectral features.

c) Product spectrum obtained from b) after subtraction of HCOOH, HCHO, CH_3ONO_2, CH_3OH, HNO_3, PNA, HONO, CO and CO_2.

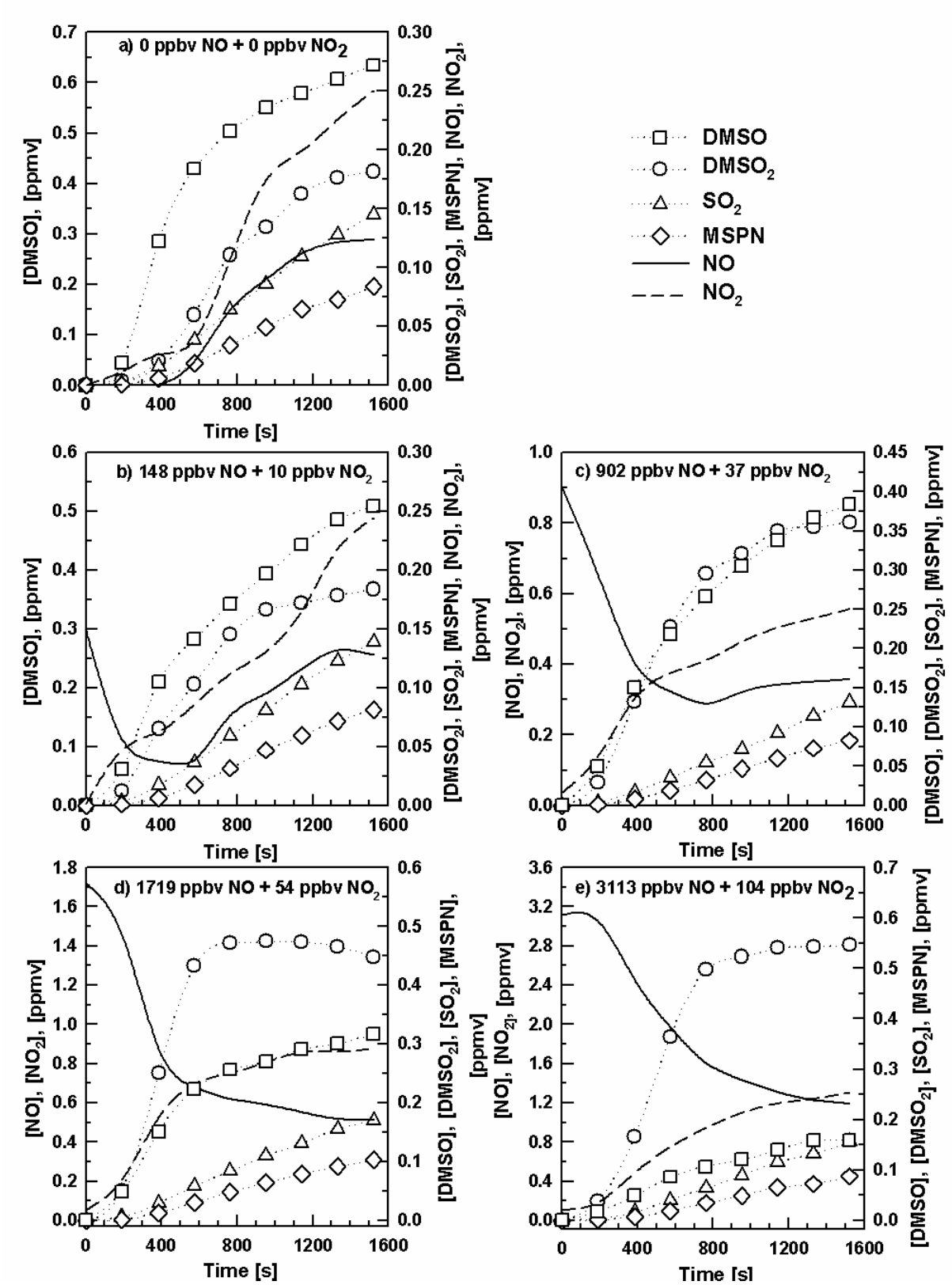

Figure 5.3: Concentration-time profiles for the sulfur-containing oxidation products identified in the reaction of OH radicals with DMS at 260 K in 1000 mbar total pressure of synthetic air with different initial NO_x concentrations.

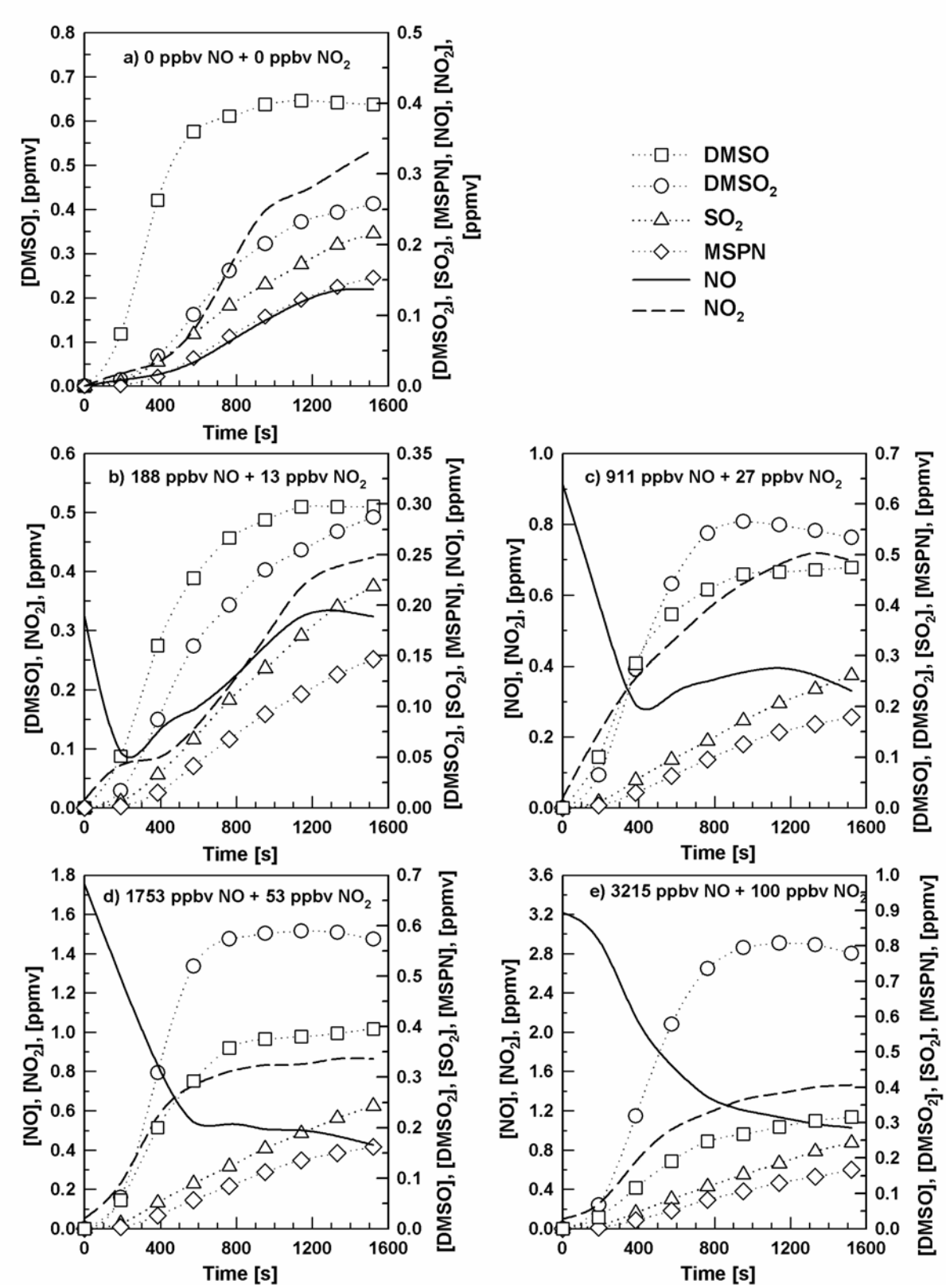

Figure 5.4: Concentration-time profiles for the sulfur-containing oxidation products identified in the reaction of OH radicals with DMS at 270 K in 1000 mbar total pressure of synthetic air with different initial NO_x concentrations.

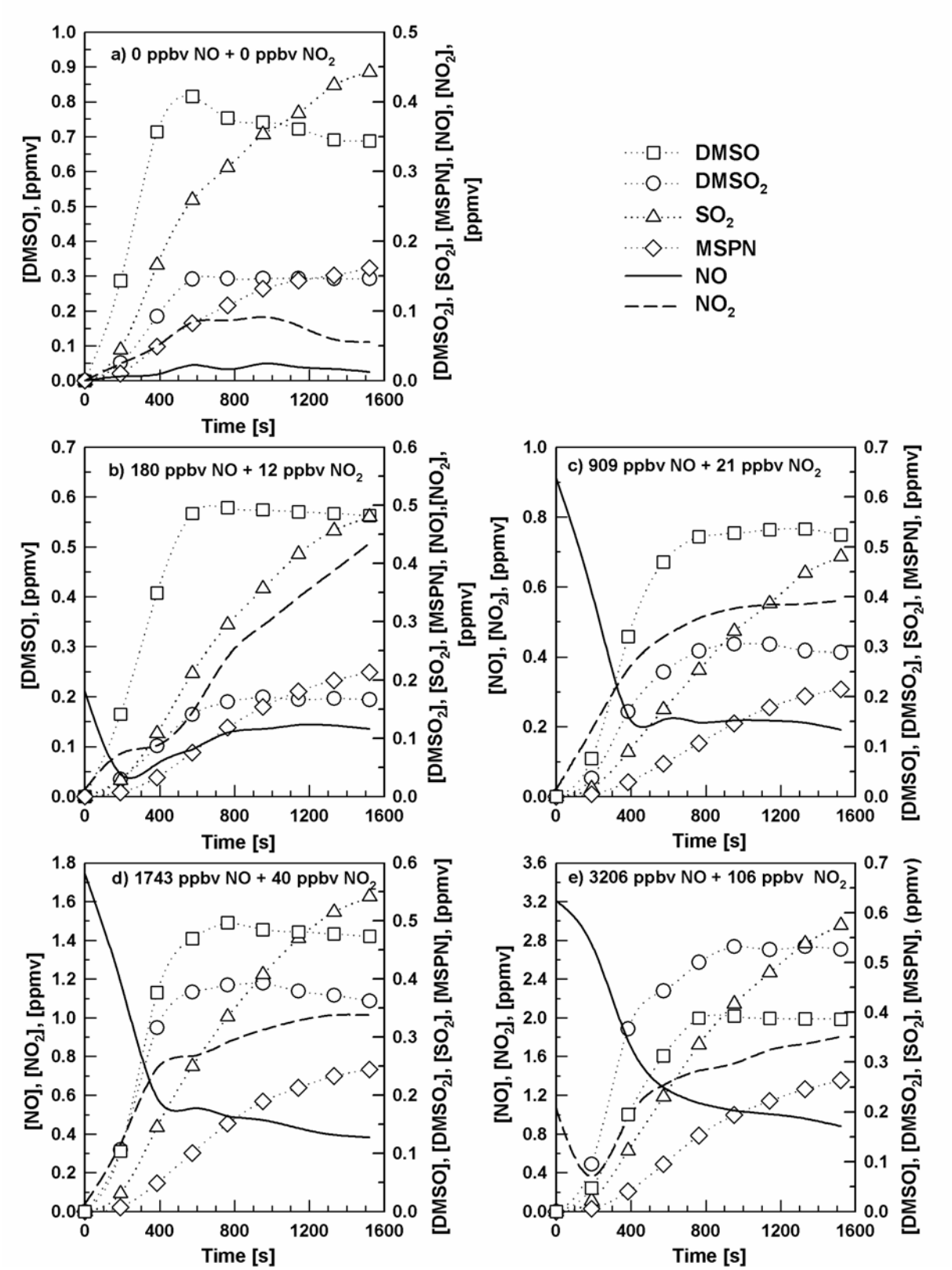

Figure 5.5: Concentration-time profiles for the sulfur-containing oxidation products identified in the reaction of OH radicals with DMS at 280 K in 1000 mbar total pressure of synthetic air with different initial NO_x concentrations.

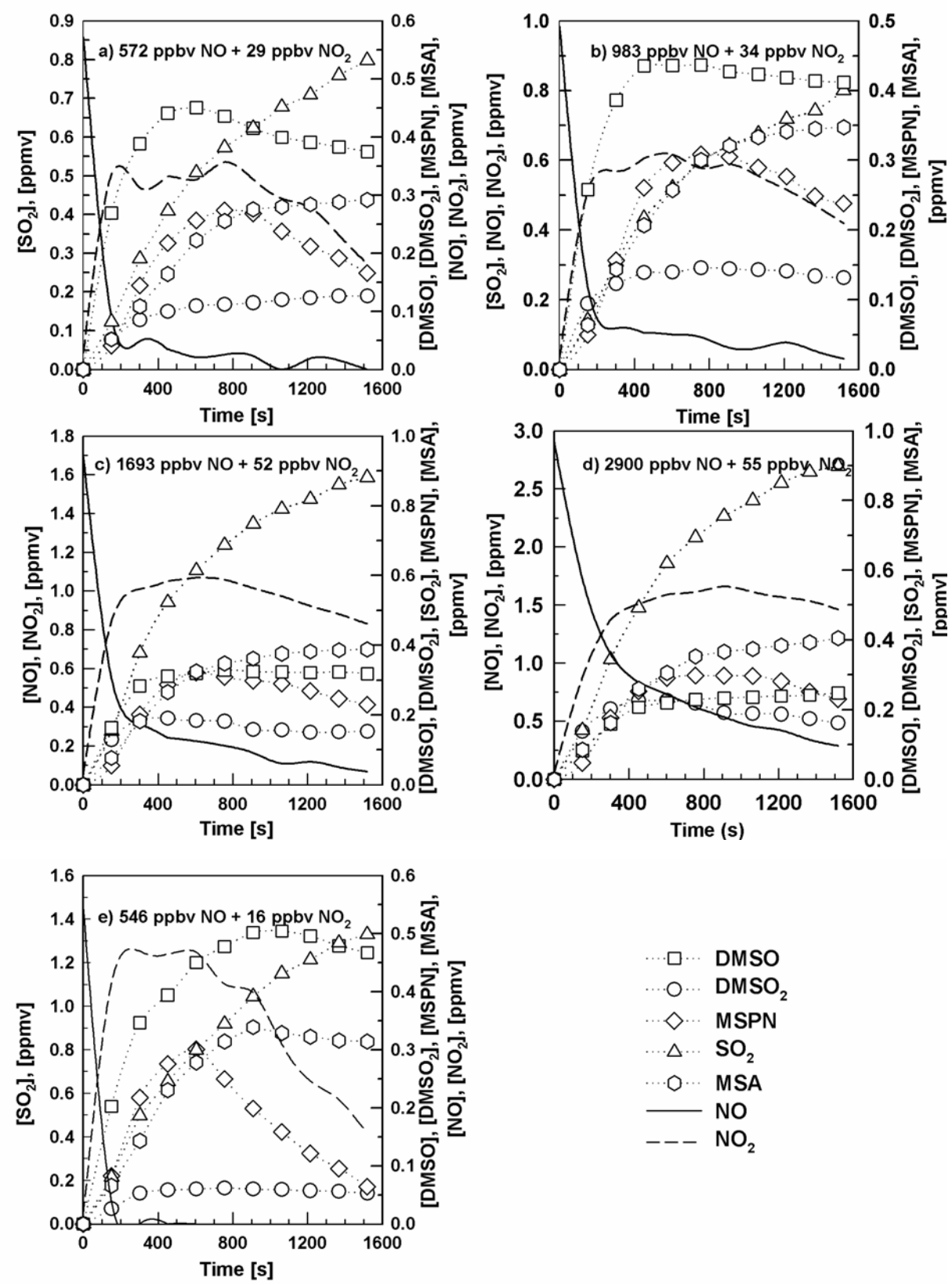

Figure 5.6: Concentration-time profiles for the sulfur-containing oxidation products identified in the reaction of OH radicals with DMS at 290 K (a, b, c, d) and at 298 K (e) in 1000 mbar total pressure of synthetic air with different initial NO_x concentrations.

In the experiments conducted in the absence of NO_x the sulfur-containing products identified and quantified by FTIR were DMSO, $DMSO_2$, SO_2, methyl thiol formate (MTF: CH_3SCHO) and carbonyl sulfide (OCS); the formation of trace amounts of MSA was also observed. Non-sulfur-containing products detected by FTIR included methanol (CH_3OH), formic acid (HCOOH), formaldehyde (HCHO), methyl hydroperoxide (CH_3OOH), carbon monoxide (CO) and carbon dioxide (CO_2). Methane sulfonic acid (MSA: $CH_3S(O)_2OH$) and methane sulfinic acid (MSIA: $CH_3S(O)OH$) were identified by IC.

Figure 5.7 shows the concentration-time profiles of DMS and sulfur-containing oxidation products from an experiment performed at 270 K on a DMS (~14 ppmv)/H_2O_2 (~25 ppmv) mixture in 1000 mbar total pressure of synthetic air.

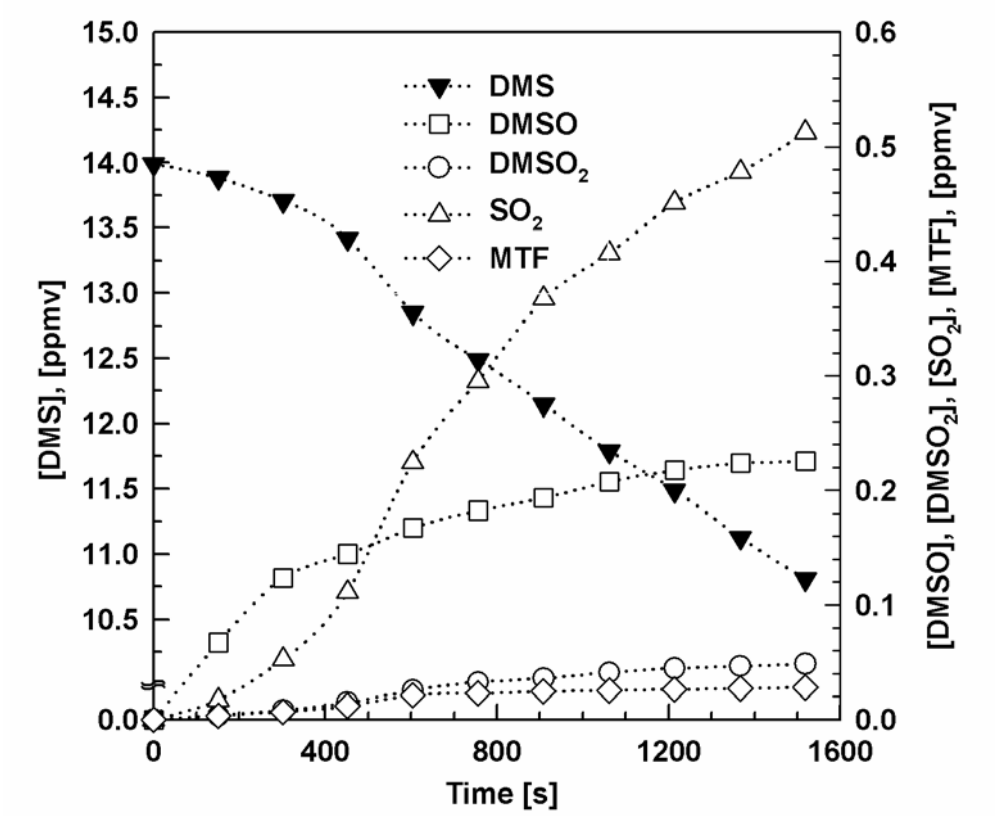

Figure 5.7: Concentration-time profiles of DMS and sulfur-containing oxidation products identified in the reaction of OH radicals with DMS from an experiment performed at 270 K on a DMS (~14 ppmv)/H_2O_2 (~25 ppmv) mixture in 1000 mbar total pressure of synthetic air in the absence of NO_x.

The concentration-time profiles of the sulfur-containing products shown in Figures 5.2 - 5.7 have not been corrected for secondary loss processes. The plots of the concentrations of the identified products versus time indicate that secondary reaction and/or wall losses of some primary products, i.e. DMSO, $DMSO_2$ and MTF, occurred during the experiments. The shapes of these product curves are determined by their production from DMS oxidation and loss processes such as reaction with OH radicals and/or wall loss (DMSO, $DMSO_2$) and photolysis (MTF). The SO_2 curves do not appear be strongly influenced by loss processes.

5.1.1 Dimethyl sulfoxide (DMSO)

DMSO was identified using FTIR spectroscopy and quantified using calibrated spectra. Calibrations were performed for each of the temperatures at which the experiments were perfomed. The Intergated Band Intensities (IBI) values for DMSO are presented in Appendix II. The quantification of DMSO, especially at the end of the experiments, was affected by the formation of formic acid, a compound whose spectral features overlap those of DMSO in the wave number range 1046 - 1148 cm^{-1}.

In Figures 5.2 - 5.7, where concentration-time profiles of the formation of DMSO are shown, it is evident that this compound is not an end-product of the oxidation of DMS. An increase in the DMSO concentration during the first minutes of the experiments is observed followed, in many cases, by a nearly steady state concentration of DMSO.

Results from NO_x-containing experiments:

The plots of the measured yield-time profiles for DMSO as a function of initial NO_x concentrations for all five temperatures studied (260, 270, 280, 290 and 298 K) are shown in Figure 5.8. From Figure 5.8 it can be seen that the yield-time behaviour of DMSO varied systematically with changes in temperature and initial NO_x concentration. The uncorrected yield-time profiles for DMSO show that at each temperature and for every initial NO_x concentration, the yield of DMSO initially increases, passes through a maximum and then decreases. The DMSO yield is strongly dependent on the initial NO_x concentration; increasing the initial NO_x concentration systematically depressed the DMSO yield maximum at each of the temperatures investigated.

The shapes of the curves for DMSO are determined by production from DMS oxidation and loss processes, i.e. loss to the reactor walls and further oxidation of DMSO by OH radicals. To derive the exact formation yields of DMSO its measured concentration has to be corrected for further reaction with OH radicals and wall loss. Corrections were performed using the mathematical procedure described in Section 3.4.2. The rate

coefficients used for the reaction of DMS with OH radicals were taken from the study of Albu *et al.* (2006a). The rate coefficient for the reaction of OH radicals with DMSO is associated with a high degree of uncertainty (Barnes *et al.*, 1989; Hynes and Wine, 1996; Urbanski *et al.*, 1998; Falbe-Hansen *et al.*, 2000; Kukui *et al.*, 2003; Resende *et al.*, 2005; González-Garcia *et al.*, 2006). For the purposes of the DMSO yield corrections, the Arrhenius expression (k_{DMSO} = $10^{-11.2\pm0.7}$ exp(800 $\pm$ 540/T) cm^3 $molecule^{-1}$ s^{-1}) from Hynes and Wine (1996) was used to calculate the rate coefficients for the individual temperatures.

DMSO is a sticky compound, and DMSO wall loss caused some experimental difficulties. Wall loss was observed at all five temperatures and the rate of this loss was found to differ significantly not only from one temperature to another but also from one experiment to another (from 4×10^{-4} s^{-1} to 3×10^{-3} s^{-1}). Consequently, the maximum value obtained in dark experiments for the first order loss rate of DMSO, for each temperature, was used in the yield correction calculations.

Plots of the corrected DMSO concentration versus the amount of DMS consumed for all of the five temperatures studied, 260, 270, 280, 290 and 298 K, and the different initial NO_x concentrations are shown in Figure 5.9.

From the representations in Figure 5.9 the yield of DMSO for every set of experimental conditions, specific temperature and NO_x concentration, can be determined from the slopes of the linies. In Figure 5.9e, at 298 K, the plot for DMSO shows two distinct linear periods: the short initial period gives a lower DMSO yield than that determined in the second period. The change in the DMSO yield occurs at the point, where the NO concentration approaches zero; this behaviour is attributed to a change in the reaction mechanism as will be discussed in Paragraph 5.2.

The corrected formation yields of DMSO, obtained by the linear regression analysis, are presented in Table 5.1. In Table 5.1 the yields of DMSO are also compared to the fraction of the reaction occurring *via* the addition reaction pathway for the specific reaction conditions calculated using the results of Albu *et al.* (2006a) and Atkinson *et al.* (2004).

From Table 5.1 it can be seen that the yield of DMSO is strongly dependent on the temperature and on the initial NO_x concentration: (i) it decreases with increasing temperature and (ii) decreases with increasing NO_x concentration.

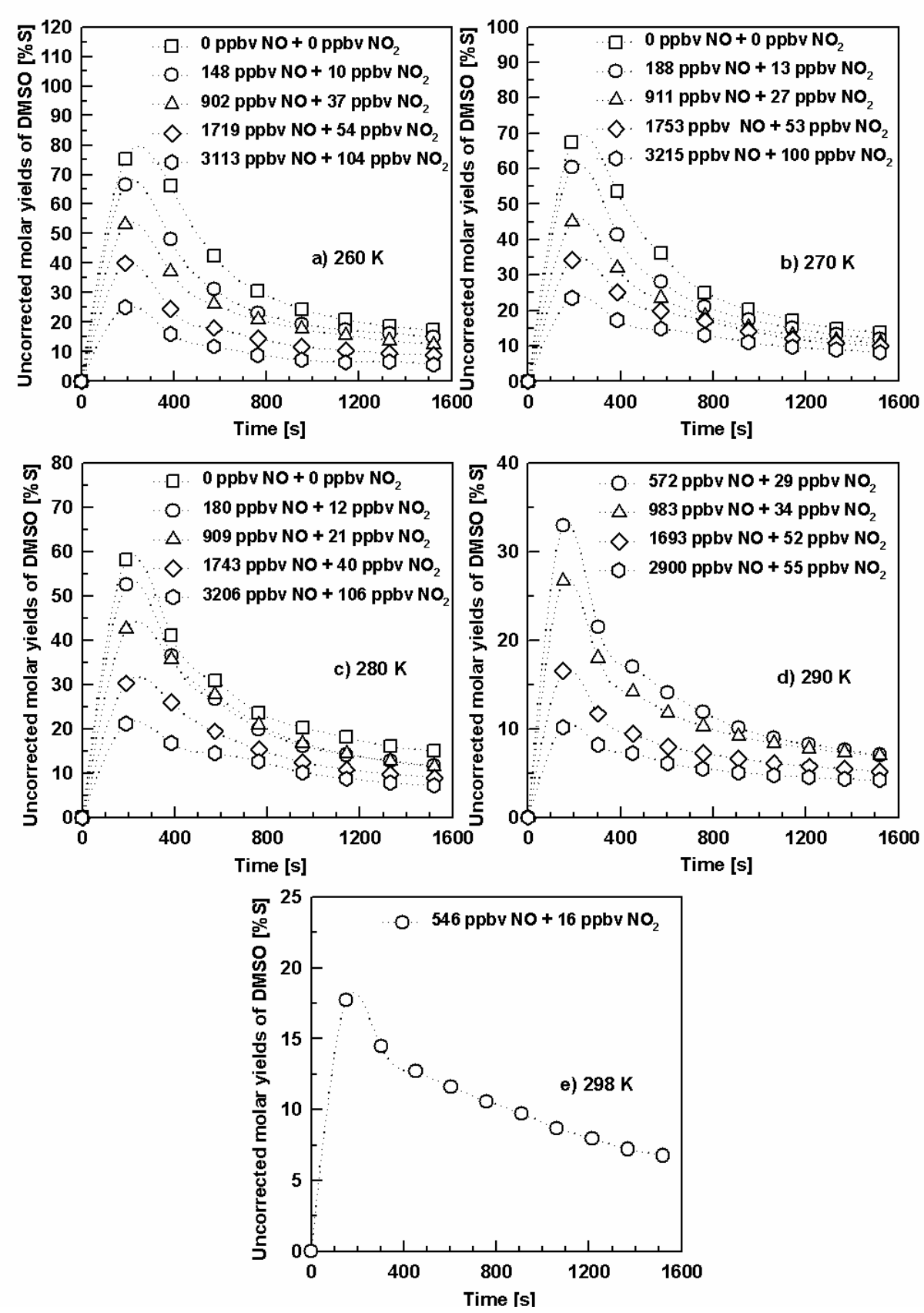

Figure 5.8: Plots of the uncorrected molar yields of DMSO, determined in 1000 mbar of synthetic air at a) 260 K, b) 270 K, c) 280 K, d) 290 K and e) 298 K for different initial NO_x concentration, versus reaction time.

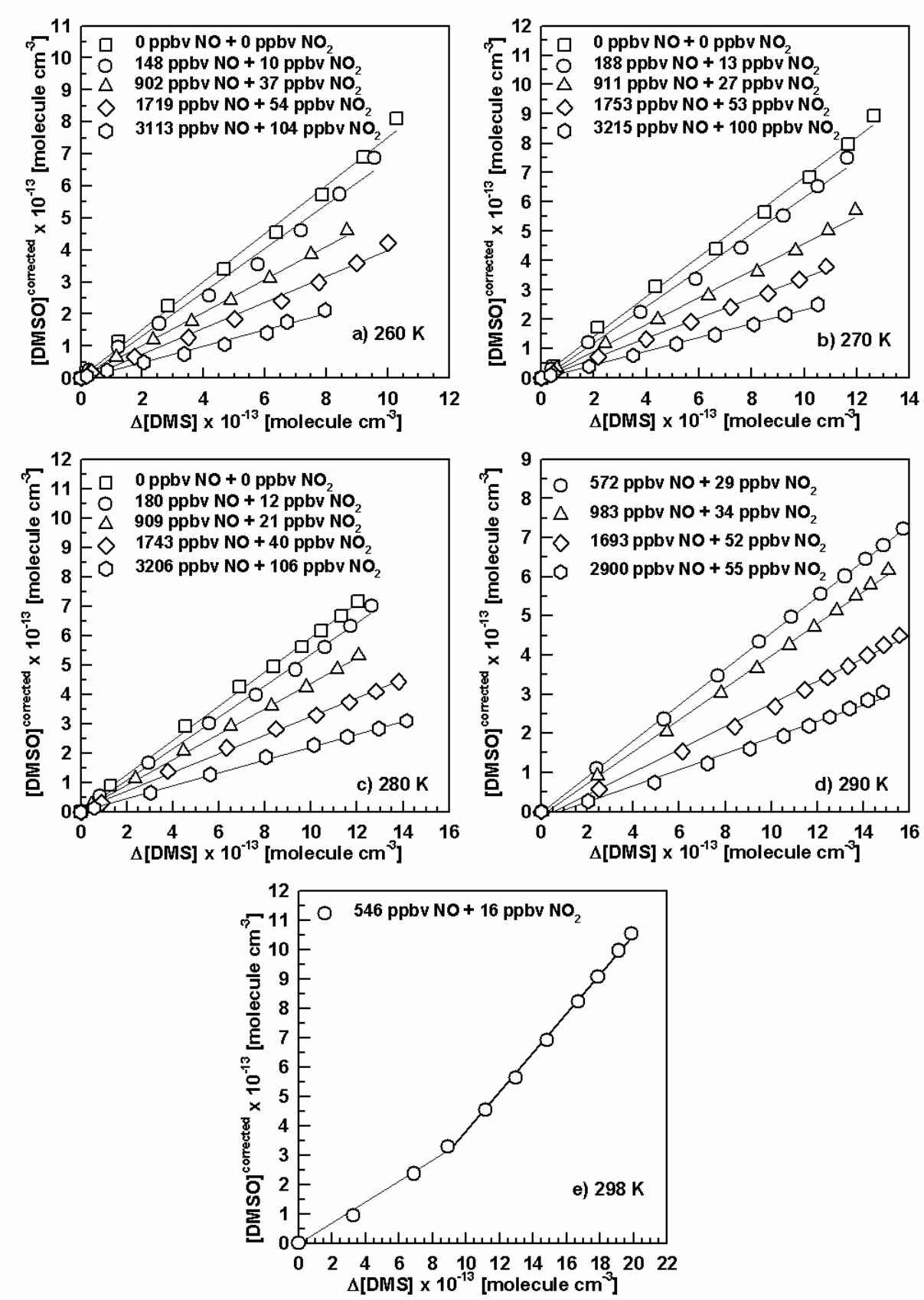

Figure 5.9: Plots of the corrected DMSO concentrations, determined in 1000 mbar synthetic air at a) 260 K, b) 270 K, c) 280 K, d) 290 K and e) 298 K for different initial NO_x concentrations, versus the consumption of DMS.

Table 5.1: Corrected yields for the formation of DMSO in the OH radical initiated oxidation of DMS in 1000 mbar synthetic air as a function of temperature and initial NO_x concentration.

Temperature (K)	NO (ppbv)	NO_2 (ppbv)	Corrected DMSO yields (% molar yield, $\pm 2\sigma$)	Contribution of addition pathway* (%)
260	0	0	75.05 ± 3.70	~ 79
	148	10	68.17 ± 4.78	
	902	37	51.64 ± 1.84	
	1719	54	40.43 ± 2.56	
	3113	104	25.48 ± 2.10	
270	0	0	67.86 ± 3.72	~ 71
	188	13	61.96 ± 3.22	
	911	27	46.05 ± 1.87	
	1753	53	34.40 ± 0.86	
	3215	100	23.40 ± 0.65	
280	0	0	58.05 ± 1.64	~ 62
	180	12	53.52 ± 3.92	
	909	21	43.24 ± 0.92	
	1743	40	31.67 ± 0.96	
	3206	106	21.99 ± 0.46	
290	572	29	45.93 ± 0.37	~ 50
	983	34	40.89 ± 0.92	
	1693	52	29.11 ± 1.20	
	2900	55	20.72 ± 1.34	
298	546	16	36.98 ± 5.06	~ 39

**fraction of the reaction occurring via the addition pathway calculated for the specific reaction conditions using the results of Albu et al. (2006a) - addition and Atkinson et al. (2004) - abstraction.*

Results from NO_x-free experiments:

In the experiments where H_2O_2 was used as the OH radical source, DMSO can only be measured accurately within the first couple of minutes of irradiation, since the concentration of DMSO quickly falls to very low levels.

The measured yield-time profiles for DMSO for all five temperatures studied, 260, 270, 280, 290 and 298 K, are plotted as a function of O_2 partial pressure, ~0, 205 and 500 mbar, in Figure 5.10. From Figure 5.10 it can be seen that the yield-time behaviour of DMSO varied with changes in temperature and O_2 partial pressure. At ~0 mbar O_2 partial pressure, the yield of DMSO was zero for all five temperatures and at a constant temperature the yield increases slightly with increasing O_2 partial pressure. As in the NO_x-containing experiments, the shapes of the DMSO yield curves, at 205 and 500 mbar O_2 partial pressure, are determined by production from DMS oxidation and loss processes, i.e. further oxidation of DMSO by OH radicals and wall loss.

The measured yield-time data for DMSO have been corrected for wall loss and reaction with OH radicals using the mathematical procedure described in Section 3.4.2. Plots of the corrected DMSO concentration versus the amount of DMS consumed for all five temperatures studied and the different initial O_2 partial pressures are shown in Figure 5.11.

The corrected DMSO yields determined from Figure 5.11 are presented in Table 5.2. In Table 5.2 the yields of DMSO are also compared to the fraction of the reaction occurring *via* the addition reaction pathway calculated using the results of Albu *et al.* (2006a) and Atkinson *et al.* (2004) for the specific reaction conditions.

From Table 5.2 it can be seen that: (i) for all five temperatures studied, at ~0 mbar O_2 partial pressure, the formation of DMSO was not observed, (ii) in synthetic air, the yield of DMSO decreases with increasing temperature and (iii) for the same temperature, the yield of DMSO increases with increasing O_2 partial pressure.

Table 5.2: Corrected yields for the formation of DMSO in the OH radical initiated oxidation of DMS in 1000 mbar diluent gas, as a function of temperature and O_2 partial pressure, in the absence of NO_x.

Temperature (K)	pO_2 (mbar)	Corrected DMSO yields (% molar yield, $\pm 2\sigma$)	Contribution of addition pathway* (%)
260	~0	0.00 ± 0.00	
	205	73.03 ± 2.09	~ 79
	500	82.96 ± 2.50	~ 82
270	~0	0.00 ± 0.00	
	205	66.99 ± 6.94	~ 71
	500	74.52 ± 4.06	~ 76
280	~0	0.00 ± 0.00	
	205	62.25 ± 3.22	~ 62
	500	69.10 ± 3.88	~ 70
290	~0	0.00 ± 0.00	
	205	51.43 ± 3.98	~ 50
	500	55.81 ± 1.98	~ 62
298	~0	0.00 ± 0.00	
	205	38.56 ± 1.36	~ 39
	500	48.80 ± 2.52	~ 55

**fraction of the reaction occurring via the addition pathway calculated for the specific reaction conditions using the results of Albu et al. (2006a) - addition and Atkinson et al. (2004) - abstraction.*

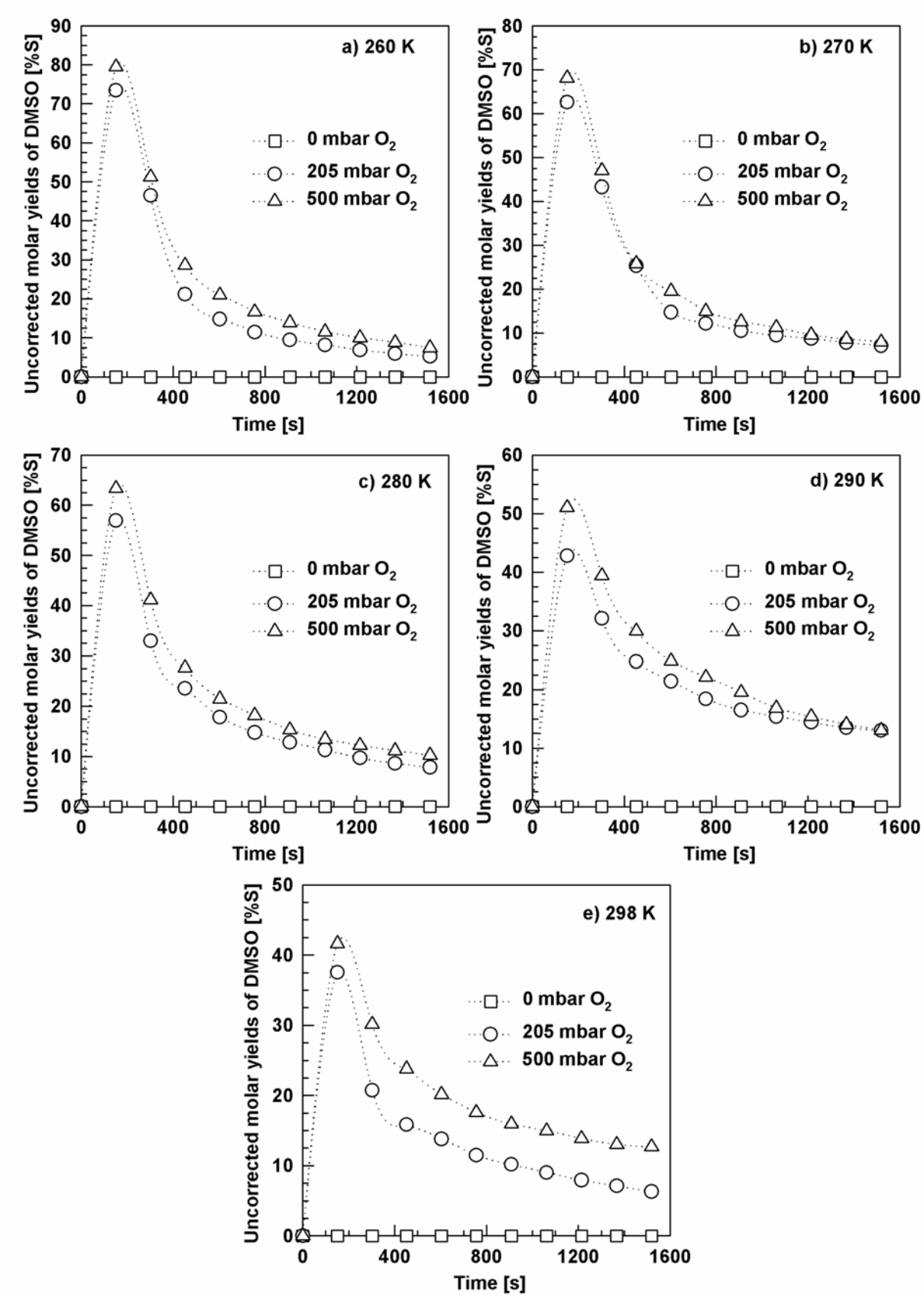

Figure 5.10: Plots of the uncorrected molar yields of DMSO, determined in the absence of NO_x in 1000 mbar diluent gas at a) 260 K, b) 270 K, c) 280 K, d) 290 K and e) 298 K for different O_2 partial pressures (~0, 205 and 500 mbar), versus reaction time.

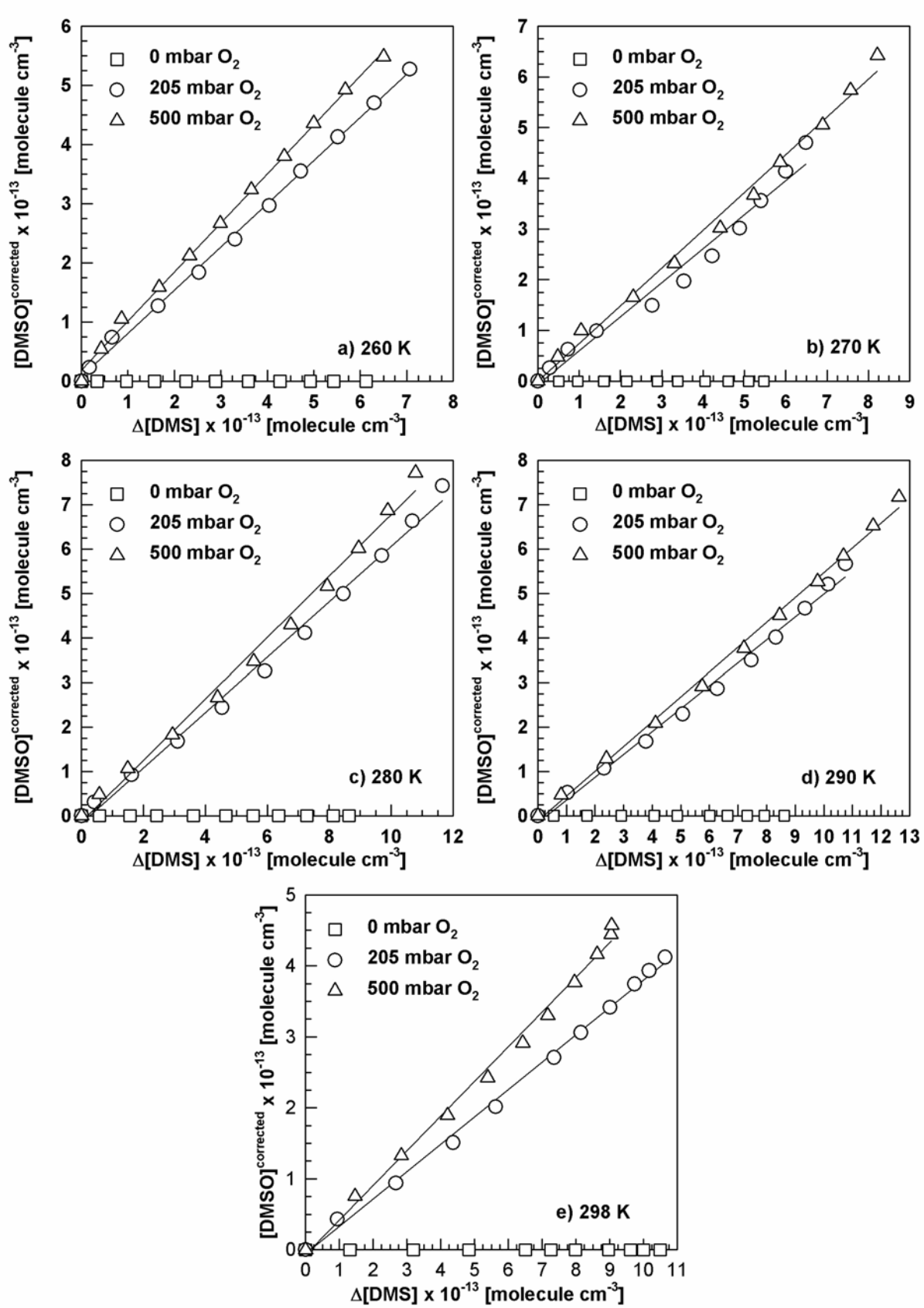

Figure 5.11: Plots of the corrected DMSO concentrations, determined in the absence of NO_x in 1000 mbar diluent gas at a) 260 K, b) 270 K, c) 280 K, d) 290 K and e) 298 K for different O_2 partial pressures (~0, 205 and 500 mbar), versus the consumption of DMS.

5.1.2 Dimethyl sulfone ($DMSO_2$)

$DMSO_2$ was determined by FTIR spectroscopy using the characteristic spectral features of $DMSO_2$ in the wave number ranges: 895 - 970 cm^{-1}, 1125 - 1216 cm^{-1} and 1300 - 1385 cm^{-1}. All three bands were used for the substraction, but quantification was made using the band in the region 1125 - 1216 cm^{-1}. Calibrated spectra, obtained in the same reaction chamber, were used for quantification. The IBI values for $DMSO_2$ are listed in Appendix II.

In Figures 5.2 - 5.7, where concentration-time profiles of the formation of $DMSO_2$ are shown, an increase in the $DMSO_2$ concentration during the first minutes of the experiments is oberved, followed by a nearly steady-state concentration of $DMSO_2$.

Results from NO_x-containing experiments:

The plots of the measured yield-time profiles for $DMSO_2$ as a function of initial NO_x concentrations for all five temperatures studied, 260, 270, 280, 290 and 298 K, are shown in Figure 5.12.

Figure 5.12 shows that for each temperature the $DMSO_2$ yield is strongly dependent on the initial NO_x concentration; the observed yield of $DMSO_2$ increases with increasing NO_x concentration. The shapes of the curves for $DMSO_2$ are determined by production from DMS oxidation and loss processes, i.e. loss to the reactor walls. The reaction between $DMSO_2$ and OH radicals is slow and will not be important in the system: at room temperature a rate coefficient of $k_{DMSO2} < 3 \times 10^{-13}$ cm^3 $molecule^{-1}$ s^{-1} has been reported by Falbe-Hansen *et al.* (2000), and an upper limit of $(1.6 \pm 1.0) \times 10^{-13}$ cm^3 $molecule^{-1}$ s^{-1} was estimated by Patroescu (1996). $DMSO_2$ was lost at all five temperatures to the wall of the reaction chamber and the rate of this loss differ from one temperature to another (from 2×10^{-4} s^{-1} to 4×10^{-3} s^{-1}). The maximum value obtained in dark experiments for the first order loss rate of $DMSO_2$, for each temperature, was used in the yield correction calculations. Corrections were performed using the mathematical procedure described in Section 3.4.2.

Plots of the corrected $DMSO_2$ concentrations versus the amount of DMS consumed for all five temperatures studied, 260, 270, 280, 290 and 298 K, and the different initial NO_x concentrations are shown in Figure 5.13.

The yield of $DMSO_2$ for every set of specific experimental conditions, temperature and NO_x concentration, have been obtained from the plots in Figure 5.13. The corrected formation yields of $DMSO_2$ were determined from linear regression analysis of the slopes of the linies and are presented in Table 5.3.

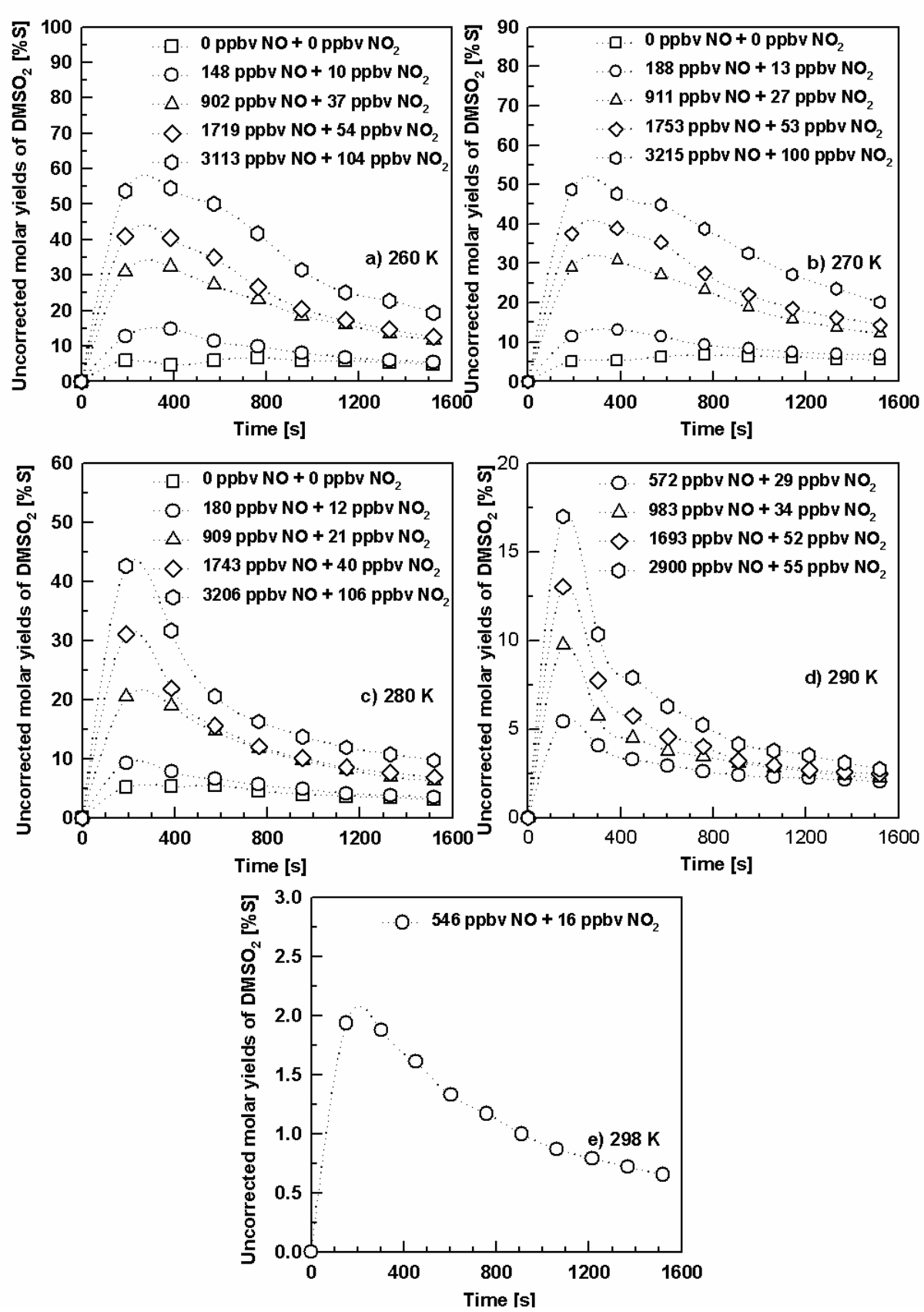

Figure 5.12: Plots of the uncorrected molar yields of $DMSO_2$, determined in 1000 mbar of synthetic air at a) 260 K, b) 270 K, c) 280 K, d) 290 K and e) 298 K for different initial NO_x concentration, versus reaction time.

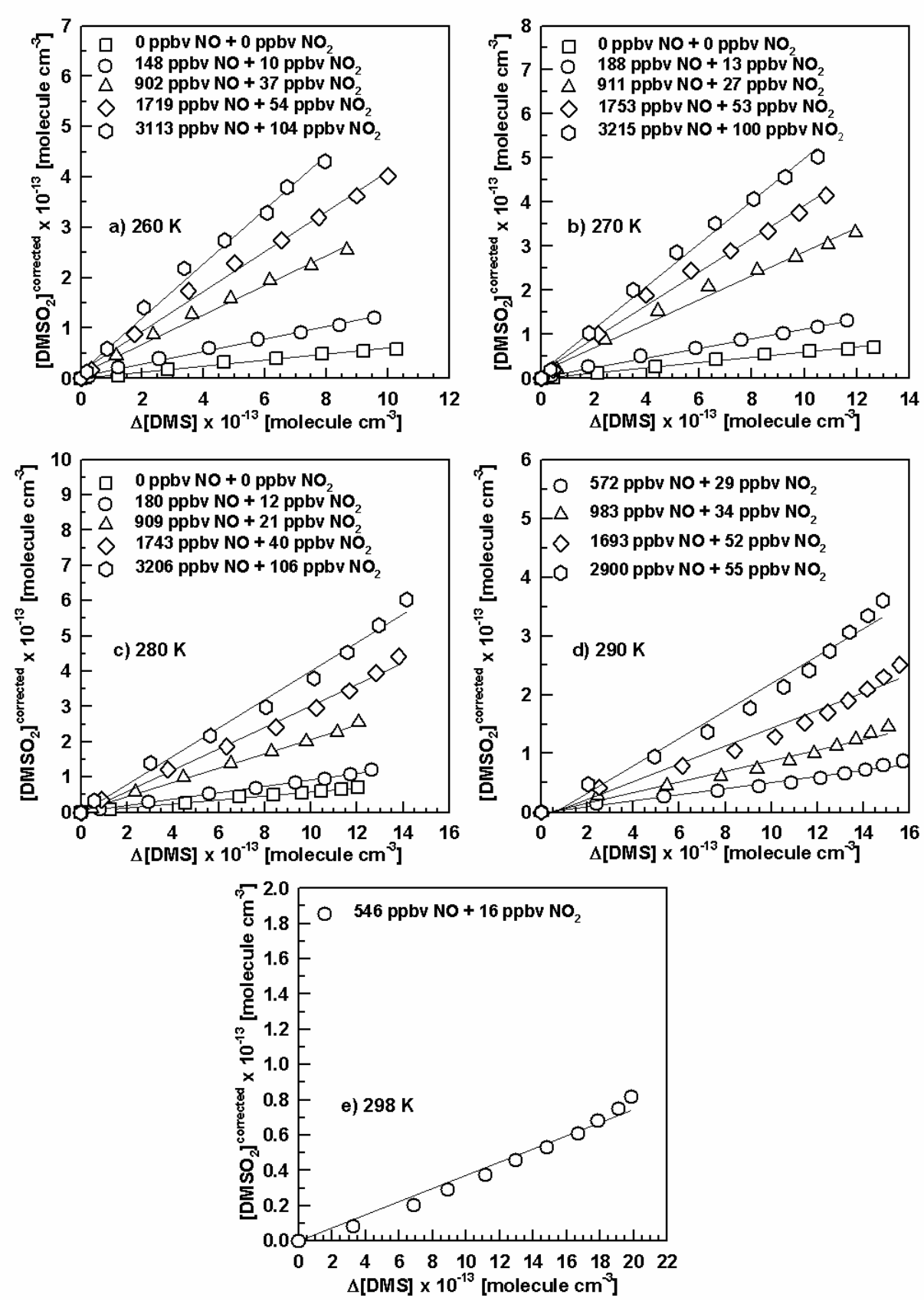

Figure 5.13: Plots of the corrected $DMSO_2$ concentrations, determined in 1000 mbar synthetic air at a) 260 K, b) 270 K, c) 280 K, d) 290 K and e) 298 K for different initial NO_x concentrations, versus the consumption of DMS.

Table 5.3: Corrected yields for the formation of $DMSO_2$ in the OH radical initiated oxidation of DMS in 1000 mbar synthetic air as a function of temperature and initial NO_x concentration.

Temperature (K)	NO (ppbv)	NO_2 (ppbv)	$DMSO_2$ yield (% molar yield, $\pm 2\sigma$)
260	0	0	5.95 ± 0.45
	148	10	12.33 ± 0.64
	902	37	29.25 ± 1.92
	1719	54	39.58 ± 2.44
	3113	104	53.87 ± 3.44
270	0	0	5.83 ± 0.48
	188	13	10.91 ± 0.52
	911	27	27.37 ± 2.14
	1753	53	37.76 ± 2.44
	3215	100	48.35 ± 3.06
280	0	0	5.74 ± 0.30
	180	12	9.07 ± 0.32
	909	21	20.40 ± 0.66
	1743	40	30.36 ± 1.86
	3206	106	40.32 ± 2.84
290	572	29	5.19 ± 0.48
	983	34	9.12 ± 0.95
	1693	52	15.21 ± 1.70
	2900	55	23.45 ± 2.26
298	546	16	4.08 ± 0.32

From Table 5.3 it can be seen that the yield of $DMSO_2$ is strongly dependent on the temperature and on the initial NO_x concentration: (i) it decreases with increasing temperature and (ii) increases with increasing NO_x concentration.

Results from NO_x-free experiments:

The measured yield-time profiles for $DMSO_2$ obtained in experiments using H_2O_2 as the OH radical source are shown in Figure 5.14 for all the temperatures, 260, 270, 280, 290 and 298 K, and O_2 partial pressures, ~0, 205 and 500 mbar, employed in the measurements. From Figure 5.14 it can be seen that for a constant temperature, increasing the O_2 partial pressure results in an increase of the $DMSO_2$ yield and for a constant O_2 partial pressure increasing the temperature appears to results in a slight increase of the $DMSO_2$ yield. In Figure 5.14 the yields of $DMSO_2$ are not corrected for secondary loss processes such as wall

loss. Corrections were performed using the mathematical procedure described in Section 3.4.2.

Plots of the corrected $DMSO_2$ concentration versus the amount of DMS consumed, for all five temperatures studied and the different O_2 partial pressure are shown in Figure 5.15. The corrected formation yields of $DMSO_2$ obtained by linear regression analysis of the plots in Figure 5.15 are collected in Table 5.4.

Table 5.4: Corrected yields for the formation of $DMSO_2$ in the OH radical initiated oxidation of DMS in 1000 mbar diluent gas, as a function of temperature and O_2 partial pressure, in the absence of NO_x.

Temperature (K)	pO_2 (mbar)	$DMSO_2$ yield (% molar yield, $\pm 2\sigma$)
260	~0	1.07 ± 0.05
	205	1.57 ± 0.07
	500	2.12 ± 0.11
270	~0	1.73 ± 0.10
	205	3.20 ± 0.10
	500	3.83 ± 0.10
280	~0	2.74 ± 0.07
	205	3.94 ± 0.19
	500	4.53 ± 0.15
290	~0	2.86 ± 0.07
	205	4.04 ± 0.15
	500	4.96 ± 0.20
298	~0	2.90 ± 0.20
	205	4.13 ± 0.22
	500	5.49 ± 0.32

From Table 5.4 it can be seen that the formation yield of $DMSO_2$ is slightly dependent on the temperature and on the O_2 partial pressure: (i) it increases with increasing O_2 partial pressure for a constant temperature and (ii) it increases with increasing temperature for a constant O_2 partial pressure. The yields of $DMSO_2$ after correction are quite variable, however, in total they represent no more than 6% S.

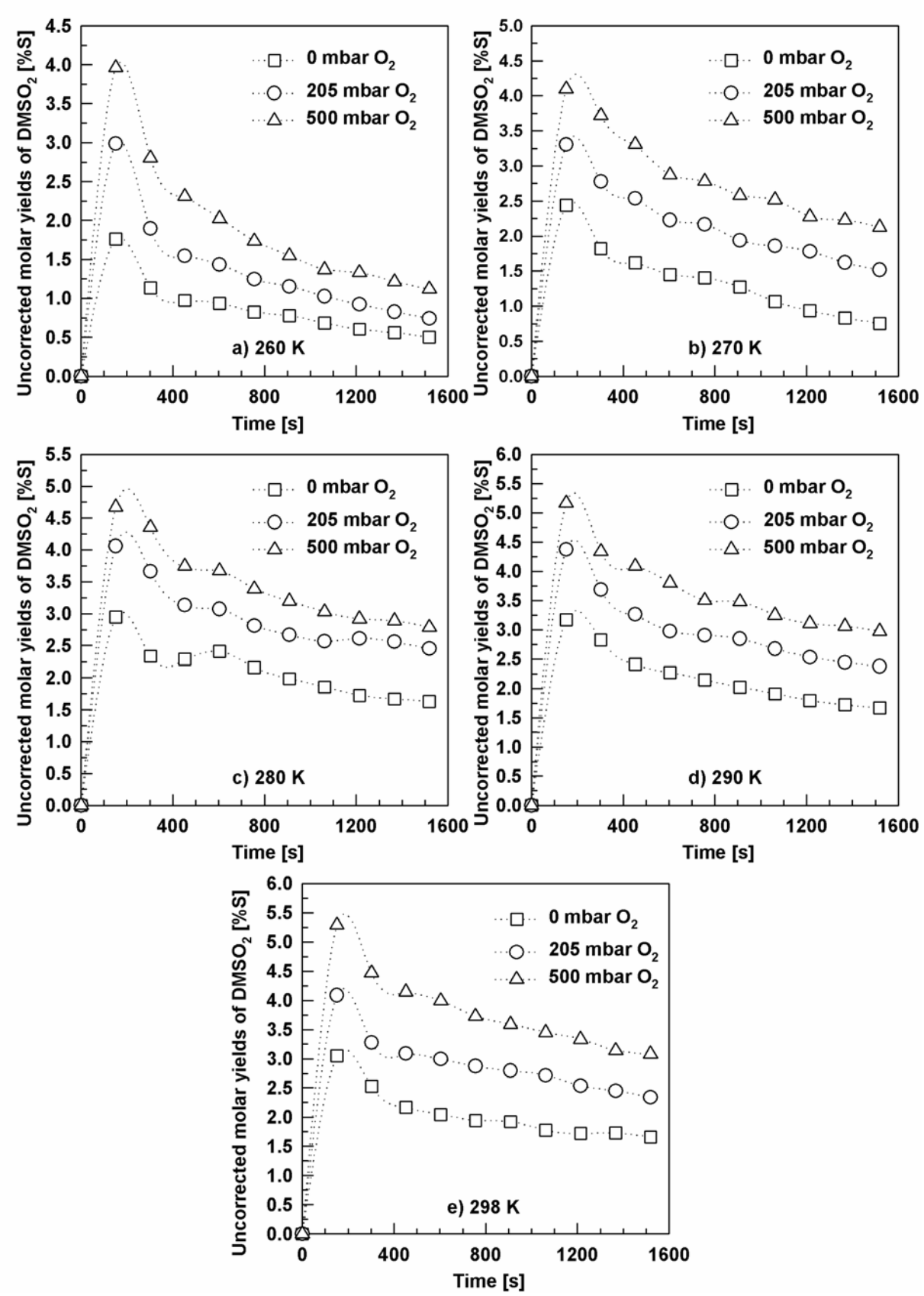

Figure 5.14: Plots of the uncorrected molar yields of $DMSO_2$, determined in the absence of NO_x in 1000 mbar diluent gas at a) 260 K, b) 270 K, c) 280 K, d) 290 K and e) 298 K for different O_2 partial pressures (~0, 205 and 500 mbar), versus reaction time.

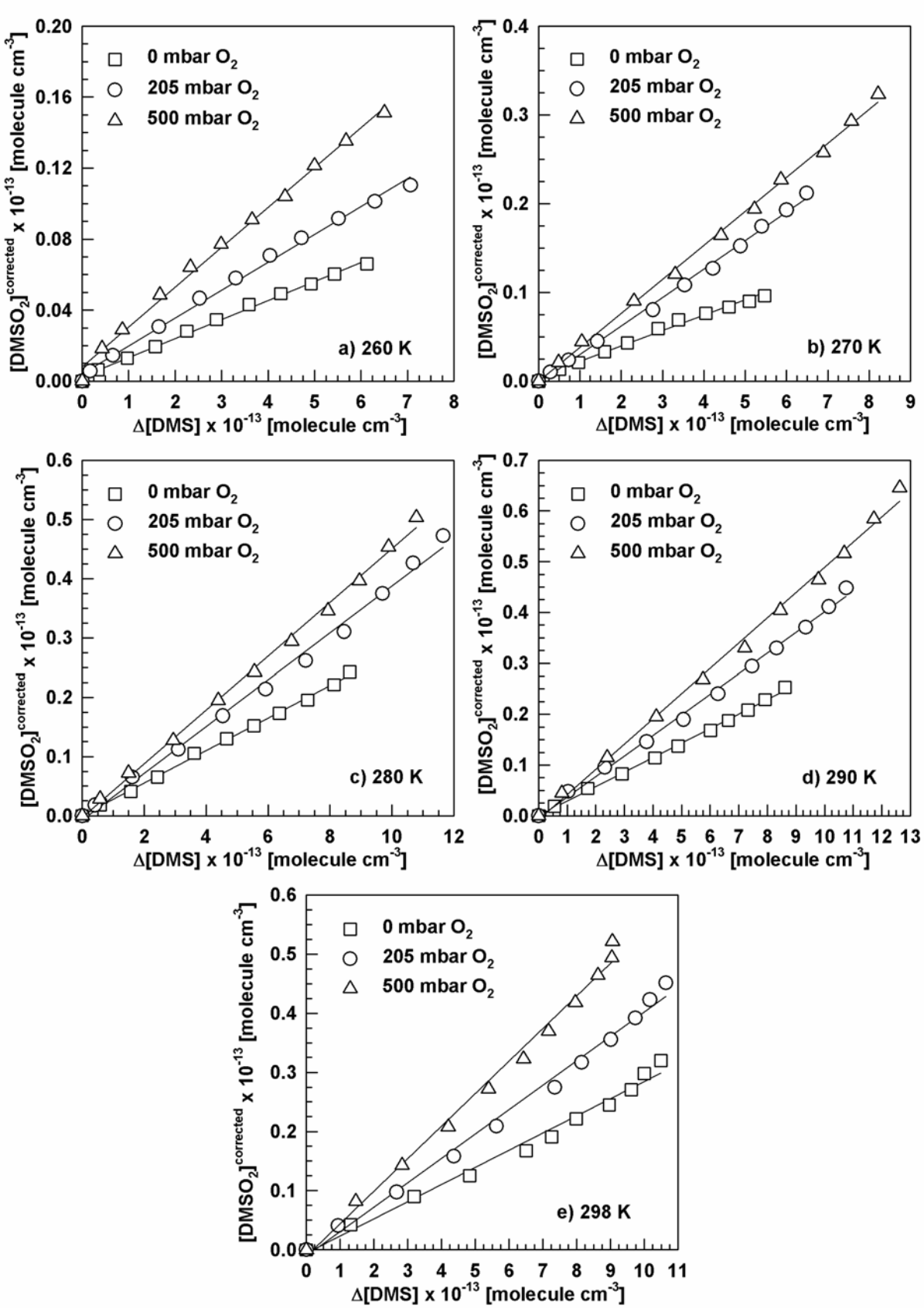

Figure 5.15: Plots of the corrected $DMSO_2$ concentrations, determined in the absence of NO_x in 1000 mbar diluent gas at a) 260 K, b) 270 K, c) 280 K, d) 290 K and e) 298 K for diferent O_2 partial pressures (~0, 205 and 500 mbar), versus the consumption of DMS.

5.1.3 Sulfur dioxide (SO_2)

SO_2 was determined by FTIR spectroscopy using the characteristic spectral features in the wave number range 1305 - 1405 cm^{-1}. SO_2 was quantified using calibrated spectra, obtained for each temperature in the reaction chamber. The IBI values for SO_2 are listed in Appendix II.

Concentration-time profiles of the formation of SO_2 are shown in Figures 5.2 - 5.7. The shapes of the SO_2 curves indicate that this compound is not strongly influenced by secondary loss processes.

Results from NO_x-containing experiments:

The measured yield-time profiles for SO_2 as a function of initial NO_x concentrations for all five temperatures studied, 260, 270, 280, 290 and 298 K, are shown in Figure 5.16.

From Figure 5.16 it can be seen that for a constant temperature, increasing the concentration of NO_x resulted in only a slight increase of the SO_2 formation yield. For approximately the same NO_x initial concentration increasing the temperature also only resulted in a moderate increase of the SO_2 formation yield. In Figure 5.16 the yields of SO_2 are not corrected for secondary loss processes such as further reaction with OH radicals or wall loss. The wall loss for SO_2 at all five temperatures was insignificant (~2×10^{-6} s^{-1}). The rate coefficient for the reaction of OH radicals with SO_2 is well established; for the purposes of the SO_2 yield corrections the values of k_{SO2} were calculated from the Arrhenius expression ($k_{SO2} = 5.07 \times 10^{-13} \exp(231/T)$ cm^3 $molecule^{-1}$ s^{-1}), which is used in modelling studies (Yin *et al.*, 1990a; Hertel *et al.*, 1994). Corrections were performed using the mathematical procedure described in Section 3.4.2.

Plots of the corrected SO_2 concentrations for all five temperatures studied, 260, 270, 280, 290 and 298 K, and the different initial NO_x concentrations, versus the amount of DMS consumed are shown in Figure 5.17. The corrected formation yields of SO_2 obtained by linear regression analysis of the plots in Figure 5.17 are collected in Table 5.5. The corrections for SO_2 secondary consumption were only of the order of 1%.

From Table 5.5 it can be seen that (i) for a constant temperature, increasing the initial NO_x concentration resulted in only a slight increase of the corrected SO_2 yield, while (ii) for approximately the same NO_x initial concentration increasing the temperature resulted in a more substantial increase of the corrected SO_2 yield.

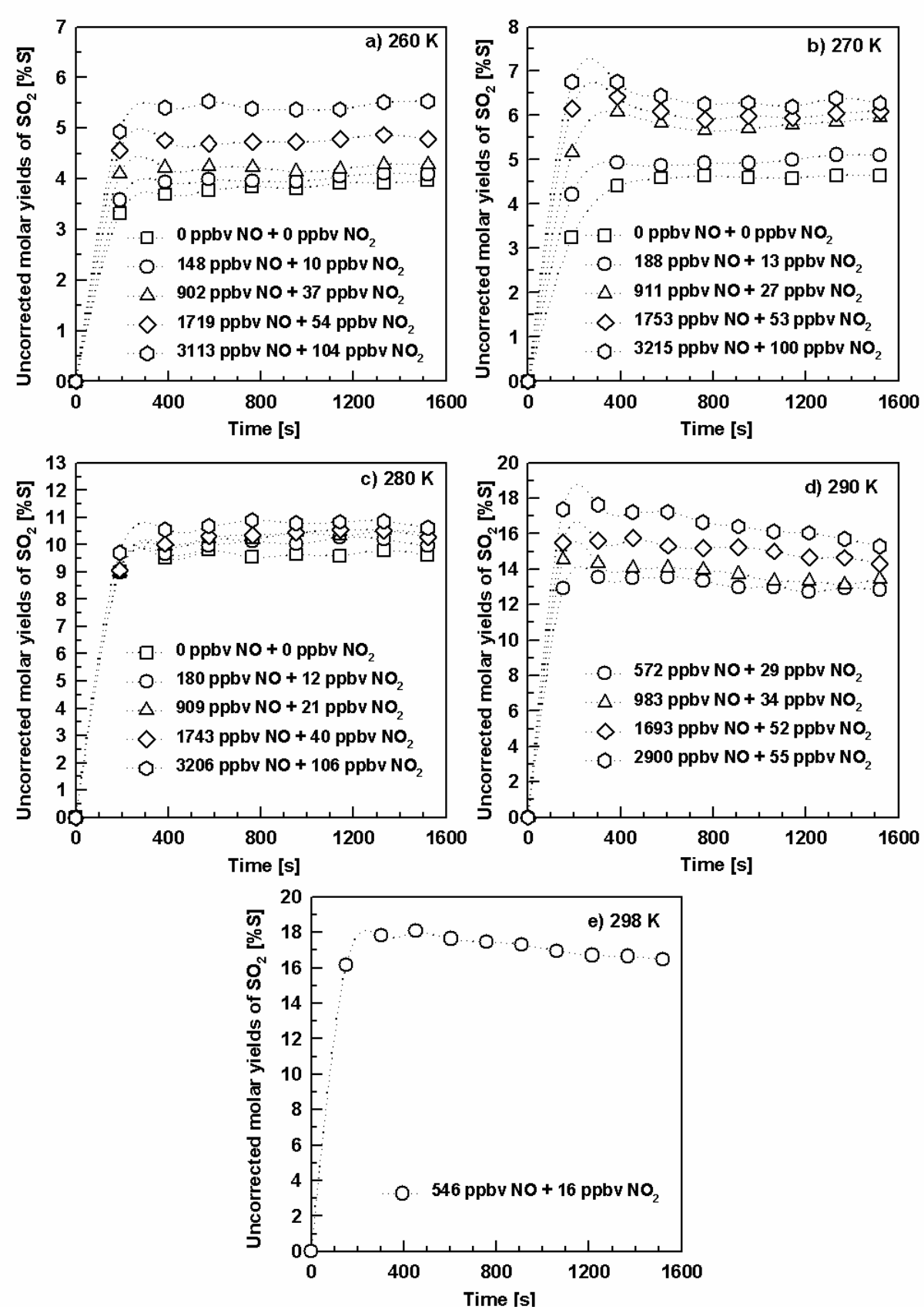

Figure 5.16: Plots of the uncorrected molar yields of SO_2, determined in 1000 mbar of synthetic air at a) 260 K, b) 270 K, c) 280 K d) 290 K and e) 298 K for different initial NO_x concentrations, versus reaction time.

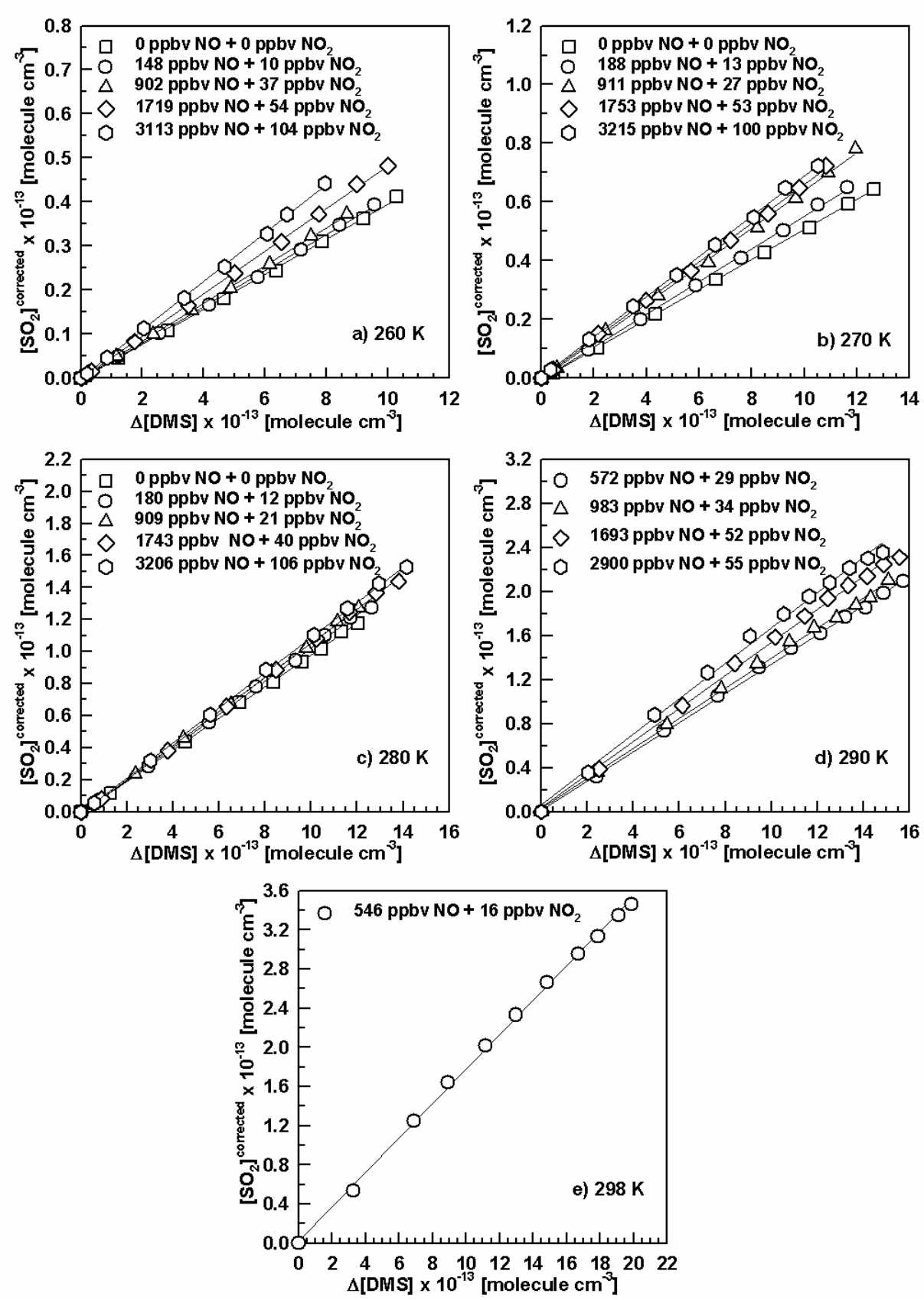

Figure 5.17: Plots of the corrected SO_2 concentrations, determined in 1000 mbar of synthetic air at a) 260 K, b) 270 K, c) 280 K, d) 290 K and e) 298 K for different initial NO_x concentrations, versus the consumption of DMS.

Table 5.5: Corrected yields for the formation of SO_2 in the OH radical initiated oxidation of DMS in 1000 mbar synthetic air as a function of temperature and initial NO_x concentrations.

Temperature (K)	NO (ppbv)	NO_2 (ppbv)	Corrected SO_2 yield (% molar yield, $\pm 2\sigma$)
260	0	0	3.97 ± 0.07
	148	10	4.11 ± 0.07
	902	37	4.28 ± 0.06
	1719	54	4.84 ± 0.07
	3113	104	5.51 ± 0.09
270	0	0	5.10 ± 0.04
	188	13	5.57 ± 0.10
	911	27	6.42 ± 0.15
	1753	53	6.58 ± 0.11
	3215	100	6.85 ± 0.11
280	0	0	9.82 ± 0.14
	180	12	10.29 ± 0.16
	909	21	10.61 ± 0.14
	1743	40	10.64 ± 0.16
	3206	106	10.94 ± 0.14
290	572	29	13.28 ± 0.26
	983	34	13.67 ± 0.35
	1693	52	15.03 ± 0.45
	2900	55	16.06 ± 0.65
298	546	55	17.66 ± 0.40

Results for NO_x-free experiments:

The measured yield-time profiles for SO_2 obtained in experiments using H_2O_2 as the OH radical source are shown in Figure 5.18 for all the temperatures, 260, 270, 280, 290 and 298 K, and O_2 partial pressures, ~0, 205 and 500 mbar, employed in the measurements.

From Figure 5.18 it is clear that for a constant temperature, increasing the O_2 partial pressure results in a decrease of the SO_2 formation yields and for a constant O_2 partial pressure increasing the temperature results in an increase of the SO_2 formation yields. In Figure 5.18 the yields of SO_2 are not corrected for secondary loss processes such as further reaction with OH radicals. Corrections were performed using the mathematical procedure described in Section 3.4.2. Plots of the SO_2 corrected concentration versus the amount of DMS consumed, for all five temperatures studied and different O_2 partial pressure are shown in Figure 5.19.

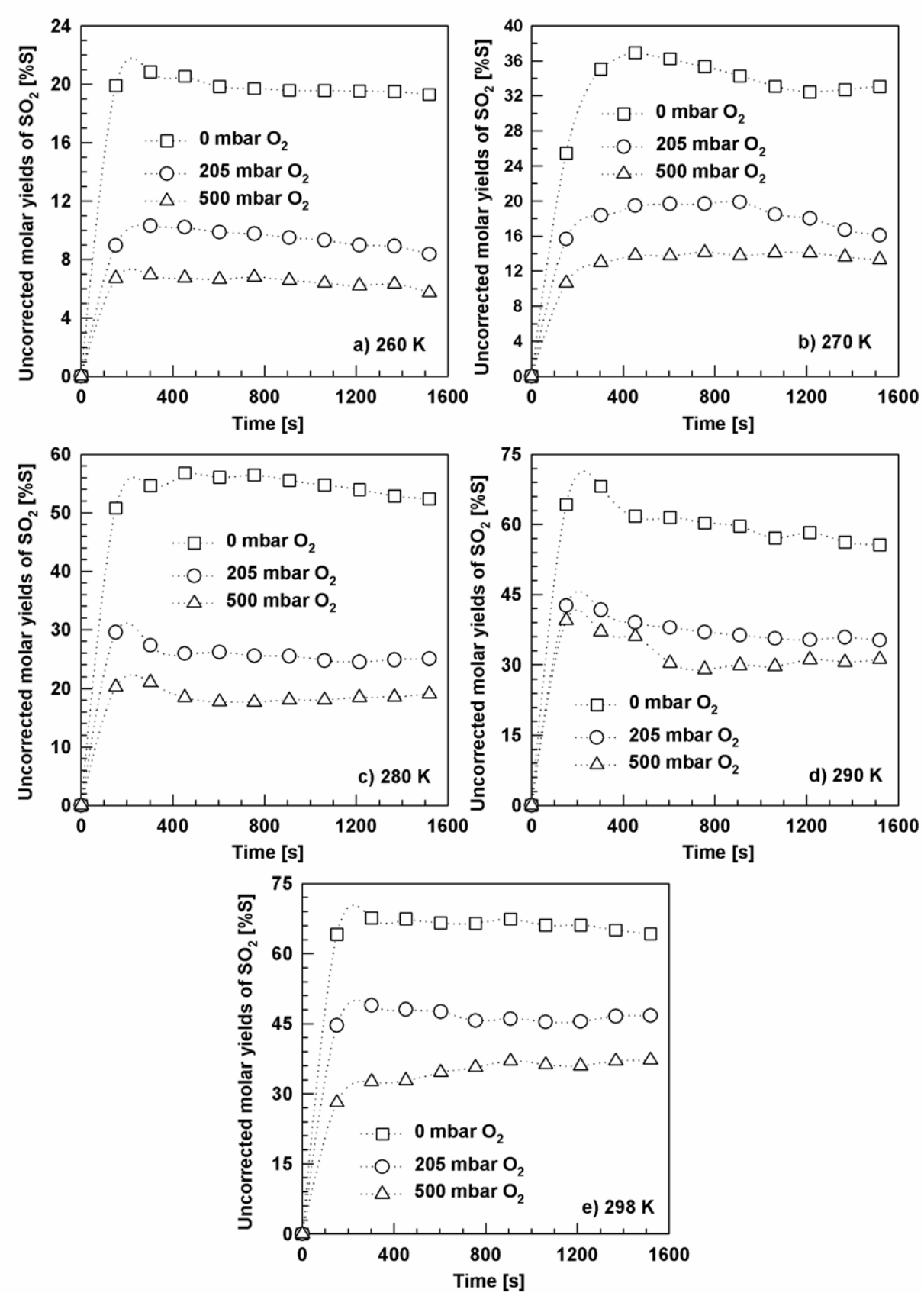

Figure 5.18: Plots of the uncorrected molar yields of SO_2, determined in the absence of NO_x in 1000 mbar diluent gas at a) 260 K, b) 270 K, c) 280, d) 290 K and e) 298 K for different O_2 partial pressures (~0, 205 and 500 mbar), versus reaction time.

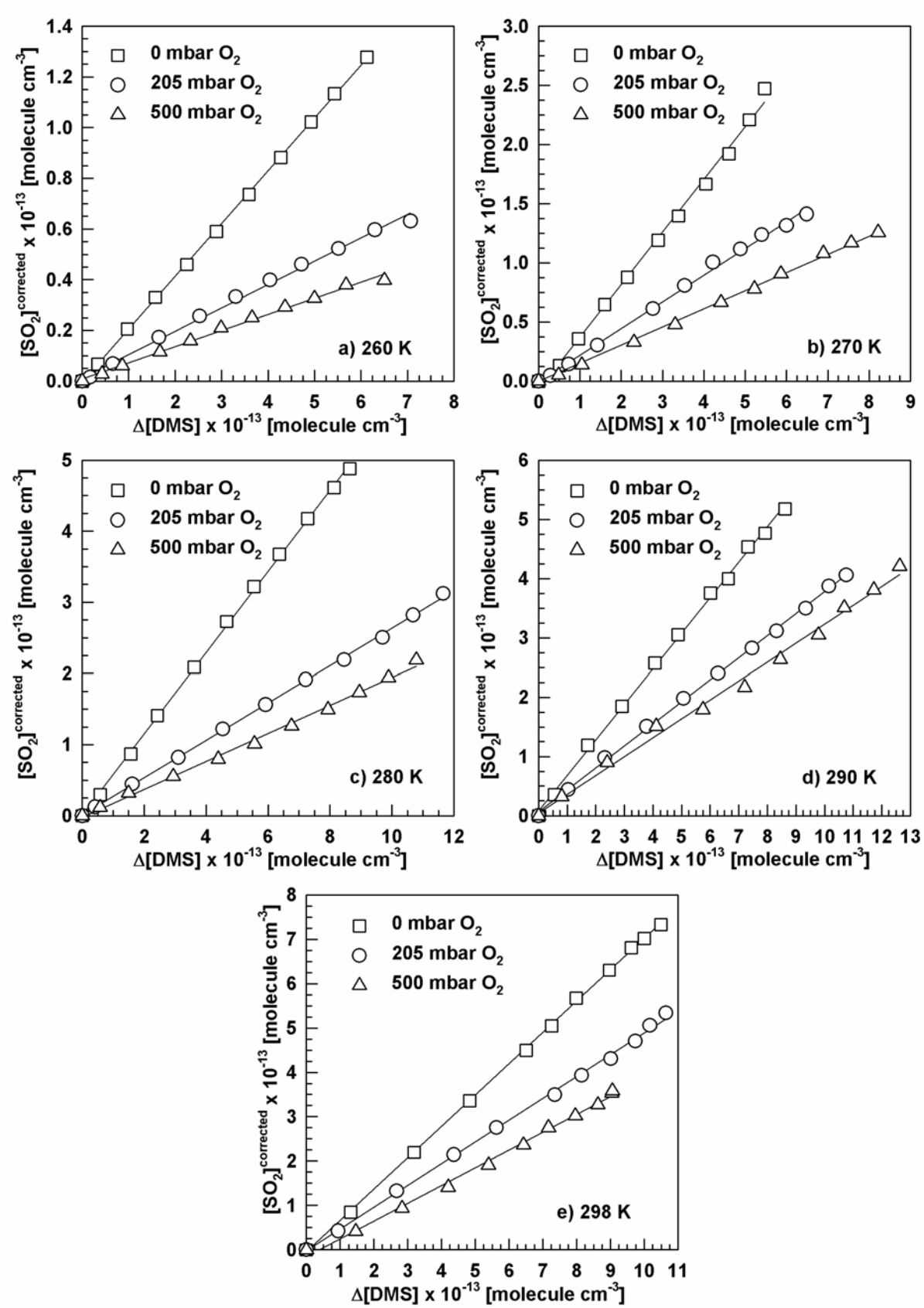

Figure 5.19: Plots of the corrected SO_2 concentrations, determined in the absence of NO_x in 1000 mbar diluent gas at a) 260 K, b) 270 K, c) 280 K, d) 290 K and e) 298 K for different O_2 partial pressures (~0, 205, 500 mbar), versus the consumption of DMS.

The corrected formation yields of SO_2 obtained by linear regression analysis of the plots in Figure 5.19 are collected in Table 5.6.

Table 5.6: Corrected yields for the formation of SO_2 in the OH radical initiated oxidation of DMS in 1000 mbar diluent gas as a function of temperature and O_2 partial pressure, in the absence of NO_x.

Temperature (K)	pO_2 (mbar)	Corrected SO_2 yield (% molar yield, $\pm 2\sigma$)
260	~0	20.80 ± 0.18
	205	9.20 ± 0.38
	500	6.37 ± 0.30
270	~0	44.33 ± 1.82
	205	22.52 ± 0.82
	500	15.67 ± 0.32
280	~0	57.14 ± 0.85
	205	26.26 ± 0.44
	500	18.83 ± 0.62
290	~0	59.94 ± 1.44
	205	37.14 ± 0.68
	500	31.88 ± 1.64
298	~0	70.75 ± 0.80
	205	49.11 ± 1.26
	500	40.07 ± 1.98

From Table 5.6 it can be seen that the yield of SO_2 is strongly dependent on the temperature and on the O_2 partial pressure: (i) it increases with increasing temperature for each O_2 partial pressure and (ii) decreases with increasing O_2 partial pressure for each temperature.

5.1.4 Methyl sulfonyl peroxynitrate (MSPN)

MSPN was determined, using FTIR spectroscopy. The spectral features of a peroxynitrate were observed in the product spectra of the OH radical initiated oxidation of DMS in the presence of NO_x. The quantification of MSPN was made using absorption cross-sections for the absorption bands centered at 777, 1303 and 1768 cm^{-1} taken from the work of Patroescu (1996) and Patroescu-Klotz (1999).

Concentration-time profiles of the formation of MSPN are shown in Figures 5.2 - 5.6. The measured yield-time profiles for MSPN as a function of initial NO_x concentrations for all

five temperatures studied from the experiments, where CH_3ONO was used as OH radical source, are shown in Figure 5.20.

The yield-time contours of MSPN at 260, 270 and 280 K show an initial increase in the yield with time, which is to be expected because of the increase in the NO_2 concentration, followed by a quasi steady state period where the rate of production of MSPN is equal to its rate of loss. In contrast the yield-time contours at 290 and 298 K initially rise and go through a maximum, which is followed by a decrease in the MSPN yield presumably due to the much larger thermal decomposition rate of MSPN at these temperatures compared to 280 K and below. The points where the yield remains constant or decay begins are at the point in the reaction system where the NO_2 concentration has reached a maximum and then remains almost constant or decreases slightly. The yields of MSPN determined at these points are collected in Table 5.7; the errors represent 20% of the determined values.

Table 5.7: Yields of MSPN in the reaction of DMS with OH radicals in 1000 mbar synthetic air as a function of temperature and initial NO_x concentrations.

Temperature (K)	NO (ppbv)	NO_2 (ppbv)	MSPN yields (% molar yield, ± 20%)
260	0	0	2.31 ± 0.46
	148	10	2.39 ± 0.48
	902	37	2.76 ± 0.55
	1719	54	2.89 ± 0.58
	3113	104	3.09 ± 0.62
270	0	0	3.29 ± 0.66
	188	13	3.43 ± 0.68
	911	27	4.19 ± 0.84
	1753	53	4.26 ± 0.85
	3215	100	4.34 ± 0.87
280	0	0	3.59 ± 0.72
	180	12	4.46 ± 0.89
	909	21	4.79 ± 0.96
	1743	40	4.85 ± 0.97
	3206	106	5.02 ± 1.00
290	572	29	7.18 ± 1.44
	983	34	8.45 ± 1.69
	1693	52	8.65 ± 1.73
	2900	55	9.04 ± 1.81
298	546	55	7.77 ± 1.55

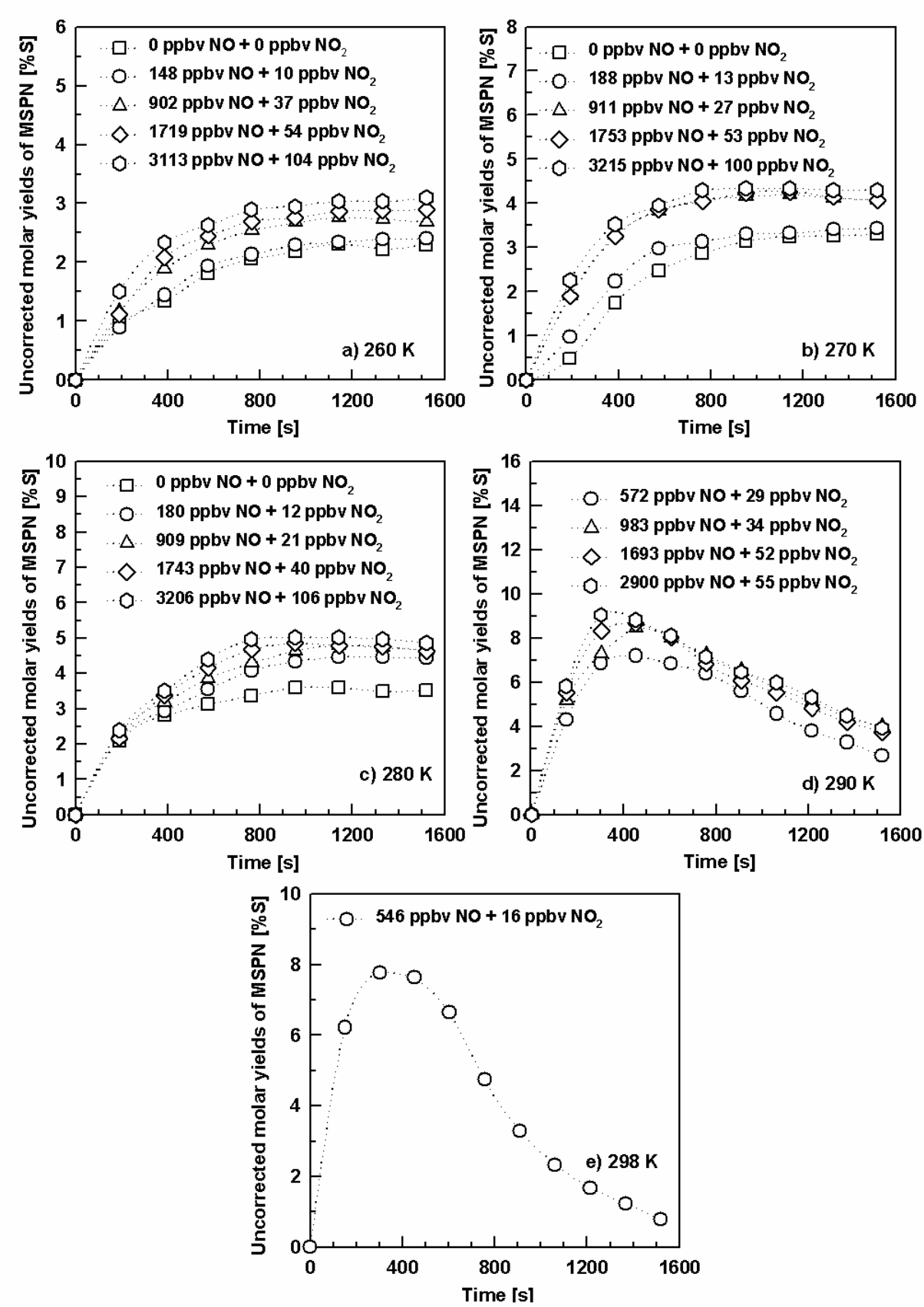

Figure 5.20: Plots of the molar yields of MSPN, determined in 1000 mbar of synthetic air at a) 260 K, b) 270 K, c) 280 K d) 290 K and e) 298 K for different initial NO_x concentrations, versus reaction time.

The yield of MSPN is not a constant in the reaction systems, however, from Table 5.7 it can be seen that (i) for a constant temperature, increasing the initial NO_x concentration resulted in only a slight increase in the amount of the MSPN formed, while (ii) for approximately the same NO_x initial concentration increasing the temperature resulted in a more substantial increase of the amount of MSPN formed in the system.

5.1.5 Methyl thiol formate (MTF)

In the present study, absorptions attributable to methyl thiol formate (767 and 1679 cm^{-1}) have been observed in the spectra obtained in the experiments of the OH radical initiated oxidation of DMS under NO_x-free conditions. The absorptions due to MTF were not observed in systems containing NO_x.

The measured yield-time profiles for MTF for all the temperatures, 260, 270, 280, 290 and 298 K, and O_2 partial pressures, ~0, 205 and 500 mbar, employed in the measurements are shown in Figure 5.21. Figure 5.21 shows that there is a tendency for the yield of MTF to increase with decreasing O_2 partial pressure at constant temperature and to increase with decreasing temperature at constant O_2 partial pressure.

Competition between production of MTF from DMS oxidation and its further oxidation by OH radicals and photolysis by the mercury lamps used to produce OH radicals determines the shape of the MTF curves. To derive the formation yields of MTF its concentration was corrected for further reaction with OH radicals and photolysis using the mathematical procedure described in Section 3.4.2.

The rate coefficient for the reaction of OH radicals with MTF is known only at room temperature, k_{MTF} = 1.11 $\times$ 10^{-11} cm^3 $molecule^{-1}$ s^{-1} (Patroescu *et al.*, 1996); in the correction procedure it has been assumed that the rate coefficient of MTF with OH radicals is constant over the experimental temperature range of 260 to 299 K. Patroescu (1996) has reported photolysis frequencies for MTF. In the correction procedure the values from Patroescu (1996) were used after adjustment to take into account the light intensity in the chamber; this adjustment was based on a comparison of the NO_2 photolysis rate coefficient (J_{NO2}) in the present chamber and that in the chamber used by Patroescu (1996).

Plots of the corrected MTF concentrations versus the amount of DMS consumed for all five temperatures studied and the different initial O_2 partial pressures are shown in Figure 5.22. The MTF corrected yields are presented in Table 5.8.

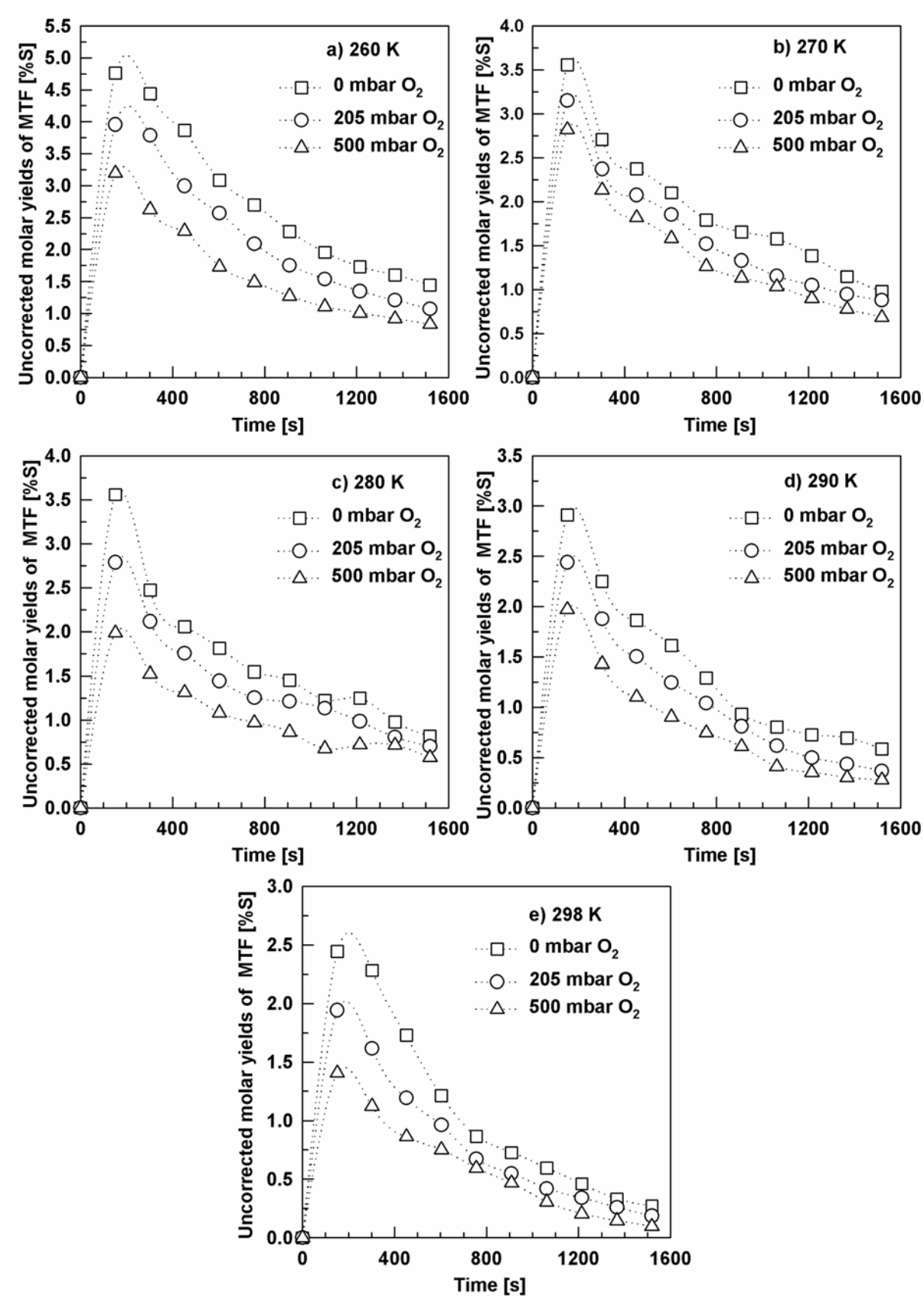

Figure 5.21: Plots of the uncorrected molar yields of MTF, determined in 1000 mbar diluent gas at a) 260 K, b) 270 K, c) 280 K, d) 290 K and e) 298 K for different O_2 partial pressures (~0, 205 and 500 mbar), versus reaction time.

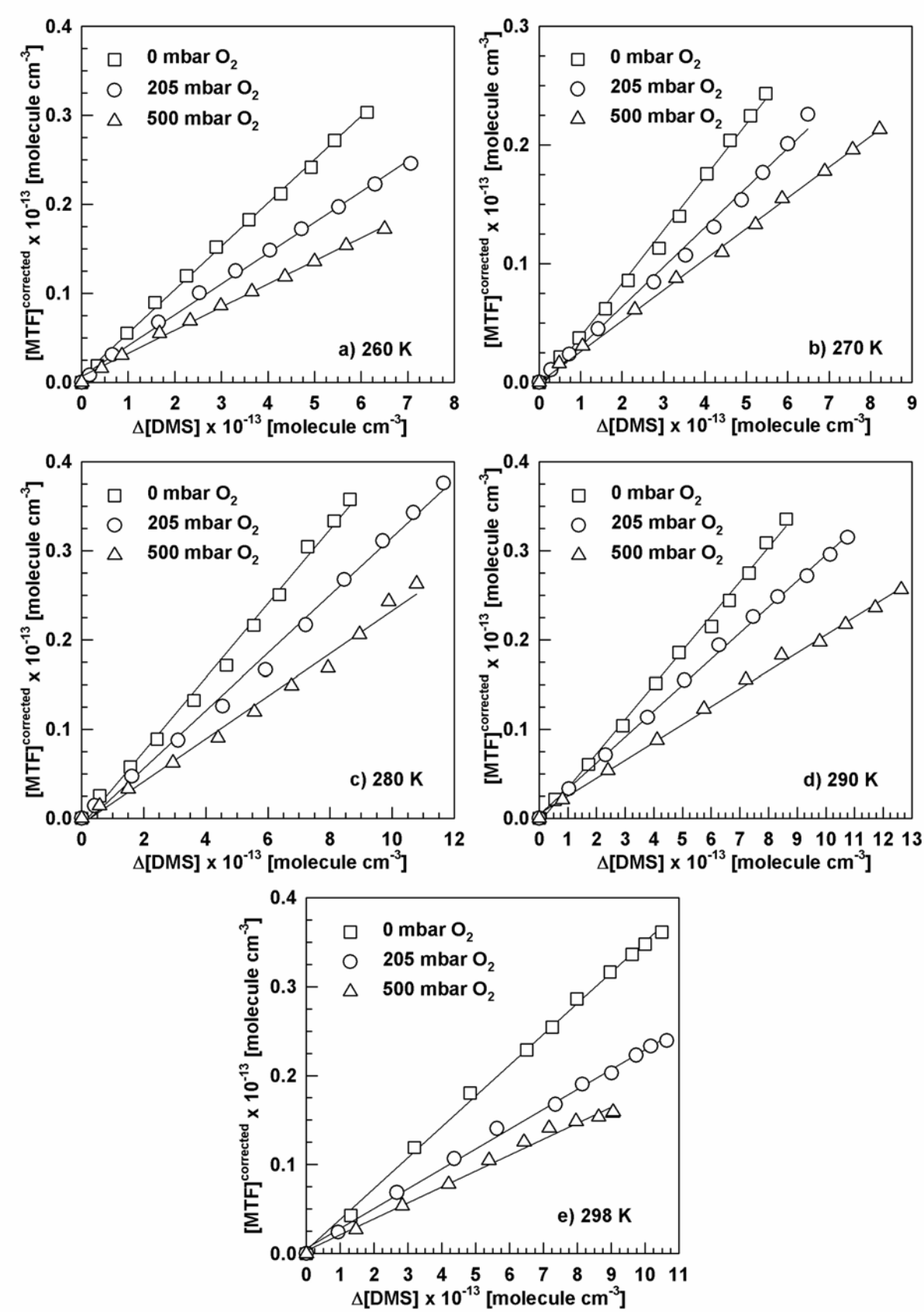

Figure 5.22: Plots of the corrected MTF concentrations, determined in 1000 mbar diluent gas at a) 260 K, b) 270 K, c) 280 K, d) 290 K and e) 298 K for different O_2 partial pressures (~0, 205, 500 mbar), versus the consumption of DMS.

Table 5.8: Corrected yields for the formation of MTF in the OH radical initiated oxidation of DMS in 1000 mbar diluent gas as a function of temperature and O_2 partial pressure.

Temperature (K)	pO_2 (mbar)	MTF yields (% molar yield, $\pm 2\sigma$)
260	~0	4.87 ± 0.12
	205	3.45 ± 0.10
	500	2.59 ± 0.09
270	~0	4.47 ± 0.18
	205	3.33 ± 0.16
	500	2.55 ± 0.05
280	~0	4.14 ± 0.18
	205	3.23 ± 0.14
	500	2.39 ± 0.14
290	~0	3.84 ± 0.14
	205	2.91 ± 0.06
	500	2.00 ± 0.06
298	~0	3.46 ± 0.09
	205	2.23 ± 0.07
	500	1.78 ± 0.11

From Table 5.8 it can be seen that the yield of MTF (i) increases with decreasing O_2 partial pressure at constant temperature and (ii) increases with decreasing temperature at constant O_2 partial pressure.

5.1.6 Carbonyl sulfide (OCS)

In the present study, absorptions attributable to carbonyl sulfide (2070 cm^{-1}) were observed in the spectra obtained in the experiments performed under NO_x-free conditions in the presence of O_2 at all five temperatures investigated. The absorptions due to OCS were most pronounced at the highest O_2 partial pressure and temperature. However, at 260, 270 and 280 K these absorptions were not much greater than the signal-to-noise ratio and quantification at these temperatures was not possible. Quantification was only possible at 290 and 298 K. Absorptions attributable to carbonyl sulfide were not observed in reaction systems containing NO_x.

The measured yield-time profiles for OCS at 290 and 298 K and different O_2 partial pressures are shown in Figure 5.23. The yield of OCS is observed to increase with time indicating that it is formed from the further oxidation of a DMS primary product.

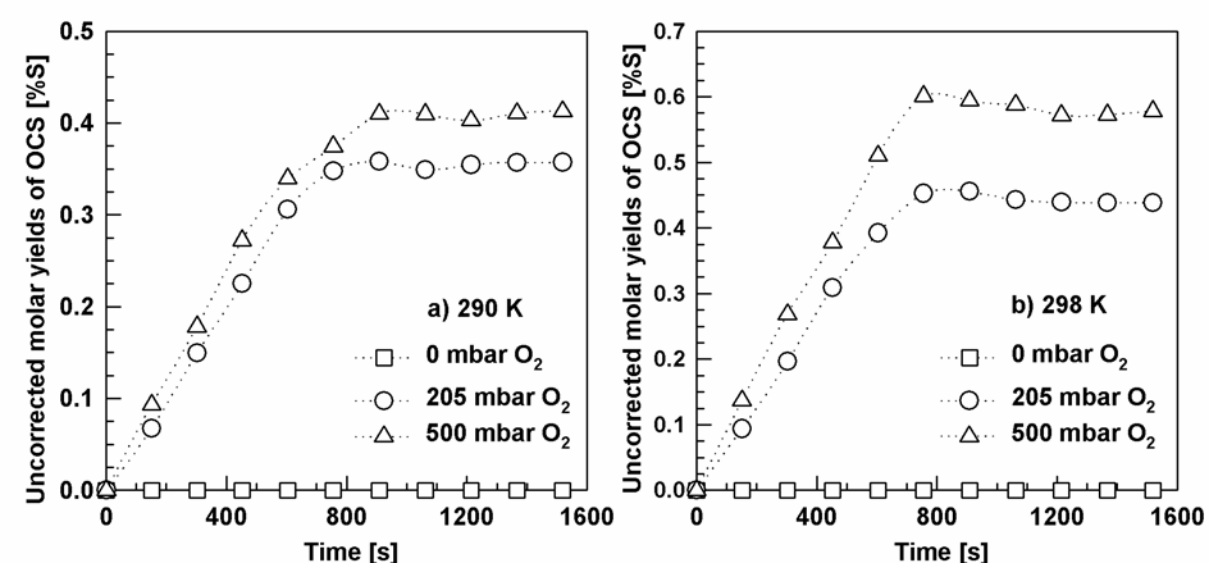

Figure 5.23: Plots of the uncorrected molar yields of OCS, determined in 1000 mbar diluent gas at a) 290 K and b) 298 K as a function of O_2 partial pressure, versus reaction time.

The yields of OCS obtained towards the end of the experiments, when the change in the OCS yield was minimal, are listed in Table 5.9.

Table 5.9: Formation yields of OCS in the reaction of DMS with OH radicals in 1000 mbar diluent gas (obtained at the end of the experiments) as a function of temperature and O_2 partial pressure.

Temperature (K)	pO_2 (mbar)	OCS yields (% molar yield, ± 20%)
290	~0	-
	205	0.35 ± 0.07
	500	0.41 ± 0.08
298	~0	-
	205	0.45 ± 0.09
	500	0.60 ± 0.12

The yields of OCS obtained from the end phase of the experiments (i) increase with increasing O_2 partial pressure at a constant temperature and (ii) increase slightly with increasing temperature at a constant O_2 partial pressure.

5.1.7. Methane sulfonic acid (MSA) and methane sulfinic acid (MSIA)

Formation of methane sulfonic acid (MSA: $CH_3S(O)_2OH$) and methane sulfinic acid (MSIA: $CH_3S(O)OH$) were observed as products in the OH radical initiated oxidation of DMS.

FTIR-Results

MSA is a compound with a very low vapour pressure, whose infrared spectrum is known (Mihalopulos *et al.*, 1992b) and hence, the identification and quantification of this compound in the gas phase was possible. In the experiments performed in the absence of NO_x, at all five temperatures (260, 270, 280, 290 and 298 K) and in the experiments performed in the presence of NO_x, at 260, 270 and 280 K, weak absorptions were found in the IR spectrum which could be assigned to gas-phase methane sulfonic acid. However, these absorptions were not much greater than the signal-to-noise ratio and quantification was not possible. Quantification of MSA in the gas phase was only possible in the experiments performed in the presence of NO_x at 290 and 298 K.

The measured yield-time profiles for gaseous MSA at 290 and 298 K and different initial NO_x concentration are shown in Figure 5.24. In Figure 5.24 the yields of MSA have not been corrected for possible secondary loss processes. The increase of the MSA yield with time indicates that secondary reactions are primarily responsible for its formation. The yields of MSA obtained towards the end of the experiments, when the change in the MSA yield was minimal, are listed in Table 5.10.

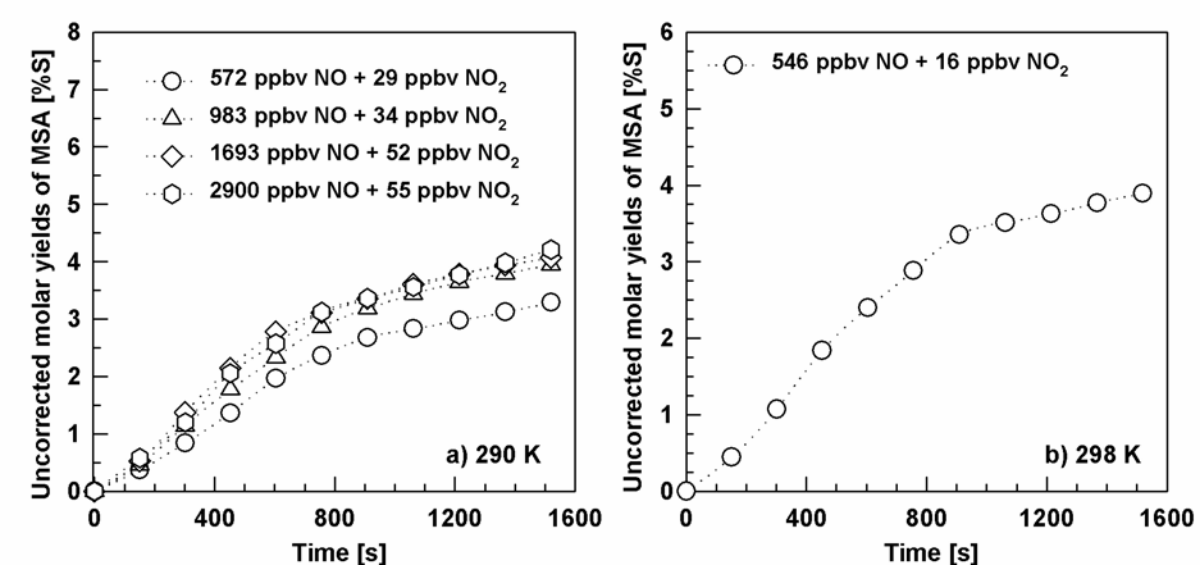

Figure 5.24: Plots of the uncorrected molar yields of MSA at a) 290 K and b) 298 K and 1000 mbar synthetic air as a function of the initial NO_x concentration versus reaction time.

Table 5.10: Formation yields of MSA in the reaction of DMS with OH radicals in 1000 mbar synthetic air (obtained at the end of the experiments) as a function of temperature and initial NO_x concentration.

Temperature (K)	NO (ppbv)	NO_2 (ppbv)	MSA yields (% molar yield, ± 20%)
290	572	29	2.95 ± 0.28
	983	34	3.31 ± 0.35
	1693	52	3.60 ± 0.39
	2900	55	3.89 ± 0.55
298	546	55	3.26 ± 0.30

From Table 5.10 it can be seen that the gas-phase MSA yields determined by FTIR spectroscopy from the end phase of the experiments increase very slightly with increasing NO_x concentration but were not more than 4% S.

The infrared spectrum of methane sulfinic acid (MSIA: $CH_3S(O)OH$) is not presently known, and it was, therefore, not possible to establish the formation of this compound in the gas phase using long path FTIR spectroscopy.

IC-Results

Ion chromatography was the analytical tool used to prove the presence of MSIA in the OH radical initiated oxidation of DMS. This analytical technique was also used to get additional information on MSA (gas + aerosol) in the DMS photooxidation system.

Collection of the samples for ion chromatographic analysis was as described in Section 3.2.2.

Figure 5.25 shows a chromatogram demonstrating the detection of the $CH_3S(O)O^-$ and $CH_3S(O)_2O^-$ anions from MSIA and MSA, respectively. The samples were taken during the irradiation of DMS/CH_3ONO/synthetic air mixture at 298 K and 1000 mbar total pressure, in the presence of 546 ppmv NO + 16 ppmv NO_2; the peaks of MSIA and MSA are well resolved.

The yields of the methane sulfinate ($CH_3(O)O^-$) and methane sulfonate ($CH_3S(O)_2O^-$) anions obtained using the samples collected during the irradiation time period of the experiments performed at all five temperatures, 260, 270, 280, 290 and 298 K, and at different O_2 partial pressure, ~0, 205 and 500 mbar, and different initial NO_x concentrations are presented in Tables 5.11 and 5.12, respectively.

The values in Tables 5.11 and 5.12 are integral yield values for the irradiation time period of the experiments and represent composite values of production and loss processes. The results from Tables 5.11 and 5.12 do not represent the formation yields of the species, however, in the case of MSIA they represent a lower limit of the formation yield.

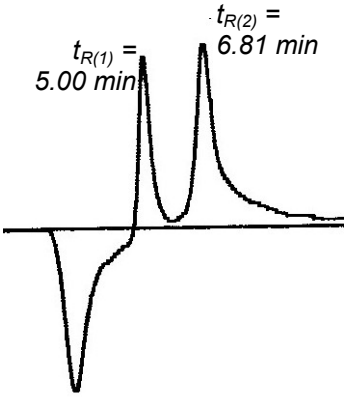

Figure 5.25: Example of a chromatogram demonstrating the detection of MSIA ($t_{R(1)}$) and MSA ($t_{R(2)}$) from samples collected from the reactor during the irradiation of a DMS/CH_3ONO/synthetic air mixture at 298 K and 1000 mbar total pressure, in the presence of 546 ppmv NO + 16 ppmv NO_2.

Table 5.11: Ion chromatographic analysis of methane sulfinate ($CH_3(O)O^-$) and methane sulfonate ($CH_3S(O)_2O^-$) anions from the samples collected from the oxidation of DMS in 1000 mbar bath gas, at different temperatures (260, 270, 280, 290 and 298 K) and different O_2 partial pressures (~0, 205 and 500 mbar), in the absence of NO_x.

T (K)	pO_2 (mbar)	Volume (l)	$CH_3S(O)O^-$		$CH_3S(O)_2O^-$	
			ppm	%S	ppm	%S
260	0	20	0.11	4.78	0.08	3.47
	205	20	0.55	20.75	0.38	14.34
	500	20	0.56	22.95	0.45	18.44
270	0	20	0.12	4.47	0.09	3.35
	205	20	0.65	19.18	0.38	11.94
	500	20	0.68	19.65	0.54	15.60
280	0	20	0.15	4.34	0.11	3.18
	205	20	0.75	16.12	0.42	9.03
	500	20	0.81	18.83	0.47	10.93
290	0	20	0.14	3.93	0.10	2.80
	205	20	0.57	12.80	0.28	6.29
	500	20	0.68	13.02	0.42	8.04
298	0	20	0.15	3.36	0.11	2.46
	205	20	0.35	7.74	0.23	5.09
	500	20	0.39	10.12	0.21	5.45

From Table 5.11 it can be seen that the yields of both MSIA and MSA (i) increase with increasing O_2 partial pressure for the same temperature and (ii) increase with decreasing temperature for a constant O_2 partial pressure. Both MSIA and MSA have also been detected in the absence of O_2 in the reaction system, but in low yields.

Table 5.12: Ion chromatographic analysis of methane sulfinate ($CH_3(O)O^-$) and methane sulfonate ($CH_3S(O)_2O^-$) anions from the samples collected from the oxidation of DMS in 1000 mbar synthetic air, at different temperatures (260, 270, 280, 290 and 298 K) and different initial NO_x concentrations.

T	NO	NO_2	Volume	$CH_3S(O)O^-$		$CH_3S(O)_2O^-$	
(K)	(ppbv)	(ppbv)	(l)	ppm	%S	ppm	%S
260	0	0	20	0.65	17.85	0.56	15.38
	148	10	20	0.50	14.74	0.39	11.50
	902	37	20	0.38	12.37	0.28	9.12
	1719	54	20	0.35	9.88	0.27	7.81
	3113	104	20	0.25	8.86	0.20	7.11
270	0	0	20	0.67	14.43	0.56	12.06
	188	13	20	0.55	12.88	0.45	10.53
	911	27	20	0.51	11.61	0.37	8.42
	1753	53	20	0.38	9.74	0.29	7.23
	3215	100	20	0.31	8.01	0.26	6.70
280	0	0	20	0.65	14.16	0.49	10.67
	180	12	20	0.58	12.03	0.43	8.92
	909	21	20	0.51	11.08	0.36	7.82
	1743	40	20	0.45	8.55	0.35	6.65
	3206	106	20	0.39	7.22	0.32	5.93
290	572	29	20	0.42	6.83	0.45	7.23
	983	34	20	0.33	5.53	0.37	6.21
	1693	52	20	0.30	4.87	0.28	4.55
	2900	55	20	0.24	3.58	0.23	3.92
298	546	16	20	0.45	5.57	0.49	6.06

The MSA yields obtained in the presence of NO_x in the gas phase at 290 and 298 K using FTIR spectroscopy are lower than the yields obtained under the same conditions using ion chromatography.

From Table 5.12 it can be seen that the yields of MSIA and MSA (i) decrease with increasing NO_x concentration for a constant temperature and (ii) decrease with increasing temperature for approximately the same NO_x initial concentration.

5.2 Discussion of the results and comparison with literature data

For ease of discussion, summaries of the corrected product yields for the major sulfur-containing compounds obtained in the present work in the absence and in the presence of NO_x are given in Table 5.13 and Table 5.14, respectively.

Table 5.13: Yields for the formation of DMSO, $DMSO_2$, SO_2, MTF and OCS in the OH radical initiated oxidation of DMS in 1000 mbar diluent gas as a function of temperature and O_2 partial pressure in the absence of NO_x.

T (K)	pO_2 (mbar)	% molar yield, $\pm 2\sigma$				
		DMSO	$DMSO_2$	SO_2	MTF	OCS[i]
260	0	0.00 ± 0.00	1.07 ± 0.05	20.80 ± 0.18	4.87 ± 0.12	-
	205	73.03 ± 2.09	1.57 ± 0.07	9.20 ± 0.38	3.45 ± 0.10	-
	500	82.96 ± 2.50	2.12 ± 0.11	6.37 ± 0.30	2.59 ± 0.09	-
270	0	0.00 ± 0.00	1.73 ± 0.10	44.33 ± 1.82	4.47 ± 0.18	-
	205	66.99 ± 6.94	3.20 ± 0.10	22.52 ± 0.82	3.33 ± 0.16	-
	500	74.52 ± 4.06	3.83 ± 0.10	15.67 ± 0.32	2.55 ± 0.05	-
280	0	0.00 ± 0.00	2.74 ± 0.07	57.14 ± 0.85	4.14 ± 0.18	-
	205	62.25 ± 3.22	3.94 ± 0.19	26.26 ± 0.44	3.23 ± 0.14	-
	500	69.10 ± 3.88	4.53 ± 0.15	18.83 ± 0.62	2.39 ± 0.14	-
290	0	0.00 ± 0.00	2.86 ± 0.07	59.94 ± 1.44	3.84 ± 0.14	-
	205	51.43 ± 3.98	4.04 ± 0.15	37.14 ± 0.68	2.91 ± 0.06	0.35 ± 0.07
	500	55.81 ± 1.98	4.96 ± 0.20	31.88 ± 1.64	2.00 ± 0.06	0.41 ± 0.08
298	0	0.00 ± 0.00	2.90 ± 0.20	70.75 ± 0.80	3.46 ± 0.09	-
	205	38.56 ± 1.36	4.13 ± 0.22	49.11 ± 1.26	2.23 ± 0.07	0.45 ± 0.09
	500	48.80 ± 2.52	5.49 ± 0.32	40.07 ± 1.98	1.78 ± 0.11	0.60 ± 0.12

[i] *the yield increases with time; the yield given is that observed toward the end of the experiment.*

Table 5.14: Yields for the formation of DMSO, $DMSO_2$, SO_2, MSPN and MSA in the OH radical initiated oxidation of DMS in 1000 mbar synthetic air as a function of temperature and initial NO_x concentration.

T (K)	NO (ppbv)	NO_2 (ppbv)	% molar yield, $\pm 2\sigma$				
			DMSO	$DMSO_2$	SO_2	MSPN[i]	MSA[ii]
260	0	0	75.05 ± 3.70	5.95 ± 0.45	3.97 ± 0.07	2.31 ± 0.46	-
	148	10	68.17 ± 4.78	12.33 ± 0.64	4.11 ± 0.07	2.39 ± 0.48	-
	902	37	51.64 ± 1.84	29.25 ± 1.92	4.28 ± 0.06	2.76 ± 0.55	-
	1719	54	40.43 ± 2.56	39.58 ± 2.44	4.84 ± 0.07	2.89 ± 0.58	-
	3113	104	25.48 ± 2.10	53.87 ± 3.44	5.51 ± 0.09	3.09 ± 0.62	-
270	0	0	67.86 ± 3.72	5.83 ± 0.48	5.10 ± 0.04	3.29 ± 0.66	-
	188	13	61.96 ± 3.22	10.91 ± 0.52	5.57 ± 0.10	3.43 ± 0.68	-
	911	27	46.05 ± 1.87	27.37 ± 2.14	6.42 ± 0.15	4.19 ± 0.84	-
	1753	53	34.40 ± 0.86	37.76 ± 2.44	6.58 ± 0.11	4.26 ± 0.85	-
	3215	100	23.40 ± 0.65	48.35 ± 3.06	6.85 ± 0.11	4.34 ± 0.87	-
280	0	0	58.05 ± 1.64	5.74 ± 0.30	9.82 ± 0.14	3.59 ± 0.72	-
	180	12	53.52 ± 3.92	9.07 ± 0.32	10.29 ± 0.16	4.46 ± 0.89	-
	909	21	43.24 ± 0.92	20.40 ± 0.66	10.61 ± 0.14	4.79 ± 0.96	-
	1743	40	31.67 ± 0.96	30.36 ± 1.86	10.64 ± 0.16	4.85 ± 0.97	-
	3206	106	21.99 ± 0.46	40.32 ± 2.84	10.94 ± 0.14	5.02 ± 1.00	-
290	572	29	45.93 ± 0.37	5.19 ± 0.48	13.28 ± 0.26	7.18 ± 1.44	2.95 ± 0.28
	983	34	40.89 ± 0.92	9.12 ± 0.95	13.67 ± 0.35	8.45 ± 1.69	3.31 ± 0.35
	1693	52	29.11 ± 1.20	15.21 ± 1.70	15.03 ± 0.45	8.65 ± 1.73	3.60 ± 0.39
	2900	55	20.72 ± 1.34	23.45 ± 2.26	16.06 ± 0.65	9.04 ± 1.81	3.89 ± 0.55
298	546	16	36.98 ± 5.06	4.08 ± 0.32	17.66 ± 0.40	7.77 ± 1.55	3.26 ± 0.30

[i]the yield depends on the NO_x conditions; the yield given is that observed toward the end of the experiment. [ii]the yield increases with time; the yield given is that observed toward the end of the experiment.

5.2.1 Dimethyl sulfoxide (DMSO) and dimethyl sulfone ($DMSO_2$) formation

With the exception of the studies carried out in one atmosphere of nitrogen, dimethyl sulfoxide (DMSO: $CH_3S(O)CH_3$) is an important product in all of the systems studied, whereas dimethyl sulfone ($DMSO_2$: $CH_3S(O)_2CH_3$) only becomes significant upon the additon of considerable quanties of NO_x. In the following discussion only changes in the final corrected yields of the sulfur species with change in reaction conditions will be considered. DMSO and $DMSO_2$ are products, which can only be formed *via* the addition reaction pathway described in Section 2.2.1. The kinetic studies allow the respective fractions of the reaction occurring *via* the addition and abstraction pathways to be calculated for the different temperature and O_2 partial pressure reaction conditions employed in this study. The relative fractions are given in Table 5.15.

Table 5.15: Relative fractions of the reaction of DMS with the OH radical occurring *via* the addition and abstraction pathways.

Temperature (K)	pO_2 (mbar)	Addition pathway* (%)	Abstraction pathway* (%)
260	~0	-	100
	205	~79	~21
	500	~82	~18
270	~0	-	100
	205	~71	~29
	500	~76	~24
280	~0	-	100
	205	~62	~38
	500	~70	~30
290	~0	-	100
	205	~50	~ 50
	500	~62	~38
298	~0	-	100
	205	~39	~61
	500	~55	~45

**the fractions have been calculated for the specific reaction conditions using the results of Albu et al. (2006a) for addition and the results of Atkinson et al. (2004) for abstraction.*

The work has achieved the following:

- In systems with oxygen present the combined yields of DMSO and $DMSO_2$ are roughly equal to the fraction of the reaction proceeding *via* the addition channel. This

holds for all the temperatures investigated and also for both the NO_x-free and NO_x-containing systems (Tables 5.13 and 5.14).

- In the presence of NO_x, increasing the initial NO concentration decreased the yield of DMSO with an accompanying compensating increase in the yield of $DMSO_2$ (Table 5.14). Relatively high initial concentrations of NO were necessary to obtain a substantial decrease in the DMSO yield and an increase in the $DMSO_2$ yield.
- The yields of DMSO and $DMSO_2$ in the NO_x-systems containing "no" initially added extra NO were very similar to the DMSO and $DMSO_2$ yields obtained in the corresponding NO_x-free systems.
- In the NO_x-free experiments the yield of $DMSO_2$ was always very low (Table 5.13).
- In one atmosphere of nitrogen formation of DMSO was not observed (Table 5.13).
- In the absence of NO_x, in synthetic air the yield of DMSO decreases with increasing temperature (Table 5.13).
- In the absence of NO_x, for the same temperature, the yield of DMSO increases with increasing O_2 partial pressure (Table 5.13).

In the absence of NO_x, the observed behaviour of the yields of DMSO with variation in temperature and O_2 partial pressure (Section 5.1.1) is generally in line with what would be expected from the current mechanistic models, the initial steps of which can be represented by the following simplified reaction scheme:

$$OH + CH_3SCH_3 \rightarrow CH_3SCH_2 + H_2O \quad \text{(abstraction pathway)} \quad (5.1a)$$

$$OH + CH_3SCH_3 + M \leftrightarrow CH_3S(OH)CH_3 + M \quad \text{(addition pathway)} \quad (5.1b, -b)$$

$$CH_3S(OH)CH_3 + O_2 \rightarrow \text{products (including DMSO, } DMSO_2\text{, MSIA etc)} \quad (5.1c)$$

Low temperatures and high O_2 partial pressure will favour the addition channel and, hence, DMSO formation, whereas high temperatures and low O_2 partial pressure will favour the abstraction pathway.

The results from the present work support that in the absence of NO_x formation of DMSO *via* reaction of the dimethyl hydroxysulfuranyl radical (DMS-OH) with molecular oxygen will be by far the dominant channel. The possible pathways leading to DMSO formation are:

$$CH_3S(OH)CH_3 + O_2 \rightarrow CH_3S(O)CH_3 + HO_2 \quad (5.2)$$

$$CH_3S(OH)CH_3 + O_2 + M \rightarrow CH_3S(OH)(OO)CH_3 + M \quad (5.3)$$

$$CH_3S(OH)(OO)CH_3 + M \rightarrow CH_3S(O)CH_3 + HO_2 + M \quad (5.4)$$

From the present results it is not possible to say whether the formation of DMSO is mainly through a direct H-atom abstraction from the DMS-OH adduct, reaction (5.2), or *via* formation of an alcoxy-peroxy radical (DMS-OH-O_2) and its subsequent decomposition, reactions (5.3) and (5.4) although as will be discussed below, addition of O_2 has been shown to occur.

In the absence of NO_x only very low yields of $DMSO_2$ (< 6%) were observed at all the temperatures and O_2 partial pressures studied. The formation yield did not show a significant variation with the concentration of oxygen in the system. $DMSO_2$ production was also observed when N_2 was used as the diluent gas. Since in N_2 formation of DMSO was not observed the majority of $DMSO_2$ production in these experiments can almost certainly be ascribed to H_2O_2/DMS interactions, probably heterogeneous in nature at the reactor walls.

Chemical routes, which may lead to $DMSO_2$ formation in the oxidation of DMS with OH radicals in the reaction system under NO_x-free conditions, include formation from the reactions of the DMS-OH and DMS-OH-O_2 adducts and/or further oxidation of DMSO:

$$CH_3S(OH)CH_3 + O_2 + M \rightarrow CH_3S(OH)(OO)CH_3 + M \quad (5.3)$$

$$CH_3S(OH)(OO)CH_3 + M \rightarrow CH_3S(O)CH_3 + HO_2 + M \quad (5.4)$$

$$CH_3S(OH)(OO)CH_3 + M \rightarrow CH_3S(O)_2CH_3 + OH + M \quad (5.5)$$

$$CH_3S(O)CH_3 + OH + M \rightarrow CH_3S(O)(OH)CH_3 + M \quad (5.6)$$

$$CH_3S(O)(OH)CH_3 + O_2 \rightarrow CH_3S(O)(OH)(OO)CH_3 \quad (5.7)$$

$$CH_3S(O)(OH)(OO)CH_3 + M \rightarrow CH_3S(O)_2CH_3 + HO_2 + M \quad (5.8)$$

$$2\ CH_3S(OH)(OO)CH_3 \rightarrow 2\ CH_3S(OH)(O)CH_3 + O_2 \quad (5.9)$$

$$CH_3S(OH)(OO)CH_3 + RO_2 + M \rightarrow CH_3S(OH)(O)CH_3 + RO + O_2 + M \quad (5.10)$$

$$CH_3S(O)(OH)CH_3 + O_2 \rightarrow CH_3S(O)_2CH_3 + HO_2 \quad (5.11)$$

where RO_2 represents other peroxy radicals formed in the system.

The low yields of $DMSO_2$ observed under NO_x-free conditions employed in the present study support that the above-proposed routes to $DMSO_2$ formation are only of minor importance in the reaction systems.

In the experiments carried out in the presence of NO_x both DMSO and $DMSO_2$ were observed in substantial yields at all five temperatures. It is evident from the results presented in Paragraph 5.1.1 and Paragraph 5.1.2 that the yield-time behaviour of DMSO and $DMSO_2$ varies systematically with the changes in temperature and initial NO_x concentration. As

stated above the combined yields of DMSO and $DMSO_2$ are approximately equal to the fraction of the reaction proceeding by the addition channel for all the reaction conditions investigated, which indicates that no major product from the addition channel is missing.

The formation behaviour of DMSO and $DMSO_2$ with changes in temperature and initial NO_x concentration in the presence of O_2 can be described by the following oxidation scheme:

$$OH + CH_3SCH_3 + M \leftrightarrow CH_3S(OH)CH_3 + M \quad (5.1b, -b)$$

$$CH_3S(OH)CH_3 + O_2 \rightarrow CH_3S(O)CH_3 + HO_2 \quad (5.2)$$

$$CH_3S(OH)CH_3 + O_2 + M \rightarrow CH_3S(OH)(OO)CH_3 + M \quad (5.3)$$

$$CH_3S(OH)(OO)CH_3 + M \rightarrow CH_3S(O)CH_3 + HO_2 + M \quad (5.4)$$

$$CH_3S(OH)(OO)CH_3 + M \rightarrow CH_3S(O)_2CH_3 + OH + M \quad (5.5)$$

$$2\ CH_3S(OH)(OO)CH_3 \rightarrow 2\ CH_3S(OH)(O)CH_3 + O_2 \quad (5.9)$$

$$CH_3S(OH)(OO)CH_3 + NO \rightarrow CH_3S(OH)(O)CH_3 + NO_2 \quad (5.12)$$

$$CH_3S(OH)(O)CH_3 + O_2 \rightarrow CH_3S(O)_2CH_3 + HO_2 \quad (5.11)$$

In this scheme, reaction of an $CH_3S(OH)(OO)CH_3$ adduct with NO to give the $CH_3S(OH)(O)CH_3$ radical and NO_2, reaction (5.12), is the reaction in competition to reaction (5.4) that prevents DMSO from being formed when NO is added. This reaction is followed by reaction of the oxy radical ($CH_3S(OH)(O)CH_3$) with O_2 to give $DMSO_2$ and HO_2, reaction (5.11). The scheme predicts that any decrease in the yield of DMSO due to reaction (5.12) should be accompanied by a corresponding increase in the yield of $DMSO_2$.

With the large concentrations of NO_x being employed in the experiments one could speculate that the reaction of $O(^3P)$ with DMS in the systems may be a source of error since the photolysis of NO_2 will produce $O(^3P)$. It is well established that the reaction of $O(^3P)$ with DMS produces CH_3SO radicals in near 100% yield, which will further oxidize to produce SO_2 in high yield (Cvetanović *et al.*, 1981; Atkinson *et al.*, 2004 and references therein); this was also confirmed in test experiments within this study. Thus, if reaction of $O(^3P)$ with DMS was a significant interfering factor it would considerably reduce the yields of DMSO and $DMSO_2$ and increase that of SO_2. The fact that the combined yields of DMSO and $DMSO_2$ approximately match the fraction of the OH + DMS reaction predicted to proceed by the addition channel supports that interference from $O(^3P)$ + DMS is insignificant.

Figures 5.26 and 5.27 show plots of the DMSO and $DMSO_2$ yields as a function of the initial NO concentrations for the different temperatures studied (this study and the work of Arsene, 2002). The $DMSO_2$ yield values obtained in 1000 mbar synthetic air without any extra NO_x in addition to that generated from the CH_3ONO radical source were observed to

vary only slightly with temperature: 5.95 ± 0.45% (at 260 K), 5.83 ± 0.48% (at 270 K) and 5.74 ± 0.30% (at 280K). As noted previously these yields are very similar to those observed in the NO_x-free experiments. All of the plots for the DMSO yield as a function of initial NO concentration show curvature. For $DMSO_2$, with the exception of the data for 290 K, which appear linear, all the plots also show curvature.

An examination of the early stages of Figures 5.26 and 5.27 and also the numbers in Table 5.14 shows that NO concentrations of 150 - 200 ppbv cause an approximate doubling of the $DMSO_2$ compared to the ~5 - 6% yield measured under "zero" initial NO conditions for 260, 270 and 280 K. At the higher temperature of 290 K the effect appears to be much lower. The dependence of the DMSO and $DMSO_2$ yields on the NO_x conditions can explain the large variation in the yields of these compounds reported in literature studies of DMS oxidation products.

Other products studies from the literature on the OH radical initiated oxidation of DMS are summarized in Table III.1 (Appendix III). These studies have been performed mainly in photoreactors under static conditions. Many of the older studies have reported end product yields which have not been corrected for secondary reactions of the products and neither has a proper account been taken of possible oxidation at the walls of the photoreactor; this makes a direct comparison with the results of this study, which have been performed under more controlled conditions, difficult. Although the influence of NO_x on the OH radical initiated oxidation of DMS has been known for many years from kinetic investigations, it is only in recent years that experiments have been performed to elucidate the influence of NO_x on the product distribution. Also here direct comparisons of the results are not always easy because of the different NO/NO_2 ratios employed and the manner in which yields have been determined. The observations from the different studies do, however, allow trends to be recognized and inferences to be made concerning different reaction pathways and their importance under atmospheric conditions.

Arsene *et al.* (1999) have performed a detailed studied on the OH radical photo-oxidation of DMS at three different temperatures (284, 295 and 306 ± 2 K) and different O_2 partial pressures (20, 200 and 500 mbar), working with mixtures DMS - H_2O_2 at a total pressure of 1000 mbar (N_2 + O_2). DMSO and $DMSO_2$ were monitored using FTIR spectroscopy and corrections for secondary reaction and wall loss were made. Arsene *et al.* (1999) observed the same trend in the yield of DMSO with temperature and O_2 partial pressure as determined in this study. The values of the DMSO yields are in good agreement, within the error limits, with those of the present study. As in this study Arsene *et al.* (1999) found the yields of $DMSO_2$ to be highly variable and generally not above 8% S with a tendency for higher yields at higher temperatures.

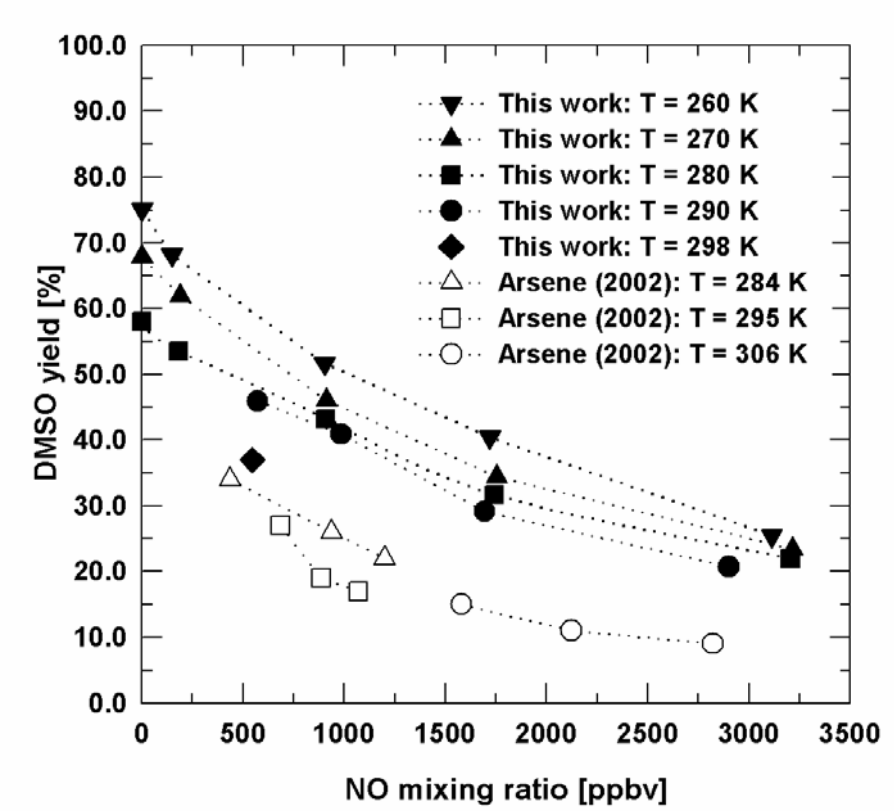

Figure 5.26: DMSO yields as a function of the initial NO concentrations for the different temperatures studied.

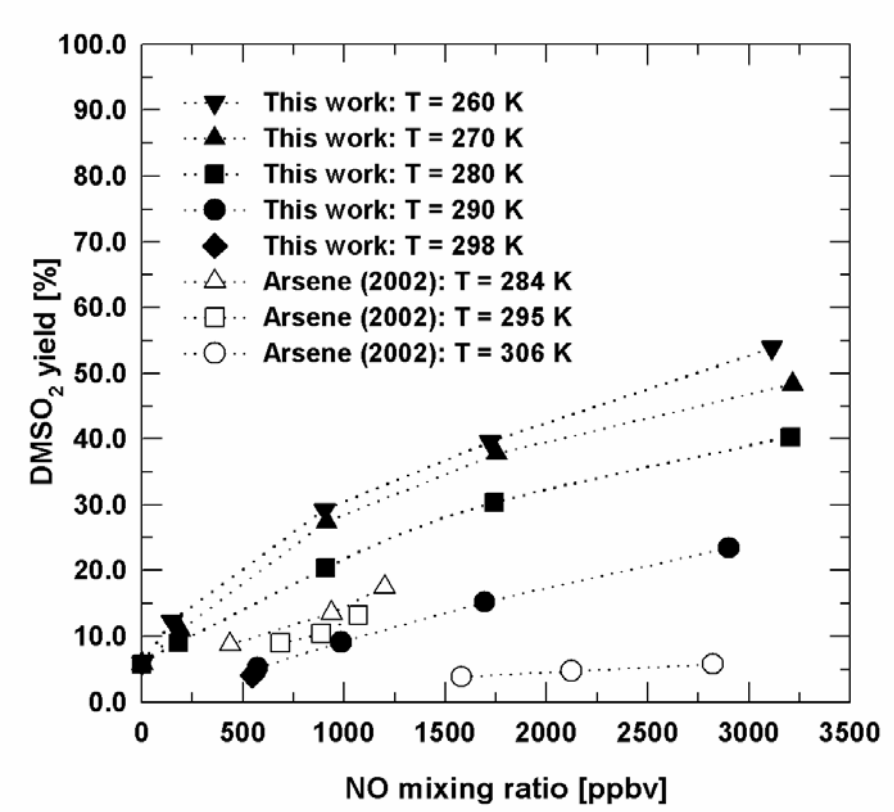

Figure 5.27: $DMSO_2$ yields as a function of the initial NO concentrations for the different temperatures studied.

The results of the present study together with those of Arsene *et al.* (1999) support that, in the absence of NO_x and over the temperature range 260 to 306 K, the O_2 dependent pathway in the OH radical initiated oxidation of DMS will result primarily in the formation of DMSO.

The study of Patroescu *et al.* (1999) was the first to systematically study the influence of the NO_x concentration on the product distribution in the OH radical initiated oxidation of DMS. At room temperature they varied the NO_x mixing ratio between 0 and ~1800 ppbv and observed changes in the yields of the observed products. As can be seen in Table III.1 (Appendix III) increasing the initial NO_x mixing ratio decreased the DMSO yield and increased the $DMSO_2$ yield as observed in this study. In the study of Patroescu *et al.* (1999) because of the experimental conditions employed the product formation yields could only be determined at 4 and 10% DMS consumption. The formation yields of DMSO and $DMSO_2$ were also not corrected for possible loss to the wall and/or further chemical reactions.

In a study similar to that presented here, Arsene *et al.* (2001) have investigated the products of the OH radical initiated oxidation of DMS at different initial NO_x concentrations for three temperatures (284, 295 and 306 $\pm$ 2 K) using H_2O_2 as the OH radical source. The studies performed within this work, however, have extended the investigations to lower temperatures and have used initial NO_x concentrations with much higher NO/NO_2 concentration ratios, i.e much lower initial NO_2 concentrations. In addition, the systems investigated in this work were less reactive, i.e. the OH radical steady state concentrations were lower than those used by Arsene *et al.* (2001) and resulted in much less secondary oxidation of the products.

Arsene *et al.* (2001) observed the same trends in the DMSO and $DMSO_2$ yields as reported here, i.e. increasing the initial NO concentration was found to depress the DMSO yield and enhance that of $DMSO_2$. They invoked the same mechanism as outlined above to explain this behaviour. Also in the study of Arsene *et al.* (2001) the combined yields of DMSO and $DMSO_2$ were roughly equal to the fraction of the reaction proceeding *via* the addition pathway at 295 and 306 K, but the agreement was not so good at 284 K. However, the yields of DMSO measured by Arsene *et al.* (2001) for the given initial NO conditions are lower than would be predicted from the NO dependence observed in this work. As mentioned above Arsene *et al.* (2001) had high NO_2 concentrations in their initial NO_x mixture, it is quite probable that under the conditions of their experiments that the fast photolysis of NO_2 led to initial levels of NO significantly higher than those present in the pre-irradiation period. Such an elevation of the initial NO concentration would explain the lower DMSO yields compared to this study due to the increased importance of reaction (5.12). Unfortunately, this

hypothesis could not be tested since Arsene *et al.* (2001) did not report concentration-time profiles for NO and NO_2.

In plots of the DMSO concentration against the amount DMS consumed to obtain the DMSO yield Arsene *et al.* (2001) observed two distinct linear periods: an initial period followed by a transition to a second period with larger slope, i.e. an increase in the DMSO yield compared to the first period. The onset of the increase was observed to occur at the point where the NO concentration approached values below the detection limit (10 ppbv), where the limiting step for DMSO formation, reaction (5.12), becomes unimportant. Apart from one experiment at 298 K (Figure 5.6e) this behaviour was not observed in the present work since sufficient NO was always present to drive reaction (5.12).

The finding in this work and the study of Arsene *et al.* (2001) of the nearly exclusive formation of DMSO in the O_2 dependent oxidation pathway of DMS is in strong contrast to the findings from the studies by Hynes *et al.* (1993) and Turnipseed *et al.* (1996). In the laser flash photolysis/pulsed laser induced fluorescence and pulsed laser photolysis/pulsed laser induced fluorescence studies on the reaction of OH radicals with DMS by Hynes *et al.* (1993) at 267 K and Turnipseed *et al.* (1996) at 234 and 258 K, branching ratios of ~0.5 and 0.5 ± 0.15 for HO_2 radical production from the $CH_3S(OH)CH_3 + O_2$ reaction were reported. The branching ratios are based on the conversion of HO_2 radical to OH radical by reaction with NO. They assumed that HO_2 radical was formed *via* abstraction of H atom from the DMS-OH adduct with the co-product DMSO in equivalent yield. The branching ratio for DMSO formation of ~0.5 from the studies of Hynes *et al.* (1993) and Turnipseed *et al.* (1996) is much lower than the ratio of slightly under 1 suggested by this study and the results of Arsene *et al*. (2001) for the temperature range 260 to 306 K. Arsene *et al*. (2001) have suggested that the discrepancy is probably due to the reaction conditions employed by Turnipseed *et al.* (1996) to produce OH radicals. Arsene *et al*. (2001) argued that addition of NO in the system employed by Turnipseed *et al.* (1996) will not only convert HO_2 radical to OH radical but will also disturb the equilibrium DMS-OH + O_2 $\leftrightarrow$ DMS-OH-O_2 through the reaction DMS-OH-O_2 + NO $\rightarrow$ DMS-OH-O + NO_2, which would change the DMSO formation branching ratio in their system.

Based on the work performed in this study and the body of evidence presented above it is suggested that in the OH radical initiated photooxidation of DMS within the temperature range 260 to 306 K, under all of the conditions that will prevail in the troposphere, the major products of the O_2-dependent pathway will be DMSO with a branching ratio of $\geq$0.95 and $DMSO_2$, if formed at all, with a ratio at the most of 0.05.

5.2.2 *Sulfur dioxide (SO_2), methyl thiol formate (MTF), methane sulfonic acid (MSA) and methyl sulfonyl peroxynitrate (MSPN) formation*

The results presented in Paragraph 5.1 and tabulated in Tables 5.13 and 5.14 show systematic changes in the yield-time behaviours of sulfur dioxide (SO_2), methyl thiol formate (MTF: CH_3SCHO), methane sulfonic acid (MSA: $CH_3S(O)_2OH$) and methyl sulfonyl peroxynitrate (MSPN: $CH_3S(O)_2OONO_2$) with temperature, O_2 partial pressure and initial NO_x conditions.

The ***experiments performed in the absence of NO_x*** (Table 5.13) will be considered first. The following generalisations can be made about the behaviours of SO_2 and MTF:

- The SO_2 yield increases with increasing temperature for each O_2 partial pressure.
- The SO_2 yield decreases with increasing O_2 partial pressure for each temperature studied.
- The yield of SO_2 is lower than the fraction of the reaction proceeding *via* the O_2-independent pathway.
- The MTF yield decreases with increasing O_2 partial pressure for each temperature studied.
- There are only moderate changes in the MTF yield on changing the temperature at a fixed O_2 partial pressure.

The observed variation in SO_2 formation with temperature and O_2 partial pressure in the absence of NO_x is generally in line with what would be expected from current mechanistic models, the initial steps of which can be represented by the following simplified reaction scheme:

$$OH + CH_3SCH_3 \rightarrow CH_3SCH_2 + H_2O \quad \text{(abstraction pathway)} \quad (5.1a)$$

$$OH + CH_3SCH_3 + M \leftrightarrow CH_3S(OH)CH_3 + M \quad \text{(addition pathway)} \quad (5.1b, -b)$$

$$CH_3S(OH)CH_3 + O_2 \rightarrow \text{products (including DMSO, } DMSO_2 \text{ etc)} \quad (5.1c)$$

$$CH_3SCH_2 + O_2 \rightarrow \text{products (including } SO_2\text{, MTF, MSA etc)} \quad (5.1d)$$

High temperatures and low O_2 partial pressure will favour the abstraction pathway and, hence, SO_2 formation, whereas low temperatures and high O_2 partial pressure favours the addition channel and DMSO formation.

The CH_3SCH_2 radicals formed in the abstraction channel by reaction (5.1a) will undergo the following reactions:

$$CH_3SCH_2 + O_2 + M \rightarrow CH_3SCH_2O_2 + M \quad (5.13)$$

$$CH_3SCH_2O_2 + CH_3SCH_2O_2\ (RO_2) \rightarrow 2CH_3SCH_2O + O_2 \quad (5.14a)$$

$$\rightarrow CH_3SCHO + CH_3SCH_2OH\ (ROH) + O_2 \quad (5.14b)$$

$$CH_3SCH_2O + M \rightarrow CH_3S + HCHO + M \quad (5.15)$$

where RO_2 represents other peroxy radicals formed in the system. The major fate of the CH_3SCH_2O radicals formed by reaction (5.14a) has been shown to be thermal decomposition to form CH_3S radicals and HCHO, reaction (5.15). The further reactions of CH_3S with O_2 in the absence of NO_x are postulated to lead to the formation of SO_2 and CH_3SO_3H. The following reaction scheme can explain the formation of SO_2 and MSA:

$$CH_3S + O_2 + M \leftrightarrow CH_3SOO + M \quad (5.16b, -b)$$

$$CH_3SOO \rightarrow \rightarrow CH_3S(O)_2 \quad (5.17)$$

$$CH_3S(O)_2 + M \rightarrow SO_2 + CH_3 + M \quad (5.18)$$

$$CH_3S(O)_2 + O_2 + M \rightarrow CH_3S(O)_2(OO) \quad (5.19)$$

$$CH_3S(O)_2(OO) + CH_3SO_{x(x=0-2)} \rightarrow CH_3S(O)_2(O) + CH_3SO_{x(x=1-3)} \quad (5.20)$$

$$CH_3S(O)_2(O) + RH \rightarrow CH_3S(O)_2(OH) + R \quad (5.21)$$

where RH = HCHO, CH_3SCH_3, CH_3SH, CH_3SOH, CH_3SO_2H, H_2O_2, CH_3OH, HO_2 (Yin *et al.*, 1990a).

In the reaction sequence (5.13) to (5.15) self-reactions of the peroxy radical $CH_3SCH_2O_2$, or reactions with other peroxy radicals will result in formation of methyl thiol formate (MTF: CH_3SCHO) and a corresponding alcohol, which would be methyl thiomethanol (CH_3SCH_2OH) in the case of the self-reaction of $CH_3SCH_2O_2$ radicals. An alternative route to MTF formation is reaction of the CH_3SCH_2O with O_2:

$$CH_3SCH_2O + O_2 \rightarrow CH_3SCHO + HO_2 \quad (5.22)$$

However, based on the available experimental evidence (Barnes *et al.*, 1994b, 1996; Patroescu *et al.*, 1996; Turnipseed *et al.*, 1996; Urbanski *et al.*, 1997), the current consensus is that this formation route is negligible and that thermal decomposition of the CH_3SCH_2O radical by reaction (5.15) dominates.

MTF has been detected and quantified in the NO_x-free experiments (Table 5.13); its formation is not observed in the experiments with NO_x. Its yield follows the same temperature

and O_2 partial pressure pattern as that shown by SO_2. Under the presumption that reaction (5.14b) is the source of MTF in the reaction systems, equal yields of CH_3SCH_2OH (methyl tiomethanol) will be formed. Unfortunately, to the best of my knowledge this compound has never been synthesized and thus no infrared spectrum of this compound is available, which could be used to verify its formation in the present experimental systems. Assuming, however, that it is the co-product of MTF then the combined yield of SO_2, MTF and CH_3SCH_2OH at 205 and 500 mbar O_2 partial pressure (Table 5.13) can account for up to 88% of the reaction proceeding by the O_2-independent abstraction channel. It is possible that the remainder is CH_3SCH_2OOH, which could be formed in the reaction $HO_2 + CH_3SCH_2OO$ (as was disscused in Chapter 2, Paragraph 2.2.2):

$$CH_3SCH_2OO + HO_2 \rightarrow CH_3SCH_2OOH + O_2 \qquad (5.23)$$

The above analysis is only valid, if production of SO_2 from the O_2-dependent addition channel is not significant under the experimental conditions employed, which is thought to be the case as will be discussed below. The analysis can also not be applied to the experiments performed under conditions without O_2 or at low O_2 partial pressure since the reaction will proceed virtually 100% *via* the abstraction channel and radical-radical reactions at the low O_2 levels present in the chamber, e.g. those between CH_3SCH_2 radicals, will produce products which can not be measured and quantified. Interestingly, at low O_2 partial pressure the SO_2 yield is highest at the highest temperature and lowest at the lowest temperature, which indicates the expected increasing importance of radical-radical combination reactions with decreasing temperature, terminating the SO_2 producing route. MTF formation is also observed at low O_2 partial pressure. The MTF yields in these experiments are only slightly higher than those observed in the experiments with high partial pressures of O_2, which is to be expected since a larger proportion of the reaction proceeds by the abstraction channel. The small dependence of the MTF yields on the O_2 partial pressures is further indirect evidence that formation of MTF *via* reaction (5.22) is negligible. The MTF yield is also observed to increase with decreasing temperature, which fully supports peroxy-peroxy reactions as main source, since these reactions will increase in importance with decreasing temperature.

Very low formation yields for MTF, up to a few percent, have also been reported in room temperature studies of the oxidation of DMS under the conditions of low and zero NO_x concentrations (Arsene *et al*., 1999; Patroescu *et al*., 1999) (see Table III.1, Appendix III).

The relatively low yield of MTF measured in the NO_x-free experiments, in which relatively high different concentrations levels of HO_2, CH_3SCH_2OO and other organosulfur peroxy radicals are generated, suggest that the production of MTF from peroxy-peroxy reaction will not be more than a few percent even at low temperatures.

The analyses of the SO_2 formation in the NO_x-free experiments did not show any indication for secondary formation of SO_2; this and the low SO_2 yields would support that under the conditions of the present experiments the observed processing of DMSO in the system does not produce SO_2 to any significant degree and fits with the recent observations that MSIA is the major product (Urbanski *et al.*, 1998; Arsene *et al.*, 2002c; Kukui *et al.*, 2003).

The high SO_2 yields reported in other DMS oxidation studies performed under NO_x-free conditions (see Table III.1, Appendix III) can be attributed to the higher OH radical steady state concentrations of the other systems which result in substantial further oxidation of MSIA which is known to produce SO_2 (Kukui *et al*., 2003).

In ***the experiments performed in the presence of NO_x*** (Table 5.14) at one atmosphere total pressure of synthetic air, the following general observations have been made:

- The yields of SO_2 are much lower than the fraction of the reaction proceeding *via* the abstraction pathway, which is generally considered the major production route for SO_2, as outlined above. Between 18 - 30% of the abtraction reaction is resulting in SO_2 formation. This is the case at all of the temperatures of this study.
- Increasing the initial NO_x concentration results in only minor increases in the SO_2 yield for all the temperatures.
- The SO_2 yields increase slightly with increasing temperature, which reflects the increase in the fraction of the reaction proceeding by the abstraction channel with increasing temperature.
- Formation of methyl sulfonyl peroxynitrate (MSPN: $CH_3S(O)_2OONO_2$) has been observed and quantified as a function of the progress of the reaction.
- Formation of methane sulfonic acid (MSA: $CH_3S(O)_2OH$) has been observed and quantified at 290 and 298 K as a function of the progress of the reaction.
- The combined yields of SO_2 and MSPN at 260, 270 and 280 K and of SO_2, MSPN and MSA at 290 and 298 K are much lower than the fraction of the reaction proceeding *via* the abstraction pathway.

In the presence of NO_x it has been shown that the H atom abstraction channel results exclusively in the formation of the CH_3S radical and HCHO, since the $CH_3SCH_2O_2$ radicals formed in reaction (5.13) react entirely with NO to give the CH_3SCH_2O radical, which decomposes to these products (as was disscused in Section 2.2.2):

$$CH_3SCH_3 + O_2 + M \rightarrow CH_3SCH_2O_2 + M \quad (5.13)$$

$$CH_3SCH_2O_2 + NO \rightarrow CH_3SCH_2O + NO_2 \quad (5.24)$$

$$CH_3SCH_2O + M \rightarrow CH_3S + HCHO + M \quad (5.15)$$

As in the NO_x-free experiments the further reactions of CH_3S will be pivotal in determining the amount of SO_2 formed in the abstraction channel.

As discussed in Section 2.2.2 Turnipseed *et al.* (1992) have discovered the formation of a weakly bound adduct between CH_3S and O_2:

$$CH_3S + O_2 + M \leftrightarrow CH_3SOO + M \quad (5.16b, -b)$$

Under atmospheric temperatures and O_2 concentrations, typically between 20 and 80% of CH_3S would be in the form of the CH_3SOO adduct. The equilibrium between CH_3S and CH_3SOO makes it difficult to assess the fate of CH_3S under atmospheric conditions. Based on the available kinetic data, reactions with O_2 and O_3 will determine the fate of CH_3S in the atmosphere. However, under the conditions of the present experiments in NO_x, reactions of CH_3S with NO_2 and especially NO will dominate over the reaction with O_2 as can be seen in Table 5.16 where the first-order loss rates (k[A]) for the reactions of CH_3S with O_2, O_3, NO and NO_2 at 298 K and atmospheric pressure are listed.

Table 5.16: First-order loss rates (k[A]) for the reaction of CH_3S with O_2, O_3, NO and NO_2 at 298 K and atmospheric pressure.

Reaction	*k*(298 K) (cm^3 $molecule^{-1}$ s^{-1})	[A] (molecules cm^{-3})	k[A] (s^{-1})
$CH_3S + O_2 \rightarrow$ products	$< 6 \times 10^{-18}$	5.17×10^{18}	< 31
$CH_3S + O_3 \rightarrow$ products	4.9×10^{-12}	9.84×10^{11} (40 ppbv)	4.8
$CH_3S + NO \rightarrow$ products	4.0×10^{-11}	2.46×10^{12} (100 ppbv)	98
		7.38×10^{13} (3000 ppbv)	2952
$CH_3S + NO_2 \rightarrow$ products	6.0×10^{-11}	2.46×10^{12} (100 ppbv)	147

The reaction of CH_3S radicals with NO will result in the formation of methyl thionitrite (CH_3SNO) at atmospheric pressure, however, under the experiments conditions this will be rapidly photolysed:

$$CH_3S + NO + M \rightarrow CH_3SNO + M \quad (5.25)$$

$$CH_3SNO + h\nu \rightarrow \text{products } (CH_3S + NO) \quad (5.26)$$

Niki *et al*. (1983a, b) have studied the spectroscopic and photochemical properties of CH_3SNO and reported IR and UV-Visible spectra. No evidence could be found in the recorded infrared spectra for the formation of CH_3SNO. Its steady state concentration, however, may be below the detection limit of the experimental set-up. Niki *et al*. reported a yield for SO_2 of ~20% for the photolysis of CH_3SNO in air at 298 K, which is similar to the yields of 18 to 30% determined here over a wider range of conditions. Niki *et al*. noted the presence of several prominent peaks belonging to gaseous MSA and also the presence other S-containing compounds, which they were unable to identify.

In the residual spectra of the experiments performed in the presence of NO_x at low temperatures, i.e. after subtraction of all identified species, some unidentified bands remained at 1723, 1301 and 795 cm^{-1}, at room temperature or around room temperature some additional bands at 1674, 1297 and 822 cm^{-1} were also present. These bands can be attribuited to peroxynitrate compounds ($CH_3S(O)OONO_2$ and possibly CH_3SOONO_2) and $CH_3S(O)ONO_2$, $CH_3S(O)NO_2$ and $CH_3S(O)NO$ (Mayer-Figge, 1997). In the present study the formation of the peroxynitrate MSPN ($CH_3S(O)_2OONO_2$) has been quantified. As was discussed in Section 2.2.2, MSPN will result from reactions of the methyl sufonyl radical (CH_3SO_2):

$$CH_3SO_2 + O_2 + M \leftrightarrow CH_3S(O)_2OO + M \quad (5.27)$$

$$CH_3S(O)_2OO + NO_2 + M \leftrightarrow CH_3S(O)_2OONO_2 + M \quad (5.28)$$

In some end product studies (Barnes *et al.*, 1987b; Jensen *et al.*, 1991, 1992) a species was observed which was tentatively assigned to methyl sulfinyl peroxynitrate ($CH_3S(O)OONO_2$). The formation of this species would imply a reaction sequence involving consecutive addition of O_2 and NO_2 to CH_3SO:

$$CH_3SO + O_2 + M \leftrightarrow CH_3S(O)OO + M \quad (5.29)$$

$$CH_3S(O)OO + NO_2 + M \leftrightarrow CH_3S(O)OONO_2 + M \quad (5.30)$$

However, it is now quite sure that the compound observed in these studies was methyl sulfonyl peroxynitrate ($CH_3S(O)_2OONO_2$) and not methyl sulfinyl peroxynitrate ($CH_3S(O)OONO_2$) (Hjorth *et al.*, 1993; Van Dingen *et al.*, 1994; Mayer-Figge *et al.*, 1997). Methyl sulfonyl peroxynitrate ($CH_3S(O)_2OONO_2$) has been observed in many other studies of the OH radical initiated oxidation of DMS, at room or around room temperature, in the presence of NO_x (Sørensen *et al.*, 1996; Patroescu *et al.*, 1999; Arsene *et al.*, 2001; Librando *et al.*, 2004), and the reported yields of MSPN are collected in Table III.1 (Appendix III). The yield of MSPN is dependent on the temperature and NO_x concentration of the system, which makes a direct comparison between the different product studies difficult. However, in all of the studies the molar yields of MSPN have never exceeded 8%.

Mayer-Figge (1997) has investigated the photolysis of CH_3SNO at low temperatures using FTIR spectroscopy for the product analysis in an attempt to detect methyl thiomethyl peroxynitrate (CH_3SOONO_2) and methyl sulfinyl peroxynitrate ($CH_3S(O)OONO_2$). The IR evidence from the study was more in keeping with the formation of $CH_3S(O)OONO_2$ rather than CH_3SOONO_2. A qualitative investigation on the thermal stability of the species implied that it would not be important under atmospheric conditions.

5.2.3 Carbonyl sulfide (OCS) formation

Formation of OCS has been observed in this study from the OH radical photooxidation of dimethyl sulfide in experiments performed in the absence of NO_x at 290 and 298 K. The present results confirm that OCS is a minor but important product of the OH radical initiated oxidation of DMS under NO_x-free conditions.

The yield of OCS at 298 K and an oxygen partial pressure of 205 mbar, as determined in the present study, is similar to that previously obtained in studies on the OH radical initiated oxidation of DMS at room temperature under NO_x-free or very low NO_x conditions (Barnes *et al.*, 1994b, 1996; Patroescu, 1996; Arsene *et al.*, 1999; Patroescu *et al.*, 1999; Arsene *et al.*, 2001; Arsene, 2002) (see Table III.1, Appendix III).

The mechanism of OCS formation is presently not known; a detailed discussion on possible pathways, which could explain the formation of OCS in the OH radical initiated oxidation of DMS, can be found in the paper of Barnes *et al.* (1996).

As was discussed in Section 2.2.2, OCS can result from reactions of CH_3S radicals with O_2, producing CH_2S (thioformaldehyde) and its subsequent oxidation:

$$CH_3S + O_2 \rightarrow CH_2S + HO_2 \quad (5.31)$$

$$CH_2S + OH/h\nu \rightarrow HCS + H_2O/H \quad (5.32)$$

$$HCS + O_2 \rightarrow OCS + OH \quad (5.33)$$

Barnes *et al.* (1994b, 1996) have presented experimental evidence, which supports the existence of this formation route for OCS. The self-reaction of CH_3S radicals leads through a minor channel to the formation of CH_2S and methyl mercaptan (CH_3SH) (Barnes *et al.*, 1996, and references therein).

This and other studies have shown that methyl thiol formate (MTF) is a product of the NO_x-free oxidation of DMS. The reaction of MTF with OH radicals or its photolysis could also lead to the formation of OCS (Patroescu *et al.*, 1996):

$$CH_3SCHO + OH/h\nu \rightarrow CH_3SCO + H_2O/H \quad (5.34)$$

$$CH_3SCO + \Delta \rightarrow CH_3 + OCS \quad (5.35)$$

In the present work formation of OCS was not observed in the experiments performed in the absence of O_2 contrary to the formation of MTF (as discussed in Chapter 4 traces of O_2 will always be present in photoreactors which can explain the formation of MTF). The photolysis of MTF in N_2 is known to produce OCS in very low yield (Patroescu *et al.*, 1996), but in the present experimental system the amount produced by photolysis of MTF in N_2 was obviously below the detection limit. The observations support the main source of OCS in the present experiments is the reaction of CH_3S with O_2 to produce CH_2S followed by oxidation of this compound to give OCS as suggested by Barnes *et al.* (1994b, 1996).

The yield of OCS is small, and it has been suggested that the oxidation of impurities such as CS_2, which can be present in the liquid samples of DMS, could explain the observed formation of OCS in the OH radical initiated oxidation of DMS. Oxidation of CS_2 with OH radicals is known to result in high yields of OCS (Barnes *et al.*, 1983; Becker *et al.*, 1990). However, the concentrations of OCS formed in experimental systems of Barnes *et al.* (1994b, 1996) were always much higher than the detection limit for CS_2 with the FTIR experimental set-up, which supported that the presence of CS_2 impurities can be excluded as the OCS source. Further, and more importantly, in studies on the OH radical initiated oxidation of CS_2 large yields of OCS were observed in the presence of NO_x (Barnes *et al.*, 1983; Becker *et al.*, 1990). Since in this study and that of Barnes *et al.* (1996), NO_x reduces the OCS yield to zero this also rules out the oxidation of CS_2 as the OCS source. Reduction of the OCS formation yield to zero by the addition of NO_2 to the reaction system can be attributed to effective scavenging of the CH_3S radicals by the reaction with NO_2 or O_3 to form CH_3SO and NO.

5.2.4 Methane sulfonic acid (MSA) and methane sulfinic acid (MSIA) formation

Methane sulfinic acid and methane sulfonic acid have been determined by ion chromatography at all temperatures and reaction conditions studied. From the IC analysis the integral yields of MSIA and MSA, incorporating all production and loss processes, show the following:

- The yields of MSIA and MSA increase with increasing O_2 partial pressure for a constant temperature.
- The yields of MSIA and MSA increase with decreasing temperature for a constant O_2 partial pressure.
- Both MSIA and MSA have also been detected in the absence of O_2 in the reaction system, but in low yields.
- The yields of MSIA and MSA decrease with increasing of NO_x concentration for a constant temperature.
- The yields of MSIA and MSA decreases with increasing temperature for approximately the same NO_x initial concentration.
- The MSA yields obtained at 290 and 298 K using ion chromatography are higher than those determined in the gas phase by FTIR spectroscopy.

From the IC analysis for the highest temperature used in the experiments, 298 K, the integral yield of MSIA is between 3.5 - 10% S and is increasing with decreasing temperature, reaching between ~5 - 23% S at 260 K, the lowest temperature used in experiments. The yields measured in this work are in accord with the yields obtained by Arsene *et al.* (2001), in which they showed that the yield of MSIA is between 4 - 10% S at 295 K and about 20% S at 284 K, but are much higher than the yield of 1.5 $\pm$ 1.1% S reported by Sørensen *et al.* (1996) and of 0.1 - 0.2 $\pm$ 0.1% S reported by Librando *et al.* (2004). This can probably be explaind by the method of sampling used by Sørensen *et al.* (1996) and Librando *et al.* (2004). In their study the samples were collected at the end of the irradiation period and not during the irradiation as in this study and in the work of Arsene *et al.* (2001). Since MSIA is subject to further fast oxidation by OH radicals (Yin *et al.*, 1990a) and wall loss processes, a low yield of MSIA will be obtained if the measurements are conducted at the end of the irradiation. In this study and in the study of Arsene *et al.* (2001) much lower collection and storage temperatures were used which probably assists in inhibiting the further oxidation of MSIA to MSA by any oxidising material co-collected in the sampling medium.

The yields of MSA obtained using IC are higher then the quantities measured in the gas phase, at 290 and 298 K, in the presence of NO_x. This is probably due to (i) the method of sampling, i.e. continuous collection of the samples during irradiation and (ii) oxidation of MSIA to MSA either in the sampling line or in the liquid sample itself. The measured values of MSA using the IC method cannot, therefore, be compared directly with the gas-phase formation yield of MSA. The measured quantities of MSA by IC are the composite values of the gas-phase MSA yield plus the contribution from the oxidation of MSIA. Because of the high reactivity of MSIA, it is very difficult to avoid its further oxidation to MSA in analytical probing systems. The higher values of methane sulfonic acid determined by IC compared to the gas-phase values of this compound obtained by long path FTIR spectroscopy are a further indication of the importance of MSIA production in the reaction system.

Test experiments showed that mixtures of DMS-H_2O_2-N_2 (-synthetic air or -N_2/O_2) or DMS-CH_3ONO-synthetic air do not produce MSIA and MSA in the dark. Thus, the only route to MSIA in the present experiments appears to be gas-phase OH radical intiated oxidation of DMS. The results of the IC analysis experiments also show an increase in the measured yield of MSIA on decreasing the temperature from 298 to 260 K. The decrease in temperature increases the importance of the addition pathway and also the formation of DMSO. Therefore, the results support the conclusion that the further oxidation of DMSO with OH will be the major pathway leading to production of MSIA in the present system by the reaction sequence:

$$CH_3S(O)CH_3 + OH + M \rightarrow CH_3S(O)(OH)CH_3 + M \quad (5.36)$$

$$CH_3S(O)(OH)CH_3 + M \rightarrow CH_3S(O)OH + CH_3 + M \quad (5.37)$$

Although, the measurements do not allow an exact determination of the formation yield of MSIA, a simple consideration based on the magnitude of the measured MSIA yield in combination with the sampling efficiency and the loss processes involved (wall loss, gas-phase oxidation, oxidation to MSA in the liquid sample) leads to the conclusion that the fraction of the OH + DMSO reaction leading to MSIA formation must be fairly considerable.

This would be in agreement with the recent studies of Urbanski *et al*. (1998), Arsene *et al*. (2002c), Wang and Zhang (2002b), Kukui *et al*. (2003), Resende *et al.* (2005) and González-Garcia *et al.* (2006).

5.3 Summary of the product results

The products from the OH radical initiated oxidation of dimethyl sulfide (DMS) has been investigated as a function of temperature and: (i) initial NO_x concentration at 1000 mbar total pressure of synthetic air and (ii) O_2 partial pressure at 1000 mbar total pressure ($O_2 + N_2$).

(i) NO_x-containing systems:

- In the presence of NO_x, the sulfur-containing products identified in the OH radical initiated oxidation of DMS were dimethyl sulfoxide (DMSO), dimethyl sulfone ($DMSO_2$), sulfur dioxide (SO_2), methyl sulfonyl peroxynitrate (MSPN) and methane sulfonic acid (MSA).
- Based on the obtained molar yields of the gas-phase products, using long path FTIR spectroscopy, it has been shown (Table 5.14 and Figure 5.28) that the level of the NO concentration in the reaction system was a crucial factor in determining the yields of the products at different temperatures. Increasing the initial NO concentration was found to depress the DMSO formation yields and enhance those of $DMSO_2$, SO_2, MSPN and MSA.
- The variation of the product yields with temperature and NO_x concentration is consistent with the occurrence of both addition and abstraction channels in the OH radical initiated oxidation of DMS.
- At all the temperatures studied, both DMSO and $DMSO_2$ were observed in substantial yields. The combined yields of DMSO and $DMSO_2$ are approximately equal to the fraction of the reaction proceeding *via* the addition channel for all the reaction conditions investigated, which indicates that no major product from the addition channel is missing.
- In the presence of NO_x, increasing the initial NO concentration decreased the yield of DMSO with an accompanying compensating increase in the yield of $DMSO_2$. Relatively high intial concentrations of NO were necessary to obtain a substantial decrease in the DMSO yield and an increase in the $DMSO_2$ yield.
- The combined yields of SO_2 and MSPN at 260, 270 and 280 K and the combined yields of SO_2, MSA and MSPN at 290 and 298 K are much lower than the fraction of the reaction proceeding *via* the abstraction pathway indicating the presence of unidentified compounds. From absorption features in the IR evidence was found for the possible presence of nitro sulfinyl or sulfonyl type compounds.

(ii) NO_x-free systems:

- In the absence of NO_x, the formation of dimethyl sulfoxide (DMSO), dimethyl sulfone ($DMSO_2$), sulfur dioxide (SO_2), methyl thiol formate (MTF) and carbonyl sulfide (OCS) was observed.
- Based on the obtained molar yields of the gas-phase products, analyzed by long path FTIR spectroscopy, it has been shown (Table 5.13 and Figure 5.29) that DMSO and SO_2 are the major oxidation products under NO_x-free conditions in the systems with oxygen. In one atmosphere of nitrogen the formation of DMSO was not observed.
- The observed behaviour of formation of SO_2 and DMSO at various temperatures and O_2 partial pressures is in agreement with current mechanistic models involving addition and abstraction channels of the primary reaction steps.
- In systems with oxygen present the combined yields of DMSO and $DMSO_2$ are approximately equal to the fraction of the reaction proceeding *via* the addition channel like the results in the NO_x-containing systems. The yield of $DMSO_2$ was always very low (<6%). The results support that in the absence of NO_x formation of DMSO *via* reaction of the DMS-OH adduct with molecular oxygen will be by far the dominant channel and the production of $DMSO_2$ from reactions of the DMS-OH or DMS-OH-O_2 adducts will be very minor.
- The total yield of SO_2 and MTF at 260, 270 and 280 K as well as the total yield of SO_2, MTF and OCS at 290 and 298 K are lower than the fraction of the reaction proceeding *via* the O_2-independent pathway, indicating a missing product, possibly CH_3SCH_2OOH.

The experimental product data obtained in the present study have helped to highlight important mechanistic features of the atmospheric degradation mechanism of dimethyl sulfide (DMS). In combination with observations from previous studies on DMS oxidation the results obtained in this study have been used to construct a general mechanism for the oxidation of DMS in the absence and in the presence of NO_x. Figure 5.30 and Figure 5.31 show the general mechanisms for the addition and abstraction channels, respectively, in the OH radical initiated oxidation of DMS.

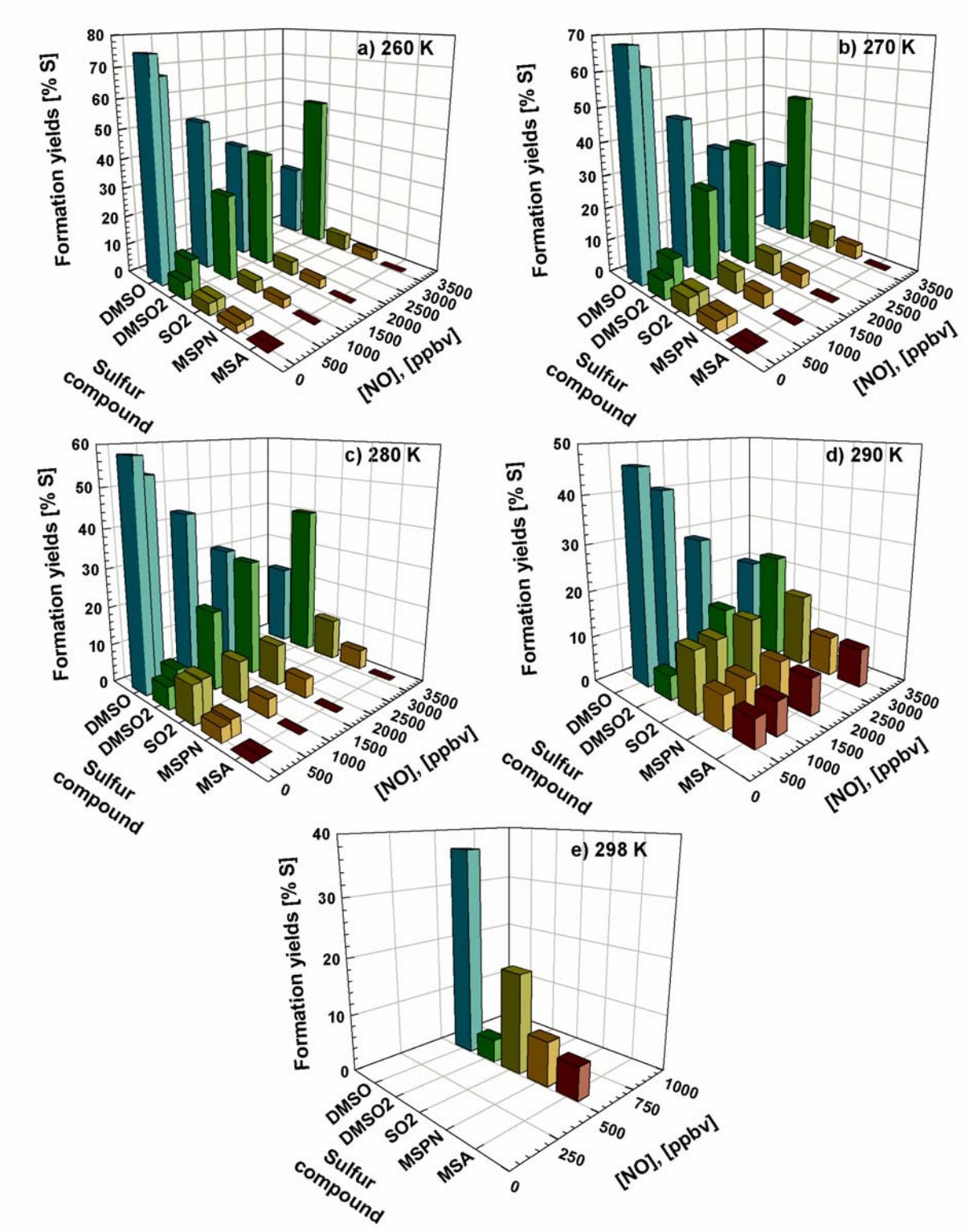

Figure 5.28: Yields of the products observed in the OH radical initiated oxidation of DMS at different temperatures as a function of the initial NO concentration.

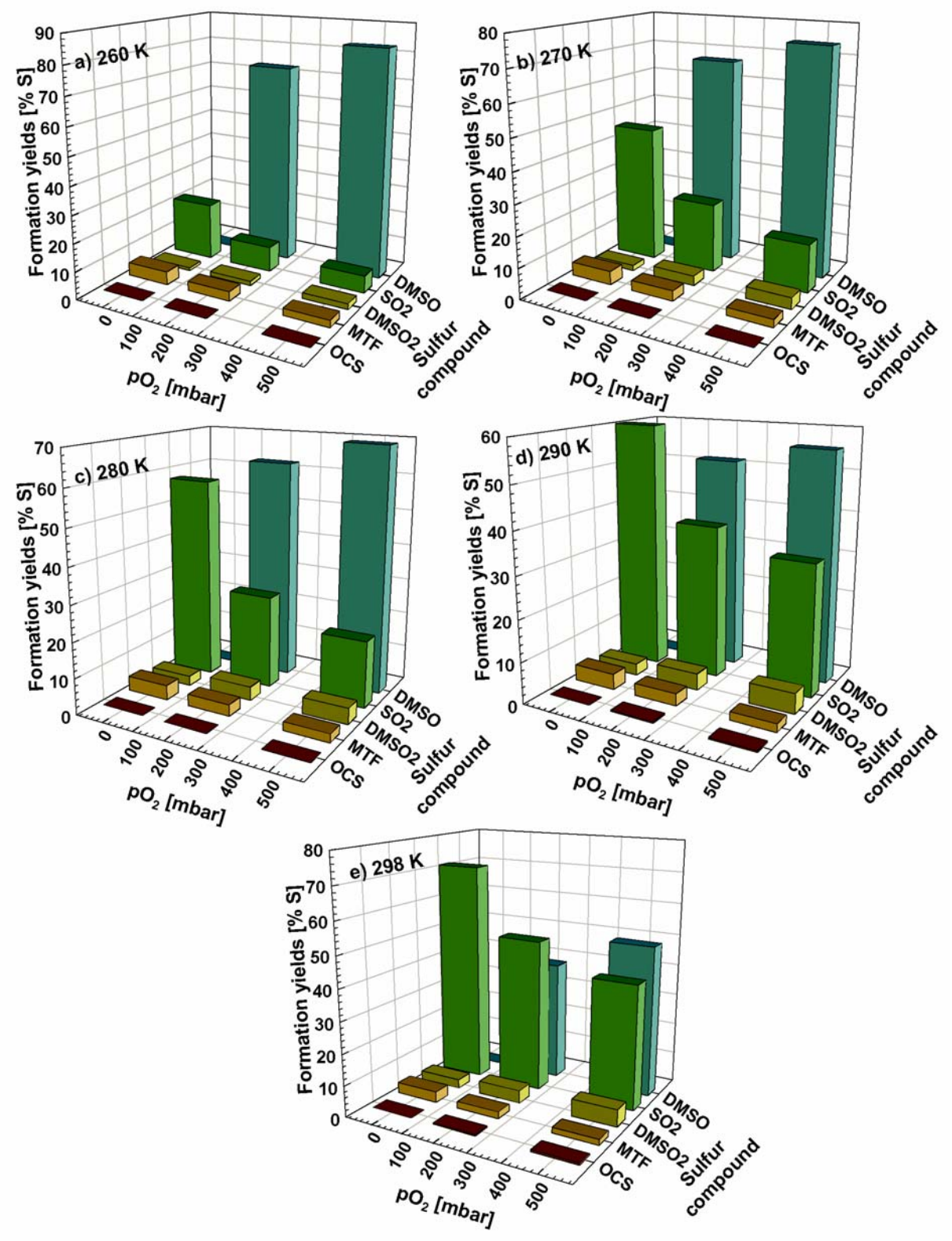

Figure 5.29: Yields of the products observed in the OH radical initiated oxidation of DMS at different temperatures as a function of the O_2 partial pressure.

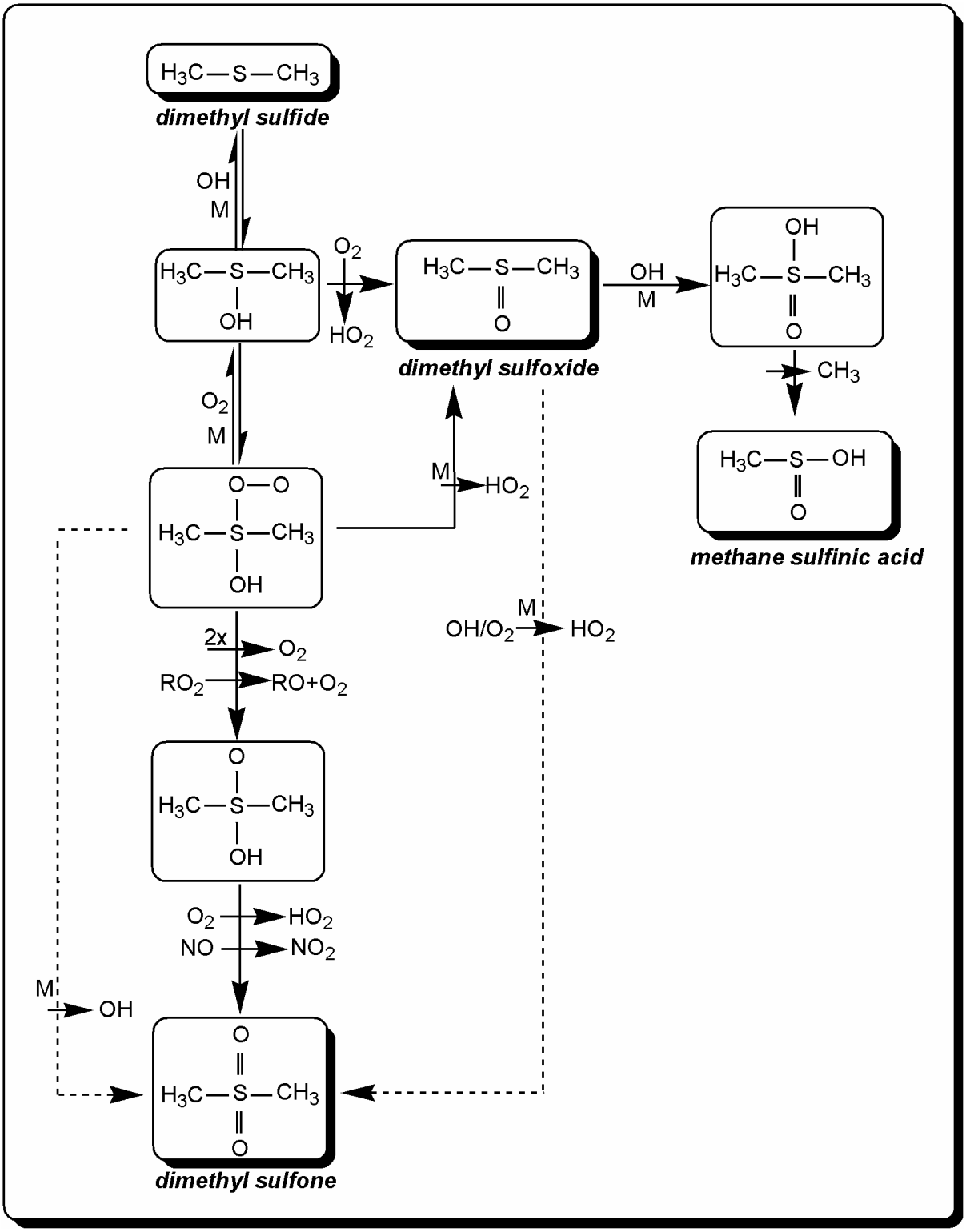

Figure 5.30: Proposed reaction mechanism for the addition channel of the OH radical initiated oxidation of DMS.

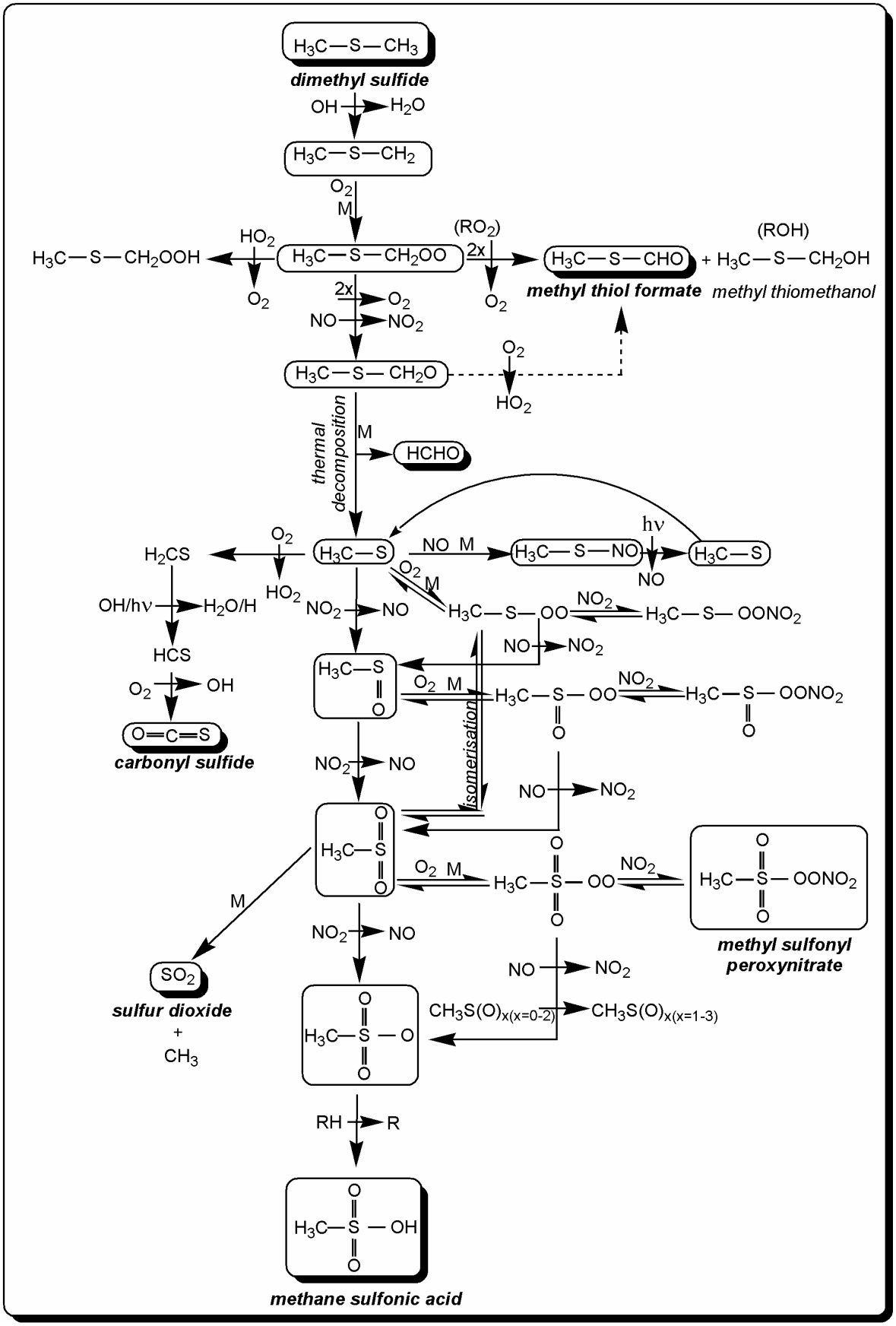

Figure 5.31: Proposed reaction mechanism for the abstraction channel of the OH radical initiated oxidation of DMS.

Chapter 6

Atmospheric implications

The kinetic results reported in Chapter 4 have confirmed the sharp increase in the rate coefficient for the reaction of OH radicals with DMS at temperatures below ~270 K observed by Williams *et al*. (2001, 2007).

Although these results are of interest from a mechanistic viewpoint they will have no impact on DMS chemistry in the lower troposphere (LT) since at temperatures below ~273 K emissions of DMS from the oceans will be extremely low. The results will only be of atmospheric significance if DMS can reach the upper troposphere/lower stratosphere (UT/LS), as has been observed for reactive VOC's, where such low temperatures prevail. Updrafts in deep convective clouds can raise boundary layer air into the upper troposphere within a matter of minutes. It has been suggested from observations of near-zero ozone concentrations over the convective Pacific that rapid convective transport of marine gaseous emissions such as DMS between the marine boundary layer and the uppermost troposphere could occur and lead to sulfate particle formation (Kley *et al.*, 1996). Up to now no measurements have confirmed this.

The distribution of the products from the reaction of OH radicals with DMS is dependent on the ratio of the two reaction channels, addition and abstraction, which is controlled by temperature and the oxygen partial pressure. The results of this study and those of Williams *et al*. (2001, 2007) have shown that for atmospheric conditions and at temperatures below ~270 K the contribution of the addition pathway is considerably higer than was predicted by extrapolation using the previously recommended Arrhenius expression of Hynes *et al*. (1986).

Product studies on the OH radical initiated oxidation of DMS as a function of temperature and oxygen partial pressure reported in Chapter 5 have shown that dimethyl sulfoxide (DMSO) is the major product from the addition channel with molar yields of around 75% at 260 K in the presence of low levels of NO_x. Only very low yields of sulfur dioxide (SO_2) and dimethyl sulfone ($DMSO_2$) are observed under these conditions.

A considerable fraction of the DMSO formed undergoes further oxidation in the system due to its rapid reaction with OH radicals. The products from the oxidation of DMSO

with OH radicals at low temperature are currently not known. A number of studies to determine the mechanism of the reaction of DMSO with OH have been carried out at room or around room temperature (Barnes *et al*., 1989; Hynes and Wine, 1996; Sørensen *et al*., 1996; Urbanski *et al*., 1998; Arsene *et al*., 2002c; Kukui *et al*., 2003; Bossoutrot *et al*., 2004). The products observed include sulfur dioxide (SO_2), dimethyl sulfone ($DMSO_2$), methyl sulfonyl peroxynitrate (MSPN), methane sulfonic acid (MSA) and methane sulfinic acid (MSIA). However, the values of the product yields reported in the various studies differ quite significantly and require further investigations. At room temperature it has been shown that the major product from the OH radical initiated oxidation of DMSO is methane sulfinic acid (Urbanski *et al.*, 1998; Arsene *et al.*, 2002c; Kukui *et al.*, 2003); *ab initio* studies (Wang and Zhang, 2002b; Resende *et al.*, 2005; González-Garcia *et al.*, 2006) also support formation of MSIA as the main product in the reaction of DMSO with OH radicals.

The analyses of the SO_2 formation in the NO_x-free experiments in this work did not show any indication for secondary formation of SO_2; this and the low SO_2 yields would support that under the conditions of the present experiments the observed processing of DMSO in the system does not produce SO_2 to any significant degree and fits with the recent observations that MSIA is the major product. The high SO_2 yields reported in other DMS oxidation studies performed under NO_x-free conditions (see Table III.1, Appendix III) can be attributed to the higher OH radical steady state concentration of the other systems which result in substantial further oxidation of MSIA which is known to produce SO_2 (Kukui *et al*., 2003).

In the remote marine boundary layer, where NO levels are typically low (2 - 8 pptv) (McFarland *et al.*, 1979; Davis *et al.*, 1987; Singh *et al.*, 1996), production of $DMSO_2$ from reactions of the DMS-OH or DMS-OH-O_2 adduct will be very minor. It is clear from this work that although very high concentrations of $DMSO_2$ can be generated in the experimental systems, initial concentrations of NO in excess of those ocurring the atmosphere are required to obtain a change in the reaction channels of the adducts. Such NO concentrations will only be found in urban-suburban areas, where NO_x mixing ratios typically range from 10 to 1000 ppbv. Therefore, the yield behaviour of $DMSO_2$ observed in the present study in the presence of NO_x supports that under the majority of the NO_x conditions encountered in the atmosphere production of $DMSO_2$ from reaction of the DMS-OH-O_2 adduct with NO will be of negligible importance. The reaction sequence will only be important in laboratory experimental systems containing 200 ppbv or higher levels of NO_x. The formation of $DMSO_2$ could possibly be of some importance in highly polluted coastal areas.

The relatively low yield of MTF measured in the NO_x-free experiments, in which relatively high different concentration levels of HO_2, CH_3SCH_2OO and other organosulfur

peroxy radicals are generated, suggests that even in the remote marine boundary layer, where the concentrations of NO are very low and peroxy-peroxy radical reaction can occur, the production of MTF will not be more than a few percent.

The results of the present work show that the OCS yield from the oxidation of DMS is low, however, because of the relatively high global DMS source of 24.45 $\pm$ 5.30 Tg S $year^{-1}$ (Watts, 2000), the OCS production from the DMS oxidation could contribute 0.15 $\pm$ 0.03 Tg OCS $year^{-1}$ which makes ~12% of the total OCS source.

The above discussion has been for conditions of 1 atm of air. However, in the UT/LS where low temperatures between 210 and 260 K can prevail the increase in the rate coefficient will be compensated, at least in part, by the decrease in the O_2 partial pressure which will fall, from approximately 110 Torr at 3 km altitude to 40 Torr around 10 km. In regions of the troposphere with an O_2 partial pressure of ~100 Torr where temperatures of approximately 250 K prevail, the present results show that the addition channel will account for ~70% of the overall reaction of OH radicals with DMS. However, in the present work no kinetic measurements were made down to 210 K, but an extrapolation of the available data set suggests that under these conditions the addition channel could account for ~80% of the overall reaction. Thus, it would appear that under the conditions prevailing in the UT/LS the contribution of the addition channel to the reaction of OH radicals with DMS will vary within a relatively narrow range, i.e. approximately 70 - 80%, since the increase in rate with decreasing temperature is compensated by the decrease with decreasing partial pressure of O_2.

Summary

A detailed knowledge of the hydroxyl (OH) radical kinetics and atmospheric oxidation mechanism for dimethyl sulfide (DMS) is necessary to asses the possible impacts of this compound on the climate. The aims of this work were therefore (i) to study the kinetics of the reaction of OH radicals with DMS as a function of temperature and oxygen partial pressure and (ii) to investigate the effects of temperature, oxygen partial pressure and NO_x concentration on the product distribution from the reaction. The results will help to better predict product pathways under atmospheric conditions. A detailed knowledge of the atmospheric oxidation mechanism for DMS is necessary because different products will have different impacts on the climate. To fulfill these aims:

- the kinetics of the OH radical initiated oxidation of DMS were investigated as a function of temperature (250, 260, 270, 280, 290 and 299 K) and O_2 partial pressure (~0, 205 and 500 mbar) at a total pressure of 1000 mbar ($O_2 + N_2$) using the relative kinetic technique and FTIR spectroscopy for the analysis

and

- the yields of important species produced in the OH radical initiated oxidation of dimethyl sulfide have been determined and quantified at different temperatures (260, 270, 280, 290 and 298 K), different O_2 partial pressures (~0, 205 and 500 mbar) and different initial NO_x concentrations ($NO + NO_2$: 0 - 3215 ppbv + 0 - 106 ppbv) using mainly *in situ* FTIR spectroscopy for the analysis of reactants and products.

The averaged values of the rate coefficients for the reaction of OH radicals with DMS determined in this work as a function of temperature and oxygen partial pressure are summarized in Table S.1. The Arrhenius expressions, valid in the range of temperature from 250 to 299 K, for the reaction of OH radicals with DMS derived from the temperature dependent rate coefficients listed in Table S.1 are given in Table S.2.

Table S.1: Summary of rate coefficients for the reaction of OH radicals with DMS determined at different temperatures and O_2 partial pressures.

Temperature (K)	$k_{DMS} \times 10^{11}$ (cm^3 $molecule^{-1}$ s^{-1})		
	~0 mbar O_2	205 mbar O_2	500 mbar O_2
299	0.50 ± 0.10	0.78 ± 0.18	0.95 ± 0.19
290	0.57 ± 0.11	0.98 ± 0.23	1.34 ± 0.27
280	0.62 ± 0.13	1.20 ± 0.26	1.54 ± 0.31
270	0.63 ± 0.14	1.51 ± 0.34	1.85 ± 0.37
260	0.64 ± 0.13	1.99 ± 0.47	2.38 ± 0.47
250	0.66 ± 0.14	2.82 ± 0.77	2.83 ± 0.62

Table S.2: Arrhenius expressions for the reaction of OH radicals with DMS as a function of O_2 partial pressure valid in the temperature range 250 to 299 K.

O_2 partial pressure (mbar)	k_{DMS} (cm^3 $molecule^{-1}$ s^{-1})
~ 0	$(1.56 \pm 0.20) \times 10^{-12} \exp[(369 \pm 27) / T]$
205	$(1.31 \pm 0.08) \times 10^{-14} \exp[(1910 \pm 69) / T]$
500	$(5.18 \pm 0.71) \times 10^{-14} \exp[(1587 \pm 24) / T]$

The results obtained in this work using the relative kinetic technique have confirmed the sharp increase in the rate coefficient for OH radicals with DMS at temperatures below 270 K observed by Williams *et al*. (2001) using an absolute kinetic method. The results of this study confirmed the findings of Williams *et al*. (2001) that for 1 atm of air and at temperatures below ~270 K the contribution of the addition pathway is considerably more than was predicted by extrapolation using the previously recommended expression of Hynes *et al*. (1986).

Product distributions for the reaction of OH radicals with DMS have been obtained over a wide range of conditions, in the absence and in the presence of NO_x, and for the first time at low temperatures (260 - 280 K). The major sulfur-containing products identified in the OH radical initiated oxidation of DMS were dimethyl sulfoxide (DMSO: $CH_3S(O)CH_3$) and sulfur dioxide (SO_2), in the absence of NO_x, and dimethyl sulfoxide, dimethyl sulfone ($DMSO_2$: $CH_3S(O)_2CH_3$) and sulfur dioxide, in the presence of NO_x; as minor sulfur-containing products have been identified dimethyl sulfone, methyl thiol formate (MTF: CH_3SCHO) and carbonyl sulfide (OCS), in the absence of NO_x, and methyl sulfonyl peroxynitrate (MSPN: $CH_3S(O)_2OONO_2$) and methane sulfonic acid (MSA: $CH_3S(O)_2OH$), in the presence of NO_x. The variation of the product yields with temperature, NO_x concentration

and O_2 partial pressure is consistent with the occurrence of both addition and abstraction channels in the OH radical initiated oxidation of DMS. The work has shown the following:

- In the absence of NO the yield of DMSO always accounts for ≥95% of the products in the addition channel over the range of temperatures studied.
- In the presence of NO, the following reaction sequence has been shown to occur:

$$OH + CH_3SCH_3 + M \leftrightarrow CH_3S(OH)CH_3 + M$$
$$CH_3S(OH)CH_3 + O_2 + M \leftrightarrow CH_3S(OH)(OO)CH_3 + M$$
$$CH_3S(OH)(OO)CH_3 + NO \rightarrow CH_3S(OH)(O)CH_3 + NO_2$$
$$CH_3S(OH)(O)CH_3 + O_2 \rightarrow CH_3S(O)_2CH_3 + HO_2$$

  The sequence has been shown to control the DMSO/$DMSO_2$ yield ratio of the addition channel in NO_x-containing DMS reaction systems.
- With the exception of the experiments performed in N_2, for all other conditions of temperature, O_2 partial pressure and NO_x concentration the combined yields of DMSO and $DMSO_2$ were always approximately equal to the fraction of the reaction proceeding *via* the addition route.
- The above reaction sequence in the presence of NO has been shown to be only important in reaction systems containing approximately 200 ppbv or more NO. Therefore, under the low NO_x conditions generally present in the remote marine boundary layer the results support that DMSO will be (i) the dominat addition channel product and (ii) the nature of its further oxidation products will determine the contribution of the addition channel to new aerosol formation.
- As has been observed in other studies the oxidation of DMS under NO_x-free conditions has been shown to produce OCS. According to the results of the present work the photolysis of MTF is not a source of OCS. The most likely source appears to be the reaction of CH_3S with O_2 to form CH_2S with further oxidation to give OCS.
- In all of the experimental systems the yield of SO_2 was always lower than the fraction of the reaction proceeding *via* the O_2-independent pathway. In the NO_x-free systems this has been attributed to the formation of products such as CH_3SCHO (methyl thiol formate), CH_3SCH_2OH (methyl thiomethanol) and possibly CH_3SCH_2OOH. Of these products only CH_3SCHO has been positively identified. The results support that in the remote marine atmosphere the yield of this compound in the oxidation of DMS will not be more than a few percent even at low temperatures. In the presence of high levels of NO_x the low SO_2 yields can be explained by the formation of sulfur reservoir

species such as $CH_3S(O)_2OONO_2$, $CH_3S(O)OONO_2$, $CH_3S(O)ONO_2$, $CH_3S(O)NO_2$ and $CH_3S(O)NO$. The low levels of SO_2 observed also support that the further oxidation of DMSO formed in the O_2-dependent pathway is not leading to formation of high yields of SO_2 under the conditions of the experiments.

The present kinetic and product studies have significantly improved the understanding of the atmospheric degradation pathways of DMS as a function of temperature. The kinetic and product studies at low temperature will be of assistance in modelling the atmospheric fate of DMS in the lower and upper troposphere. It will also be helpful in modelling the seasonal effects of the anthropogenic DMS emissions.

Appendix I

Synthesis of methyl nitrite (CH_3ONO)

Methyl nitrite, which is a gas at room temperature (Bp. = -16^0C), has been synthesised following the method of Taylor *et al.* (1980) with some small modifications. Methyl nitrite was produced by the reaction of sodium nitrite ($NaNO_2$) with methanol (CH_3OH) in the presence of sulfuric acid (H_2SO_4).

The following quantities of chemicals were used:

- (I) 69 g (1 mol) $NaNO_2$
- (II) solution of CH_3OH: 48.7 ml CH_3OH + 38.5 ml H_2O
- (III) solution of H_2SO_4: 49 ml H_2O + 26.8 ml H_2SO_4 (conc.)

$NaNO_2$ (I) and the solution of CH_3OH (II) were mixed in a 2 l three-neck flask fitted with a magnetic stirrer and a dropping funnel. The flask was cooled and kept during the time of synthesis in an ice bath (at ~0^0C) because of the exotermic reaction, which takes place on the addition of H_2SO_4. The solution of H_2SO_4 (III) was added drop wise (using the dropping funnel) to the mixture over a period of ~3 hours; the addition of the acid has to be very slow because the reaction is very fast. The gaseous methyl nitrite produced was swept out of the reaction flask, and passed through a glass tube containing anhydrous calcium chloride ($CaCl_2$) in order to remove water, and then collected in a glass cylinder placed in a cooling trap at -68^0C (dry ice/ethanol mixture). The pale yellow liquid methyl nitrite was stored in the glass cylinder in the dark at -78^0C (in dry ice) to prevent thermal decomposition.

Methanol (CH_3OH) was not detectable in the FTIR spectrum of the freshly synthesised methyl nitrate. When the methyl nitrate is left for a long period in the glass cylinder, it has been observed that traces of methyl nitrate (CH_3ONO_2) can be formed.

Appendix II

Gas-phase infrared absorption cross sections

Calibration method

The 336 l glass reactor was used to determine absorption cross sections in the IR spectral region of sulfur and non-sulfur containing compounds used as reactants or identified as products in this work. The integral cross sections were determined using the procedure outlined by Etzkorn *et al.* (1999). A brief description of the method employed is given below.

Absorption cross sections are defined by Lambert-Beer's law:

$$\ln\left(\frac{I_0(\nu)}{I(\nu)}\right) = \sigma_{e(\nu)} \cdot c \cdot l = D_{(\nu)} \qquad \text{(II.1)}$$

were $I_{(\nu)}$ and $I_{0(\nu)}$ denote the measured light intensities at wave number ν with and without absorber present in the cell, $\sigma_{e(\nu)}$ is the absorption cross section at the wave number ν, c is the analyte concentration and l the optical path length through the cell. The term $\ln(I_{0(\nu)}/I_{(\nu)})$ is also known as the optical density $D_{(\nu)}$ at the wave number ν.

From equation II.1, an expression for the integrated band intensity (IBI) can be derived by integrating over the wave numbers covered by the absorption band of interest. This is a mathematical process, which is performed by the computer software. The IBI value is an often-used parameter for the absorption intensity of a given molecule, because the IBI value normally is considered constant for a molecular absorption band if pressure, temperature and instrumental resolution are constant. Therefore, if the IBI value for a compound is known, the concentration can be found by equation (II.2):

$$\mathrm{IBI} = \frac{\int_{\nu} \ln\frac{I_0(\nu)}{I(\nu)}\,\mathrm{d}\nu}{c \cdot l} \Leftrightarrow c = \frac{\int_{\nu} \ln\frac{I_0(\nu)}{I(\nu)}\,\mathrm{d}\nu}{(\mathrm{IBI}) \cdot l} \qquad \text{(II.2)}$$

If the IBI value is not known for a compound, a calibration of the compound has to be made. A calibration is normally made by adding known amounts of the compound into the reactor and by calculating the integral area. This is performed for several different concentrations of the compound. The method is valid only for reasonably volatile compounds.

Some of compounds used in this work (liquids or solids) have a very low vapour pressure. In order to obtain a reproducible and quantitative transfer of the compounds into the gas phase, measured volumes or weighed amounts of the compounds were dissolved in HPLC grade dichloromethane (CH_2Cl_2). The concentrations of the solutions were chosen to result in a total injected volume between 100 and 1000 µl for the calibration. For injection of the dissolved samples, a lockable syringe Hamilton 1001 SLK equipped with an extra long needle was used.

The transfer of the sample solutions into the gas phase was accomplished by injecting the needle of the syringe into the evacuated cell through the septum. The valve controlling the nitrogen was then opened to produce a strong nitrogen flow across the needle tip. The lock of the syringe was opened and the solution allowed vaporising into the cell. The syringe was then removed and the cell was filled with nitrogen to a final pressure of 1000 mbar. Approximately 5 min were allowed for fan assisted mixing by and the adjustment of a thermal equilibrium before a FTIR spectrum was recorded.

For the calculation of the concentration in the cell the uncertainty of the injected volume has to be taken into account. Because the volume of the needle is unknown and syringe calibration ticks possess a certain width, the “true” concentration, $c_{i,t}$ in the cell will be different from the concentration calculated from the injected volumes c_i by an offset a. By injecting different volumes (i) for one compound, this offset can be corrected.

$$c_i = (\alpha_i \cdot c_{ref,t}) - a \qquad \text{(II.3)}$$

In this work at least five different volumes were injected into the cell for each compound. In the evaluation, the optical density D_i (see Eqn II.1) was separately calculated for each injected concentration. Then the ratios $\alpha_i(D_i/D_{ref})$ were obtained by subtraction of the non-calibrated reference spectra of the pure compounds recorded in absence of a solvent from the spectra recorded for different injected volumes in the chamber. The subtraction factors obtained were plotted as a function of the calculated concentrations of the analyte in the glass reactor. A linear least square fit through these data point was performed, with the slope of the fit giving the concentration corresponding to reference spectrum. Integrated

band intensities were determined using Lambert-Beer's law: integrated optical densities of the reference spectra were divided by the concentrations determined (Eqn II.3) and the optical path length of the White mirror system (see Eqn II.2).

The following tables list the FTIR absorption cross sections (cm molecule^{-1}) determined in this work. The measured values have an uncertainty of ± 10%.

DMS – σ_{10}

T (K)	Wavelength (cm^{-1})		
	2780 - 3050	1380 - 1500	1260 - 1360
301	$(1.54 \pm 0.05) \times 10^{-17}$	$(3.49 \pm 0.09) \times 10^{-18}$	$(6.94 \pm 0.19) \times 10^{-19}$
290	$(1.52 \pm 0.07) \times 10^{-17}$	$(3.58 \pm 0.17) \times 10^{-18}$	$(6.92 \pm 0.38) \times 10^{-19}$
280	$(1.57 \pm 0.04) \times 10^{-17}$	$(3.65 \pm 0.08) \times 10^{-18}$	$(6.77 \pm 0.15) \times 10^{-19}$
270	-	$(3.63 \pm 0.04) \times 10^{-18}$	-
260	$(1.61 \pm 0.14) \times 10^{-17}$	$(3.88 \pm 0.29) \times 10^{-18}$	$(6.89 \pm 0.42) \times 10^{-19}$
250	$(1.61 \pm 0.08) \times 10^{-17}$	$(3.84 \pm 0.23) \times 10^{-18}$	$(6.99 \pm 0.37) \times 10^{-19}$

SO_2 – σ_{10}

T (K)	Wavelength (cm^{-1})
	1305 - 1405
298	$(2.48 \pm 0.19) \times 10^{-17}$
290	$(2.41 \pm 0.04) \times 10^{-17}$
280	$(2.37 \pm 0.02) \times 10^{-17}$
270	$(2.49 \pm 0.07) \times 10^{-17}$
260	$(2.45 \pm 0.06) \times 10^{-17}$
250	$(2.26 \pm 0.17) \times 10^{-17}$

DMSO – σ_{10}

T (K)	Wavelength (cm^{-1})
	1046 - 1148
298	$(1.51 \pm 0.09) \times 10^{-17}$
290	$(1.25 \pm 0.05) \times 10^{-17}$
280	$(1.05 \pm 0.06) \times 10^{-17}$
270	$(1.37 \pm 0.11) \times 10^{-17}$
260	$(1.15 \pm 0.08) \times 10^{-17}$

$DMSO_2$ – σ_{10}

T (K)	Wavelength (cm^{-1})
	1125 - 1216
299	$(1.63 \pm 0.12) \times 10^{-17}$
290	$(1.17 \pm 0.05) \times 10^{-17}$
280	$(8.06 \pm 0.52) \times 10^{-18}$
270	$(4.44 \pm 1.00) \times 10^{-18}$
260	-

NO_2 – σ_{10}

T (K)	Wavelength (cm^{-1})	
	2800 - 2950	1500 - 1700
297	$(4.56 \pm 0.31) \times 10^{-18}$	$(8.59 \pm 0.50) \times 10^{-17}$
280	$(4.11 \pm 0.13) \times 10^{-18}$	$(7.50 \pm 0.37) \times 10^{-17}$
270	$(3.88 \pm 0.57) \times 10^{-18}$	$(7.26 \pm 0.76) \times 10^{-17}$
260	$(3.99 \pm 0.34) \times 10^{-18}$	$(7.25 \pm 0.58) \times 10^{-17}$

MeOH – σ_{10}

T (K)	Wavelength (cm^{-1})	
	2700 - 3150	900 - 1160
297	$(1.78 \pm 0.19) \times 10^{-17}$	$(1.59 \pm 0.15) \times 10^{-17}$
280	$(2.07 \pm 0.16) \times 10^{-17}$	$(1.63 \pm 0.12) \times 10^{-17}$
270	$(1.99 \pm 0.12) \times 10^{-17}$	$(1.57 \pm 0.08) \times 10^{-17}$
260	$(2.13 \pm 0.24) \times 10^{-17}$	$(1.73 \pm 0.19) \times 10^{-17}$

Appendix III

Literature product yields in the reaction of dimethyl sulfide with OH radicals.

Table III.1: Reported literature yields for the formation of DMSO, $DMSO_2$, SO_2, SO_4^{2-}/H_2SO_4, MSPN, MTF, OCS, MSA and MSIA in the reaction of DMS with OH radicals in 1000 mbar synthetic air (or different p_{O2}(mbar)[d]).

[DMS] (ppmv)	$[NO_x]$[a](ppbv)= $[NO]$[b]+$[NO_2]$[c]/ p_{O2}(mbar)[d]	OH source (ppmv)	Volume of reactor (l)	T (K)	% molar yield	
					DMSO	$DMSO_2$
8-20 830	(2-39.4)×10[3a] (400-1210) ×10[3a]	CH_3ONO 46	11 Q 1 G	303±2	- -	- -
1.0-1.5	280-360[b]+ 240-130[c]	-	8×10^4 T	-	-	-
0.2-2.5	86-580[a]	-	4/80× 10^3 T	-	-	-
20	10×10[3b]	C_2H_5ONO 10	-	-	-	-
~1.3	~700	-	6×10^3 P	303±1	-	-
20-45 20	- 10[b]	H_2O_2 20-40 -	420 G 420 G	298±3 298±3	- -	20±5 20
0.48-0.70	0.12-0.31[b]+ 0.02-0.14[c]	-	2.5×10^4 T	306-310	-	-
1-5 1-5	- 0.2-5[c]	H_2O_2 5-20	1080 Q	~296	20-30 -	- -
5-15 60-100	- -	CH_3ONO 10-20	480 T	295±3	- 15±5.0 (7.7±3.0)	0.9±0.6 -
6.5±0.5	140[b]	H_2O_2 25	1080 Q	297±1	25±6[g]/ 16±4[h]	1.9±0.5[g]/ 1.7±0.5[h]
	234[b]				22.2±4[g]/ 19.1±5[h]	4.5±2.8[g]/ 6.9±2[h]
	380[b]				20.4±1[g]/ 13.3±5[h]	6.1±1.3[g]/ 7.6±3.3[h]
	1160[b]				16.1±6[g]/ 8.1±2[h]	16.5±7.4[g]/ 10.8±2.7[h]
	1760[b]				16.4±4.7[g]/ 4.4±1.5[h]	9.6±7.1[g]/ 5.7±2.7[h]

Table III.1: Reported literature yields for the formation of DMSO, $DMSO_2$, SO_2, SO_4^{2-}/H_2SO_4, MSPN, MTF, OCS, MSA and MSIA in the reaction of DMS with OH radicals in 1000 mbar synthetic air (or different p_{O2}(mbar)[d]).

% molar yield							Reference
SO_2	[e]SO_4^{2-}/ [f]H_2SO_4	MSPN	MTF	OCS	MSA	MSIA	
20.7±1.2 -	- <2[e]	- -	- -	- -	- >50	- -	Hatakeyama *et al.* (1982, 1983)
40-74	-	-	-	-	-	-	Grosjean and Lewis (1982)
37-94	1.0-16.9[e]	-	-	-	0.6-13.4	-	Grosjean (1984)
22	-	-	-	-	-	-	Niki *et al.* (1983a, b)
21±5 29±7	-	-	-	-	>50	-	Hatakeyama *et al.* (1985)
70±10 20-30	- -	- -	- -	- -	- -	- -	Barnes *et al.* (1988)
61-71	1.2-4.7[f]	-	-	-	1.2-7.3	-	Yin *et al.* (1990b)
80±10 20-30	- -	- -	- -	0.7±0.2	- -	- -	Barnes *et al.* (1994b, 1996)
27.1±4.0 -	0.3±0.2[e]	3.8±2.8	-	-	5.9±4.4	1.5±1.1	Sørensen *et al.* (1996)
16.9±9[g]/ 31±2[h]	-	2.0±1.0[g]/ 3.1±0.6[h]	0[g]/ 0.3±0.2[h]	0[g]/ 0.05[h]	1.9±0.5[g]/ 1.7±0.5[h]	-	Patroescu *et al.* (1999)
20.4±2[g]/ 25.8±6[h]	-	3.2±1.0[g]/ 6.0±0.2[h]	0[g]/≤0.6[h]	-	4.5±2.8[g]/ 6.9±2.0[h]	-	
11.4±5[g]/ 16.2±6[h]	-	4.0±2.0[g]/ 8.0±0.6[h]	-	-	6.1±1.3[g]/ 7.6±3.3[h]	-	
9.5±5.7[g]/ 22.4±7[h]	-	4.0±2.0[g]/ 7.0±3.0[h]	-	-	16.5±7.4[g]/ 10.8±2.7[h]	-	
12.7±4.7[g]/ 21±5[h]	-	1.0±0.5[g]/ 3.8±2.0[h]	-	-	12.1±4.9[g]/ 15.5±4[h]	-	

Table III.1: continuation

[DMS] (ppmv)	$[NO_x]^a$(ppbv) = $[NO]^b+[NO_2]^c$/ p_{O2}(mbar)^d	OH source (ppmv)	Volume of reactor (l)	T (K)	% molar yield	
					DMSO	$DMSO_2$
6.5±0.5	0^c	H_2O_2 25	1080 Q	297±1	23±5^g/ 18.7±3^h	1.9±0.3^g/ 1.5±0.3^h
	27^c				26±8^g/ 16.4±3.5^h	3.6±2^g/ 5.6±0.5^h
	60^c				32.7±3.3^g/ 17±3^h	7.3±1.3^g/ 5.4±1.7^h
	210^c				38±16^g/ 12.1±5^h	5±1.7^g/ 8±1.3^h
	457^c				28±2^g/ 13.5±4^h	10.6±1.7^g/ 6.6±2^h
	600^c				33±6^g/ 13.6±4^h	9.6±7.1^g/ 5.7±2.7^h
6.5-7.5	20^d 200^d 500^d	H_2O_2 32	1080 Q	284±2	- 46.3±5.0 -	<8
	20^d 200^d 500^d			295±2	- 38.4±7.6 -	
	20^d 200^d 500^d			306±2	- 24.4±2.8 -	
6-7	434^b+135^c 937^b+356^c 1200^b+515^c	H_2O_2 32	1080 Q	284	34 26 22	8.74±0.94 13.56±1.34 17.52±1.36
	685^b+251^c 886^b+368^c 1070^b+505^c			295	27 19 17	8.97±0.92 10.43±1.49 13.23±1.53
	1579^b+141^c 2123^b+689^c 2821^b+739^c			306	15 11 9	3.84±0.83 4.71±1.03 5.75±1.06
3-7	<20^a 1000^a (24^b) 10000^a (953^b)	H_2O_2 9-25	480 Q	-	6.3±1.6 6.5±2.4 9.3±1.0	4.5±1.7 5.1±1.2 17.4±1.8

$^a NO_x$ mixing ratio (ppbv); ^{b}NO mixing ratio (ppbv); $^c NO_2$ mixing ratio (ppbv); $^d O_2$ partial pressure (mbar); ^{g}yields obtained for 4% conversion of DMS; ^{h}yields obtained for 10% conversion of DMS.

Table III.1: continuation

% molar yield							Reference
SO_2	[e]SO_4^{2-}/ [f]H_2SO_4	MSPN	MTF	OCS	MSA	MSIA	
32.8±4[g]/ 53±5[h]	-	0[g]/0[h]	2±0.5[g]/ 3.8±1[h]	0.2±0.1[g]/ 0.4±0.2[h]	1.6±0.2[g]/ 3.4±0.6[h]	-	Patroescu *et al.* (1999)
40±5[g]/ 59.5±5[h]	-	0[g]/0[h]	2.5±1.6 [g]/2.8±1[h]	0.2±0.1[g]/ 0.4±0.2[h]	22.4±7.3 [g]/8±3[h]	-	
34.8±2[g]/ 48.4±4[h]	-	≤1[g]/ 1.0±0.5[h]	≤2[g]/ 1±0.5[h]	0[g]/ 0.3±0.03[h]	20±6[g]/ 6.8±3[h]	-	
19.7±9[g]/ 34±6[h]	-	2.0±0.6[g]/ 3.0±0.6[h]	0[g]/≤1[h]	0[g]/ 0.19±0.04[h]	25.5±13[g] /12±3[h]	-	
29±8[g]/ 39±9[h]	-	3.0±1.0[g]/ 4.0±1.0[h]	0[g]/≤1[h]	0[g]/ 0.15±0.02[h]	31.8±6[g]/ 16.3±6[h]	-	
17±7.4[g]/ 24.7±3[h]	-	6.0±2.0[g]/ 9.0±3.0[h]	0[g]/0.8± 0.2[h]	0[g]/ 0[h]	28.5±13[g] /18±6[h]	-	
- 84.3±6.5 -	- 20.83-42.06[e]	- - -	- - -	0.23±0.05 0.37±0.04 0.38±0.06	1-4 14.3-23.22	- 17.35-19.24	Arsene *et al.* (1999), Arsene (2002)
- 95.0±3.8 -	- 14.42-17.32[e]	- - -	- 7.2±1.4 -	0.29±0.04 0.53±0.06 0.44±0.05	1-4 4.98-10.44	- 2.53-10.26	
- 99.0±6.5 -	- - -	- - -	- - -	0.31±0.06 0.63±0.06 0.71±0.07	1-4	-	
65 43 35	- - -	- - -	- - -	0.24±0.05 0.16±0.03 -	- - -	- - -	Arsene *et al.* (2001), Arsene (2002)
41 36 33	- - -	- - -	- - -	0.16±0.04 0.17±0.05 0.16±0.05	- - -	- - -	
41 34 33	- - -	- - -	- - -	- - -	- - -	- - -	
54±14 51.7±4.2 27.1±8.1	1.3±0.7[e] 1.0±0.3[e] 1.3±0.1[e]	- - 13.8±1.0	- - -	- - -	1.0±0.7 1.4±0.3 0.5±0.1	0.2±0.1 0.2±0.1 0.1±0.1	Librando *et al.* (2004)

G = glass; P = PFA (tetrafluoroethylene-perfluoroalkyl vinyl ether copolymer); Q = quartz; T = Teflon.

Appendix IV

Gases and chemicals

IV.1: Gases employed in this work

Gas	Supplier	Purity (%)
Nitrogen (N_2)	Messer-Griesheim	99.999
Oxygen (O_2)	Messer-Griesheim	99.999
Synthetic air	Messer-Griesheim	Hydrocarbon free
(20.5:79.5 = O_2:N_2(%))		99.995
Nitrogen oxide (NO)	Messer-Griesheim	$\geq$ 99.5
Nitrogen dioxide (NO_2)	Messer-Griesheim	$\geq$ 98.0
Carbon monoxide (CO)	Messer-Griesheim	99.7
Carbon dioxide (CO_2)	Messer-Griesheim	99.995
Sulfur dioxide (SO_2)	Messer-Griesheim	$\geq$ 99.0
Ethene (C_2H_4)	Messer-Griesheim	99.95
Propene (C_3H_6)	Messer-Griesheim	99.95
2-methylpropene (C_4H_8)	Messer-Griesheim	$\geq$ 99

IV.2: Chemicals employed in this work

Compound	State at room temperature, 1 bar	Supplier	Purity (%)
Dimethyl sulfide (CH_3SCH_3)	liquid	Sigma-Aldrich	99.0
Dimethyl sulfoxide ($CH_3S(O)CH_3$)	liquid	Aldrich	99.9
Dimethyl sulfone ($CH_3S(O)_2CH_3$)	solid	Fluka	$>$ 98.0
Dichlormethane (CH_2Cl_2)	liquid	Aldrich	99.9
Formic acid (HCOOH)	liquid	Fluka	98.0
Hydrogen peroxide (H_2O_2)	liquid	Peroxide Chemie	85.0
Methanol (CH_3OH)	liquid	Carl Roth	99.9
Methane sulfinic acid sodium salt	solid	Lancaster	97.0
Methane sulfonic acid sodium salt	solid	Aldrich	99.5
Sodium carbonate	solid	Fluka	99.5
Sodium hydrogen carbonate	solid	Fluka	99.7

Appendix V

Abbreviations

BDE	bond dissociation energy
BL	boundary layer
CIMS	chemical ionization mass spectrometry
CP	continuous photolysis
CS_2	carbon disulfide
CCN	cloud condensation nuclei
DF	discharge flow
DMDS	dimethyl disulfide
DMS	dimethyl sulfide
DMS-d_6	dimethyl sulfide - deuterated analogue
DMSO	dimethyl sulfoxide
$DMSO_2$	dimethyl sulfone
DMSP	dimethyl sulfonium propionate
Δ[DMS]	the change in DMS concentration
ΔH^0	the reaction enthalpy
EPR	electron paramagnetic resonance
FP	flash photolysis
FT	free troposphere
FTIR	Fourier transform infrared
GC	gas chromatography
HPF	high pressure flow
HPLC	high performance liquid chromatography
HPTR	high pressure turbulent flow reactor
H_2S	hydrogen sulfide
H_2SO_4	sulfuric acid
IC	ion chromatography
ID	internal diameter
IR	infrared
J_{NO2}	NO_2 photolysis rate coefficient
KS	kinetic spectroscopy
LIF	laser induced fluorescence
LS	lower stratosphere
LT	lower trophosphere
MBL	marine boundary layer

MCT	mercury-cadmium-tellurium
MS	methane sulfonate
MSA	methane sulfonic acid
MSEA	methane sulfenic acid
MSIA	methane sulfinic acid
MSPN	methyl sulfonyl peroxynitrate
MeSH	methyl mercaptan
MTF	methyl thiolformate
MTM	methylthiomethyl radical
MTP	methylthiylperoxy radical
NMHC	non methane hydrocarbon
NO_x	$NO + NO_2$
nss-SO_4^{2-}	non-sea-salt sulfate
OCS	carbonyl sulfide
P	pressure
PLIF	pulsed laser induced fluorescence
PLP	pulsed laser photolysis
ppmv	parts per million by volume:
	1 ppmv = 2.93×10^{13} molecules cm^{-3} at 1 bar and 250 K
	1 ppmv = 2.82×10^{13} molecules cm^{-3} at 1 bar and 260 K
	1 ppmv = 2.71×10^{13} molecules cm^{-3} at 1 bar and 270 K
	1 ppmv = 2.61×10^{13} molecules cm^{-3} at 1 bar and 280 K
	1 ppmv = 2.52×10^{13} molecules cm^{-3} at 1 bar and 290 K
	1 ppmv = 2.46×10^{13} molecules cm^{-3} at 1 bar and 298 K
	1 ppmv = 2.45×10^{13} molecules cm^{-3} at 1 bar and 299 K
ppbv	parts per billion by volume:
	1 ppbv = 2.46×10^{10} molecules cm^{-3} at 1 bar and 298 K
pptv	parts per trillion by volume:
	1 pptv = 2.46×10^{7} molecules cm^{-3} at 1 bar and 298 K
PR	pulse radiolysis
RF	resonance fluorescence
T	temperature
UT	upper trophosphere
UV	ultraviolet (200-400 nm)
VIS	visible (400-700 nm)
VOC	volatile organic compound

References

Abbatt, J.P.D., F.F. Fenter and J.G. Anderson:
High-pressure discharge flow kinetics study of OH + CH_3SCH_3, CH_3SSCH_3 → products from 297 to 368 K,
Journal of Physical Chemistry, **96** (4), 1780-1785, **1992**

Albu, M., C. Arsene and I. Barnes:
Product investigations of the OH initiated oxidation of dimethyl sulphide at sub-zero temperatures,
Proceedings of the 7th Scientific Conference of the International Global Atmospheric Chemistry Project (IGAC), Creta Maris, Hersonissos, Heraklion, Crete, 18-25 September, **2002**

Albu, M., I. Barnes, I. Patroescu-Klotz, C. Arsene and R. Mocanu:
Simulation chamber experiments on the OH-initiated oxidation of dimethyl sulphide at low temperatures,
Proceedings of EGS-AGU-EUG Joint Assembly, Nice, France, 6-11 April, **2003**

Albu, M., I. Barnes and R. Mocanu:
Studies of the reaction of dimethyl sulfide with OH - temperature and O_2 partial pressure dependence,
Proceedings of EGU 1st General Assembly, Nice, France, 25-30 April, **2004a**

Albu, M., I. Barnes and R. Mocanu:
Kinetic study of the temperature dependence of the OH initiated oxidation of dimethyl sulphide,
Proceedings of the 18th International Symposium on Gas Kinetics, Bristol, U.K., 7-12 August, **2004b**

Albu, M., I. Barnes, K.H. Becker, I. Patroescu-Klotz, R. Mocanu and Th. Benter:
Rate coefficients for the gas-phase reaction of OH radicals with dimethyl sulfide: temperature and O_2 partial pressure dependence,
Physical Chemistry Chemical Physics, **8**, 728-736, **2006a**

Albu, M., I. Barnes and R. Mocanu:
Kinetic study of the temperature dependence of the OH initiated oxidation of dimethyl sulfide,
Proceedings of the NATO Advanced Research Workshop on Environmental Simulation Chambers: Application to Atmospheric Chemical Processes, Zakoppane, Poland, 1-4 October 2004, I. Barnes and K.J. Rudzinski (Eds), NATO Science Series IV: Earth and Environmental Sciences - Vol. 62, Springer, Dordrecht, The Netherlands, pp. 223-230, **2006b**

Albu, M., I. Barnes, K.H. Becker, I. Patroescu-Klotz, R. Mocanu and Th. Benter:
FT-IR product study on the OH-initiated oxidation of dimethyl sulfide: temperature and O_2 partial pressure dependence,

Proceedings of the NATO Advanced Research Workshop, Alushta, Ukraine, 1-4 October, **2007**

Albu, M., I. Barnes, C. Arsene, K.H. Becker, I. Patroescu-Klotz, R. Mocanu and Th. Benter:
Product study on the OH-initiated oxidation of dimethyl sulfide: temperature, NO_x, and O_2 partial pressure dependence,
to be published, **2008**

Allen, A.G., A.L. Dick and B.M. Davison:
Sources of atmospheric methanesulphonate, non-sea-salt sulphate, nitrate and related species over the temperate south Pacific,
Atmospheric Environment, **31** (2), 191-205, **1997**

Andreae, M.O., and H. Raemdonck:
Dimethyl sulfide in the surface ocean and the marine atmosphere: a global view,
Science, **221**, 744-747, **1983**

Andreae, M.O., and W.R. Barnard:
The marine chemistry of dimethylsulfide,
Marine Chemistry, **14**, 267-279, **1984**

Andreae, M.O., R.J. Ferek, F. Bermond, K.P. Byrd, R.T. Engstrom, S. Hardin, P.D. Houmere, F. LeMarrec, H. Raemdonck and R.B. Chatfield:
Dimethyl sulfide in the marine atmosphere,
Journal of Geophysical Research, **90** (D7), 12,891-12,900, **1985**

Andreae, M.O.:
Ocean-atmosphere interactions in the global biogeochemical sulfur cycle,
Marine Chemistry, **30**, 1-29, **1990**

Andreae, M.O., and W.A. Jaeschke:
Exchange of sulphur between biosphere and atmosphere overe temperate and tropical regions,
Sulphur Cycling on the Continents: Wetlands, Terrestrial Ecosystems, and Associated Water Bodies, SCOPE 48, R.W. Howarth, J.W.B. Stewart and M.V. Ivanov (Eds), Wiley, Chichester, pp. 27-61, **1992**

Andreae, T.W., M.O. Andreae and G. Schebeske:
Biogenic sulfur emissions and aerosols over the tropical South Atlantic. 1. Dimethylsulfide in seawater and in the atmospheric boundary layer,
Journal of Geophysical Research, **99** (D11), 22,819-22,829, **1994**

Andreae, M.O., and P.J. Crutzen:
Atmospheric aerosols: biogeochemical sources and role in atmospheric chemistry,
Science, **276**, 1052-1058, **1997**

Aneja, V.P.:
Natural sulfur emissions into the atmosphere,
Journal of Air and Waste Management Association, **40** (4), 469-476, **1990**

Arsene, C., I. Barnes and K.H. Becker:
FT-IR product study on the photo-oxidation of dimethyl sulphide: temperature and O_2 partial pressure dependence,
Physical Chemistry Chemical Physics, **1**, 5463-5470, **1999**

Arsene, C., I. Barnes, K.H. Becker and R. Mocanu:

FT-IR product study on the photo-oxidation of dimethyl sulphide in the presence of NO_x - temperature dependence*,*
Atmospheric Environment, **35**, 3769-3780, **2001**

Arsene, C.:
Atmospheric Degradation Mechanisms of Organic Sulphur Compounds,
Ph.D. Thesis, Physikalische Chemie/Fachbereich C, Bergische Universität Wuppertal, Germany, **2002**

Arsene, C., I. Barnes and M. Albu:
Chlorine atom reaction kinetics with organo-sulphur compounds as a function of temperature and O_2 partial pressure,
Proceedings of the 17th International Symposium on Gas Kinetics, Essen, Germany, 24-29 August, **2002a**

Arsene, C., I. Barnes and M. Albu:
Product study of the Cl atom initiated photooxidation of dimethyl sulphide,
Proceedings of the 7th Scientific Conference of the International Global Atmospheric Chemistry Project (IGAC), Creta Maris, Hersonissos, Heraklion, Crete, 18-25 September, **2002b**

Arsene, C., I. Barnes, K.H. Becker, W.F. Schneider, T.J. Wallington, N. Mihalopoulos and I.V. Patroescu-Klotz:
Formation of methane sulfinic acid in the gas-phase OH-radical initiated oxidation of dimethyl sulfoxide,
Environmental Science and Technology, **36**, 5155-5163, **2002c**

Arsene, C., I. Barnes and M. Albu:
Evaluation of the Climatic Impact of Dimethyl Sulphide (EL CID), contract number: EVK2-CT-1999-00033, final report to the European Commission, Brussels, **2003**

Arsene, C., I. Barnes, M. Albu, R.I. Olariu, K.H. Becker and K. Wirtz:
Mechanistic studies on the atmospheric oxidation of organic sulphur compounds,
The European Photoreactor EUPHORE 4th REPORT 2001, I. Barnes (Ed.), Compiled and Produced by: Institut Physikalische Chemie, Bergische Universität Wuppertal and Fundación Centro de Estudios Ambientales del Mediterráneo Valencia, pp. 152-165, February **2004**

Arsene, C., I. Barnes, K.H. Becker and Th. Benter:
Gas-phase reaction of Cl with dimethyl sulfide: temperature and oxygen partial pressure dependence of the rate coefficient,
International Journal of Chemical Kinetics, **37**, 66-73, **2005**

Atkinson, R., R.A. Perry and J.N. Pitts, Jr.:
Rate constants for the reaction of OH radicals with COS, CS_2 and CH_3SCH_3 over the temperature range 299-430 K,
Chemical Physics Letters, **54** (1), 14-18, **1978**

Atkinson, R., J.N. Pitts, Jr., and S.M. Aschmann:
Tropospheric reactions of dimethyl sulfide with NO_3 and OH radicals,
Journal of Physical Chemistry, **88** (8), 1584-1587, **1984**

Atkinson, R.:
Gas-phase tropospheric chemistry of volatile organic compounds: 1. alkanes and alkenes,
Journal of Physical Chemistry. Reference Data, **26** (2), 215-290, **1997**

Atkinson, R., D.L. Baulch, R.A. Cox, J.N. Crowley, R.F. Hampson, R.G. Hynes, M.E. Jenkin, M.J. Rossi and J. Troe:
Evaluated kinetic and photochemical data for atmospheric chemistry: volume 1 - gas phase reactions of O_x, HO_x, NO_x and SO_x species,
Atmospheric Chemistry and Physics, **4**, 1461-1738, **2004**

Aumont, O., S. Belviso and P. Monfray:
Dimethylsulfoniopropionate (DMSP) and dimethylsulfide (DMS) sea surface distributions simulated from a global three-dimensional ocean carbon cycle model,
Journal of Geophysical Research, **107** (C4), 10.1029/1999JC000111, **2002**

Baker, J., and J.M. Dyke:
A photoelectron and ab initio study of the CH_3SCH_2 radical,
Chemical Physics Letters, **213** (3, 4), 257-261, **1993**

Balla, R.J., and J. Heicklen:
Oxidation of sulfur compounds. I: The photolysis of CH_3SH and $(CH_3S)_2$ in the presence of NO,
Canadian Journal of Chemistry, **62** (1), 162-170, **1984**

Balla, R.J., H.H. Nelson and J.R. McDonald:
Kinetics of the reaction of CH_3S with NO, NO_2 and O_2,
Chemical Physics, **109**, 101-107, **1986**

Ballesteros, B., N.R. Jensen and J. Hjorth:
FT-IR study of the kinetics and products of the reactions of dimethylsulphide, dimethylsulphoxide and dimethylsulphone with Br and BrO,
Journal of Atmospheric Chemistry, **43** (2), 135-150, **2002**

Bandy, A.R., D.L. Scott, B.W. Blomquist, S.M. Chen and D.C. Thornton:
Low yields of SO_2 from dimethyl sulfide oxidation in the marine boundary layer,
Geophysical Research Letters, **19** (11), 1125-1127, **1992**

Bandy, A.R., D.C. Thornton, B.W. Blomquist, S. Chen, T.P. Wade, J.C. Ianni, G.M. Mitchell and W. Nadler:
Chemistry of dimethyl sulfide in the equatorial Pacific atmosphere,
Geophysical Research Letters, **23** (7), 741-744, **1996**

Bardouki, H., H. Berresheim, M. Vrekoussis, J. Sciare, G. Kouvarakis, K. Oikonomou, J. Schneider and N. Mihalopoulos:
Gaseous (DMS, MSA, SO_2, H_2SO_4 and DMSO) and particulate (sulfate and methanesulfonate) sulfur species over the northeastern coast of Crete,
Atmospheric Chemistry and Physics, **3**, 1871-1886, **2003**

Barnard, W.R., M.O. Andreae, W.E. Watkins, H. Bingemer and H.-W. Georgii:
The flux of dimethylsulfide from the oceans to the atmosphere,
Journal of Geophysical Research, **87** (C11), 8787-8793, **1982**

Barnes, I., K.H. Becker, E.H. Fink, A. Reimer, F. Zabel and H. Niki:
Rate constant and products of the reaction $CS_2 + OH$ in the presence of O_2,
International Journal of Chemical Kinetics, **15**, 631-645, **1983**

Barnes, I., K.H. Becker, P. Carlier and G. Mouvier:
FTIR study of the DMS/NO_2/I_2/N_2 photolysis system: the reaction of IO radicals with DMS,
International Journal of Chemical Kinetics, **19** (6), 489-501, **1987a**

Barnes, I., V. Bastian and K.H. Becker:
FTIR spectroscopic studies of the $CH_3S + NO_2$ reaction under atmospheric conditions, *Chemical Physics Letters*, **140** (5), 451-457, **1987b**

Barnes, I., V. Bastian and K.H. Becker:
Kinetics and mechanisms of the reaction of OH radicals with dimethyl sulphide, *International Journal of Chemical Kinetics*, **20** (6), 415-431, **1988**

Barnes, I., V. Bastian, K.H. Becker and D. Martin:
Fourier Transform IR studies of the reactions of dimethyl sulfoxide with OH, NO_3, and Cl radicals,
Biogenic Sulphur in the Environment, E.S. Saltzman and W.J. Cooper (Eds), American Chemical Society, Washington, pp. 476-488, **1989**

Barnes, I., V. Bastian, K.H. Becker and R.D. Overath:
Kinetic studies of the reactions of IO, BrO, and ClO with dimethylsulfide, *International Journal of Chemical Kinetics*, **23** (7), 579-591, **1991**

Barnes, I.:
Overview and atmospheric significance of the results from laboratory kinetic studies performed within the CEC project "OCEANO-NOX",
Dimethylsulphide: Oceans, Atmosphere and Climate, G. Restelli and G. Angeletti (Eds), Kluwer Academic Publishers, Dordrecht, pp. 223-237, **1993**

Barnes, I., K.H. Becker and N. Mihalopoulos:
An FTIR product study of the photooxidation of dimethyl disulfide, *Journal of Atmospheric Chemistry*, **18**, 267-289, **1994a**

Barnes, I., K.H. Becker and I. Patroescu:
The tropospheric oxidation of dimethyl sulfide: a new source of carbonyl sulphide, *Geophysical Research Letters*, **21** (22), 2389-2392, **1994b**

Barnes, I., K.H. Becker and I. Patroescu:
FTIR product study of the OH initiated oxidation of dimethyl sulphide: observation of carbonyl sulphide and dimethyl sulphoxide, *Atmospheric Environment*, **30** (10/11), 1805-1814, **1996**

Barnes, I., J. Hjorth and N. Mihalopoulos:
Dimethyl sulfide and dimethyl sulfoxide and their oxidation in the atmosphere, *Chemical Reviews*, **106** (3), 940-975, **2006**

Barone, S.B., A.A. Turnipseed and A.R. Ravishankara:
Role of adducts in the atmospheric oxidation of dimethyl sulfide, *Faraday Discussions*, **100**, 39-54, **1995**

Barone, S.B., A.A. Turnipseed and A.R. Ravishankara:
Reaction of OH with dimethyl sulfide (DMS). 1. Equilibrium constant for OH + DMS reaction and the kinetics of the $OH{\cdot}DMS + O_2$ reaction, *Journal of Physical Chemistry*, **100** (35), 14,694-14,702, **1996**

Bates, T.S., J.D. Cline, R.H. Gammon and S.R. Kelly-Hansen:
Regional and seasonal variations in the flux of oceanic dimethylsulfide to the atmosphere,
Journal of Geophysical Research, **92** (C3), 2930-2938, **1987**

Bates, T.S., B.K. Lamb, A. Guenther, J. Dignon and R.E. Stoiber:
Sulphur emissions to the atmosphere from natural sources,

Journal of Atmospheric Chemistry, **14**, 315-337, **1992**

Becker, K.H., W. Nelsen, Y. Su and K. Wirtz:
A new mechanism for the reaction CS_2 + OH,
Chemical Physics Letters, **168** (6), 559-563, **1990**

Bedjanian, Y., G. Poulet and G. LeBras:
Kinetic study of the reaction of BrO radicals with dimethylsulfide,
International Journal of Chemical Kinetics, **28** (5), 383-389, **1996**

Berresheim, H.:
Biogenic sulfur emissions from the Subantarctic and Antarctic oceans,
Journal of Geophysical Research, **92** (D11), 13,245-13,262, **1987**

Berresheim, H., D.J. Tanner and F.L. Eisele:
Real-time measurement of dimethyl sulfoxide in ambient air,
Analytical Chemistry, **65** (1), 84-86, **1993a**

Berresheim, H., D.J. Tanner and F.L. Eisele:
Method for real-time detection of dimethyl sulfone in ambient air,
Analytical Chemistry, **65** (21), 3168-3170, **1993b**

Berresheim, H., F.L. Eisele, D.J. Tanner, L.M. McInnes, D.C. Ramsey-Bell and D.S. Covert:
Atmospheric sulphur chemistry and cloud condensation nuclei (CCN) concentrations over the north eastern Pacific coast,
Journal of Geophysical Research, **98** (D7), 12,701-12,711, **1993c**

Berresheim, H., P.H. Wine and D.D. Davis:
Sulphur in the atmosphere,
Composition, Chemistry, and Climate of the Atmosphere, H.B. Singh (Ed.), Van Nostrand Reinhold, New York, pp. 251-307, **1995**

Berresheim, H., and F.L. Eisele:
Sulfur chemistry in the Antarctic trophosphere experiment: an overview of project SCATE,
Journal of Geophysical Research, **103** (D1), 1619-1627, **1998**

Berresheim, H., J.W. Huey, R.P. Thorn, F.L. Eisele, D.J. Tanner and A. Jefferson:
Measurements of dimethyl sulfide, dimethyl sulfoxide, dimethyl sulfone, and aerosol ions at Palmer station, Antarctica,
Journal of Geophysical Research, **103** (D1), 1629-1637, **1998**

Black, G., and L.E. Jusinski:
Laser-induced fluorescence studies of the CH_3S radical,
Journal of the Chemical Society, Faraday Transactions 2, **82**, 2143-2151, **1986**

Bopp, L., O. Aumont, S. Belviso and P. Monfray:
Potential impact of climate change on marine dimethyl sulfide emissions,
Tellus, **55B**, 11-22, **2003**

Borissenko, D., A. Kukui, G. Laverdet and G. LeBras:
Experimental study of SO_2 formation in the reactions of CH_3SO radical with NO_2 and O_3 in relation with atmospheric oxidation mechanism of dimethyl sulfide,
Journal of Physical Chemistry A, **107**, 1155-1161, **2003**

Bossoutrot, V., G. LeBras, C. Arsene, M. Albu and I. Barnes:
OH-initiated oxidation of dimethyl sulphoxide,

The European Photoreactor EUPHORE 4th REPORT 2001, I. Barnes (Ed.), Compiled and Produced by: Institut Physikalische Chemie, Bergische Universität Wuppertal and Fundación Centro de Estudios Ambientales del Mediterráneo Valencia, pp. 171-174, February **2004**

Butkovskaya, N.I., and G. LeBras:
Mechanism of the NO_3 + DMS reaction by discharge flow mass spectrometry,
Journal of Physical Chemistry, **98** (10), 2582-2591, **1994**

Butkovskaya, N.I., G. Poulet and G. LeBras:
Discharge flow study of the reactions of chlorine and fluorine atoms with dimethyl sulfide,
Journal of Physical Chemistry, **99** (13), 4536-4543, **1995**

Butkovskaya, N.I., and I. Barnes:
Model study of the photooxidation of CH_3SSCH_3 and $CH_3SO_2SCH_3$ in a static reactor at 253-295 K,
Proceedings of the 8th European Symposium on the Physico-Chemical Behaviour of Atmospheric Pollutants, Torino, Italy, 17-20 September, **2001**

Butkovskaya, N.I., and I. Barnes:
Model study of the photooxidation of $CH_3SO_2SCH_3$ at atmospheric pressure: thermal decomposition of the CH_3SO_2 radical,
Proceedings of the NATO Advanced Research Workshop on Global Atmospheric Change and its Impact on Regional Air Quality, Irkutsk, Russian Federation, 21-27 August 2001, I. Barnes (Ed.), NATO Science Series IV: Earth and Environmental Scieneces - Vol. 16, Kluwer Academic Publishers, Dordrecht, The Netherlands, pp. 147-152, **2002**

Butkovskaya, N.I., and I. Barnes:
Evaluation of the Climatic Impact of Dimethyl Sulphide (EL CID), contract number: EVK2-CT-1999-00033, final report to the European Commission, Brussels, **2003**

Cainey, J.M., G.P. Ayers, R.W. Gillett, J.L. Gras, J.P. Ivey and P.W. Selleck:
Sulfur aerosol/CCN relationship in marine air at Cape Grim,
Baseline Atmospheric Program, 58-65, **1996**

Campolongo, F., A. Saltelli, N.R. Jensen, J. Wilson and J. Hjorth:
The role of multiphase chemistry in the oxidation of dimethylsulphide (DMS). A latitude dependent analysis,
Journal of Atmospheric Chemistry, **32**, 327-356, **1999**

Challenger, F., and M.I. Simpson:
Studies on biological methylation. Part XII. A precursor of dimethyl sulphide evolved by Polysiphonia fastigiata. Dimethyl-2-carboxyethylsulphonium hydroxide and its salts,
Journal of the Chemical Society, 1591-1597, **1948**

Chang, P.-F., T.T. Wang, N.S. Wang, Y.-L. Hwang and Y.-P. Lee:
Temperature dependence of rate coefficients of reactions of NO_2 with CH_3S and C_2H_5S,
Journal of Atmospheric Chemistry A, **104** (23), 5525-5529, **2000**

Charlson, R.J., J.E. Lovelock, M.O. Andreae and S.G. Warren:
Oceanic phytoplankton, atmospheric sulphur, cloud albedo and climate,
Nature, **326**, 655-661, **1987**

Chen, G., D.D. Davis, P. Kasibhatla, A.R. Bandy, D.C. Thornton, B.J. Huebert, A.D. Clarke and B.W. Blomquist:
A study of DMS oxidation in the tropics: comparison of Christmas island field observations of DMS, SO_2, and DMSO with model simulations,
Journal of Atmospheric Chemistry, **37**, 137-160, **2000**

Chin, M., D.J. Jacob, G.M. Gardner, M.S. Foreman-Fowler, P.A. Spiro and D.L. Savoie:
A global three-dimensional model of tropospheric sulfate,
Journal of Geophysical Research, **101** (D13), 18,667-18,690, **1996**

Chin, M., R.B. Rood, D.J. Allen, M.O. Andreae, A.M. Thompson, S.-J. Lin, R.M. Atlas and J.V. Ardizzone:
Processes controlling dimethylsulfide over the ocean: Case studies using a 3-D model driven by assimilated meteorological fields,
Journal of Geophysical Research, **103** (D7), 8341-8353, **1998**

Cline, J.D., and T.S. Bates:
Dimethyl sulfide in the equatorial Pacific ocean: a natural source of sulfur to the atmosphere,
Geophysical Research Letters, **10** (10), 949-952, **1983**

Cox, R.A., and D. Sheppard:
Reactions of OH radicals with gaseous sulphur compounds,
Nature, **284**, 330-331, **1980**

Cvetanović, R.J., D.L. Singleton and R.S. Irwin:
Gas-phase reactions of $O(^3P)$ atoms with methanethiol, ethanethiol, methyl sulfide, and dimethyl disulfide. 2. Reaction products and mechanisms,
Journal of American Chemical Society, **103**, 3530-3539, **1981**

Dacey, J.W.H., and S.G. Wakeham:
Oceanic dimethylsulfide: production during zooplankton grazing on phytoplankton,
Science, **233**, 1314-1316, **1986**

Dacey, J.W.H., F.A. Howse, A.F. Michaels and S.G. Wakeham:
Temporal variability of dimethylsulfide and dimethylsulfoniopropionate in the Sargasso Sea,
Deep-Sea Research, **Part I 45**, 2085-2104, **1998**

Davis, D., J.D. Bradshaw, M.O. Rodgers, S.T. Sandholm and S. KeSheng:
Free tropospheric and boundary layer measurements of NO over the central and eastern North Pacific Ocean,
Journal of Geophysical Research, **92** (D2), 2049-2070, **1987**

Davis, D., G. Chen, P. Kasibhatla, A. Jefferson, D. Tanner, F. Eisele, D. Lenschow, W. Neff and H. Berresheim:
DMS oxidation in the Antarctic marine boundary layer: comparison of model simulations and field observations for DMS, DMSO, $DMSO_2$, H_2SO_4(g), MSA(g), and MSA(p),
Journal of Geophysical Research, **103** (D1), 1657-1678, **1998**

Davis, D., G. Chen, A. Bandy, D. Thornton, F. Eisele, L. Mauldin, D. Tanner, D. Lenschow, H. Fuelberg, B. Huebert, J. Heath, A. Clarke and D. Blake:
Dimethyl sulfide oxidation in the equatorial Pacific: Comparison of model simulations with field observations for DMS, SO_2, H_2SO_4(g), MSA(g), MS, and NSS,
Journal of Geophysical Research, **104** (D5), 5765-5784, **1999**

Davison, B., and C. N. Hewitt:
Elucidation of the trophospheric reactions of biogenic sulfur species from a field measurement campaign in NW Scotland,
Chemosphere, **28** (3), 543-557, **1994**

Davison, B., C. O'Dowd, C.N. Hewitt, M.H. Smith, R.M. Harrison, D.A. Peel, E. Wolf, R. Mulvaney, M. Schwikowski and U. Baltensperger:
Dimethyl sulfide and its oxidation products in the atmosphere of the Atlantic and southern oceans,
Atmospheric Environment, **30** (10/11), 1895-1906, **1996**

Daykin, E.P., and P.H. Wine:
Rate of reaction of IO radicals with dimethylsulfide,
Journal of Geophysical Research, **95** (D11), 18,547-18,553, **1990**

De Bruyn, W.J., M. Harvey, J.M. Cainey and E.S. Saltzman:
DMS and SO_2 at Baring Head, New Zealand: implications for the yield of SO_2 from DMS,
Journal of Atmospheric Chemistry, **41**, 189-209, **2002**

Denman, K., E. Hofmann and H. Marchant:
Marine biotic responses to environmental change and feedbacks to climate,
Climate Change, The Science of Climate Change, J.T. Hougton *et al.* (Eds), Cambridge University Press, U.K., pp. 483-516, **1995**

Diaz-de-Mera, Y., A. Aranda, D. Rodriguez, R. Lopez, B. Cabañas and E. Martinez:
Gas-phase reactions of chlorine atoms and ClO radicals with dimethyl sulfide. Rate coefficients and temperature dependences,
Journal of Physical Chemistry A, **106**, 8627-8633, **2002**

Dlugokencky, E.J., and C.J. Howard:
Laboratory studies of NO_3 radical reactions with some atmospheric sulfur compounds,
Journal of Physical Chemistry, **92**, 1188-1193, **1988**

Dockery, D.W., C.A. Pope III, X. Xu, J.D. Spengler, J.H. Ware, M.E. Fay, B.G. Ferris and F.E. Speizer:
An association between air pollution and mortality in six U.S. cities,
The New England Journal of Medicine, **329**, 1753 - 1759, **1993**

Dominé, F., T.P. Murrells and C.J. Howard:
Kinetics of the reactions of NO_2 with CH_3S, CH_3SO, CH_3SS, and CH_3SSO at 297 K and 1 torr,
Journal of Physical Chemistry, **94** (15), 5839-5847, **1990**

Dominé, F., A.R. Ravishankara and C.J. Howard:
Kinetics and mechanisms of the reactions of CH_3S, CH_3SO, and CH_3SS with O_3 at 300 K and low pressure,
Journal of Physical Chemistry, **96** (5), 2171-2178, **1992**

Dyke, J.M., M.V. Ghosh, D.J. Kinnison, G. Levita, A. Morris and D.E. Shallcross:
A kinetics and mechanistic study of the atmospherically relevant reaction between molecular chlorine and dimethyl sulfide (DMS),
Physical Chemistry Chemical Physics, **7**, 866-873, **2005**

El-Nahas, A.M., T. Uchimaru, M. Sugie, K. Tokuhashi and A. Sekiya:
Hydrogen abstraction from dimethyl ether (DME) and dimethyl sulfide (DMS) by OH radical: a computational study,

Journal of Molecular Structure. Theochem, **722** (1-3), 9-19, **2005**

Enami, S., Y. Nakano, S. Hashimoto, M. Kawasaki, S. Aloisio and J.S. Francisco:
Reactions of Cl atoms with dimethyl sulfide: a theoretical calculation and an experimental study with cavity ring-down spectroscopy,
Journal of Physical Chemistry A, **108**, 7785-7789, **2004**

Erickson III, D.J., S.J. Ghan and J.E. Penner:
Global ocean-to-atmosphere dimethyl sulfide flux,
Journal of Geophysical Research, **95** (D6), 7543-7552, **1990**

Etzkorn, T., B. Klotz, S. Sørensen, I.V. Patroescu, I. Barnes, K.H. Becker and U. Platt:
Gas-phase absorption cross sections of 24 monocyclic aromatic hydrocarbons in the UV and IR spectral ranges,
Atmospheric Environment, **33**, 525-540, **1999**

Falbe-Hansen, H., S. Sørensen, N.R. Jensen, T. Pedersen and J. Hjorth:
Atmospheric gas-phase reactions of dimethylsulphoxide and dimethylsulphone with OH and NO_3 radicals, Cl atoms and ozone,
Atmospheric Environment, **34**, 1543-1551, **2000**

Feichter, J., E. Kjellström, H. Rodhe, F. Dentener, J. Lelieveld and G.-J. Roelofs:
Simulation of the trophospheric sulfur cycle in a global climate model,
Atmospheric Environment, **30** (10/11), 1693-1707, **1996**

Finlayson-Pitts, B.J., and J.N. Pitts, Jr.:
Chemistry of the Upper and Lower Atmosphere. Theory, Experiments and Applictions, Academic Press, San Diego, **2000**

Georgii, H.W., and P. Warnek:
Chemistry of the tropospheric aerosol and of clouds,
Global Aspects of Atmospheric Chemistry, R. Zellner, H. Baumgärtel, W. Grünbein and F. Hensel (Eds), Steinkopff Darmstadt, Springer New York, pp. 111-179, **1999**

Ghosh, M.V., D.E. Shallcross and J.M. Dyke:
Study of the atmospherically important reaction - Cl_2 with dimethylsulphide,
Proceedings of the 18th International Symposium on Gas Kinetics, Bristol, U.K., 7-12 August, **2004**

Gondwe, M., M. Krol, W. Gieskes, W. Klaassen and H. DeBaar:
The contribution of ocean-leaving DMS to the global atmospheric burdens of DMS, MSA, SO_2, and NSS SO_4^{2-},
Global Biogeochemical Cycles, **17** (2), 1056, 10.1029/2002GB001937, **2003**

Gonzáles-García, N., À. Gonzáles-Lafont and J.M. Lluch:
Variational transition-state theory study of the dimethyl sulfoxide (DMSO) and OH reaction,
Journal of Physical Chemistry A, **110**, 798-808, **2006**

Gonzáles-García, N., À. Gonzáles-Lafont and J.M. Lluch:
Kinetic study on the reaction of OH radical with dimethyl sulfide in the absence of oxygen,
ChemPhysChem, **8** (2), 255-263, **2007**

Gravestock, T., M.A. Blitz and D.E. Heard:
Kinetics study of the reaction of iodine monoxide radicals with dimethyl sulfide,
Physical Chemistry Chemical Physics, **7**, 2173-2181, **2005**

Grosjean, D., and R. Lewis:
Atmospheric photooxidation of methyl sulfide,
Geophysical Research Letters, **9** (10), 1203-1206, **1982**

Grosjean, D.:
Photooxidation of methyl sulfide, ethyl sulfide, and methanethiol,
Environmental Science and Technology, **18**, 460-468, **1984**

Gross, A., I. Barnes, R.M. Sørensen, J. Kongsted and K.V. Mikkelsen:
A theoretical study of the reaction between $CH_3S(OH)CH_3$ and O_2,
Journal of Physical Chemistry A, **108** (41), 8659-8671, **2004**

Gu, M., and F. Turecek:
The elusive dimethylhydroxysulfuranyl radical. An intermediate or a transition state?
Journal of American Chemical Society, **114** (18), 7146-7151, **1992**

Haas, P.:
The liberation of methyl sulphide by seeweed,
Biochemical Journal, **29**, 1297-1299, **1935**

Hatakeyama, S., M. Okuda and H. Akimoto:
Formation of sulfur dioxide and methanesulfonic acid in the photooxidation of dimethyl sulfide in the air,
Geophysical Research Letters, **9** (5), 583-586, **1982**

Hatakeyama, S., and H. Akimoto:
Reactions of OH radicals with methanethiol, dimethyl sulfide, and dimethyl disulfide in air,
Journal of Physical Chemistry, **87** (13), 2387-2395, **1983**

Hatakeyama, S., K. Izumi and H. Akimoto:
Yield of SO_2 and formation of aerosol in the photo-oxidation of DMS under atmospheric conditions,
Atmospheric Environment, **19** (1), 135-141, **1985**

Hertel, O., J. Christensen and Ø. Hov:
Modelling of the end products of the chemical decomposition of DMS in the marine boundary layer,
Atmospheric Environment, **28** (15), 2431-2449, **1994**

Hewitt, C.N., and B. Davison:
Field measurements of dimethyl sulphide and its oxidation products in the atmosphere,
Phil. Trans. R. Soc. Lond. B, **352**, 183-189, **1997**

Hjorth, J., N.R. Jensen, F. Raes and R. Van Dingen:
Laboratory and modelling studies of the formation of a stable intermediate in the night-time oxidation of DMS,
Dimethylsulphide: Oceans, Atmosphere and Climate, G. Restelli and G. Angeletti (Eds), Kluwer Academic, Publishers, Dordrecht, pp. 261-272, **1993**

Hsu, Y.-C., D.-S. Chen and Y.-P. Lee:
Rate constant for the reaction of OH radicals with dimethyl sulfide,
International Journal of Chemical Kinetics, **19** (12), 1073-1082, **1987**

Huebert, B.J., D.J. Wylie, L. Zhuang and J.A. Heath:

Production and loss of methanesulfonate and non-sea salt sulfate in the equatorial Pacific marine boundary layer,
Geophysical Research Letters, **23** (7), 737-740, **1996**

Hynes, A.J., P.H. Wine and D.H. Semmes:
Kinetics and mechanism of OH reactions with organic sulphides,
Journal of Physical Chemistry, **90**, 4148-4156, **1986**

Hynes, A.J., and P.H. Wine:
Kinetics of the OH + CH_3SH reaction under atmospheric conditions,
Journal of Physical Chemistry, **91** (13), 3672-3676, **1987**

Hynes, A.J., R.E. Stickel, A.J. Pounds, Z. Zhao, T. McKay, J.D. Bradshaw and P.H. Wine:
Mechanistic studies of the OH-initiated oxidation of dimethylsulfide,
Dimethylsulphide: Oceans, Atmosphere and Climate, G. Restelli and G. Angeletti (Eds), Kluwer Academic Publishers, Dordrecht, pp. 211-221, **1993**

Hynes, A.J., R.B. Stoker, A.J. Pounds, T. McKay, J.D. Bradshaw, J.M. Nicovich and P.H. Wine:
A mechanistic study of the reaction of OH with dimethyl-d_6 sulfide. Direct observation of adduct formation and the kinetics of the adduct reaction with O_2,
Journal of Physical Chemistry, **99** (46), 16,967-16,975, **1995**

Hynes, A.J., and P.H. Wine:
The atmospheric chemistry of dimethylsulfoxide (DMSO). Kinetics and mechanism of the OH + DMSO reaction,
Journal of Atmospheric Chemistry, **24** (1), 23-37, **1996**

Ingham, T., D. Bauer, R. Sander, P.J. Crutzen and J.N. Crowley:
Kinetics and products of the reactions BrO + DMS and Br + DMS at 298 K,
Journal of Physical Chemistry A, **103** (36), 7199-7209, **1999**

Jefferson, A., J.M. Nicovich and P.H. Wine:
Temperature-dependent kinetics studies of the reactions $Br(^2P_{3/2})$ + $CH_3SCH_3 \leftrightarrow CH_3SCH_2$ + HBr. Heat of formation of the CH_3SCH_2 radical,
Journal of Physical Chemistry, **98** (29), 7128-7135, **1994**

Jefferson, A., D.J. Tanner, F.L. Eisele and H. Berresheim:
Sources and sinks of H_2SO_4 in the remote Antarctic marine boundary layer,
Journal of Geophysical Research, **103** (D1), 1639-1645, **1998a**

Jefferson, A., D.J. Tanner, F.L. Eisele, D.D. Davis, G. Chen, J. Crawford, J.W. Huey, A.L. Torres and H. Berresheim:
OH photochemistry and methane sulfonic acid formation in the coastal Antarctic boundary layer,
Journal of Geophysical Research, **103** (D1), 1647-1656, **1998b**

Jensen, N.R., J. Hjorth, C. Lohse, H. Skov and G. Restelli:
Products and mechanism of the reaction between NO_3 and dimethylsulphide in air,
Atmospheric Environment, **25A** (9), 1897-1904, **1991**

Jensen, N.R., J. Hjorth, C. Lohse, H. Skov and G. Restelli:
Products and mechanisms of the gas phase reactions of NO_3 with CH_3SCH_3, CD_3SCD_3, CH_3SH and CH_3SSCH_3,
Journal of Atmospheric Chemistry, **14**, 95-108, **1992**

Jonas, P.R., R.J. Charlson and H. Rodhe:
Aerosols,
Climate Change 1994. Radiative Forcing of Climate Change and an Evalation of the IPCC 1992 IS92 Emission Scenarios, J.T. Houghton *et al.* (Eds), Intergovernamental Panel on Climate Change, Cambridge University Press, U.K., pp. 127-162, **1995**

Karl, M., A. Gross, C. Leck and L. Pirjola:
Intercomparison of dimethylsulfide oxidation mechanisms for the marine boundary layer: gaseous and particulate sulfur constituents,
Journal of Geophysical Research, **112**, D15304, doi: 10.1029/ 2006JD007914, **2007**

Katoshevski, D., A. Nenes and J.H. Seinfeld:
A study of processes that govern the maintenance of aerosols in the marine boundary layer,
Journal of Aerosol Science, **30** (4), 503-532, **1999**

Keller, M.D.:
Dimethyl sulfide production and marine phytoplankton: the importance of species composition and cell size,
Biological Oceanography, **6**, 375-382, **1989**

Kettle, A.J., M.O. Andreae, D. Amouroux, T.W. Andreae, T.S. Bates, H. Berresheim, H. Bingemer, R. Boniforti, M.A.J. Curran, G.R. DiTullio, G. Helas, G.B. Jones, M.D. Keller, R.P. Kiene, C. Leck, M. Levasseur, G. Malin, M. Maspero, P. Matrai, A.R. McTaggart, N. Mihalopoulos, B.C. Nguyen, A. Novo, J.P. Putaud, S. Rapsomanikis, G. Roberts, G. Schebeske, S. Sharma, R. Simo, R. Staubes, S. Turner and G. Uher:
A global data base of sea surface dimethylsulfide (DMS) measurements and a procedure to predict sea surface DMS as a function of latitude, longitude, and month,
Global Biogeochemical Cycles, **13** (2), 399-445, **1999**

Kettle, A.J., and M.O. Andreae:
Flux of dimethylsulfide from the oceans: a comparison of updated data sets and flux models,
Journal of Geophysical Research, **105** (D22), 26,793-26,808, **2000**

Kieber, D.J., J. Jiao, R.P. Kiene and T.S. Bates:
Impact of dimethylsulfide photochemistry on methyl sulfur cycling in the equatorial Pacific ocean,
Journal of Geophysical Research, **101** (C2), 3715-3722, **1996**

Kim, K.-H., G. Lee and Y.P. Kim:
Dimethylsulfide and its oxidation products in coastal atmospheres of Cheju Island,
Environmental Pollution, **110**, 147-155, **2000**

Kinnison, D.J., W. Mengon and J.A. Kerr:
Rate coefficients for the room temperature reaction of Cl atoms with dimethyl sulfide and related alkyl sulfides,
Journal of the Chemical Society, Faraday Transactions, **92** (3), 369-372, **1996**

Kirst, G.O., C. Thiel, H. Wollf, J. Nothangel, M. Wanzek and R. Ulmke:
Dimethylsulphoniopropionate (DMSP) in ice-algae and its possible biological role,
Marine Chemistry, **35**, 381-388, **1991**

Kley, D., P.J. Crutzen, H.G.J. Smit, H. Vömel, S.J. Oltmans, H. Grassl and V. Ramanathan:

Observations of near-zero ozone concentrations over the convective Pacific: effects on air chemistry,
Science, **274**, 230-233, **1996**

Kloster, S., J. Feichter, E. Maier-Reimer, K.D. Six, P. Stier and P. Wetzel:
DMS cycle in the marine ocean-atmosphere system - a global model study,
Biogeosciences, **3**, 29-51, **2006**

Knight, G.P., and J.N. Crowley:
The reactions of IO with HO_2, NO and CH_3SCH_3: flow tube studies of kinetics and product formation,
Physical Chemistry Chemical Physics, **3**, 393-401, **2001**

Koga, S., and H. Tanaka:
Numerical study of the oxidation process of dimethylsulfide in the marine atmosphere,
Journal of Atmospheric Chemistry, **17**, 201-228, **1993**

Kuhns, D.W., T.B. Tran, S.A. Shaffer and F. Tureček:
Methyltiomethyl radical. A variable-time neutralization-reionization and *ab initio* study,
Journal of Physical Chemistry, **98** (18), 4845-4853, **1994**

Kukui, A., V. Bossoutrot, G. Laverdet and G. LeBras:
Mechanism of the reaction of CH_3SO with NO_2 in relation to atmospheric oxidation of dimethyl sulfide: experimental and theoretical study,
Journal of Physical Chemistry A, **104** (5), 935-946, **2000**

Kukui, A., D. Borissenko, G. Laverdet and G. LeBras:
Gas-phase reactions of OH radicals with dimethyl sulfoxide and methane sulfinic acid using turbulent flow reactor and chemical ionization mass spectrometry,
Journal of Physical Chemistry A, **107** (30), 5732-5742, **2003**

Kurylo, M.J.:
Flash photolysis resonance fluorescence investigation of the reaction of OH radicals with dimethyl sulfide,
Chemical Physics Letters, **58** (2), 233-237, **1978**

Langner, J., and H. Rodhe:
A global three-dimensional model of the thropospheric sulfur cycle,
Journal of Atmospheric Chemistry, **13**, 225-263, **1991**

Leck, C., U. Larsson, L.E. Bagander, S. Johansson and S. Hajdu:
Dimethyl sulfide in the Baltic Sea: annual variability in relation to biological activity,
Journal of Geophysical Research, **95** (C3), 3353-3363, **1990**

Ledyard, K.M., and J.W.H. Dacey:
Microbial cycling of DMSP and DMS in coastal and oligotrophic seawater,
Limnology and Oceanography, **41** (1), 33-40, **1996**

Legrand, M., C. Feniet-Saigne, E.S. Saltzmann, C. Germain, N.I. Barkov and V.N. Petrov:
Ice-core record of oceanic emissions of dimethylsulphide during the last climate cycle,
Nature, **350**, 144-146, **1991**

Legrand, M., C. Hammer, M. DeAngelis, J. Savarino, R. Delmas, H. Clausen and S.J. Johnsen:
Sulfur-containing species (methanesulfonate and SO_4) over the last climatic cycle in the Greenland ice core project (central Greenland) ice core,
Journal of Geophysical Research, **102** (C12), 26,663-26,679, **1997**

Legrand, M., and E.C. Pasteur:
Methane sulfonic acid to non-sea-salt sulfate ratio in coastal Antarctic aerosol and surface snow,
Journal of Geophysical Research, **103** (D9), 10,991-11,006, **1998**

Librando, V., G. Tringali, J. Hjorth and S. Coluccia:
OH-initiated oxidation of DMS/DMSO: reaction products at high NO_x levels,
Environmental Pollution, **127**, 403-410, **2004**

Lightfoot, P.D., R.A. Cox, J.N. Crowley, M. Destriau, G.D. Hayman, M.E. Jenkin, G.K. Moortgat and F. Zabel:
Organic peroxy radicals: kinetics, spectroscopy and tropospheric chemistry,
Atmospheric Environment, **26A** (10), 1805-1961, **1992**

Liss, P.S., G. Malin, S.M. Turner and P.M. Holligan:
Dimethyl sulphide and *Phaeocystis*: a review,
Journal of Marine Systems, **5**, 41-53, **1994**

Lovelock, J.E., R.J. Maggs and R.A. Rasmussen:
Atmospheric dimethyl sulphide and the natural sulphur cycle,
Nature, **237**, 452-453, **1972**

Lucas, D.D., and R.G. Prinn:
Mechanistic studies of dimethylsulfide oxidation products using an observationally constrained model,
Journal of Geophysical Research, **107** (D14), 10.1029/2001JD000843, **2002**

Lucas, D.D., and R.G. Prinn:
Parametric sensitivity and uncertainty analysis of dimethylsulfide oxidation in the clear-sky remote marine boundary layer,
Atmospheric Chemistry and Physics, **5**, 1505-1525, **2005**

MacLeod, H., J.L. Jourdain, G. Poulet and G. LeBras:
Kinetic study of reactions of some organic sulfur comounds with OH radicals,
Atmospheric Environment, **18** (12), 2621-2626, **1984**

MacLeod, H., S.M. Aschmann, R. Atkinson, E.C. Tuazon, J.A. Sweetman, A.M. Winer and J.N. Pitts, Jr.:
Kinetics and mechanisms of the gas phase reactions of the NO_3 radical with a series of reduced sulfur compounds,
Journal of Geophysical Research, **91** (5), 5338-5346, **1986**

Maguin, F., A. Mellouki, G. Laverdet, G. Poulet and G. LeBras:
Kinetics of the reactions of the IO radical with dimethyl sulfide, methanethiol, ethylene, and propylene,
International Journal of Chemical Kinetics, **23** (3), 237-245, **1991**

Malin, G., S. Turner, P. Liss, P. Holligan and D. Harbour:
Dimethylsulphide and dimethylsulphoniopropionate in the northeast Atlantic during the summer coccolithophore bloom,
Deep Sea Research, **40** (7), 1487-1508, **1993**

Mari, C., K. Suhre, R. Rosset, T.S. Bates, B.J. Huebert, A.R. Bandy, D.C. Thornton and S. Businger:
One-dimensional modeling of sulfur species during the first aerosol characterization experiment (ACE 1) Lagrangian B,
Journal of Geophysical Research, **104** (D17), 21,733-21,749, **1999**

Maroulis, P.J., and A.R. Bandy:
Estimate of the contribution of biologically produced dimethyl sulfide to the global sulfur cycle,
Science, **196**, 647-648, **1977**

Martin, D., J.L. Jourdain and G. LeBras:
Kinetic study for the reactions of OH radicals with dimethylsulfide, diethylsulfide, tetrahydrothiophene, and thiophene,
International Journal of Chemical Kinetics, **17**, 1247-1261, **1985**

Martin, D., J.L. Jourdain, G. Laverdet and G. LeBras:
Kinetic study for the reaction of IO with CH_3SCH_3,
International Journal of Chemical Kinetics, **19** (6), 503-512, **1987**

Martinez, E., J. Albaladejo, E. Jiménez, A. Notario and A. Aranda:
Kinetics of the reaction of CH_3S with NO_2 as a function of temperature,
Chemical Physics Letters, **308**, 37-44, **1999**

Martinez, E., J. Albaladejo, A. Notario and E. Jiménez:
A study of the atmospheric reaction of CH_3S with O_3 as a function of temperature,
Atmospheric Environment, **34**, 5295-5302, **2000**

Mauldin III, R.L., D.J. Tanner, J.A. Heath, B.J. Huebert and F.L. Eisele:
Observations of H_2SO_4 and MSA during PEM-Tropics-A,
Journal of Geophysical Research, **104** (D5), 5801-5816, **1999**

Maurer, T., I. Barnes and K.H. Becker:
FT-IR kinetic and product study of the Br-initiated oxidation of dimethyl sulfide,
International Journal of Chemical Kinetics, **31** (12), 883-893, **1999**

Mayer-Figge, A.:
Thermischer Zerfall von Peroxynitraten verschiedener Struktur: Experimentelle Untersuchungen und Berechnungen,
Ph.D. Thesis, Physikalische Chemie/Fachbereich C, Bergische Universität Wuppertal, Germany, **1997**

McFarland, M., D. Kley, J.W. Drummond, A.L. Schmeltekopf and R.H. Winkler:
Nitric oxide measurements in the equatorial Pacific region,
Geophysical Research Letters, **6** (7), 605-608, **1979**

McKee, M.L.:
Computational study of addition and abstraction reactions between OH radical and dimethyl sulfide. A difficult case,
Journal of Physical Chemistry, **97**, 10,971-10,976, **1993a**

McKee, M.L.:
Theoretical study of the CH_3SOO radical,
Chemical Physics Letters, **211** (6), 643-648, **1993b**

McKee, M.L.:
Theoretical study of the CH_3SCH_2OO and CH_3SCH_2O radicals,
Chemical Physics Letters, **231**, 257-262, **1994**

McKee, M.L.:
Comparison of gas-phase and solution-phase reactions of dimethyl sulfide and 2-(methylthio) ethanol with hydroxyl radical,
Journal of Physical Chemistry A, **107** (35), 6819-6827, **2003**

Mellouki, A., J.L. Jourdain and G. LeBras:
Discharge flow study of the $CH_3S + NO_2$ reaction mechanism using $Cl + CH_3SH$ as the CH_3S source,
Chemical Physics Letters, **148** (2, 3), 231-236, **1988**

Mihalopoulos, N., B.G. Nguyen, C. Boissard, J.M. Campin, J.P. Putaud, S. Belviso, I. Barnes and K.H. Becker:
Field study of dimethylsulfide oxidation in the boundary layer: variations of dimethylsulfide, methanesulfonic acid, sulfur dioxide, non-sea-salt sulphate and Aitken nuclei at a coastal site,
Journal of Atmospheric Chemistry, **14**, 459-477, **1992a**

Mihalopoulos, N., I. Barnes and K.H. Becker:
Infrared absorption spectra and integrated band intensities for gaseous methanesulphonic acid (MSA),
Atmospheric Environment, **26A** (5), 807-812, **1992b**

Minikin, A., M. Legrand, J. Hall, D. Wagenbach, C. Kleefeld, E. Wolff, E.C. Pasteur and F. Ducroz:
Sulfur-containing species (sulfate and methanesulfonate) in coastal Antarctic aerosol and precipitation,
Journal of Geophysical Research, **103** (D9), 10,975-10,990, **1998**

Mousavipour, S.H., L. Emad and S. Fakhraee:
Theoretical study on the unimolecular dissociation of CH_3SCH_3 and CH_3SCH_2,
Journal of Physical Chemistry A, **106** (11), 2489-2496, **2002**

Nakano, Y., M. Goto, S. Hashimoto, M. Kawasaki and T.J. Wallington:
Cavity ring-down spectroscopic study of the reactions of Br atoms and BrO radicals with dimethyl sulfide,
Journal of Physical Chemistry A, **105**, 11,045-11,050, **2001**

Nakano, Y., S. Enami, S. Nakamichi, S. Aloisio, S. Hashimoto and M. Kawasaki:
Temperature and pressure dependence study of the reaction of IO radicals with dimethyl sulfide by cavity ring-down laser spectroscopy,
Journal of Physical Chemistry A, **107**, 6381-6387, **2003**

Nguyen, B.C., A. Gaudry, B. Bonsang and G. Lambert:
Reevaluation of the role of dimethyl sulfide in the sulphur budget,
Nature, **275**, 637-639, **1978**

Nguyen, B.C., S. Belviso, N. Mihalopoulos, J. Gostan and P. Nival:
Dimethyl sulfide production during natural phytoplanktonic blooms,
Marine Chemistry, **24**, 133-141, **1988**

Nguyen, B.C., N. Mihalopoulos, J.P. Putaud, A. Gaudry, L. Gallet, W.C. Keene and J.N. Galloway:
Covariations in oceanic dimethyl sulfide, its oxidation products and rain acidity at Amsterdam island in the southern Indian Ocean,
Journal of Atmospheric Chemistry, **15**, 39-53, **1992**

Nielsen, O.J., H.W. Sidebottom, L. Nelson, J.J. Treacy and D.J. O'Farrell:
An absolute and relative rate study of the reaction of OH radicals with dimethyl sulfide,
International Journal of Chemical Kinetics, **21** (12), 1101-1112, **1989**

Nielsen, O.J., H.W. Sidebottom, L. Nelson, O. Rattigan, J.J. Treacy and D.J. O'Farrell:
Rate constants for the reactions of OH radicals and Cl atoms with diethyl sulfide, di-*n*-propyl sulfide, and di-*n*-buthyl sulfide,
International Journal of Chemical Kinetics, **22** (6), 603-612, **1990**

Nielsen, O.J., J. Sehested and T.J. Wallington:
Atmospheric chemistry of dimethyl sulfide. Kinetics of the $CH_3SCH_2O_2 + NO_2$ reaction in the gas phase at 296 K,
Chemical Physics Letters, **236**, 385-388, **1995**

Niki, H., P.D. Maker, C.M. Savage and L.P. Breitenbach:
An FTIR study of the mechanism for the reaction $HO + CH_3SCH_3$,
International Journal of Chemical Kinetics, **15**, 647-654, **1983a**

Niki, H., P.D. Maker, C.M. Savage and L.P. Breitenbach:
Spectroscopic and photochemical properties of CH_3SNO,
Journal of Physical Chemistry, **87** (1), 7-9, **1983b**

Pandis, S.N., L.M. Russell and J.H. Seinfeld:
The relationship between DMS flux and CCN concentration in remote marine regions
Journal of Geophysical Research, **99** (D8), 16,945-16,957, **1994**

Patroescu, I.V.:
Reaktionen von organischen Schwefelverbindungen in der Atmosphäre,
Ph.D. Thesis, Physikalische Chemie/Fachbereich C, Bergische Universität Wuppertal, Germany, **1996**

Patroescu, I.V., I. Barnes and K.H. Becker:
FTIR kinetic and mechanistic study of the atmospheric chemistry of methyl thiolformate,
Journal of Physical Chemistry, **100** (43), 17,207-17,217, **1996**

Patroescu, I.V., I. Barnes, K.H. Becker and N. Mihalopoulos:
FT-IR product study of the OH-initiated oxidation of DMS in the presence of NO_x,
Atmospheric Environment, **33**, 25-35, **1999**

Patroescu-Klotz, I.:
Reactions of organic sulphur compounds in the atmosphere. Photochemical oxidation of dimethyl sulphide, dimethyl sulphoxide and methyl thiolformate / Reactii ale compusilor organici cu sulf in atmosfera. Oxidarea fotochimica a dimetil sulfurii, dimetil sulfoxidului si a tioformiatului de metil, Ed. Royal Company, Bucuresti, **1999**

Pham, M., J.-F. Müller, G.P. Brasseur, C. Granier and G. Megie:
A three-dimensional study of the tropospheric sulfur cycle,
Journal of Geophysical Research, **100** (D12), 26,061-26,092, **1995**

Plane, J.M.C.:
Gas-phase atmospheric oxidation of biogenic sulfur compounds,
Biogenic Sulfur in the Environment, E.S. Saltzman and W.J. Cooper (Eds), American Chemical Society, Washington, pp. 404-423, **1989**

Platt, U., and G. Honninger:
The role of halogen species in the trophosphere,
Chemosphere, **52** (2), 325-338, **2003**

Preunkert, S., M. Legrand, B. Jourdain, C. Moulin, S. Belviso, N. Kasamatsu, M. Fukuchi and T. Hirawake:

Interannual variability of dimethylsulfide in air and seawater and its atmospheric oxidation by-products (methanesulfonate and sulfate) at Dumont d'Urville, coastal Antarctica (1999-2003),
Journal of Geophysical Research, **112**, D06306, doi:10.1029/2006JD007585, **2007**

Prinn, R.G., R.F. Weiss, B.R. Miller, J. Huang, F.N. Alyea, D.M. Cunnold, P.J. Fraser, D.E. Hartley and P.G. Simmonds:
Atmospheric trends and lifetime of CH_3CCl_3 and global OH concentrations,
Science, **269**, 187-192, **1995**

Putaud, J.P., N. Mihalopoulos, B.C. Nguyen, J.M. Campin and S. Belviso:
Seasonal variations of atmospheric sulfur dioxide and dimethylsulfide concentrations at Amsterdam island in the southern Indian Ocean,
Journal of Atmospheric Chemistry, **15**, 117-131, **1992**

Putaud, J.P., B.M. Davison, S.F. Watts, N. Mihalopoulos, B.C. Nguyen and C.N. Hewitt:
Dimethylsulfide and its oxidation products at two sites in Brittany (France),
Atmospheric Environment, **33**, 647-659, **1999**

Ravishankara, A.R., Y. Rudich, R. Talukdar and S.B. Barone:
Oxidation of atmospheric reduced sulphur compounds: perspective from laboratory studies,
Phil. Trans. R. Soc. Lond. B, **352**, 171-182, **1997**

Ray, A., I. Vassalli, G. Laverdet and G. LeBras:
Kinetics of the thermal decomposition of the CH_3SO_2 radical and its reaction with NO_2 at 1 Torr and 298 K,
Journal of Physical Chemistry, **100** (21), 8895-8900, **1996**

Resende, S.M., and W.B. De Almeida:
Theoretical study of the atmospheric reaction between dimethyl sulfide and chlorine atoms,
Journal of Physical Chemistry A, **101** (50), 9738-9744, **1997**

Resende, S.M., and W.B. De Almeida:
Mechanism of the atmospheric reaction between the radical CH_3SCH_2 and O_2,
Journal of Physical Chemistry A, **103** (21)**,** 4191-4195, **1999a**

Resende, S.M., and W.B. De Almeida:
Thermodynamical analysis of the atmospheric fate of the $CH_3SCH_2O_2$ radical,
Physical Chemistry Chemical Physics, **1**, 2953-2959, **1999b**

Resende, S.M., J.C. de Bona and P. de Souza Sombrio:
Theoretical study of the role of adducts in the atmospheric oxidation of dimethyl sulfoxide by OH, O_2 and O_3 and the kinetics of the rection DMSO + OH,
Chemical Physics, **309** (2-3), 283-289, **2005**

Restad, K., I.S.A. Isaksen and T.K. Berntsen:
Global distribution of sulphate in the trophosphere. A three-dimensional model study,
Atmospheric Environment, **32** (20), 3593-3609, **1998**

Saltelli, A., and J. Hjorth:
Uncertainty and sensitivity analyses of OH-initiated dimethyl sulphide (DMS) oxidation kinetics,
Journal of Atmospheric Chemistry, **21**, 187-221, **1995**

Sayin, H., and M.L. McKee:

Computational study of the reactions between XO (X = Cl, Br, I) and dimethyl sulfide,
Journal of Physical Chemistry A, **108** (37)**,** 7613-7620, **2004**

Sciare, J., E. Baboukas and N. Mihalopoulos:
Short-term variability of atmospheric DMS and its oxidation products at Amsterdam island during summer time,
Journal of Atmospheric Chemistry, **39**, 281-302, **2001**

Seinfeld, J.H., and S.N. Pandis:
Atmospheric Chemistry and Physics. From Air Pollution to Climate Change, John Wiley & Sons Inc., New York, **1998**

Sekušak, S., P. Piecuch, R.J. Bartlett and M.G. Cory:
A general reaction path dual-level direct dynamics calculation of the reaction of hydroxyl radical with dimethyl sulfide,
Journal of Physical Chemistry A, **104** (38), 8779-8786, **2000**

Shaw, G.E.:
Bio-controlled thermostasis involving the sulfur cycle,
Climate Change, **5**, 297-303, **1983**

Shon, Z.-H., D. Davis, G. Chen, G. Grodzinsky, A. Bandy, D. Thornton, S. Sandholm, J. Bradshaw, R. Stickel, W. Chameides, G. Kok, L. Russell, L. Mauldin, D. Tanner and F. Eisele:
Evaluation of the DMS flux and its conversion to SO_2 over the southern ocean,
Atmospheric Environment, **35**, 159-172, **2001**

Singh, H.B., D. Herlth, R. Kolyer, L. Salas, J.D. Bradschaw, S.T. Sandholm, D.D. Davis, J. Crawford, Y. Kondo, M. Koike, R. Talbot, G.L. Gregory, G.W. Sachse, E. Browell, D.R. Blake, F.S. Rowland, R. Newell, J. Merrill, B. Heikes, S.C. Liu, P.J. Crutzen and M. Kanakidou:
Reactive nitrogen and ozone over the western Pacific: distribution, partitioning, and sources,
Journal of Geophysical Research, **101** (D1), 1793-1808, **1996**

Sørensen, S., H. Falbe-Hansen, M. Mangoni, J. Hjorth and N.R. Jensen:
Observation of DMSO and $CH_3S(O)OH$ from the gas phase reaction between DMS and OH,
Journal of Atmospheric Chemistry, **24**, 299-315, **1996**

Spiro, P.A., D.J. Jacob and J.A. Logan:
Global inventory of sulfur emissions with $1^o \times 1^o$ resolution,
Journal of Geophysical Research, **97** (D5), 6023-6036, **1992**

Stark, H., S.S. Brown, P.D. Goldan, M. Aldener, W.C. Kuster, R. Jakoubek, F.C. Fehsenfeld, J. Meagher, T.S. Bates and A.R. Ravishankara:
Influence of nitrate radical on the oxidation of dimethyl sulfide in a polluted marine environment,
Journal of Geophysical Research, **112**, D10S10, doi:10.1029/2006JD007669, **2007**

Staubes, R., and H.-W. Georgii:
Measurements of atmospheric and seawater DMS concentrations in the Atlantic, the Arctic and Antarctic region,
Dimethylsulphide: Oceans, Atmosphere and Climate, G. Restelli and G. Angeletti (Eds), Kluwer Academic Publishers, Dordrecht, pp. 95-102, **1993**

Stickel, R.E., J.M. Nicovich, S. Wang, Z. Zhao and P.H. Wine:

Kinetic and mechanistic study of the reaction of atomic chlorine with dimethyl sulfide, *Journal of Physical Chemistry*, **96** (24), 9875-9883, **1992**

Stickel, R.E., Z. Zhao and P.H. Wine:
Branching ratios for hydrogen transfer in the reactions of OD radicals with CH_3SCH_3 and $CH_3SC_2H_5$,
Chemical Physics Letters, **212** (3,4), 312-318, **1993**

Taylor, W.D., T.D. Allston, M.J. Moscato, G.B. Fazekas, R. Kozlowski and G.A. Takacs:
Atmospheric photodissociation lifetime for nitromethane, methyl nitrite, and methyl nitrate,
International Journal of Chemical Kinetics, **12**, 231-240, **1980**

Thompson, K.C., C.E. Canosa-Mas and R.P. Wayne:
Kinetics and mechanism of the reaction between atomic chlorine and dimethyl selenide; comparison with the reaction between atomic chlorine and dimethyl sulfide,
Physical Chemistry Chemical Physics, **4**, 4133-4139, **2002**

Tuazon, E.C., H. MacLeod, R. Atkinson and W.P.L. Carter:
α-Dicarbonyl yields from the NO_x-air photooxidations of a series of aromatic hydrocarbons in air,
Environmental Science and Technology, **20**, 383-387, **1986**

Tureček, F.:
The dimethylsulfide-hydroxyl radical reaction. An ab initio study,
Journal of Physical Chemistry, **98** (14), 3701-3706, **1994**

Tureček, F.:
Franck-Condon dominated chemistry. Formation and dissociations of the dimethylhydroxysulfuranyl radical,
Collection Czech Chemical Communications, **65**, 455-476, **2000**

Turner, S.M., G. Malin, P.D. Nightingale and P.S. Liss:
Seasonal variation of dimethyl sulphide in the North Sea and an assessment of fluxes to the atmosphere,
Marine Chemistry, **54** (3-4), 245-262, **1996**

Turnipseed, A.A., S.B. Barone and A.R. Ravishankara:
Observation of CH_3S addition to O_2 in the gas phase,
Journal of Physical Chemistry, **96** (19), 7502-7505, **1992**

Turnipseed, A.A., and A.R. Ravishankara:
The atmospheric oxidation of dimethyl sulphide: elementary steps in a complex mechanism,
Dimethylsulphide: Oceans, Atmosphere and Climate, G. Restelli and G. Angeletti (Eds), Kluwer Academic Publishers, Dordrecht, pp. 185-195, **1993**

Turnipseed, A.A., S.B. Barone and A.R. Ravishankara:
Reaction of CH_3S and CH_3SOO with O_3, NO_2, and NO,
Journal of Physical Chemistry, **97** (22), 5926-5934, **1993**

Turnipseed, A.A., S.B. Barone and A.R. Ravishankara:
Reaction of OH with dimethyl sulphide. 2. Products and mechanisms,
Journal of Physical Chemistry, **100** (35), 14,703-14,713, **1996**

Tyndall, G.S., J.P. Burrows, W. Schneider and G.K. Moortgat:
Rate coefficient for the reaction between NO_3 radicals and dimethyl sulphide,

Chemical Physics Letters, **130** (5), 463-466, **1986**

Tyndall, G.S., and A.R. Ravishankara:
Kinetics and mechanism of the reactions of CH_3S with O_2 and NO_2 at 298 K,
Journal of Physical Chemistry, **93** (6), 2426-2435, **1989a**

Tyndall, G.S., and A.R. Ravishankara:
Kinetics of the reaction of CH_3S with O_3 at 298 K,
Journal of Physical Chemistry, **93** (12), 4707-4710, **1989b**

Tyndall, G.S., and A.R. Ravishankara:
Atmospheric oxidation of reduced sulfur species,
International Journal of Chemical Kinetics, **23** (6), 483-527, **1991**

Uchimaru, T., S. Tsuzuki, M. Sugie, K. Tokuhashi and A. Sekiya:
A theoretical study on the strength of two-center three-electron bond in $(CH_3)_2S$-OH and H_2S-OH adducts,
Chemical Physics Letters, **408** (4-6), 216-220, **2005**

Urbanski, S.P., R.E. Stickel, Z. Zhao and P.H. Wine:
Mechanistic and kinetic study of formaldehyde production in the atmospheric oxidation of dimethyl sulfide,
Journal of the Chemical Society, Faraday Transactions, **93** (16), 2813-2819, **1997**

Urbanski, S.P., R.E. Stickel and P.H. Wine:
Mechanistic and kinetic study of the gas-phase reaction of hydroxyl radical with dimethyl sulfoxide,
Journal of Physical Chemistry A, **102** (51), 10,522-10,529, **1998**

Urbanski, S.P., and P.H. Wine:
Chemistry of gas phase organic sulfur-centred radicals,
S-Centred Radicals, Z.B. Alfassi (Ed.), John Wiley and Sons, pp. 97-140, **1999a**

Urbanski, S.P., and P.H. Wine:
Spectroscopic and kinetic study of the Cl-S$(CH_3)_2$ adduct,
Journal of Physical Chemistry A, **103** (50), 10,935-10,944, **1999b**

Vairavamurthy, A., M.O. Andreae and R.L. Iverson:
Biosynthesis of dimethylsulfide and dimethylpropiothetin by *Hymenomonas carterae* in relation to sulfur source and salinity variations,
Limnology and Oceanography, **30** (1), 59-70, **1985**

Van Dingenen, R., N.R. Jensen, J. Hjorth and F. Raes:
Peroxynitrate formation during the night-time oxidation of dimethylsulfide: its role as a reservoir species for aerosol formation,
Journal of Atmospheric Chemistry, **18**, 211-237, **1994**

Wallington, T.J., R. Atkinson, A.M. Winer and J.N. Pitts, Jr.:
Absolute rate constants for the gas-phase reactions of the NO_3 radical with CH_3SCH_3, NO_2, CO, and a series of alkanes at 298 $\pm$ 2 K,
Journal of Physical Chemistry, **90** (19), 4640-4644, **1986a**

Wallington, T.J., R. Atkinson, A.M. Winer and J.N. Pitts, Jr.:
Absolute rate constants for the gas-phase reactions of the NO_3 radical with CH_3SH, CH_3SCH_3, CH_3SSCH_3, H_2S, SO_2, and CH_3OCH_3 over the temperature range 280-350 K,
Journal of Physical Chemistry, **90** (21), 5393-5396, **1986b**

Wallington, T.J., R. Atkinson, E.C. Tuazon and S.M. Aschmann:
The reaction of OH radicals with dimethyl sulfide,
International Journal of Chemical Kinetics, **18** (8), 837-846, **1986c**

Wallington, T.J., P. Dagaut and M.J. Kurylo:
Ultraviolet absorption cross sections and reaction kinetics and mechanisms for peroxy radicals in the gas phase,
Chemical Reviews, **92** (4), 667-710, **1992**

Wallington, T.J., T. Ellermann and O.J. Nielsen:
Atmospheric chemistry of dimethyl sulfide: UV spectra and self-reaction kinetics of CH_3SCH_2 and $CH_3SCH_2O_2$ radicals and kinetics of the reactions $CH_3SCH_2 + O_2 \rightarrow CH_3SCH_2O_2$ and $CH_3SCH_2O_2 + NO \rightarrow CH_3SCH_2O + NO_2$,
Journal of Physical Chemistry, **97** (32), 8442-8449, **1993**

Wang, L., and J. Zhang:
Addition complexes of dimethyl sulfide (DMS) and OH radical and their reactions with O_2 by ab initio and density functional theory,
Journal of Molecular Structure: THEOCHEM, **543** (1 - 3), 167-175, **2001**

Wang, L., and J. Zhang:
Ab initio calculation on thermochemistry of CH_3SO_xH (x = 1 - 3) and H_2SO_y (y = 2, 3)
Journal of Molecular Structure: THEOCHEM, **581** (1-3), 129-138, **2002a**

Wang, L., and J. Zhang:
Ab initio study of reaction of dimethyl sulfoxide (DMSO) with OH radical,
Chemical Physics Letters, **356**, 490-496, **2002b**

Watts, S.F.:
The mass budgets of carbonyl sulfide, dimethyl sulfide, carbon disulfide and hydrogen sulfide,
Atmospheric Environment, **34**, 761-779, **2000**

Wayne, R.P.:
Chemistry of Atmospheres, 3th Ed., Oxford University Press Inc., New York, **2000**

Williams, M.B., P. Campuzano-Jost, D. Bauer and A.J. Hynes:
Kinetic and mechanistic studies of the OH-initiated oxidation of dimethylsulfide at low temperature - a reevaluation of the rate coefficient and branching ratio,
Chemical Physics Letters, **344**, 61-67, **2001**

Williams, M.B., P. Campuzano-Jost, B.M. Cossairt, A.J. Hynes and A.J. Pounds:
Experimental and theoretical studies of the reaction of the OH radical with alkyl sulfides: 1. direct observations of the formation of the OH-DMS adduct-pressure dependence of the forward rate of addition and development of a predictive expression at low temperature,
Journal of Physical Chemistry A, **111**, 89-104, **2007**

Wilson, C., and D.M. Hirst:
Kinetics of gas phase oxidation of reduced sulfur compounds,
Progression Reaction Kinetics, **21**, 69-132, **1996**

Wilson, C., and D.M. Hirst:
Ab initio study of the reaction of chlorine atoms with H_2S, CH_3SH, CH_3SCH_3 and CS_2,
Journal of the Chemical Society, Faraday Transactions, **93** (16), 2831-2837, **1997**

Wine, P.H., N.M. Kreutter, C.A. Gump and A.R. Ravishankara:

Kinetics of OH reactions with the atmospheric sulfur compounds H_2S, CH_3SH, CH_3SCH_3, and CH_3SSCH_3,
Journal of Physical Chemistry, **85**, 2660-2665, **1981**

Wine, P.H., J.M. Nicovich, R.E. Stickel, Z. Zhao, C.J. Shackelford, K.D. Kreutter, E.P. Daykin and S. Wang:
Halogen and sulfur reactions relevant to polar chemistry,
The Tropospheric Chemistry of Ozone in Polar Regions, H. Niki and K.H. Becker (Eds), NATO ASI Series I: Global Environmental Change, Vol. 7, Springer-Verlag Berlin, pp. 385-395, **1993**

Yin, F., D. Grosjean and J.H. Seinfeld:
Photooxidation of dimethyl sulfide and dimethyl disulfide. I: Mechanism development,
Journal of Atmospheric Chemistry, **11** (4), 309-364, **1990a**

Yin, F., D. Grosjean, R.C. Flagan and J.H. Seinfeld:
Photooxidation of dimethyl sulfide and dimethyl disulfide. II: Mechanism evaluation,
Journal of Atmospheric Chemistry, **11** (4), 365-399, **1990b**

Zhao, Z., R.E. Stickel and P.H. Wine:
Branching ratios for methyl elimination in the reactions of OD radicals and Cl atoms with CH_3SCH_3,
Chemical Physics Letters, **251**, 59-66, **1996**

Zhang, H., G.-L. Zhang, L. Wang, B. Liu, X.-Y. Yu and Z.-S. Li:
Theoretical study on the Br + CH_3SCH_3 reaction,
Journal of Computational Chemistry, **28** (7), 1153-1159, **2007**